Universität Rostock

Development of thermodynamic frameworks for the reliable prediction of properties of key compounds and intermediates obtained from biomass

Dissertation

zur

Erlangung des Grades

doctor rerum naturalium (Dr. rer. nat.)

am Institut für Chemie

der Mathematisch-Naturwissenschaftlichen Fakultät

der Universität Rostock

vorgelegt von

Irina Andreeva

aus Moscow, Russland

Rostock 2021

Acknowledgment

First of all, I would like to thank my supervisor Professor Doctor Sergey Verevkin for his ideas, inspiration, support and help. I would like to admit also that Professor Sergey Verevkin believed in my ability to come back into science after almost 10 years break, he has given me an opportunity not only to make my PhD research, but also to perform studies in different scientific directions related to the work of our scientific group and our colleagues from other laboratories, institutes and universities.

I would like to share this achievement with my former scientific supervisor and manager Professor Doctor Victor Bagratashvili who has died a few years ago. He was and remains one of the brightest and the most talented people I have ever met in my life. I want to dedicate this work to him.

My special words of gratitude are for Doctor Dzmitry Zaitsau who always helped me with valuable scientific advices during the whole period of my research as well as gave numerous technical support in the use of all scientific equipment throughout the research period.

With regard to technical support and regular repairs of devices that I carried out while researching, I really appreciate Peter Kumm and Thomas Kröger-Badge for their reliability and readiness to help.

I thank all my colleagues from Professor Doctor Ralf Ludwig's group and colleagues from LLM department for these three years of mutual work, their presence in my life, support and understanding.

My special gratitude goes to Doctor Sergey Bokarev and Doctor Olga Bokareva for their friendship and emotional presence in my life.

I would like to thank Riko Siewert for his help in arrangement of my life when I just arrived in Rostock and could hardly speak German.

I dedicate this work also to Tuvia Khokhlov, Ekaterina Gilod, Tuulia Vikkila-Qvick and Sirpa Tiittanen.

I am infinitely grateful to my parents, whose merit is in the formation and development of my personality. I dedicate this work to my father, who fights against cancer and has always been an example of strength and resilience for me.

And a special acknowledgment I would like to express to German Science Foundation, grant VE 265/12-1 for the financial support of the current research.

Selbstständigkeitserklärung

Ich versichere hiermit an Eides statt, dass diese Arbeit selbstständig und ausschließlich mit Hilfe der von mir angegebenen Quellen und Hilfsmittel angefertigt wurde.

Irina Andreeva   17.05.2021

Universität Rostock
Institut für Chemie
Abteilung Physikalische Chemie
Dr. Lorenz Weg 2
D-18051
irina.andreeva@uni-rostock.de

Summary

The reliable thermochemical data are required for the design and development of new technologies for valorisation biomass. Based on expanded experimental work, a "centerpiece" approach to predict thermodynamic properties such as enthalpies of formation and enthalpies of vaporization of key compounds and intermediates from biomass was developed. Classical combustion calorimetry was used to measure combustion energies and derive enthalpies of formation in the condensed state. Differential scanning calorimetry was used to measure heat capacities and the solid-solid and solid-liquid phase transitions. The static and transpiration method were used to study vapor pressure temperature dependences and derive vaporization/sublimation enthalpies. We used different empirical methods, structure-property correlations, and the high-level quantum-chemical calculations for evaluation of new experimental results. The evaluated thermochemical properties of substituted benzenes, glycerol ethers, and indole derivatives were used for validation and refinement of the "centerpiece" approach.

Zusammenfassung

Die zuverlässigen thermochemischen Daten werden für das Design und die Entwicklung neuer Technologien zur Steigerung des Werts von Biomasse benötigt. Basierend auf erweiterten experimentellen Arbeiten wurde ein „Herzstück" -Ansatz zur Vorhersage thermodynamischer Eigenschaften wie Bildungsenthalpien und Verdampfungsenthalpien von Schlüsselverbindungen und Zwischenprodukten aus Biomasse entwickelt. Die klassische Verbrennungskalorimetrie wurde verwendet, um Verbrennungsenergien zu messen und Bildungsenthalpien im kondensierten Zustand abzuleiten. Die Differentialscanningkalorimetrie wurde verwendet, um die Wärmekapazitäten und die Fest-Fest- und Fest-Flüssig-Phasenübergänge zu messen. Die Statische- und die Transpirations-Methode wurden verwendet, um Dampfdrucktemperaturabhängigkeiten zu messen und Verdampfungs-/Sublimationsenthalpien abzuleiten. Wir verwendeten verschiedene empirische Methoden, Struktur-Eigenschafts-Korrelationen und die quantenchemischen Berechnungen auf hoher Ebene zur Evaluierung neuer experimenteller Ergebnisse. Die evaluierten thermochemischen Eigenschaften von substituierten Benzolen, Glycerinethern und Indolderivaten wurden zur Validierung und Verfeinerung des „Herzstück" -Ansatzes verwendet.

Content

List of tables

List of figures

1. Introduction

The modern technologies for the valorisation of biomass into valuable fuels, chemicals, materials, and products are required to replace the depleted petroleum sources. The lignin and triglycerides (from plants oils and fats) are among the best suitable sources. Lignin is the most abundant polymer material that is based on aromatic units in nature. Lignin is broadly used either directly or chemically modified, as component for composites and copolymers, dispersant agent for pesticides, emulsifier, etc. Millions of tons of lignin are produced in the paper industry every year. Despite the natural abundance of lignin, valorisation of this polymer into more useful chemicals has proven to be a major challenge. Lignin is comprised by a number of different aromatic sub-units and this inherent complexity makes it difficult to achieve selectivity in chemical conversions. Also, the biodiesel from the plants oils is on-going substitute for fossil fuels in the near future. The glycerol appears as a by-product by the manufacturing of the biodiesel, representing ca. 10 wt% of the total output. The valorization of glycerol is one of the most researched topics of today. Chemical feasibility of new strategies to utilize renewable feedstocks (lignin and glycerol) into value-added products can be easily assessed by thermodynamic calculations, provided that reliable data are available [1-4].

In order to develop the valorisation technologies and understand the energetics and mechanisms that control the products formation and distribution, reliable thermodynamic data have to be collected and evaluated for building blocks that result from the thermal conversion of lignin. The fundamental properties such as enthalpies of phase transitions (vaporisation, sublimation, and fusion) and enthalpies of formation, are used in the design and optimization of chemical processes involved in renewable feedstocks valorisation technologies [5,6]. The key compounds and intermediates obtained from the lignin and glycerol valorization have been in focus of this study.

Admittedly, the number of compounds that is possible to obtain from biomass is countless. Knowledge of their physico-chemical and thermodynamic properties is required for the separation and further utilization of these products. The capacity of experimental investigations of all these compounds is rather limited. Alternatively, there are numerous techniques that can be used to predict thermochemical parameters of organic substances [1–3]. However, most of them are generally too detailed to be applied to the relatively large molecules obtained from the lignin and glycerol valorization.

The idea of this approach is to select an appropriate "centerpiece" molecule with reliable thermodynamic properties [10,11]. The "centerpiece" molecule should be large enough to bear major structural features specific to the series of compounds being studied (*e.g.* benzene, anisole, glycerol, *etc*). Various substituents can be attached (or "subtracted") to the "centerpiece" in different positions. The enthalpic contributions for each substituent and their mutual interactions are usually quantified from the group-additivity method. The thermochemical properties of substituted benzenes, glycerol ethers, and indole derivatives were measured in this work and used for validation and refinement of the "centerpiece" approach.

2. Materials and Methods

2.1. Materials

There were two types of substances used in this work. The first were commercial samples with a purity greater than 0.99 mass fraction (as specified by the manufacturer). In most cases the samples were additionally purified before the thermochemical experiments. The second type were substances that were synthesized and purified by cooperation partners. The degree of purity was determined (short before the thermochemical experiments) using a GC equipped with a FID. A capillary column HP-5 was used with a column length of 30 m, an inside diameter of 0.32 mm, and a film thickness of 0.25 μm. Water mass fraction in the samples was determined using a Mettler Toledo DL38 Karl Fischer titrator with HYDRANAL™ as the reagent.

2.2. Methods

2.2.1. Vapour pressure measurements: transpiration method

Transpiration is a convenient method to measure absolute vapour pressures at different temperatures in order to derive the vaporization and sublimation enthalpies. There are several advantages for this method, *e.g.* it is not influenced by a small amount of volatile impurities and it is possible to measure the equilibrium vapor pressure within a reasonable time. Vapor pressure can be measured over temperature ranges that are close to ambient. This method is particularly applicable for vapor pressures in the range 0.01 to 3000 Pa. In principle, the method is free of serious errors and has proved to give results being in excellent agreement with other established techniques for determining vapor pressures of pure substances and enthalpies of vaporization from the temperature dependence of the vapor pressure.

Figure 1. U-shaped glass saturator.
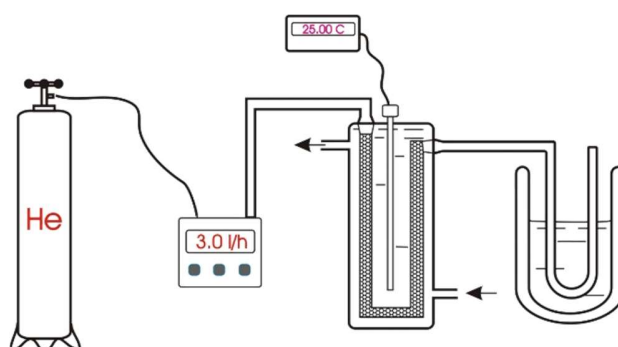
Figure 2. Schematic diagram of the transpiration apparatus.

To carry out an experiment approximately 0.7 g of a studied substance was mixed with glass beads with diameter 1.0 mm (#11079110, BioSpec Products) and placed in a U-shaped glass saturator with a controlled internal temperature (Figure 1). The scheme of the saturator is shown

in the Figure 2. If the studied compound is solid, the same amount of the compound was dissolved in such solvent as methanol or acetonitrile, then mixed with glass beads and further the solvent was fully evaporated and as a result the glass beads were covered by a tiny layer of the compound; further they were also placed into the U-shaped glass saturator. In the case of presence impurities in an investigated substance, the substance was preconditioned in the saturator at 1-2 L/h nitrogen flow rate, 20-60°C during 30-60 min. The presence of impurities after the preconditioning procedure was detected by the GC analysis of the collected sample.

A nitrogen flow with stabilized by a thermostat temperature with deviation ± 0.1 K flew through the saturator; the value of the temperature under experimental conditions was measured and controlled with Pt-100 thermometer. In the saturator the gas was saturated by the substance, and was then collected in the cold trap installed in the outlet of the saturator. To collect it for the further gas chromatography (GC) analysis, the internal surface of the cold trap was washed carefully by a solvent such as methanol, acetonitrile, benzene, toluene or by a binary mixture of these agents. In addition, 200 μL of solution of an external standard with defined concertation was added. In each experiment values of ambient temperature, T, as well as air pressure, p, were measured.

The velocity of the nitrogen gas flow varied from 1 to 3 l/h. The choice of the parameter is conditioned by the fact that if the flow velocity is lower than 1 L/h, the substance will be transferred from the cold trap due to diffusion. In the case of the gas flow speed higher than 3 l/h, the passing carrying gas won't be saturated by the substance. The velocity of the gas flow was detected with use of a soap-film flow meter (0101-0113 Hewlett-Packard). The correction and reproducibility of the work of the soap-film flow meter was verified with the use of a digital gas flow controller (Bronkhorst Hi-Tec E-7500-AAA).

The amount of the substance was detected with the aid of GC analysis (method of an external standard). A calibration for each sample was performed using an n-alkanes as the external standard. For the calibration 4 or 5 mixtures of the solutions of the studied substance and the external standard with defined concertation were studied chromatographically. In the case of GC analysis, a capillary column HP-5 (stationary phase crosslinked 5% PH ME silicone) was used with a column length of 30 m, an inside diameter of 0.32 mm, and a film thickness of 0.25 μm. As a detector a flame-ionisation detector was applied. For each studied substance and individual GC research regime was developed to allow clear splitting peaks of the substance and the external standard in the obtained chromatograms.

2.2.2. Vapour pressure measurements: static method

The static self-made experimental setup [4] was used in this work to measure vapor pressures temperature dependences. The construction is shown in Figure 3.
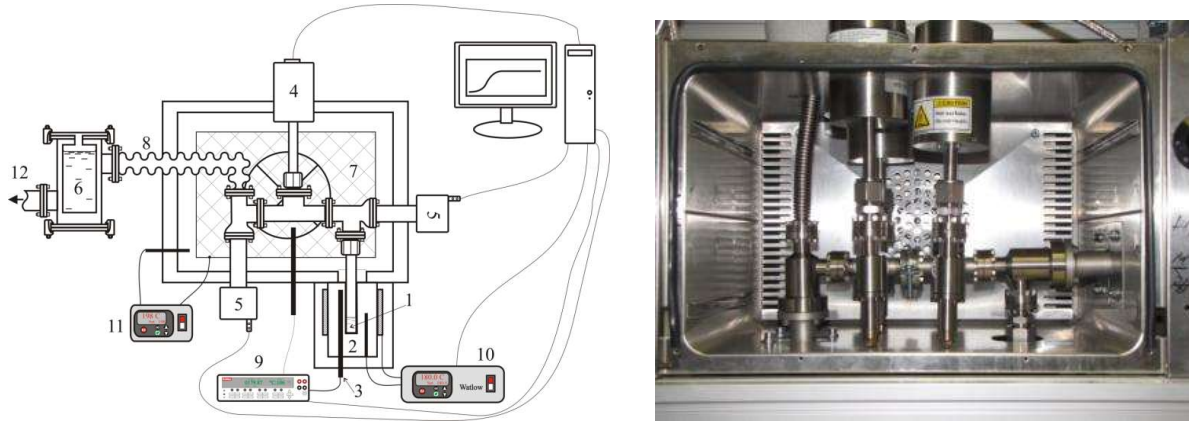
Figure 3. Schematic representation of the measuring system for the static method: 1-measurement cell, 2 - aluminum thermostating block, 3 - Burster 42510 class A 4 wire resistance thermometer, 4 - capacitance diaphragm absolute gauge MKS Baratron, 5 - all-metal angle valves VAT series 571, 6 - liquid nitrogen cold trap, 7 - orced air convection oven, 8 - bellows connection to the vacuum system, 9 - keithley 2100 multimeter, 10 - Watlow PM6C1CA-AAAAAAA temperature controller with 3-wires resistance thermometer and heating ring, 11 - rough temperature controller for the oven, 12 - Agilent HS-2 diffusion pump.

It was constructed from commercially available stainless steel UHV tubing of internal diameter d = 17 mm with ConFlat DN 16 CF connections and all-metal angle valves (VAT series 571 for high-temperatures) for UHV, operated pneumatically. The ConFlat connections and the all metal angle valve VAT provided low leakage in the vacuum system. The absence of any measurable leakage in the system was always checked before and after each experimental run. The absolute pressure in the static apparatus was measured by a combination of three absolute capacitance diaphragm gauges (manometers) covering the range of very low pressures (up to 10 Pa), low pressures (up to 1000 Pa), and the moderate pressure range (up to 10^5 Pa). Calibrations for all three gauges were traceable to the National Institute of Standards and Technology (NIST). Each manometer was connected to the measuring system through the individual all metal angle pneumatic valve VAT (series 57), and it was disconnected during the preliminary thermal equilibration of the system

During measurement a stainless still cylindrical cell with the sample was kept at a constant temperature within ±0.02 K. The sample cell was connected to the high temperature capacitance manometers covering the working range of (0.1 to 105) Pa. Uncertainties of 0.5 % for the pressure readings for both manometers were stated by the manufacturer. The temperature of tubing

connections between the measuring cell and pressure gauges was kept higher by 30-50 K than those in the sample cell in order to avoid condensation of sample vapors in the tubing system. The uncertainty of absolute temperature determination was ±0.05 K over the working temperature interval of the system.

2.3. Approximation of experimental vapour pressures

The absolute vapor pressure p_i at each temperature T_i was determined from the amount of the substance collected within a certain period of time. For calculations of p_i Dalton's law applied to the nitrogen stream saturated with the substance was assumed to be valid; the values were calculated with Equation 1.

$$p_i = m_i \cdot R \cdot T_a / V \cdot M_i \tag{1}$$

where $V = V_{N2} + V_i$ and $V_{N2} >> V_i$. In the Equation 1, R is the universal gas constant and it is equal to 8.314446 J·K⁻¹, m_i is a mass of the examined substance i, M_i is a molar mass of the substance i and V is a summed volume of V_{N2}, that is the volume of nitrogen as the carrier gas and V_i is a volume contribution of the substance to the gas phase. T_a is the temperature of a bubble meter used to measure flow rates. V_{N2} was calculated from values for flow rate and time that were specified for each individual experimrent.

The data on absolute vapour pressure, p_i, at each value of temperature, T, were fitted with the use of the Equation 2 [5]:

$$R \times \ln(p_i / p_{ref}) = a + \frac{b}{T} + \Delta_{cr,l}^g C_{p,m}^o \times \ln\left(\frac{T}{T_0}\right) \tag{2}$$

where a and b are parameters of correlation and $\Delta_{cr,l}^g C_{p,m}^o$ is the difference of the molar heat capacities of the gas and the crystalline (or liquid) phase. T_0 is an arbitrary reference temperature that has been chosen as $T_0 = 298.15$ K, $p_{ref} = 1$ Pa and R is the molar gas constant. To derive the standard molar enthalpy of vaporization, $\Delta_l^g H_m^o$, or the standard molar enthalpy of sublimation, $\Delta_{cr}^g H_m^o$, at the chosen standard temperature $T_o = 298.15$ K. For estimation of $\Delta_{cr,l}^g C_{p,m}^o$ there are different techniques [6,7]. Values of $C_{p,m}^o(cr)$ and $C_{p,m}^o(l)$ can be easily measured by DSC [8] or they can be assessed by additivity rules [9]. Since the experimental determination of the $C_{p,m}^o(g)$-values (especially for low volatile compounds) is not possible, the $\Delta_{cr,l}^g C_{p,m}^o$-values were derived from different empirical equations as follows.

2.3.1. Derivation from empirical and theoretical heat capacities $C_{p,m}^o(cr, l)$ and $C_{p,m}^o(g)$

The values of $C_{p,m}^o(cr, l)$ can be directly measured using adiabatic calorimetry method or differential scanning calorimetry (DSC) [8], but due to difficulties of direct measurement of the

gas-phase heat capacities, $C_{p,m}^o(g)$, this parameter is estimated by group additivity method [10] or by statistical thermodynamics (using the frequency spectrum calculated by high level quantum chemical methods) [7].

Another possibility to estimate the values is suggested by Chickos and Acree [11,12] using the following empirical Equation 3:

$$\Delta_l^g C_{p,m}^\circ(298.15 \text{ K}) = -0.26 \times C_{p,m}^\circ(l, 298.15) + 10.58 \tag{3}$$

where $C_{p,m}^o(l, 298.15 \text{ K})$-data are of experimental origin or estimated according to the group additivity procedure [9].

2.3.2. Derivation from vapour pressure measurements

It is well-established [13,14], that the fitting of the experimental vapor pressures measured over the broad temperature range by using the Clarke and Glew [15] equation is able to provide the reliable and independent assessment of the $\Delta_{cr}^g C_{p,m}^o$-values. The Clarke and Glew Equation (the Equation 4) is given as follows:

$$R\ln\left(\frac{p}{p^0}\right) = -\frac{\Delta_{cr}^g G_m^o(\theta)}{\theta} + \Delta_{cr}^g H_m^o(\theta)\left(\frac{1}{\theta} - \frac{1}{T}\right) + \Delta_{cr}^g C_{p,m}^o(\theta)\left[\frac{\theta}{T} - 1 + \ln\left(\frac{T}{\theta}\right)\right] \tag{4}$$

where p is the vapor pressure at the temperature T, p^o is an arbitrary reference pressure ($p^o = 1$ Pa in this work), θ is an arbitrary reference temperature (in this work we use $\theta = 298.15$ K), R is the molar gas constant, $\Delta_{cr}^g G_m^o(\theta)$ is the difference in the standard molar Gibbs energy between the gaseous and the crystalline phases at the selected reference temperature, $\Delta_{cr}^g H_m^o(\theta)$ is the standard molar enthalpy of sublimation. An advantage of Equation 4 is that the fitting coefficients of the Clarke and Glew equation are directly related to the thermodynamic functions of vaporization/sublimation.

2.3.3. Derivation from volumetric properties

This indirect and sophisticated method of $\Delta_l^g C_{p,m}^o$ estimation is based on the experimental liquid phase volumetric properties such as thermal expansion of the liquid sample, isothermal compressibility, and molar volume [13,14]:

$$\Delta_l^g C_{p,m}^\circ(298.15 \text{ K}) = -2R - (C_{p,m}^\circ - C_{v,m}^\circ)_l \tag{5}$$

where $\left(C_{p,m}^o - C_{v,m}^o\right)_l$ can be estimated as

$$\left(C_{p,m}^o - C_{v,m}^o\right)_l = n\alpha_p\left(\Delta_l^g H_m^o - RT\right) \tag{6}$$

where n is an adjustable parameter [16].

2.3.4. Derivation from the Kirchhoff Law

The $\Delta_{cr,l}^g C_{p,m}^o$-values can be derived from the Kirchhoff Law according to Equation 7 [13]:

$$\Delta_{cr,l}^g C_{p,m}^o = [\Delta_{cr,l}^g H_m^o(T_{av}) - \Delta_{cr,l}^g H_m^o(298.15\ K)]/\ (298.15\ K - T_{av}) \tag{7}$$

where T_{av} is an averaged temperature of the temperature range of vapour pressure measurements.

2.4. Vaporization/sublimation thermodynamics

Vapor pressure measured at different temperatures, T, were used to derive the standard molar enthalpies of vaporization/sublimation using the following Equation:

$$\Delta_{l,cr}^g H_m^o(T)\ = -b + \Delta_{l,cr}^g C_{p,m}^o \times T \tag{8}$$

Vaporization/sublimation entropies at temperatures T were also derived from the vapor pressures temperature dependences using Equation (9):

$$\Delta_{l,cr}^g S_m^o(T) = \Delta_{l,cr}^g H_m^o/T + R \cdot \ln(p_i/p^o) \tag{9}$$

with $p^o = 0.1$ MPa.

As a rule the uncertainties of vaporization/sublimation enthalpies $u(\Delta_{l,cr}^g H_m^o)$ are presented as the standard uncertainty (at 0.68 level of confidence, k = 1). They are calculated according to a procedure described in [17]. It includes uncertainties from the experimental conditions, uncertainties of vapor pressure, uncertainties from the fitting equation, and uncertainties from temperature adjustment to $T = 298.15$ K.

2.5. Validation of experimental vaporization enthalpies with structure-property relationships

2.5.1. Kovats´s retention indices method

The Correlation Gas-Chromatographic (CGC) method is often used to validate the experimental enthalpies of vaporization [18]. In this method vaporization enthalpies, $\Delta_l^g H_m^o$, appear to be a function of the Kovat's indices in a homologous series of such organic substances as alkanes, alcohols, and aliphatic ethers [19] as well as of alkylbenzenes [20]. It is based on correlating the experimental $\Delta_l^g H_m^o(298.15\ K)$-values with their Kovats`s indices [3]. The n-alkanes are used as standards for the calculating the Kovats´s retention index, J_x, as follows:

$$J_x\ = \frac{\lg(t_x) - \lg(t_N)}{\lg(t_{N+1}) - \lg(t_N)} \times 100 + 100N \tag{10}$$

where x refers to the adjusted retention time t_x of compound under determination; N is the number of carbon atoms of the n-alkane eluting before, and ($N + 1$) is the number of carbon atoms of the n-alkane eluting after the peak of interest. According to the established CGC procedure, all retention times are corrected for the "dead" retention time. The advantage of the method is

availability data on Kovats´s retention index [21]. Consequently, it can be considered to apply to other organic homologues substances. After the collection of data on vaporization enthalpies of similar structure compounds, $\Delta_l^g H_m^o$, and their Kovats´s retention index, J_x, and subsequent getting correlation of these two parameters, the obtained by transpiration of other technique results can be estimated with this linear correlation. This method can be also used for accurate predictions of vapour pressures and vaporization enthalpies of organic substances, but it is recommended to check its applicability in the case of each set of studied homologous substances.

2.5.2. Chain-length dependence method

Another possibility to validate experimental results and to predict vapour pressures and vaporization enthalpies is to get a correlation between enthalpies of vaporization, $\Delta_l^g H_m^o$, with the number of C-atoms within the series of homologues compounds [18]. It was shown that vaporization enthalpies is a function of a number atoms of the alkanes [22] or nitriles [23]. Thus, after getting a plot of correlation between vaporization enthalpies of homologous compounds taken from literature data and the number of their carbon atoms, N_C, the own experimental data can be considered and validated.

2.5.3. Boiling temperatures validation method

It was shown that the correlations between vaporization enthalpies, $\Delta_l^g H_m^o$, of methoxy substituted phenols and methoxy substituted benzaldehydes with their normal boiling temperatures exist [24,25]. In this way, this method can be also applied for validation of experimental results of transpiration methods for other types of organic substances. To apply this validation method a set of normal boiling temperatures as well as vaporization enthalpies of homologues to the studied substances compounds should be collected and the obtained linear correlation can be used for validation of own sets of experimental results and for prediction of missing values of vaporization enthalpies of homologous structure substances.

2.6. Differential scanning calorimetry

The standard molar enthalpies of fusion, $\Delta_{cr}^l H_m^o$, of crystalline compounds were measured by using differential scanning calorimetry (DSC) [26]. Thermal behavior of solid samples including melting temperatures and enthalpies of fusion was studied with a commercial Mettler Toldeo DSC (822e or 823e units equipped by Huber TC125 series coolers). Approximately 10 mg of a sample was placed in the standard non-pinned aluminium pan of 40 µl volume. Pan and sample were weighted with a microbalance (Sartorius MSE3.6P-000-DM) with the standard uncertainty of $5 \cdot 10^{-6}$ g. For each substance a regime of measurement was chosen individually that depended

on the expected value of the fusion temperature or on the value of the same parameter found in the literature. The character of the regime was also determined by features of crystallization of each sample. In general, in the first DSC run each sample was heated with a rate 10 K·min^{-1} up to the value of temperature that was ~ 30-40 K higher than the melting temperature of studied substance. Then the sample was cooled down to be crystallized with the rate10 K·min^{-1}. Such procedure provided sufficient contact between the sample and the bottom of pan. The DSC experiments were repeated 5 times. The calibration of the DSC was checked with melting behaviour of reference indium, gallium, lead and octane samples. The twice standard deviation of the enthalpy of fusion in the test measurements for reference compound was ± 0.3 kJ·mol^{-1} and ± 0.3 K for the melting temperature. Uncertainties of the enthalpy of fusion values are expressed as expanded uncertainties (at a level of confidence of 0.95, k=2). They include uncertainties from fusion experiment and calibration. The transition temperatures were evaluated as the onset temperature of observed transition adjusted to the zero-heating rate.

Usually, thermochemical calculations are commonly performed at the reference temperature $T = 298.15$ K. The adjustment of $\Delta_{cr}^{l}H_{m}^{o}(T_{fus})$ was performed with help of the equation [27]:

$$\Delta_{cr}^{l}H_{m}^{o}(298.15\text{ K})/(\text{J·mol-1}) = \Delta_{cr}^{l}H_{m}^{o}(T_{fus}/K) - (\Delta_{cr}^{g}C_{p,m}^{o} - \Delta_{l}^{g}C_{p,m}^{o}) \times [(T_{fus}/K) - 298.15\text{ K}] \quad (11)$$

where $\Delta_{cr}^{g}C_{p,m}^{o}$ and $\Delta_{l}^{g}C_{p,m}^{o}$ were the difference of the molar heat capacities of a studied substance of the gas and the crystal or liquid phases respectively. With this adjustment, the molar enthalpies of fusion, $\Delta_{cr}^{l}H_{m}^{o}(298.15$ K$)$ were calculated. Uncertainties in the temperature adjustment of fusion enthalpy from T_{fus} to the reference temperature were estimated to account with 30 % to the total adjustment [28].

2.7. Heat capacity measurement

Heat capacities were measured by the differential scanning calorimetry (DSC) [8]. We useda Perkin Elmer DSC Pyris 1 calorimeter equipped with Huber TC100 series chiller. Each experimental protocol of heat capacity determination included the three equal iterations with an empty pan, a reference sample of sapphire and a sample of each researched compound. For each iteration there was an equal thermal program of study; for all steps of each measurement the same pan was used. In each iteration the sample was heated with the step of 50 K at heating rate of 10 K·min^{-1}. Before and after each scanning step sample was kept isothermally for two minutes. Inside each iteration the temperature range was divided into intervals of 50 K to heat samples and between them there was a shift of 25 K. Each step for all iterations was repeated 4 times.

The heat capacity was derived with the Perkin Elmer software and then subsequently with Excel software. The heat capacity determination technique was tested with a reference sample of benzoic acid by Parr Instrument Company. In the used temperature ranges the experimental values agreed with the reference values within ±1 %. The expanded uncertainty (k = 2) for the heat capacity measured by this method was thus estimated to be $0.02 \cdot C_{s,m}$. If any mass loss takes place during the measurement, it was accounted in calculation of average heat capacities.

2.8. Combustion calorimetry

Combustion calorimetry is a technique for obtaining enthalpies of formation of chemical compounds [29–31]. In the case where an organic substance comprises only carbon, hydrogen and oxygen atoms, the combustion reactions in the oxygen atmosphere can be written:

$$C_aH_b(\text{cr or liq}) + \left(a + \frac{b}{4}\right)O_2 \xrightarrow{\Delta_cH_m^o} aCO_2(g) + \frac{b}{2}H_2O(\text{liq}) \tag{12}$$

$$C_aH_bO_c(\text{cr or liq}) + \left(a + \frac{b}{4} - \frac{c}{2}\right)O_2 \xrightarrow{\Delta_cH_m^o} aCO_2(g) + \frac{b}{2}H_2O(\text{liq}) \tag{13}$$
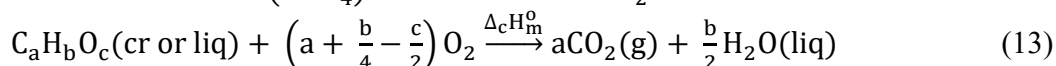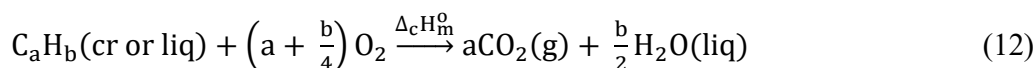
If an organic compound contains also nitrogen, the relevant combustion reactions will look like:

$$C_aH_bN_d(\text{cr or liq}) + \left(a + \frac{b}{4}\right)O_2 \xrightarrow{\Delta_cH_m^o} aCO_2(g) + \frac{b}{2}H_2O(\text{liq}) + \frac{d}{2}N_2(g) \tag{14}$$

$$C_aH_bO_cN_d(\text{cr or liq}) + \left(a + \frac{b}{4} - \frac{c}{2}\right)O_2 \xrightarrow{\Delta_cH_m^o} aCO_2(g) + \frac{b}{2}H_2O(\text{liq}) + \frac{d}{2}N_2(g) \tag{15}$$
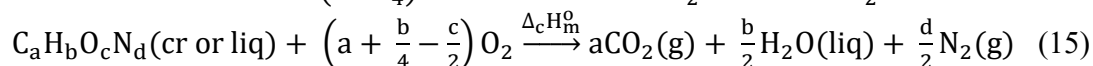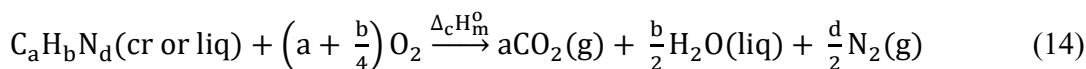
In each case the enthalpy of formation of the studied substance can be obtained from the enthalpy of combustion reaction, $\Delta_cH_m^o$, and the enthalpies of formation of CO_2 and H_2O, $\Delta_fH_m^o(CO_2, g)$ and $\Delta_fH_m^o(H_2O, \text{liq})$ which are -393.51 kJ/mol and -285.83 kJ/mol thereafter and recommended by CODATA committee [32,33].

For the determination of all enthalpies of formation an isoperibol static bomb combustion calorimeter was used; the scheme of the isoperibol static bomb combustion calorimeter is shown in the Figure 4. In all experiments, a stainless steel bomb with an internal volume 320 ml was used. A sample of an investigated compound was pelleted if the substance was a crystal or sealed in a polyethylene ampoule which is characterized by the empirical formula $CH_{1.93}$ if the substance was liquid. If the purity of a studied substance was less than 99.9%, the substance was purified by the sublimation in vacuum. Each sample was placed in two platinum crucibles sticked one into another. Each crucible has been treated with the flame of a gas burner to remove all traces of organic substances. A platinum wire of diameter 0,05 mm (Heraeus) was fixed between the ignition electrodes located on the basement part of the bomb. To connect the sample to the wire, a cotton thread of empirical formula $CH_{1.774}O_{0.887}$ was used. The masses of the crucibles, cotton thread, polythene ampule and sample were measured to an accuracy of $\pm 10^{-6}$ g using a Mettler Toledo balance (Mettler AT21 Comparator). About 1 ml of distilled and deionized water was

added to the basement part of the bomb (Figure 5), the exact mass of this amount of water was measured with the application of a Sartorius (Sartorius Fast Factory Special Version 4-21-5904) balance.
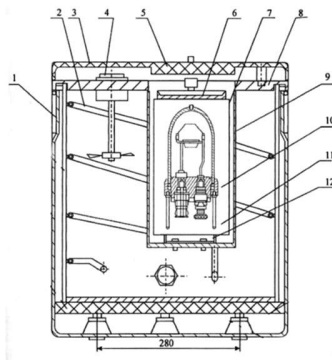
Figure 4. Static bomb combustion calorimeter:1 – thermostat inner wall, 2 – heater for the initial temperature adjustment, 3 – external wall, 4 – synchronous motor, 5 – lid of calorimetry cell, 6 – lid of calorimetry vessel, 7 – calorimetry vessel, 8 – lid of the thermostat, 9 – calorimetric cell, 10 – static stainless steel bomb, 11 – basis of the bomb, 12 – fixing of the calorimetry cell.

Figure 5. Placement of a sample in the central part of the bomb.

The stainless steel bomb was assembled and then purged three times by charging it with oxygen at a pressure of 1.01 MPa to remove the atmosphere nitrogen from the bomb. After the purging, the bomb was charged with oxygen at a pressure of 3.04 MPa and transferred to the interior of the calorimeter proper, which was then filled (on average) with 3030 g of distilled water; the bomb was electrically connected with the calorimeter proper with 2 cables. The calorimeter proper was closed and placed in the thermostat jacket of the combustion calorimeter, the temperature of which was kept at ~ 301 K; the electrical connections of the firing circuit were attached to the bomb head through calorimeter proper electrical port. The duration of the pre-, main and post periods was approximately 30 minutes each one.

The combustion of the sample was initiated at the end of the previous period by discharging a capacitor through the platinum wire. After the end of the after period, experimental data were read and stored with combustion calorimeter software in a personal computer for subsequent treatment. The bomb was removed from the calorimeter proper and then slowly discharged until atmospheric pressure was reached. If soot was detected on the surface of the crucible, the mass of the soot was measured gravimetrically and taken into account in the treatment of the results; for this purpose, the crucibles were dried in an oven at 403 K for 30 minutes, then cooled, and the soot mass was determined as the difference between the current mass of the crucibles and their initial mass determined before the experiment. The sample masses were reduced to vacuum, taking into

consideration the density values; the values of the densities were taken from the literature or the SciFinder database [34]. The atomic weights used were those recommended by the IUPAC commission [35].

The inside of a cap of the bomb and the surface of the basement part of the bomb were washed with distilled and deionized water, which was further collected to detect an amount of nitric acid formed from traces of atmospheric N_2 remaining in the bomb or from the nitrogen being a part of the investigated compound by titration with 0.1 mol·dm^{-3} NaOH (aq) using methyl red as an indicator. To avoid the presence of other types of nitrous acids, the collected water was heated to complete the oxidation of any nitrous acids to nitric acid. The detected amount of nitric acid was taken to correct the result of the experiment.

The energy equivalent of the calorimeter, ε_{calor}, was obtained from combustion calorimetry experiments with benzoic acid samples (sample SRM 39j, Parr Instrument, Parr Lot Code # 05791) whose massic combustion energy under the certificate conditions was $\Delta_c u^o$(sample SRM 39i, Parr Instrument) $= -26\ 454 \pm 12$ J·g^{-1}. At least 10 experiments were carried out to obtain the value of the energy equivalent. For any changes in the design of the combustion calorimeter, the permanence of the energy equivalent was checked with the same type of experiments with the benzoic acid samples.

For any chemical reaction the enthalpy of reaction is defined according to Hess´s Law as the sum of enthalpies of formation of all products minus the sum of enthalpies of formation of all reagents:

$$\Delta_r H_m^o = \sum \Delta_f H_m^o (\text{products}) - \sum \Delta_f H_m^o (\text{reagents}) \tag{16}$$

Because combustion calorimetry experiments take place at constant volume conditions, and consequently the heat of the combustion reactions, q, is equivalent to alteration of the internal energy, $\Delta_c U$, at pressure, p, and temperature, T:

$$q = \Delta_c U = U(\text{products}, p, T) - U(\text{reagents}, p, T) \tag{17}$$

As the result of the treatment of experimental data with the combustion calorimeter software the value of the internal energy of combustion is obtained, $\Delta_c U$. To transform it into the molar enthalpy of formation of the studied substance in the case of the reaction X as an example it should be transferred into the standard molar internal energy of combustion $\Delta_c U_m^o$:

$$\Delta_c U_m^o = \Delta_c U \cdot M(C_a H_b) \tag{18}$$

where M – molar mass of the studied substance $C_a H_b$. Further the standard molar enthalpy of the combustion reaction is calculated according to the following equation:

$$\Delta_c H_m^o = \Delta_c U_m^o + RT \cdot \Delta n \tag{19}$$

where $R = 8.31446 \ \text{J·K}^{-1}\text{·mol}^{-1}$ is the molar gas constant, T is a reference temperature that is equal to 298.15 K and Δn is an alteration of gas phase amount between products and reagents of the reaction X that is calculated as $\Delta n = n(CO_2) - n(O_2) = a - \left(a + \frac{b}{4}\right) = -\frac{b}{4}$. Further, because the enthalpies of formation of products of reaction (X), water and CO_2, are well defined, the value of the standard molar enthalpy of formation of the substance C_aH_b can be derived as:

$$\Delta_f H_m^o(C_aH_b) = a \cdot \Delta_f H_m^o(CO_2, \text{gas}) + \frac{b}{2} \cdot \Delta_f H_m^o(H_2O, \text{liq}) - \Delta_c H_m^o \tag{20}$$

2.9. Quantum-chemical calculations

The structure of the most stable conformers was found in the ADF program [36] with the methods M06L/TZ2P and M06/QZ4P based on the Slater Cartesian functions. The convergence of energy was better than 10^{-6} a.u. and for the gradients (forces) not more than 10^{-6} a.u./Å. The fundamental harmonic frequencies were obtained using M06L/TZ2P and corrected to anharmonic using a cubic polynomial. For this we found the harmonic frequencies of benzoquinone and methyl-benzoquinone [37] according to the M06L/TZ2P method, which contain a similar amount of atoms and well-established spectra, and the parameters of the third degree approximation polynomial were calculated based on the total set of frequencies available for the two molecules compared to the experimental values.

The harmonic and anharmonic frequencies of the most stable conformers were used to determine the zero point of energy and temperature contributions to enthalpy for M06/QZ4P in the "rigid rotator - anharmonic oscillator" (RRAO) approximation. Enthalpies H_{298} of the most stable conformers for each isomer were calculated by using the G3MP2, G4MP2, and G4 methods. The H_{298}-values have been converted to the standard molar enthalpies of formation $\Delta_f H_m^o(\text{g}, 298.15 \text{ K})_{\text{theor}}$ using the atomization or well-balanced reactions.

3. Results and Discussions

Chapter 1 Thermochemistry of disubstituted benzenes: ortho-, meta-, and para-substituted acetophenones with methyl, ethyl, cyano, and acetoxy substituents

1.1. Introduction

Structure-property relationships are one of the basic principles of organic and physical chemistry. Substituted benzenes are a remarkable model for the manifestation of structure – property relationships. The type and position of substituents on benzene ring significantly influences the physico-chemical properties of the compound and the appropriate chemical, physical or biological effect. The quantification of these relationships in series of substituted benzenes has been a longstanding goal of our laboratory [25,38–41]. The aim of the research is therefore to continue this research on series of acetophenones substituted with the methyl, ethyl, cyano and acetoxy groups shown in Figure 6.
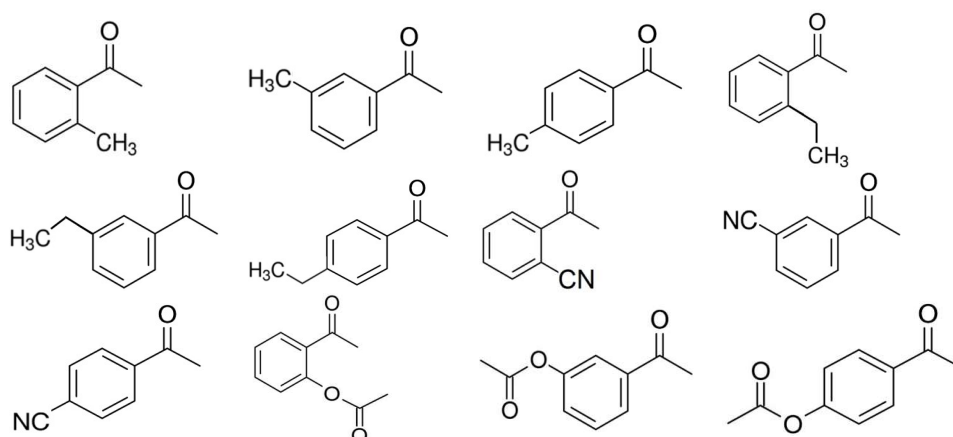
Figure 6. The studied substituted acetophenones.

The fundamental properties of these substituted benzenes such as enthalpies of formation, vapour pressures and enthalpies of phase transitions (sublimation, vaporization, and fusion) available in the literature and new experimental results were evaluated and checked for internal consistency with the help of complementary experiments, empirical and the high level quantum-chemical calculations. The consistent enthalpic data sets for disubstituted benzenes were analysed using a "centerpiece" group-contribution approach [25,38–41] in order to quantify energetics of substituent interactions on the benzene ring.

1.2. Results and discussion

1.2.1. Vapor pressures of substituted acetophenones

The absolute vapor pressures for methyl- and cyano-acetophenones are given in Table A.2. Absolute vapor pressures values of 2-methyl-acetophenone, 3-methyl-acetophenone, 2-cyano-acetophenone, 3-cyano-acetophenone and 4-cyano-acetophenone were measured for the first time. Temperature dependences of available vapor pressures for 4-methyl-acetophenone are shown in Figure A.1. The agreement of our transpiration results with those from the Knudsen method [42] is poor. It should be noted that the Knudsen method is normally used for measurements of very low pressures (usually below 1 Pa) over the solid samples. As a consequence, the disagreement observed could be attributed to the limitations specific for the Knudsen method. Vapor pressures derived for 4-methylacetophenone from the Antoine coefficients given in the compilation by Stephenson and Malanowski [43] are also questionable as neither the method nor the purity of the sample are available.

The limited data on vapour pressures of ethyl-substituted acetophenones prompted to collect experimental boiling temperatures at different pressures compiled by SciFinder [34]. The accuracy of this data is questionable as it comes from the distillation of a compound after its synthesis and not from special physico-chemical studies. However, the numerous data on boiling temperatures at standard pressure, as well as at reduced pressures (Table A.3) provide at least a reliable level of the experimental vapour pressures and a reliable trend of the dependence of the vapour pressure temperature. For example, in Figure A.2 for 2-ethylacetophenone the boiling points at different pressures compiled by SciFinder are in fair agreement with the available data set [43]. In this work for the sake of comparison, the data available in SciFinder for ethyl-acetophenones were systematically collected (Table A.3. and Figures A.2. – A.4). The comparisons of these results with those available from the literature are shown in Figure A. 2 - Figure A. 4. From these comparisons it was found that the static method results by Khorevskaya et al. [44] for 3-ethyl- and 4-ethylacetophenone are mistakable.

1.2.2. Vaporization/sublimation thermodynamics of substituted acetophenones

The compilation of the standard molar enthalpies of vaporization of substituted acetophenones at the reference temperature $T = 298.15$ K, calculated according to Equations 2 and 8 is given in Table 1.

Table 1. Compilation of data on enthalpies of vaporization $\Delta_l^g H_m^o$ and enthalpies of sublimation $\Delta_{cr}^g H_m^o$ derived acetophenones measuring in this work and from the data available in the literature.

Compound, CAS	Method[a]	T- range	$\Delta_{l,cr}^g H_m^o$ (T_{av})	$\Delta_{l,cr}^g H_m^o$ (298.15 K)	Ref.
		K	kJ·mol⁻¹	kJ·mol⁻¹	
2-methylacetophenone (liq)	C	339	65.7±0.2	58.9±0.9	[45]
577-16-2	T	293.3-332.7	58.6±0.3	59.3±0.4	this work
	T_b			59.5±1.5	Table 2
	J_x			58.8±0.7	Table 3
				59.2±0.3	*average*
3-methylacetophenone (liq)	T	285.5-334.0	59.0±0.3	59.8±0.4	this work
585-74-0	T_b			60.8±1.5	Table 2
	J_x			60.2±0.7	Table 3
				59.9±0.3	*average*
4-methylacetophenone (liq)	K	291.0-313.6	59.3±1.7	59.5±1.8	[42]
122-00-9	n/a	288-333	59.5±	60.4±1.6	[43]
	C	339	67.5±0.3	60.7±1.0	[45]
	T	302.6-354.2	59.6±0.2	61.6±0.3	this work
	T_b			62.2±1.5	Table 2
	J_x			61.6±0.7	Table 3
				61.5±0.3	*average*
2-ethylacetophenone (liq)	n/a	363-397	52.8±1.0	59.4±1.2	[43]
2142-64-5	SF	357.2-391.2	54.5±2.1	60.6±2.2	Table A.3
	T_b			63.4±1.5	Table 2
	J_x			63.3±0.7	Table 3
				62.3±0.5	*average*
3-ethylacetophenone (liq)	S	292.3-416.2	23.7±0.5	(27.7±0.6)	[44]
22699-70-3	SF	386.2-514.2	52.1±1.5	63.9±1.7	Table A.3
	T_b			65.5±1.5	Table 2
	J_x			64.7±0.7	Table 3
				64.7±0.6	*average*
4-ethylacetophenone (liq)	S	294.6-367.2	40.4±0.3	(42.9±0.4)	[44]
937-30-4	SF	367.2-518.2	54.7±0.8	65.7±1.1	Table A.3
	T_b			66.3±1.5	Table 2
	J_x			66.8±0.7	Table 3
				66.4±0.6	*average*
2-cyanoacetophenone (liq)	T	322.9-372.4	69.3±0.3	**72.9±0.4**	this work
91054-33-0					
2-cyanoacetophenone (cr)				**86.6±0.5**	Table 4
3-cyanoacetophenone (cr)	C	360.1	105.5±0.5	94.7±1.5	[46]
6136-68-1	T	318.4-362.3	95.8±0.4	97.1±0.6	this work
				96.8±0.6	*average*
3-cyanoacetophenone (liq)				74.5±1.6	Table 4
4-cyanoacetophenone (cr)	T	303.2-331.1	87.1±0.4	87.7±0.7	this work
4-cyanoacetophenone (liq)	T	333.2-369.2	68.2±0.2	72.1±0.4	this work
1443-80-7				71.8±1.6	Table 4
				72.0±0.5	*average*
2-acetoxyacetophenone (cr)	S	313.0-356.5	103.1±0.1	104.4±0.5	[47]
7250-94-4	K	298.0-321.3	104.3±0.4	104.7±0.8	[47]
				104.5±0.4	*average*
2-acetoxyacetophenone (liq)	S	344.7-398.0	68.6±0.1	75.0±0.4	[47]
				75.5±1.4	Table 4
				75.1±0.4	*average*
3-acetoxyacetophenone (cr II)	K	297.7-307.7	100.4±1.1	**100.5±1.9**	[47]
3-acetoxyacetophenone (liq)	S	305.1-368.5	75.6±0.1	78.9±0.3	[47]
2454-35-5				77.2±3.9	Table 4

				78.8±1.0	*average*
4-acetoxyacetophenone (cr II)	K	298.1-309.3	99.4±0.5	**99.6±1.5**	[47]
4-acetoxyacetophenone (cr I)	S	315.0-323.9	98.5±0.6	99.3±2.0	[47]
4-acetoxyacetophenone (liq)	S	328.9-378.3	74.3±0.1	79.1±0.4	[47]
13031-43-1				79.6±3.1	Table 4
				79.1±1.0	*average*

[a] Methods: T = transpiration; K = Knudsen effusion method; C = Calvet calorimetry; n/a – not available; S = static method; SF = from experimental boiling temperatures reported at different pressures compiled by SciFinder [34]; T_b – estimation based on use of normal boiling temperatures; J_x – correlation gas chromatography.

Our result for 2-methylacetophenone $\Delta_l^g H_m^o(298.15 \text{ K}) = 59.3\pm0.4 \text{ kJ·mol}^{-1}$ agrees well with the value $\Delta_l^g H_m^o(298.15 \text{ K}) = 58.9\pm0.9 \text{ kJ·mol}^{-1}$, directly measured with Calvet calorimetry [45]. The enthalpy of vaporization for 4-methylacetophenone, $\Delta_l^g H_m^o(298.15 \text{ K}) = 60.7\pm1.0 \text{ kJ·mol}^{-1}$, directly measured by Calvet calorimetry [45] and the values derived from the vapor pressures temperature dependences [42,43] are in very good agreement (Table 2). The enthalpy of sublimation $\Delta_{cr}^g H_m^o(298.15 \text{ K}) = 97.1\pm0.6 \text{ kJ·mol}^{-1}$ of 3-cyano-acetophenone measured in this work by the transpiration method is in agreement with the is $\Delta_{cr}^g H_m^o(298.15 \text{ K}) = 94.7\pm1.5 \text{ kJ·mol}^{-1}$ measured with a Calvet calorimeter [46].

Vapor pressures over the liquid and crystalline samples of 2-acetoxy-, 3-acetoxy, and 4-acetoxy-acetophenones, were systematically studied by combination of the static and Knudsen methods [47]. These experimental vapor pressures were approximated by Equation 2 and calculated the vaporization and sublimation enthalpies and entropies according to Equations 8 and 9 with the heat capacity differences given in Table A.1. As it can be seen from Table 1, the liquid-gas and the crystal-gas phase transition for all three isomers are very consistent and these values can be recommended for thermochemical calculations.

1.2.3. Validation of experimental vaporization enthalpies

The limited amount of data on enthalpies of vaporization for substituted acetophenones and the inconsistency of vapor pressures observed for ethyl-acetophenones have prompted the search for additional methods to validate our new transpiration results.

1.2.3.1. Validation with help of the normal boiling temperatures

As with other series of investigated compounds, it was decided to validate our transpiration results with the correlation between boiling temperatures and their enthalpies of vaporization. The available literature data on the normal boiling temperatures, T_b, for substituted acetophenones [48] and [34] were used for correlation with the $\Delta_l^g H_m^o(298.15 \text{ K})$-values measured in this work (Table 2). For the set of substituted benzenes (Table 2) the linear correlation is the following:

$$\Delta_l^g H_m^o(298.15 \text{ K}) /(\text{kJ·mol}^{-1}) = -47.6 + 0.2199 \times T_b \qquad \text{with } (R^2 = 0.966) \qquad (21)$$

As it can be seen from Table 2, the results calculated from this correlation with the boiling temperatures agree well within the uncertainties with the values obtained by the transpiration method. Such good agreement can be considered as a successful way of validation of the experimental data on the $\Delta_l^g H_m^o$(298.15 K) measured in this work using the transpiration method (Table A. 2). From Table 2 it can be seen that differences between experimental and calculated according to Equation 21 values are mostly below 2 kJ·mol^{-1}. Consequently, the uncertainties of the enthalpies of vaporization, which are estimated from the correlation $\Delta_l^g H_m^o$(298.15 K) – T_b, are assessed to be at the level of ±1.5 kJ·mol^{-1}. The Equation 21 was used to calculate the questionable enthalpies of vaporization of isomeric ethyl-acetophenones (Table 2). The latter values were denoted by a symbol T_b and shown in Table 1 for comparison with values obtained by other methods.

Table 2. Correlation of vaporization enthalpies $\Delta_l^g H_m^o$(298.15 K) of substituted acetophenones with their T_b normal boiling temperatures.

CAS	Compound	T_b [b]	$\Delta_l^g H_m^o$(298.15 K)$_{exp}$	$\Delta_l^g H_m^o$(298.15 K)$_{calc}$ [b]	Δ
		K	kJ·mol^{-1}	kJ·mol^{-1}	kJ·mol^{-1}
108-88-3	toluene	384	38.1±0.2 [49]	36.8	1.3
100-41-4	ethylbenzene	409	42.3±0.2 [49]	42.4	-0.1
98-86-2	acetophenone	475	55.4±0.3 [50]	56.9	-1.5
577-16-2	2-methylacetophenone	487	59.2±0.2 [c]	59.5	-0.3
585-74-0	3-methylacetophenone	493	59.8±0.2 [c]	60.8	-1.0
122-00-9	4-methylacetophenone	499	61.4±0.2 [c]	62.2	-0.8
2142-64-5	2-ethylacetophenone	505	-	63.4	
22699-70-3	3-ethylacetophenone	514	-	65.5	
937-30-4	4-ethylacetophenone	518	-	66.3	
93-55-0	1-phenyl-1-propanone	491	60.9±0.8 [51]	60.3	0.6
103-79-7	1-phenyl-2-propanone	490	57.7±0.3 [52]	60.1	-2.4
15764-15-5	2,3,5-trimethylacetophenone	521	70.9±0.7 [53]	66.9	4.0

[a] Normal boiling temperatures are from [48] and [34], [b] Calculated using Equation 21, [c] Experimental data measured by using the transpiration method Table A. 2).

1.2.3.2. Validation with Kovats´s retention indices

Another method that has been used to validate the experimental results is the application of Kovats´s retention indices. The literature data available on the Kovats´s retention indices, J_x, for substituted benzenes [54] were taken for correlation with the $\Delta_l^g H_m^o$(298.15 K)-values measured in this work (Table A. 2). Results from this correlation are given in Table 3.

It is known that the $\Delta_l^g H_m^o$(298.15 K)-values correlate linearly with Kovats´s indices in various homologous series of alkylbenzenes, alkanes, aliphatic ethers, alcohols, or in a series of structurally similar compounds [50]. As it was anticipated, the $\Delta_l^g H_m^o$(298.15 K)-values correlated

linearly with J_x values for the structurally parent sets of substituted benzenes collected in Table 4. For these J_x - $\Delta_l^g H_m^o$(298.15 K) correlation the same set of substituted benzenes and acetophenones as we used for the T_b-correlation was taken. For this set of Kovats´s indices (Table 3), the following linear correlation was obtained:

$$\Delta_l^g H_m^o(298.15 \text{ K}) \text{ /(kJ·mol}^{-1}) = -5.7 + 0.0582 \times J_x \quad \text{with } (R^2 = 0.989) \tag{22}$$

Table 3. Correlation of vaporization enthalpies, $\Delta_l^g H_m^o$(298.15 K), of substituted acetophenones with their Kovats´s indices (J_x).

CAS	Compound	J_x [a]	$\Delta_l^g H_m^o$(298.15 K)$_{exp}$ kJ·mol^{-1}	$\Delta_l^g H_m^o$(298.15 K)$_{calc}$[b] kJ·mol^{-1}	Δ kJ·mol^{-1}
71-43-2	benzene	670	33.9±0.2 [49]	33.3	0.6
108-88-3	toluene	750	38.1±0.2 [49]	38.0	0.1
100-41-4	ethylbenzene	840	42.3±0.2 [49]	43.2	-0.9
	acetophenone	1050	55.4±0.3 [50]	55.4	0.0
577-16-2	2-methylacetophenone	1108	59.3±0.4 [c]	58.8	0.4
585-74-0	3-methylacetophenone	1132	59.8±0.4 [c]	60.2	-0.4
122-00-9	4-methylacetophenone	1156	61.6±0.3 [c]	61.6	-0.2
2142-64-5	2-ethylacetophenone	1186	-	63.3	
22699-70-3	3-ethylacetophenone	1210	-	64.7	
937-30-4	4-ethylacetophenone	1245	-	66.8	
93-55-0	1-phenyl-1-propanone	1140	60.9±0.8 [51]	60.6	0.3
103-79-7	1-phenyl-2-propanone	1091	57.7±0.3 [52]	57.8	-0.1
15764-15-5	2,3,5-trimethyl-acetophenone	1312	70.9±0.7 [53]	70.7	0.2

[a] Kovats´s indices, J_x, [55], [b] Calculated using Equation 22, [c] from Figure A. 5. Typical thermogram of 4-methylacetophenone.

The results of the correlations with the Kovats´s indices agree perfectly with the values obtained with the transpiration method (Table 1 and Table A.2.). Such good agreement can be regarded as an additional method to validate the experimental data measured in this work using the transpiration method. From Table 3 it is clear that the differences between the experimental values and the values according to Equation 22 are mainly below 1 kJ·mol^{-1}. Therefore, the uncertainties of the enthalpies of vaporization, which are estimated from the correlation $\Delta_l^g H_m^o$(298.15 K) - J_x are evaluated within ± 0.7 kJ·mol^{-1}. We also used Equation 22 to calculate the questionable enthalpies of vaporization of isomeric ethyl-acetophenones (Table 3). The latter values were denoted by a symbol J_x and shown in Table 1 for comparison with values obtained by other methods.

1.2.3.3. Consistency of solid-liquid, solid-gas, and liquid-gas phase transitions

All cyano-acetophenones and all acetoxy-acetophenones are solids at room temperatures. We have collected in Table 4 the solid-liquid and solid-solid phase transition data available for these compounds.

Table 4. Thermodynamics of phase transitions of substituted acetophenones (in kJ·mol^{-1}).

Compound	T_{fus}/K	$\Delta_{\text{cr}}^{\text{l}}H_{\text{m}}^{\text{o}}$	$\Delta_{\text{cr}}^{\text{l}}H_{\text{m}}^{\text{o}}$ [a]	$\Delta_{\text{cr}}^{\text{g}}H_{\text{m}}^{\text{o}}$	$\Delta_{\text{l}}^{\text{g}}H_{\text{m}}^{\text{o}}$ [d]
		at T_{fus}	298.15 K		
1	2	3	4	5	6
4-methylacetophenone	251.8±0.1	14.3±0.1	12.3±0.3	73.8±0.5	61.5±0.3
2-cyanoacetophenone	322.4±0.1	14.8±0.1	13.7±0.3	86.6±0.9	72.9±0.4
3-cyanoacetophenone	370.4±0.1	25.6±0.1	22.3±1.0	96.8±1.2	74.5±1.6
4-cyanoacetophenone	331.6±0.1	17.4±0.1	15.9±0.4	87.7±1.4	71.8±1.5
2-acetoxyacetophenone	361.8±0.1	32.3±0.4 [47]	29.0±1.1	104.5±0.8	75.5±1.4
3-acetoxyacetophenone(cr II)	316.2±0.3	24.2±0.6 [47][b]	23.3±0.9	100.5±3.8	77.2±3.9
4-acetoxyacetophenone (cr II)	324.1±0.5	21.4±0.5 [47][c]	20.0±0.6	99.6±3.0	79.6±3.1

[a] adjusted to 298.15 K according to Equation 23, [b] Calculated according to [56] as the sum of phase transition [47] and enthalpy of fusion [47] at T_{fus} and adjusted to the reference temperature with Equation 23, [c] Calculated according to [56] as the sum of phase transition [47] and enthalpy of fusion [47] at T_{fus} and adjusted to the reference temperature with of Equation 23.

The enthalpy of fusion of 4-methylacetophenone $\Delta_{\text{cr}}^{\text{l}}H_{\text{m}}^{\text{o}}(T_{\text{fus}})$ = 14.3±0.1 kJ·mol^{-1} at T_{fus} = 251.8±0.1 K was measured for the first time. A typical DSC-thermogram of 4-methylacetophenone is shown in Figure A. The only available for comparison T_{fus} = 208.7 K [57] is significantly lower than the value we obtained. Taking into account the absence of purity attestation for the sample measured in [57] our result for the sample of 4-methylacetophenone, which was carefully purified by fractional sublimation and appears to be more reliable due to a purity of 99.1 ± 0.1%.

The enthalpies of fusion and melting temperatures of 2-, 3- and 4-cyanoacetophenone (Table 4) were measured for the first time. The enthalpies of fusion and melting temperatures of 2-, 3- and 4-acetoxyacetophenone (Table 4) were taken from the literature [47].

According to the common practice of thermochemistry, the experimental fusion enthalpies have to be adjusted to the reference temperature T = 298.15 K using Equation 23 [58]:

$$\Delta_{\text{cr}}^{\text{l}}H_{\text{m}}^{\text{o}}(298.15 \text{ K})/(\text{J·mol}^{-1}) = \Delta_{\text{cr}}^{\text{l}}H_{\text{m}}^{\text{o}}(T_{\text{fus}}/\text{K}) - (\Delta_{\text{cr}}^{\text{g}}C_{p,\text{m}}^{\text{o}} - \Delta_{\text{l}}^{\text{g}}C_{p,\text{m}}^{\text{o}}) \times [(T_{\text{fus}}/\text{K}) - 298.15 \text{ K}] \quad (23)$$

The values of $\Delta_{\text{cr}}^{\text{g}}C_{p,\text{m}}^{\text{o}}$ and $\Delta_{\text{l}}^{\text{g}}C_{p,\text{m}}^{\text{o}}$ are listed in Table A. 1. The standard molar enthalpies of fusion, $\Delta_{\text{cr}}^{\text{l}}H_{m}^{\text{o}}(298.15 \text{ K})$, calculated according to Equation 23 are given in Table 4. These values can now be used to establish consistency of the solid-gas and liquid-gas phase transitions for cyano-acetophenones and acetoxy-acetophenones collected in Table 1 as follows. The values of the enthalpies of vaporization, fusion and sublimation are generally linked with Equation 24:

$$\Delta_l^g H_m^o(298.15 \text{ K}) = \Delta_{cr}^g H_m^o(298.15 \text{ K}) - \Delta_{cr}^l H_m^o(298.15 \text{ K}) \qquad (24)$$

where all enthalpies are adjusted to the common reference temperature $T = 298.15$ K.

For example, the vapor pressures of 4-cyano-acetophenone was deliberately measured below and above the melting temperature using the transpiration method (Table A. 2). The sublimation enthalpy $\Delta_{cr}^g H_m^o(298.15 \text{ K}) = 87.7 \pm 0.7$ kJ·mol^{-1} and the vaporization enthalpy $\Delta_l^g H_m^o(298.15 \text{ K}) = 72.1 \pm 0.4$ kJ·mol^{-1} of 4-cyano-acetophenone are given in Table 1. According to Equation 24 and with help of fusion enthalpy $\Delta_{cr}^l H_m^o(298.15 \text{ K}) = 15.9 \pm 0.4$ kJ·mol^{-1}, the "theoretical" vaporization enthalpy of 4-cyano-acetophenone was estimated as $\Delta_l^g H_m^o(298.15 \text{ K})$ = 87.7 - 15.9 = 71.8 $\pm$ 0.5 kJ·mol^{-1}. The latter value is in excellent agreement with the experiment, proving consistency of phase transition data for this compound. In the similar way, the consistency of data for other cyano-acetophenones and acetoxy-acetophenones was established (calculations in Table 4 and the final values in Table 1).

1.2.3.4. Evaluation of available vaporization enthalpies

In order to ascertain information on vaporization thermodynamics of alkyl-substituted acetophenones, three empirical methods ($\Delta_l^g H_m^o(298.15 \text{ K})$ - T_b correlation), ($\Delta_l^g H_m^o(298.15 \text{ K})$ - J_x correlation) and consistency of phase transitions were applied. The *experimental* and "*theoretical*" vaporization enthalpies derived for each set of substituted acetophenones are given in Table 1. From this table it is clear that for each substituted acetophenone agreement among available $\Delta_l^g H_m^o(298.15 \text{ K})$-values and $\Delta_{cr}^g H_m^o(298.15 \text{ K})$-values, derived in different ways are all within the assigned error bars. To get more confidence and reliability, the weighted average (the uncertainty was used as a weighing factor) for each substituted acetophenone given in Table 1 were calculated. These values are highlighted in bold and are recommended for thermochemical calculations and the general quantitative analysis of the results. For example, in our previous works [29,59–64] it was found that *meta*- and *para*-disubstituted benzenes have similar values of the enthalpies of vaporization. For *ortho*-disubstituted benzenes, they usually differ from those for *meta*- and *para*-disubstituted species. The size of the differences depends on the nature of the substituents. The general trend, however, is that the enthalpies of vaporization of the *ortho*-species are somewhat lower compared to *meta*- and *para*-substitution. The enthalpies of vaporization of methyl, ethyl, cyano and acetoxyacetophenones follow this general trend (Table 1) and confirm the consistency of the data evaluated.

1.2.4. Standard molar enthalpies of formation

A few number of data on substituted acetophenones are available in the literature. The standard molar enthalpies of formation, $\Delta_f H_m^o(298.15)$, of 2-methyl- and 4-methylacetophenone are measured by Amaral *et al.* [45] by the static bomb combustion calorimetry. Later, the standard molar enthalpy of formation of 3-cyanoacetophenone was measured in the same laboratory [46]. The numerical data available are summarized in Table 5.

Table 5. Thermochemical data at T = 298.15 K (p° = 0.1 MPa) (in kJ·mol⁻¹).

compound	$\Delta_f H_m^o$(l or cr)	$\Delta_{l,cr}^g H_m^o$	$\Delta_f H_m^o(g)_{exp}$	$\Delta_f H_m^o(g)_{ther}$
1	2	3	4	5
2-methylacetophenone (liq)	-174.6±2.2 [45]	59.2±0.6	-115.4±2.3	-110.7±2.6
3-methylacetophenone (liq)		59.9±0.6		-120.1±2.6
4-methylacetophenone (liq)	-183.3±2.2 [45]	61.5±0.6	-121.8±2.3	-120.8±2.6
2-cyanoacetophenone (cr)		86.6±0.9		60.3±2.6
3-cyanoacetophenone (cr)	-42.3±1.5 [46]	96.8±1.2	54.5±1.9	50.4±2.6
4-cyanoacetophenone (cr)		87.7±1.4		50.0±2.6
2-acetoxyacetophenone (cr)		104.5±0.8		-435.4±2.6
3-acetoxyacetophenone (cr II)		100.5±3.8		-444.9±2.6
4-acetoxyacetophenone (cr II)		99.6±3.0		-445.1±2.6

In order to compensate for the lack of enthalpic data, the molar gas-phase enthalpies of formation for methyl, ethyl, cyano and acetoxysubstituted acetophenones were calculated using a high-level quantum chemical methods. The H_{298} enthalpies of the most stable conformers of substituted acetophenones estimated by the composite methods were converted into the *theoretical* enthalpies of formation using the *experimental* gas phase standard molar enthalpies of formation $\Delta_f H_m^o$(g, 298.15 K) of benzene, toluene, ethylbenzene, cyanobenzene, acetoxybenzene, and acetophenone (Table A. 4) using the following well-balanced reactions:

$$x\text{-}methyl\text{-}acetophenone + benzene = toluene + acetophenone \qquad (25)$$

$$x\text{-}ethyl\text{-}acetophenone + benzene = ethylbenzene + acetophenone \qquad (26)$$

$$x\text{-}cyano\text{-}acetophenone + benzene = cyanobenzene + acetophenone \qquad (27)$$

$$x\text{-}acetoxy\text{-}acetophenone + benzene = acetoxybenzene + acetophenone \qquad (28)$$
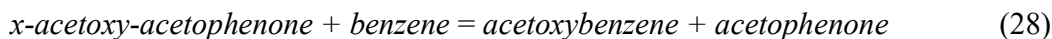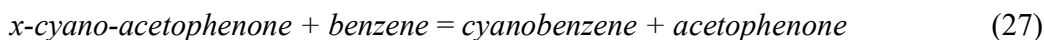
Theoretical gas phase enthalpies of the formation of substituted acetophenones are summarized in Table 6. In the last part of the research the G3MP2 and G4 methods for thermochemical calculations were applied. Using two methods simultaneously helps to avoid possible systematic errors caused by calculations. The *theoretical* values $\Delta_f H_m^o$(g, 298.15 K) as calculated by the G3MP2 and the G4 method are very close for each compound (Table 6). Therefore, we calculated the weighted average value for each substituted acetophenone in Table 6 and designated it as the *theoretical* values, $\Delta_f H_m^o$(g, 298.15 K)$_{theor}$, for comparison with the *experimental* values, $\Delta_f H_m^o$(g,

298.15 K)$_{exp}$, compiled in Table 5. Comparison of column 5 with column 4 in Table 5 shows good agreement (within the ascribed uncertainties) between the *theoretical* and *experimental* $\Delta_f H_m^o$(g, 298.15 K)-values for 2-methyl-acetophenone, 4-methyl-acetophenone and 3-cyano-acetophenone.

This good agreement can be considered as proof of the internal consistency of the thermochemical results evaluated in this work (Table 5). These results can now be recommended as reliable benchmark properties for further thermochemical calculations, *e.g.* of the liquid phase enthalpies of formation $\Delta_f H_m^o$(liq, 298.15 K) according to a general equation:

$$\Delta_f H_m^o(\text{liq, 298.15 K}) = \Delta_f H_m^o(\text{g, 298.15 K}) - \Delta_l^g H_m^o(\text{298.15 K}) \tag{29}$$

Table 6. Theoretical gas-phase enthalpies of formation at T = 298.15 K (p° = 0.1 MPa) for methyl, ethyl-, cyano- and acetoxysubstituted acetophenones calculated by using the G3MP2 and G4 methods (in kJ·mol^{-1}).

compound	$\Delta_f H_m^o$(g) $_{G3MP2}$	$\Delta_f H_m^o$(g)$_{G4}$	$\Delta_f H_m^o$(g)$_{theor}$
2-methylacetophenone	-109.7	-111.6	-110.7±2.6
3-methylacetophenone	-119.0	-120.9	-120.1±2.6
4-methylacetophenone	-119.7	-121.6	-120.8±2.6
2-ethylacetophenone	-	-130.9	-130.9±3.5
3-ethylacetophenone	-	-141.4	-141.4±3.5
4-ethylacetophenone	-	-141.9	-141.9±3.5
2-cyanoacetophenone	60.1	60.5	60.3±2.6
3-cyanoacetophenone	50.1	50.6	50.4±2.6
4-cyanoacetophenone	49.7	50.2	50.0±2.6
2-acetoxyacetophenone	-433.9	-436.6	-435.4±2.6
3-acetoxyacetophenone	-443.3	-446.1	-444.9±2.6
4-acetoxyacetophenone	-443.6	-446.3	-445.1±2.6

Table 7. Estimation of the liquid-phase enthalpies of formation $\Delta_f H_m^o$(liq) at T = 298.15 K (p° = 0.1 MPa) for substituted acetophenones (in kJ·mol^{-1}).

compound	$\Delta_f H_m^o$(g)$_{theor}$	$\Delta_l^g H_m^o$	$\Delta_f H_m^o$(liq)$_{theor}$	$\Delta_f H_m^o$(liq)$_{exp}$
2-methylacetophenone	-110.7±2.6	59.2±0.6	-169.9±2.7	-174.6±2.2 [45]
3-methylacetophenone	-120.1±2.6	59.8±0.6	-179.8±2.7	
4-methylacetophenone	-120.8±2.6	61.5±0.6	-182.1±2.7	-183.3±2.2 [45]
2-ethylacetophenone	-130.9±3.5	62.3±1.0	-193.2±3.6	
3-ethylacetophenone	-141.4±3.5	64.7±1.2	-206.1±3.7	
4-ethylacetophenone	-141.9±3.5	66.4±1.2	-208.3±3.7	
2-cyanoacetophenone	60.3±2.6	72.9±0.8	-12.6±2.7	
3-cyanoacetophenone	50.4±2.6	74.5±1.6	-24.1±3.1	-20.0±1.8 [46]
4-cyanoacetophenone	50.0±2.6	72.0±0.8	-22.0±2.7	
2-acetoxyacetophenone	-435.4±2.6	75.1±0.8	-510.3±2.7	
3-acetoxyacetophenone	-444.9±2.6	78.8±0.8	-523.5±2.7	
4-acetoxyacetophenone	-445.1±2.6	79.1±0.8	-524.1±2.7	

Indeed, the reliable *theoretical* enthalpies of formation $\Delta_f H_m^o$(g)$_{theor}$ given in Table 6 have compensated the lack of required for Equation 29 data. Together with the reliable enthalpies of

vaporization evaluated in Table 1, these results can therefore be used to calculate the *theoretical* liquid-phase enthalpies of formation (Table 7).

Comparison of column 5 with column 4 in Table 7 shows agreement (within the combined uncertainties) between the *theoretical* and *experimental* $\Delta_f H_m^o$(liq, 298.15 K)-values available for 2-methyl-acetophenone, 4-methyl-acetophenone, and 3-cyano-acetophenone. These results for the liquid phase enthalpies of formation of substituted acetophenones can therefore now be recommended for thermochemical calculations.

1.2.5. Development of a "centerpiece" group-contribution approach for substituted benzenes

The consistent sets of thermochemical data on $\Delta_l^g H_m^o$(298.15 K), $\Delta_f H_m^o$(g, 298.15 K), and $\Delta_f H_m^o$(liq, 298.15 K) evaluated in the research have been used for developing a "centerpiece" group contribution approach that is particularly suitable for aromatic compounds. The main idea of this approach is to select an appropriate "centerpiece" molecule (*e.g.* benzene or acetophenone or toluene, *etc.*) with reliable thermodynamic properties. Various substituents can be attached to the "centerpiece" in different positions on the benzene ring. The enthalpic contribution for each substituent is quantified from the differences between the enthalpy of the substituted benzene and the enthalpy of the benzene itself. Using this scheme, the contributions ΔH(H→CH_3), ΔH(H→C_2H_5), ΔH(H→$COCH_3$), ΔH(H→CN), and ΔH(H→$OCOCH_3$) were derived using the reliable thermochemical data for toluene, ethylbenzene, acetophenone, cyanobenzene, acetoxybenzene and benzene compiled in Table 8.

These enthalpic contributions ΔH(H→R) can be now applied to construct a framework of any desired substituted benzene arbitrary starting from the "centerpieces" namely acetophenone, or even starting from the benzene itself. In terms of energy, however, this framework is not complete, as the interactions between the substituents on the benzene ring are still missing.

The enthalpic contributions for mutual pairwise interactions of substituents are specific for the *ortho-*, *meta-* and *para-*positions of substituents placed in the benzene ring. The usual method for quantifying these interactions are reaction enthalpies, $\Delta_r H_m^o$(g or liq), according to Equation 25 to 28, written in reverse (*e.g.* for Equation 25 it is written as follows: *toluene + acetophenone = x-methylacetophenone + benzene*). This approach also applies to the estimation of contributions to the enthalpy of vaporization. The pairwise interactions for all three thermodynamic properties derived in this way are given in Table 8.

Quantitatively, the intensity of substituent interactions depends strongly on the type of *ortho-*, *meta-* or *para*-pairs. It is suggested to consider the strength of pairwise interaction in terms of $\Delta_f H_m^o$(g). From Table 8 it is clear that all *ortho*-substituted-benzenes exhibit a strong destabilization at the level of 10 - 15 kJ·mol^{-1} due to the sterical repulsions of bulky groups placed in the close proximity. Usually, the *meta-* and *para*-interactions of substituents on the benzene ring are less profound compared to *ortho*-interactions. This trend also applies to the interactions of the substituents examined in this work. The moderate stabilization or destabilization at the level from 2 to 5 kJ·mol^{-1} (Table 8.) is observed for the *meta-* and *para*-isomers. These effects can be explained by the specific electron density distribution within the substituted benzene ring. The pairwise interaction in terms of $\Delta_f H_m^o$(liq) follow the similar trends as for the gaseous species

Table 8. Parameters for calculation of thermodynamic properties of substituted acetophenones at 298.15 K (in kJ·mol^{-1}).

Contribution	$\Delta_l^g H_m^o$	$\Delta_f H_m^o$(g)	$\Delta_f H_m^o$(liq)
benzene	33.9 [49]	82.9[49]	49.0 [49]
ΔH(H→COCH₃	21.5	-170.0	-191.5
ΔH(H→CH₃	4.2	-32.8	-37.0
ΔH(H→CH₂CH₃	8.3	-53.0	-61.3
ΔH(H→CN	17.2	132.8	115.6
ΔH(H→OCOCH₃	25.1	-358.7	-383.8
ortho CH₃-COCH₃	-0.4	9.2	9.6
meta CH₃-COCH₃	0.2	-0.1	-0.3
para CH₃-COCH₃	1.8	-0.8	-2.6
ortho CH₂CH₃-COCH₃	-1.4	9.2	10.6
meta CH₂CH₃-COCH₃	1.0	-1.3	-2.3
para CH₂CH₃-COCH₃	2.7	-1.8	-4.5
ortho CN-COCH₃	0.3	14.6	14.3
meta CN-COCH₃	3.7	4.7	1.0
para CN-COCH₃	-0.6	4.3	4.9
ortho OCOCH₃-COCH₃	-5.4	10.6	16.0
meta OCOCH₃-COCH₃	-1.7	1.1	2.8
para OCOCH₃-COCH₃	-1.4	0.8	2.2

The discussion of the magnitudes of the pairwise interactions with respect to $\Delta_l^g H_m^o$ is rather limited, since these contributions reflect the tightness of the molecular packing in the liquid. However, these contributions are not of negligible size (Table 8. Column 2)and they have to be considered as empirical constants for the correct prediction of the vaporization energetics.

Chapter 2 Webbing a network of reliable thermochemistry around lignin building blocks: trimethoxybenzenes

2.1. Introduction

Lignin has received considerable attention as a renewable source of aromatics [65]. Catalytic processing or pyrolysis of lignin is important for a sustainable production of platform chemicals and biofuels. A better understanding of lignin processing at the molecular level is indispensable for developing process control strategies to optimize the product formation [66]. In order to understand the energetics and mechanisms that control the entire monomer formation and distribution, reliable thermodynamic data must be collected and evaluated for building blocks that result from the thermal conversion of lignin. The basic properties such as enthalpies of formation and enthalpies of phase transitions (vaporization, sublimation and fusion) are required for energy balance calculations and dynamic equilibrium determinations in valorization reactions [64,67–69].

The correlation of thermodynamic properties of lignin constituting monomers with their molecular structures can open a window of opportunity for reliable predicting the energetics of large lignin building blocks. Such prediction is crucial for optimizing the lignin conversion into value-adding and sustainable platform chemicals.

The aim of the research is to use experimental and computational methods to obtain reliable thermodynamic information for the development of quantitative structure-property relationships in molecules that are relevant for the valorization of lignin. In order to facilitate the understanding of the reactions of the lignin conversion and to control the chemical processes, "model compounds" (which imitate the structural units present in lignin) can be examined instead [39,70,71]. The tri-methoxy-substituted benzenes modelling lignin structural units examined in this work are shown in Figure 7.
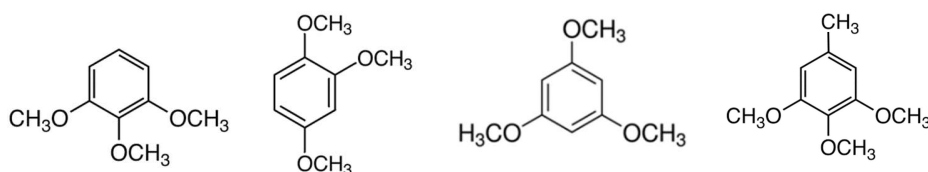
Figure 7. Trimethoxybenzenes studied in the research.

The thermochemical information available on trimethoxybenzenes is scarce [70,71]. Enthalpies of sublimation and enthalpies of formation of 1,2,3-trimethoxy and 1,3,5-trimethoxybenzene were determined by using drop and combustion calorimetry by Matos *et al* [70]. The enthalpy of vaporization of 1,3,5-trimetoxybenzene is reported from the correlation gas-chromatography [71].

The research continues the previous systematic studies of our working group [39,64,69,72–74] on the investigation of model compounds relevant to the valorization of biomass. The results on enthalpies of formation, phase transitions, and vapor pressures of a series of trimethoxybenzenes from Figure 7 have been obtained. The data available in the literature and new experimental results were evaluated and checked for internal consistency. The consistent thermochemical data sets for tri-methoxy-benzenes have been used for the design and the development of a "centerpiece" group-contribution approach being necessary for appraisal of enthalpies of formation and enthalpies of vaporization of substituted benzenes important for downstream processing of lignin-derived feedstock into end products.

2.2. Results and discussion

2.2.1. Standard molar heat capacity, $C^o_{p,m}$, measurements

Experimental heat capacity measurements are important in order to calculate heat balances in technological processes. In addition, heat capacities are required for adjustment sublimation/vaporization enthalpies to any temperature of interest, and to reduce the results of combustion calorimetry to the standard conditions. From our experiences, the empirical group contribution method developed by Chickos $et.$ at [9] can be reliably applied for capacity $C^o_{p,m}(cr)$ and capacity $C^o_{p,m}(liq)$ estimations. However, the validity of this approach towards tri-methoxy-benzenes have to be checked. In this work we measured heat capacity of 1,2,3-trimethoxy-benzene. Primary experimental results are given in Table B. 2. The experimental value $C^o_{p,m}(cr, 298.15 \text{ K})$ = 240.9 J·K^{-1}·mol^{-1} (Table B. 2.) is in excellent agreement with the estimate $C^o_{p,m}(cr, 298.15 \text{ K})$ = 243.3 J·K^{-1}·mol^{-1} (Table B. 1). Hence, the heat capacities at the reference temperature T = 298.15 K estimated according to Chickos $et.$ $al.$ [9] (Table B. 1) have been used for the temperature adjustments of experimental vaporization enthalpies as it shown in 2.2.2.

2.2.2. Thermodynamics of sublimation/vaporization

The experimental vapor pressures p_i for the trimethoxybenzenes (Table B. 3) at different temperatures were measured with help of the transpiration method. They were fitted according to the method described in 2.3 and 2.4. A short compilation of these data referenced to T = 298.15 K is given in Table 9. The method for calculating the combined uncertainties of the vaporization/sublimation enthalpies includes uncertainties from the experimental conditions of transpiration, uncertainties in vapor pressure and uncertainties due to the temperature adjustment to T = 298.15 K as described elsewhere [75,76].

Table 9. Results from the transpiration method: coefficient a and b of Equation 2 related to the studied substances, standard molar sublimation/vaporization enthalpies $\Delta_{cr,l}^{g}H_{m}^{o}$, standard molar sublimation/vaporization entropies $\Delta_{cr,l}^{g}S_{m}^{o}$, and standard molar vaporization Gibb's energies $\Delta_{cr,l}^{g}G_{m}^{o}$ at the reference temperature T = 298.15 K.

	a	$-b$	$-\Delta_{l}^{g}C_{p,m}^{o}$ [a]	$\Delta_{l}^{g}H_{m}^{o}$ [b]	$\Delta_{l}^{g}S_{m}^{o}$ [c]	$\Delta_{l}^{g}G_{m}^{o}$
			$J\cdot K^{-1}\cdot mol^{-1}$	$kJ\cdot mol^{-1}$	$J\cdot K^{-1}\cdot mol^{-1}$	$kJ\cdot mol^{-1}$
1,2,3-trimethoxybenzene (cr)	348.4	103494.0	37.2	92.4±0.7	215.5±1.3	28.2±0.1
1,2,3-trimethoxybenzene (liq)	348.3	102212.3	97.9	73.0±0.5	154.6±1.2	26.9±0.1
1,2,4-trimethoxybenzene (liq)	350.8	104844.6	97.9	75.7±0.5	157.2±1.2	28.8±0.1
1,3,5-trimethoxybenzene (cr)	333.9	101366.0	37.2	90.3±0.5	201.0±1.1	30.4±0.1
1,3,5-trimethoxybenzene (liq)	329.3	97850.6	97.9	68.7±0.4	135.7±0.5	28.2±0.1
3,4,5-trimethoxytoluene (liq)	366.9	109273.7	105.8	77.7±0.5	165.3±1.0	28.4±0.1

[a] From Table B. 2, [b] calculated by Equation 8 (data from Table B.3), [c] calculated by Equation 9 (data in Table B. 3).

Table 10. Compilation of enthalpies of sublimation/vaporization $\Delta_{cr,l}^{g}H_{m}^{o}$ of trimethoxybenzenes.

Compound/CAS	Method[a]	T- range	$\Delta_{cr,l}^{g}H_{m}^{o}(T_{av})$	$\Delta_{cr,l}^{g}H_{m}^{o}(298.15\ K)$	Ref.
		K	$kJ\cdot mol^{-1}$	$kJ\cdot mol^{-1}$	
1,2,3-trimethoxybenzene (cr)	DC	375	113.4±0.8	(98.0±3.2)	[70]
	T	288.2-314.3	92.3±0.4	92.4±0.7	this work
	F			92.0±0.7	Table 12
				92.2±1.0	average
1,2,3-trimethoxybenzene (liq)	T	318.1-346.3	69.7±0.3	73.0±0.5	this work
	J_x			72.9±0.5	Table 11
				73.0±0.7	average
1,2,4-trimethoxybenzene (liq)	T	309.7-350.1	72.5±0.3	75.7±0.5	this work
	J_x			76.0±0.5	Table 11
				75.9±0.7 [c]	average
1,3,5-trimethoxybenzene (cr)	DC	375	116.0±1.9	(100.6±3.6)	[70]
	T	288.0-326.2	89.9±0.3	90.3±0.5	this work
	F			90.7±0.7	Table 12
				90.4±0.8	average
1,3,5-trimethoxybenzene (liq)	CGC	298		68.2±2.0	[71]
	T	330.5-375.3	63.4±0.2	68.7±0.4	this work
	J_x			69.0±1.0	Table 12
				68.7±0.8	average
3,4,5-trimethoxytoluene (liq)	T	327.2-366.2	72.7±0.3	77.7±0.5	this work
	J_x			77.6±0.5	Table 11
				77.7±0.7	average

[a] Techniques: DC = drop calorimetry; T = transpiration method; J_x – derived from correlation of experimental vaporization enthalpies with Kovat´s indices; *CGC* – correlation gas-chromatographic method. *F* = derived from experimental data according to Equation 31.

Vapor pressures of tri-methoxy-benzenes have been measured for the first time. However, the sublimation enthalpies of 1,2,3-trimethoxy- and 1,3,5-trimethoxybenzenes were measured at 375 K (Table 10) using the "vacuum sublimation" drop microcalorimetric method [70]. The observed enthalpies of sublimation were adjusted to the reference temperature T = 298.15 K by using values of $\Delta_{298.15\ K}^{T}H_{m}^{o}(g)$ estimated by a group-contribution method with values from Stull *et al.* [77]. These results are listed in Table 10 for the sake of comparison with values derived in this work. However, in contrast to our transpiration results, the original uncertainties reported for

the calorimetric values do not include the uncertainties due to the temperature adjustments. In order to get a fair comparison, we assumed that the uncertainties in the temperature adjustment of vaporization/sublimation enthalpies from the experimental T to the reference temperature add 20 % to the total adjustment [56]. The calorimetric results for 1,2,3-trimethoxy- and 1,3,5-trimethoxybenzene with the reassessed uncertainties are listed in Table 10. As can be seen from this table, our "indirect" transpiration values are in disagreement with the "direct" calorimetric results even taking into account large experimental uncertainties of the latter values. There is no plausible explanation for this disagreement and it was decided to validate our new experimental results as follows in 2.2.3.

2.2.3. Kovats´s retention indices for validation of experimental vaporization enthalpies

The disagreement of sublimation enthalpies observed for 1,2,3-trimethoxybenzene and 1,3,5-trimethoxybenzene have prompted the search for additional methods to validate our transpiration results. In this context, we have applied our experiences with the CGC method [39,69,71]. The literature data available on the Kovats´s retention indices, J_x, for methoxy substituted benzenes were taken for correlation with the $\Delta_l^g H_m^o(298.15\ \text{K})$-values measured in this work. Results from these correlations are given in Table 11 and Table 12.

Table 11. Correlation of vaporization enthalpies, $\Delta_l^g H_m^o(298.15\ \text{K})$, of 1,2-dimethoxysubstituted benzenes with their Kovats´s indices (J_x).

Compound	J_x [a]	$\Delta_l^g H_m^o(298.15\ \text{K})_{exp}$ kJ·mol⁻¹	$\Delta_l^g H_m^o(298.15\ \text{K})_{calc}$ [b] kJ·mol⁻¹	Δ kJ·mol⁻¹
1,2-dimethoxybenzene	1146	64.5±0.3 [64]	64.5	0.0
1,2,3-trimethoxybenzene	1315	73.0±0.5 [c]	72.9	0.1
1,2,4-tri-methoxybenzene	1378	75.7±0.5 [c]	76.0	-0.3
3,4,5-trimethoxytoluene	1410	77.7±0.5 [c]	77.6	0.1
2,3,5-trimethoxytoluene	1527	-	83.3	-

[a] Kovats´s indices, J_x, on standard non-polar columns from [78], [b] calculated with Equation 29, [c] experimental data from Table 10.

It is known, that the $\Delta_l^g H_m^o(298.15\ \text{K})$-values correlate linearly with Kovats`s indices in various homologous series of alkylbenzenes, alkanes, aliphatic ethers, alcohols, or in a series of structurally similar compounds [18]. As expected, the $\Delta_l^g H_m^o(298.15\ \text{K})$-values correlated linearly with J_x values of methoxysubstituted benzenes, but it has turned out that the 1,2-dimethoxysubstituted species (Table 11) and the 1,3- together with the 1,4-dimetoxysubstituted species (Table 12) belong to the different lines. For the set of the methoxy-benzenes collected in Table 11, the following linear correlation was obtained:

$$\Delta_l^g H_m^o(298.15\ \text{K})\ /(\text{kJ·mol}^{-1}) = 7.9 + 0.0494 \times J_x \text{ with } (R^2 = 0.999) \qquad (29)$$

For the set of the methoxy-benzenes collected in Table 12, the following linear correlation was obtained:

$$\Delta_l^g H_m^o(298.15 \text{ K}) / (\text{kJ·mol}^{-1}) = 24.3 + 0.0318 \times J_x \text{ with } (R^2 = 0.953) \tag{30}$$

Table 12. Correlation of vaporization enthalpies, $\Delta_l^g H_m^o(298.15 \text{ K})$, of 1,3- and 1,4-dimethoxysubstituted benzenes with their Kovats's indices (J_x).

Compound	J_x [a]	$\Delta_l^g H_m^o(298.15 \text{ K})_{\text{exp}}$ kJ·mol⁻¹	$\Delta_l^g H_m^o(298.15 \text{ K})_{\text{calc}}$ [b] kJ·mol⁻¹	Δ kJ·mol⁻¹
1,3-dimethoxybenzene	1143	59.7±0.2 [64]	60.6	-0.9
1,4-dimethoxybenzene	1158	61.6±0.2 [64]	61.1	0.5
3,5-dimethoxytoluene	1233	64.5±1.2 [43]	63.5	1.0
1,3,5-trimethoxybenzene	1405	68.7±0.4 [c]	69.0	-0.3
2,4,6-trimethoxytoluene	1486	-	71.6	-

[a] Kovats's indices, J_x, on standard non-polar columns from [78], [b] calculated with Equation 30, [c] experimental from Table 10.

The results of the correlations with Kovats's indices are in a good agreement with those of the transpiration method (Table 10). Such good agreement can be seen as additional validation of the experimental data measured in this work by using the transpiration method (Table 10). It can be seen from Table 11 that differences between experimental and calculated according to Equation 29 are mostly below 0.5 kJ·mol⁻¹. Results are given in Table 12, show that differences between experimental and calculated according to Equation 30 are mostly below 1.0 kJ·mol⁻¹. Hence, the uncertainties of enthalpies of vaporization which are estimated from the correlation the $\Delta_l^g H_m^o(298.15 \text{ K})$ - J_x are evaluated with these uncertainties of ±0.5 kJ·mol⁻¹ (Table 11) and of ±1.0 kJ·mol⁻¹ (Table 12).

2.2.4. Thermodynamics of liquid-gas, solid-gas, and solid-liquid phase transitions

Another valuable option for establishing the consistency of experimental data on phase transitions (liquid-gas, solid-gas, and solid-liquid) for the compound examined is the common thermochemical equation:

$$\Delta_{cr}^g H_m^o(298.15 \text{ K}) = \Delta_l^g H_m^o(298.15 \text{ K}) + \Delta_{cr}^l H_m^o(298.15 \text{ K}) \tag{31}$$

We have used this option for 1,2,3-trimethoxybenzene and 1,3,5-trimethoxybenzene. Indeed, for 1,2,3-trimethoxybenzene, the sublimation enthalpy $\Delta_{cr}^g H_m^o(298.15 \text{ K}) = 92.4\pm0.7$ kJ·mol⁻¹ was measured using the transpiration method below the melting point (Table 10) and the vaporization enthalpy $\Delta_l^g H_m^o(298.15 \text{ K}) = 73.0\pm0.5$ kJ·mol⁻¹ was derived from vapor pressures measured above the melting point (Table 10). The latter value is also in agreement with those from J_x-correlation $\Delta_l^g H_m^o(298.15 \text{ K}) = 72.9\pm0.5$ kJ·mol⁻¹ (Table 11). The consistency of phase transitions available for

1,2,3-trimethoxybenzene can be easily established with help of Equation 31 and the experimental enthalpy of fusion for this compound $\Delta_{cr}^{l}H_m^o(298.15\ K) = 19.0\pm0.5$ kJ·mol^{-1} (Table 13) as follows:

$$\Delta_{cr}^{g}H_m^o(298.15\ K,\ 1,2,3\text{-trimethoxybenzene}) = 73.0 + 19.0 = 92.0\pm0.7\ \text{kJ·mol}^{-1} \qquad (32)$$

This estimate is in an excellent agreement with the transpiration experiment $\Delta_{cr}^{g}H_m^o(298.15\ K) = 92.4\pm0.7$ kJ·mol^{-1}. In the same way we checked the consistency of phase transitions for 1,2,3-trimethoxybenzene with the data compiled in Table 13. The estimated according to Equation 30 sublimation enthalpy $\Delta_{cr}^{g}H_m^o(298.15\ K) = 90.7\pm0.7$ kJ·mol^{-1} is an excellent agreement with the transpiration experiment $\Delta_{cr}^{g}H_m^o(298.15\ K) = 90.3\pm0.5$ kJ·mol^{-1} (Table 10).

Table 13. Phase transitions thermodynamics of trimethoxybenzenes (in kJ·mol^{-1}).

Compounds	T_{fus}, K	$\Delta_{cr}^{l}H_m^o$ at T_{fus}	$\Delta_{cr}^{l}H_m^{o\ a}$	$\Delta_{l}^{g}H_m^{o\ b}$	$\Delta_{cr}^{g}H_m^o$
				298.15 K	
1	2	3	5	6	7
1,2,3-trimethoxybenzene	318.3±0.5	20.2±0.3	19.0±0.5	73.0±0.5	92.0±0.7
1,3,5-trimethoxybenzene	329.4±0.5	23.9±0.3	22.0±0.6	68.7±0.4	90.7±0.7

[b] The experimental enthalpies of fusion $\Delta_{cr}^{l}H_m^o$ measured at T_{fus} were adjusted to 298.15 K with help of the equation: $\Delta_{cr}^{l}H_m^o(298.15\ K)/(\text{J·mol}^{-1}) = \Delta_{cr}^{l}H_m^o(T_{fus}/K) - (\Delta_{cr}^{g}C_{p,m}^o - \Delta_{l}^{g}C_{p,m}^o) \times [(T_{fus}/K) - 298.15\ K]$ [56], [c] from Table 10.

The consistency of the solid-liquid, solid-gas, and liquid-gas phase transitions for 1,2,3-trimethoxybenzene and 1,2,3-trimethoxybenzene derived in this work could be regarded as an indirect support of the reliability of our new transpiration results.

2.2.5. Standard molar enthalpies of formation from combustion calorimetry

Table 14. Thermochemical data for methoxy-substituted benzenes at T=298.15 K (p^o=0.1 MPa, in kJ·mol^{-1}).

compound	$-\Delta_c H_m^o(cr,l)$	$\Delta_f H_m^o(cr,l)_{exp}$	$\Delta_{cr,l}^{g}H_m^{o\ a}$	$\Delta_f H_m^o(g)_{exp}$	$\Delta_f H_m^o(g)_{theor}{}^{b}$
1	2	3	4	5	6
1,2,3-trimethoxybenzene (cr)	4819.5±2.5[70]	-437.0±2.8			
	4817.7±1.8 [c]	-438.9±2.1			
		-438.2±1.7	92.2±1.0	-346.0±2.0	-350.6±2.4
1,2,4-trimethoxybenzene (liq)	-4820.1±1.9 [c]	-436.5±2.2	75.9±0.7	-360.6±2.3	-360.6±2.3
1,3,5-trimethoxybenzene (cr)	4784.6±2.9 [70]	-472.0±3.1	90.4±0.8	-381.6±3.2	-382.1±1.2
3,4,5-trimethoxytoluene (liq)	-5475.0±2.0 [c]	-460.9±2.4	77.7±0.7	-383.2±2.5	-382.1±1.2

[a] From Table 10, [b] calculated as the average from G4, G3MP2, and M06/QZ4P results (Table 15), [c] this study.

Specific energies of combustion, $\Delta_c u^o$, of highly pure samples of 1,2,3-trimethoxybenzene, 1,2,4-trimethoxybenzene and 3,4,5-trimethoxytoluene were measured by using combustion calorimetry. The standard molar enthalpies of combustion $\Delta_c H_m^o(cr)$ and the standard molar enthalpies of formation $\Delta_f H_m^o(cr)$ are presented in Table B.5. Compilation of thermochemical data for methoxy-substituted benzenes is given in Table 14. The $\Delta_f H_m^o(liq)$-values of 1,2,4-trimethoxybenzene and 3,4,5-trimethoxytoluene were measured for the first time. The $\Delta_f H_m^o(cr,l)$-

values for 1,2,3-trimethoxybenzene and 1,3,5-trimethoxybenzene were previously reported by Matos *et al*. [70] (Table 14). Our new result for 1,2,3-trimethoxybenzene agrees well with their result. Nevertheless, it is reasonable to validate all available results for the methoxy-substituted benzenes with help of quantum-chemical calculations as it shown in 2.2.6.

2.2.6. Gas-phase enthalpies of formation: experiment and theory

The experimental gas-phase standard molar enthalpies of formation $\Delta_f H_m^o(g)_{exp}$ are derived from experimental results on sublimation/vaporization enthalpies (Table 10) and results from the combustion calorimetry (Tables 14, B.5) according to the common thermochemical equations:

$$\Delta_f H_m^o(g, 298.15\ \text{K})_{exp} = \Delta_{cr}^g H_m^o(298.15\ \text{K}) + \Delta_f H_m^o(cr, 298.15\ \text{K})_{exp} \qquad (33)$$

$$\Delta_f H_m^o(g, 298.15\ \text{K})_{exp} = \Delta_l^g H_m^o(298.15\ \text{K}) + \Delta_f H_m^o(liq, 298.15\ \text{K})_{exp} \qquad (34)$$

Results derived with help Equations 33 and 34 are listed in Table 14.

Conformational analysis and optimization of structures of methoxy-substituted benzenes were carried out within the framework of molecular mechanics in a force field UFF [36]. In almost all molecules located several low-lying conformers have been located, but their energies have been found to be close to each other within 1-2 kJ·mol^{-1}. The subsequent geometry optimization with the M06L/TZ2P method led to some permutations between them. Therefore, the conformers of all structures were also optimized with G3MP2 method [36]. The resulting energy distribution confirmed the M06L/Z2P results. The harmonic and anharmonic frequencies of the most stable conformers of methoxy-substituted benzenes were used to determine the zero point of energy and temperature contributions to enthalpy for M06/QZ4P in the "rigid rotator - anharmonic oscillator" (RRAO) approximation. Enthalpies H_{298} of the most stable conformers for each isomer (Figure 8) were calculated by using the G4, G3MP2, and M06/QZ4P methods.

| 1,2,3-trimethoxybenzene | 1,2,4-trimethoxybenzene | 1,3,5-trimethoxybenzene | 3,4,5-trimethoxytoluene |
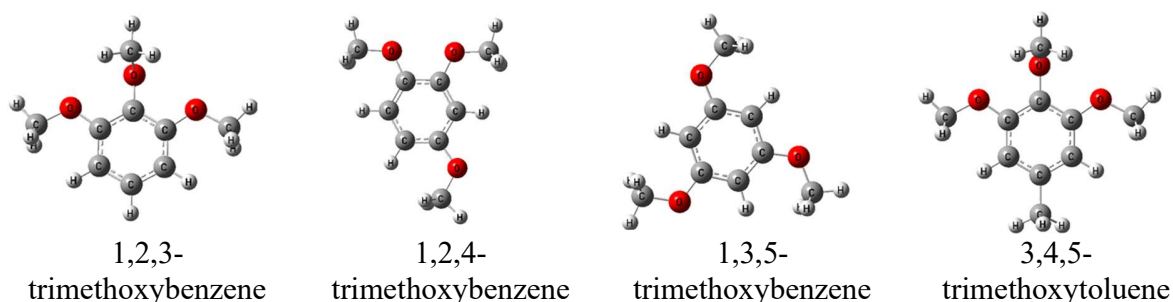
Figure 8. The most stable conformers of substituted benzenes.

Based on our experience with the quantum chemical calculations, the enthalpies of formation from the atomization reaction sometimes systematically deviate from the experimental values [79]. However, a simple linear correlation could be found between calculated by the atomisation

reaction and experimental enthalpies of formation of methoxy substituted benzenes (details are given in Table B. 9. - Table B. 12:

$$\Delta_f H_m^o(g)_{theor}/ \text{ kJ·mol}^{-1} = 1.0023 \times \Delta_f H_m^o(g, \text{AT}) + 4.1 \text{ with } R^2 = 0.9992 \text{ for G4} \tag{35}$$

$$\Delta_f H_m^o(g)_{theor}/ \text{ kJ·mol}^{-1} = 1.0064 \times \Delta_f H_m^o(g, \text{AT}) + 8.7 \text{ with } R^2 = 0.9993 \text{ for G3MP2} \tag{36}$$

$$\Delta_f H_m^o(g)_{theor}/ \text{ kJ·mol}^{-1} = 0.9739 \times \Delta_f H_m^o(g, \text{AT}) + 2.1 \text{ with } R^2 = 0.9992 \text{ for M06/Q4P} \tag{37}$$

Using these correlations, the "corrected" enthalpies of formation of substituted benzene have been calculated (Table 15).

Table 15. Comparison of the experimental, $\Delta_f H_m^o(g)_{exp}$, and theoretical, $\Delta_f H_m^o(g)_{theor}$, gas-phase standard molar enthalpies of formation of methoxy-substituted benzenes at T = 298.15 K and p° = 0.1 MPa (in kJ·mol^{-1}).

compound	$\Delta_f H_m^o(g)_{exp}$	G4	G4	G3MP2	G3MP2	M06/QZ4P	M06/QZ4P	$\Delta_f H_m^o(g)_{theor}$
	Exp.[a]	AT[b]	*WBR*[c]	AT[b]	*WBR*[c]	AT[b]	*WBR*[c]	*average*
1,2,3-trimethoxybenzene	-346.0±2.0	-351.8	-352.2	-350.2	-351.5	-348.3	-349.3	**-350.6±2.4**
1,2,4-trimethoxybenzene	-360.6±2.3	-360.7	-361.0	-359.8	-361.1	-358.5	-360.8	**-360.3±1.6**
1,3,5-trimethoxybenzene	-381.6±3.2	-382.0	-382.3	-381.1	-382.2	-381.5	-383.4	**-382.1±1.2**
3,4,5-trimethoxytoluene	-383.2±2.5	-383.4	-381.8	-382.3	-381.2	-381.6[d]	-382.1[e]	**-382.1±1.2**

[a] From Table 14, [b] calculated by the G4, G3MP2, or M06/QZ4P method, [c] Calculated by the G4, G3MP2 or M06/QZ4P methods with reactions R1 to R4 using experimental $\Delta_f H_m^o(g)$-values (Table B. 4); data for reactions R1 to R4 are given in Table B. 9 - Table B. 12, [d] calculated by the G4MP2 according to the standard atomization procedure, [e] calculated by the G4MP2 method with reaction R4 using experimental $\Delta_f H_m^o(g)$-values; for reaction R4 is given in Table B. 11.

The following general reactions were used for the *WBR* method (detailed reactions are given in Figure B. 1 and Figure B. 2):

$$x,x,x\text{-}trimethoxy\text{-}benzene + 2 \times benzene = 3 \times methoxybenzene \tag{R1 to R3}$$

$$x,x,x\text{-}trimethoxy\text{-}toluene + 2 \times benzene = 3 \times methoxy\text{-}benzene + toluene \tag{R4}$$
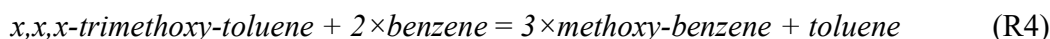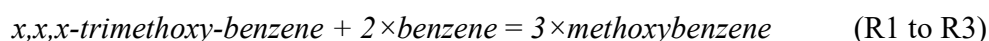
using the reliable experimental gas-phase enthalpies of formation $\Delta_f H_m^o(g, 298.15 \text{ K})$ of benzene, methoxybenzene, and toluene from Table B. 4. The theoretical enthalpies of formation of substituted benzenes were derived by using the G4, G3MP2, and M06/QZ4P methods. The results of quantum-chemical calculations are summarized in Table 15.

As can be seen from Table 15, a very good agreement with the experimental results is evident for all four quantum-chemical methods (G4, G3MP2, and M06/QZ4P) used, as well as for both atomization and WBR procedures. For this reason, the theoretical values for each compound were averaged and the final theoretical gas-phase enthalpies of formation, $\Delta_f H_m^o(g)_{theor}$, are given in Table 14. The good agreement between the experimental and theoretical standard molar enthalpies of formation for benzene derivatives can be seen as proof of the internal consistency of

the thermochemical results evaluated in this work (Table 14), which can now be recommended as reliable benchmark properties for further thermochemical calculations with substituted benzene.

2.2.7. Development of a "centerpiece" group-contribution approach

The polyphenolic lignin structure is well known as a complex 3D molecular structure that comprises a great variety of bonds with naturally around 50% ether linkages [80]. An idealized structural unit of lignin is given in Figure 9. It is obvious that all components of this unit are arranged in close proximity and interact energetically with each other. The total energetics of the structural unit of lignin consists of enthalpic contributions from structural elements (*e.g.* OH, OCH_3, C_bH *etc.*), and the contribution from mutual non-bonded interactions among these structural elements. The first contribution could be approximated with any kind of group-additivity [1,81]. An exact accounting of the non-bonded interactions even for the simplified lignin unit is hardly possible due to the complex 3D molecular structure. The only way to assess the lignin energetics is therefore to develop an approach that requires a certain degree of simplification of the real structure.

In our previous studies [39,64,69,73,74,82] we have already launched the systematic study of the energetics of compounds that can be considered as the renewable feedstock and the lignin-broken bits (*e.g.* anethole, eugenol, hydroxy-, methoxy- *etc.*). These compounds are not only relevant for the processing of lignin, but also model the constituent elements of the lignin units. These preliminary studies have helped to envisage a "centerpiece" group-contribution approach which is necessary for a basic evaluation of the energetics (enthalpies of formation and enthalpies of vaporization) of substituted benzenes, which make the main contributions to the lignin structure units. The consistent sets of thermochemical data for tri-methoxy-benzenes evaluated in Table 14 have been used for the development of a "centerpiece" group-contribution approach as follows.

2.2.7.1. Construction of a strain-free theoretical framework

It is obvious from the idealized structural unit of lignin (Figure 9, left) that alkoxy-substituted benzenes (Figure 9, right) can also be seen as one of the constituent "building blocks". For this work, however, it is more important to consider these molecules as "models" in order to develop an approach for a quick assessment of the energetics of the lignin building blocks.

The idea of this approach is that to select a "centerpiece" molecule (*e.g.* benzene or methoxybenzene, or toluene or *etc.*) with the well-established thermodynamic properties. Various substituents (mostly relevant for the lignin are alkoxy, hydroxy and carbonyl substituents) can be attached to these "centerpieces" in different positions on the benzene ring. The enthalpic contributions for these substituents can be easily quantified (Figure 10) from the differences

between the enthalpy of the substituted benzene and the enthalpy of the benzene itself. Using this scheme, the contributions $\Delta H(\text{H} \rightarrow CH_3)$ and $\Delta H(\text{H} \rightarrow CH_3O)$ were derived (Table 16) using the reliable thermochemical data for toluene, methoxybenzene, and benzene compiled in Table B. 4. Details on calculations conducted in this chapter are given in Table B. 13 and Table B. 14.
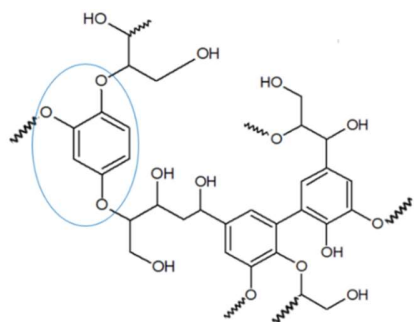
Figure 9. Idealized structural unit of lignin (left) and graphical presentation of the idea of a "centerpiece" group-contribution approach (right).
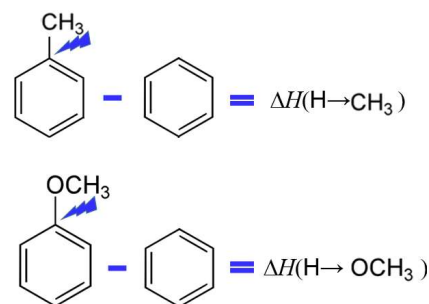
Figure 10. Example of quantification of the enthalpic contributions for the methyl- and methoxysubstituents.

These enthalpic contributions $\Delta H(\text{H} \rightarrow CH_3O)$ and $\Delta H(\text{H} \rightarrow CH_3)$ can be now applied to construct a framework of any desired methoxy-substituted benzene or toluene (*e.g.* 1,2,4-trimethoxybenzene or 3,4,5-trimethoxytoluene given in Figure 9), arbitrary starting from the one of the "centerpieces" namely methoxybenzene or toluene, or even starting from the benzene itself. In terms of energy, however, this framework is not perfect due to the lack of energetics of the interactions between the substituents.

Table 16. Parameters and pairwise nearest and non-nearest neighbour interactions of substituents on the "centerpieces" for calculation of thermodynamic properties of substituted benzenes at 298.15 K (in kJ·mol⁻¹).

Contribution	$\Delta_f H_m^o(g)$ [a]	$\Delta_l^g H_m^o$ [b]
benzene	82.9	33.9
$\Delta H(\text{H} \rightarrow CH_3O)$	-153.6	12.5
$\Delta H(\text{H} \rightarrow CH_3)$	-32.8	4.2
ortho CH₃O - CH₃O	14.3	5.6
meta CH₃O - CH₃O	-0.5	0.8
para CH₃O - CH₃O	7.4	2.7
ortho CH₃O - CH₃	-3.1	-0.4
meta CH₃O - CH₃	0.9	2.2
para CH₃O - CH₃	4.5	2.7

[a] Calculated from Table B. 13 and Table B. 14, [b] calculated from Table B. 15 and Table B. 16.

2.2.7.2.   Pairwise interactions of substituents on the benzene ring

Nearest (*e.g. ortho*-interactions) and non-nearest neighbour interactions (*e.g. meta*- or *para*- interactions) of substituents on the "centerpieces" (benzene, methoxybenzene, and toluene)

are generally stipulating the overall amount of the non-additive interactions specific for the particular structural unit of the lignin (Figure 9, left).
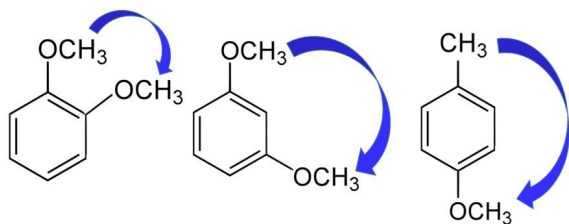
Figure 11. Example for a quantification of the enthalpic contributions "CH₃O - R" for the non-nearest neighbour interactions of the CH₃O-group with the methoxy or methyl substituents attached in the different positions to the "centerpieces".
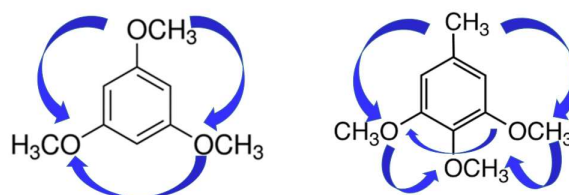
Figure 12. Agglomeration of the enthalpic contributions for the nearest and non-nearest neighbour interactions in the three and four substituted benzene derivatives.

For practical reasons, however, it is first necessary to subdivide the entire non-additive interactions into easily definable pairwise interactions. The mutual enthalpic pairwise interactions of substituents in the benzene ring can be accounted for by the three types of contributions that are specific for the *ortho*, *para* and *meta* positions of substituents placed in the benzene ring. How the pairwise interactions can be derived is shown in Figure 11. Indeed, to quantify the enthalpic contribution "*meta CH₃O - CH₃O*" for the non-bonded interaction of the *CH₃O*-groups in the *meta*-position on the methoxybenzene (taken as the "centerpiece") we must first construct the "theoretical framework" of the 1,3-dimethoxybenzene (Figure 11, middle). To do that, the contribution $\Delta H(\text{H}\rightarrow CH_3O)$ from Table 16 was added to the experimental enthalpy (enthalpy of formation or enthalpy of vaporization) of the methoxybenzene from Table B. 4. Alternatively, we could add two contributions $\Delta H(\text{H}\rightarrow CH_3O)$ to the benzene as the "centerpiece". This "theoretical framework" of 1,3-dimethoxybenzene does not contain the "*meta CH₃O - CH₃O*" interaction. However, this interaction is present in the real 1,3-dimethoxybenzene (blue arrow in Figure 11). The arithmetic difference between the experimental enthalpy (enthalpy of formation or enthalpy of vaporization) of 1,3-dimethoxybenzene and the enthalpy of the "theoretical framework" therefore provides the quantitative size of the pairwise interaction "*meta CH₃O - CH₃O*" directly (Table 16). Using the same logic, the enthalpic contributions for the "*ortho CH₃O - CH₃O*" and "*para CH₃O – CH₃*" shown in Figure 11 can be derived (Table 16) by using the parameters $\Delta H(\text{H}\rightarrow CH_3O)$ and $\Delta H(\text{H}\rightarrow CH_3)$ respectively. In the same way, the required enthalpic contributions for the *ortho*-, *meta* and *para*-pairwise interactions of substituents were obtained and summarized in Table 16.

Quantitatively, the strength of the interactions depends strongly on the type of *ortho*-, *meta*- or *para*-pairs. Let us consider the intensity of pairwise interaction in terms of $\Delta_f H_m^o(g)$. From Table 16 it can be seen that the *ortho*-dimethoxy-benzene shows a strong destabilization of 14.3 kJ·mol$^-$^{1} due to the sterical repulsions of bulky methoxy groups [64]. In contrast, the *ortho*-substituted methoxy-toluene is noticeably stabilized of -3.1 kJ·mol^{-1}, however the reason for such stabilization is not quite apparent [30]. From our experiences, the *meta*- and *para*-interactions of substituents on the benzene ring are less profound compared to *ortho*-interactions [39,64]. Indeed, the *meta*-interactions of the substituents examined can be considered as negligible since they are below 1 kJ·mol^{-1} (Table 16). In contrast, the significant destabilization at the level from 4.5 to 7.4 kJ·mol$^-$^{1} is observed for the *para*-isomers of dimethoxy-benzene and methoxy-toluene. These noticeable destabilizing effects can be explained by the specific electron density distribution within the substituted benzene ring. The discussion of the magnitudes of the pairwise interactions with respect to $\Delta_l^g H_m^o$ is rather limited, since these contributions reflect the tightness of the molecular packing in the liquid. However, these contributions are not of negligible size (Table 16, last column) and they have to be considered as empirical constants for the correct prediction of the vaporization energetics.

2.2.7.3. Effect of agglomeration of substituents on the benzene ring

It is apparent (blue arrows in Figure 12), that the introduction of the third and fourth substituents in the benzene ring is expected to increase the intensity of the mutual interactions of the substituents compared to two substituents. As can be seen in Figure 12, all three possible types of *ortho*-, *meta*- and *para*-interactions are present simultaneously in the 3,4,5-trimethoxytoluene. Does the energetics of these interactions additive with the growing number of substituents? Can be the individual contributions given in Table 16 just summarized? Or are there additional effects due to a perturbation in the electron density within the congested benzene ring?

In order to get the answer in terms of $\Delta_f H_m^o(g)$, the "theoretical framework" for each investigated molecule was calculated (Table B. 13). The difference between the $\Delta_f H_m^o(g)$ of the real molecule and the enthalpy of its model represented by the "theoretical framework" (Table B. 14 and Table B. 15) provides the total amount of pairwise nearest and non-nearest neighbour interactions of substituents on the "centerpieces" in terms of $\Delta_f H_m^o(g)$. The numerical results of these differences are compiled in Table 17.

The actual amount of interactions in tri-methoxy-substituted benzenes is given in Table 17, column 3 and it is quite comparable (within uncertainties ascribed to $\Delta_f H_m^o(g)$-values) to the

theoretical sum of nearest and non-nearest neighbour interactions of substituents (Table 17, column 4). At first glance, no additional interactions between three substituents in the benzene ring appear to occur. It is noticeable, however, that the theoretical amount of interactions is systematically overestimated up to 3.6 kJ·mol^{-1} (Table 17, column 5). This trend is more apparent for 3,4,5-trimethoxytoluene, in which the theoretical amount of interactions is already overestimated of -5.8 kJ·mol^{-1} (Table 17, last column). This observation contradicts our expectations, but it could be explained that the "real" molecule of the trimethoxybenzenes becomes noticeably more relaxed compared to the di-methoxy-substituted benzene, despite the introduction of the third substituent.

Table 17. Analysis of the total Amount of pairwise nearest and non-nearest neighbour interactions of substituents on the "centerpieces" in terms of $\Delta_f H_m^o(g)$ for tri-methoxy-substituted benzenes at 298.15 K (in kJ·mol^{-1}).

Compound	$\Delta_f H_m^o(g)$[a]	Actual amount of Interactions [b]	Theoretical amount of interactions [b]	Δ
1	2	3	4	5
1,2,3-trimethoxybenzene	-350.6±2.4	27.3	28.1	-0.8
1,2,4-trimethoxybenzene	-360.3±1.6	17.6	21.2	-3.6
1,3,5-trimethoxybenzene	-382.1±1.2	-4.2	-1.5	-2.7
3,4,5-trimethoxytoluene	-382.1±1.2	28.6	34.4	-5.8

[a] from Table 14, [b] calculated from Table B. 17 and Table B. 18.

To summarize observations regarding the $\Delta_f H_m^o(g)$-values we can conclude, that overall interactions of three methoxy-substituents placed in the benzene ring are systematically decreasing by 3 to 4 kJ·mol^{-1} compared to the theoretical value (collected from the sum of the pairwise interactions). Analysis of the total amount of pairwise nearest and non-nearest neighbour interactions of substituents on the "centerpieces" in terms of $\Delta_l^g H_m^o$ for trimethoxysubstituted benzenes is given in Table 18. As can be seen from Table 18 (and from Table B. 16 - Table B. 18), the vaporization enthalpies of the "real" tri-methoxy-benzenes are in most cases only somewhat higher in comparison to those for the "theoretical framework" (Table 18, column 3). It means, that contrary to our expectations the large values of theoretical amount of interactions (collected from the pairwise interactions given in Table 16) is virtually disappears in the "real" tri-methoxy-benzenes! Most noticeable is the difference of -10.4 kJ·mol^{-1} (Table 18, column 5) observed for the 1,2,3-trimethoxybenzene, since the theoretical value for this compound is expected to be 12.0 kJ·mol^{-1} (Table 18, column 4). This trend can be seen more profoundly for 3,4,5-trimethoxytoluene, in which the difference of -17.0 kJ·mol^{-1} (Table 18, column 5) is observed. This means that the liquid phase for these both compounds is significantly more isotropic

compared to the dimethoxysubstituted benzenes due to the less favourable intermolecular networking.

Table 18. Analysis of the total amount of pairwise nearest and non-nearest neighbour interactions of substituents on the "centerpieces" in terms of $\Delta_l^g H_m^o$ for trimethoxy-substituted benzenes at 298.15 K (in kJ·mol^{-1}).

Compound	$\Delta_l^g H_m^{o\ a}$	Actual amount of interactions[b]	Theoretical amount of interactions[b]	Δ
1	2	3	4	5
1,2,3-trimethoxybenzene	73.0±0.7	1.6	12.0	-10.4
1,2,4-trimethoxybenzene	75.9±0.7	4.5	9.1	-4.6
1,3,5-trimethoxybenzene	68.7±0.8	-2.7	2.4	-5.1
3,4,5-trimethoxytoluene	77.7±0.7	2.1	19.1	-17.0

[a] Results from Table 9 and Table 10, [b] Calculated in Table B. 15.

To summarize observations regarding the $\Delta_l^g H_m^o$ values, it was assumed that vaporization enthalpies of substituted benzene derivatives approximately (with an uncertainty of 2 to 3 kJ·mol^{-1}) equal to the value of "theoretical framework". This assumption is very practical for the quick appraisal of vaporization enthalpies of poly-substituted benzenes considered as the building blocks of the lignin. However, this assumption requires further investigation.

The parameters and pair-wise interactions of substituents in the benzene ring listed in Table 16 are aimed at predicting $\Delta_f H_m^o$(g, 298.15 K) and $\Delta_l^g H_m^o$ (298.15 K) values for benzene derivatives resulting from the lignin valorization technologies. Taking into account the complex structure of the lignin fragments, the question of the energetic consequences of the agglomeration of substituents in the benzene ring deserves further systematic investigations.

Chapter 3 Glycerol Valorisation Towards Biofuel Additivities: Thermodynamic Studies of Glycerol Ethers

3.1. Introduction

Most processes in the chemical industry use the traditional organic solvents. Although there are apparent advantages in the use of these kinds of solvents, such as availability and low price, there are some important drawbacks such as their volatility, flammability, and toxicity. That is why, the development of inexpensive, harmless and environmentally friendly alternative solvents is of great importance. The desirable properties of alternative green solvents include: low volatility, toxicity, and price, as well as renewable origin, easy availability and biodegradability. The glycerol ethers fully meet the renewable green solvent requirements and have attracted a great deal of attention in various applications. Glycerol ethers in particular have proven to be promising candidates for solvent substitution, since their physicochemical properties can be modulated by

the number, size, and type of their alkyl groups, which among other things leads to a wide range of polarities [83]. Knowledge of reliable thermodynamic data is essential for the design and development of new technologies. In this work, we present a systematic study of the thermodynamic properties of glycerol ethers given in Table 19.

Table 19. Glycerol ethers studied in this work (source – laboratory synthesis).

Structure	Name, CAS	Purity	H_2O
	1,3-dimethoxy-2-propanol, 623-69-8	0.9991	156 ppm
	1,3-diethoxy-2-propanol, 4043-59-8	0.9993	110 ppm
	1,3-di-isopropoxy-2-propanol, 13021-54-0	0.9996	111 ppm
	2,5,9,12-tetraoxatridecan-7-ol, 130670-52-9	0.9992	286 ppm
	1,3-bis(2,2,2-trifluoroethoxy)-2-propanol, 691-26-9	0.9994	246 ppm

This research continues our studies of thermodynamic properties of glycerol ethers [84,85]. The focus of this work was on heat capacities, vapour pressures, and combustion calorimetry. In order to establish the consistency of new results, the experimental values were validated with the empirical methods and with the high-level quantum-chemical calculations.

3.2. Results and discussion

3.2.1. Measurement of standard molar heat capacity, $C_{p,m}^{o}$(liq)

The heat balances in technological processes are usually based on experimental heat capacities. The heat capacities of glycerol ethers were measured for the first time. Primary experimental data measured in this work are given in Table C. 1 - Table C. 5 in the supporting information. The results were fitted to a polynomial in the temperature range between 232 K and 377 K (with $R = 8.314462$ J·K^{-1}·mol^{-1}):

1,3-dimethoxy-2-propanol: $C_{p,m}^{o}$(liq)/$R = 32.38 + 4.424 \times 10^{-2}(T/K -298.15 K) + 4.942 \times 10^{-5}(T/K -298.15 K)^2$ from 232.1 to 320.1 K (38)

1,3-diethoxy-2-propanol: $C_{p,m}^{o}$(liq)/$R = 42.00 + 4.737 \times 10^{-2} (T/K -298.15/K)$ from 232.6 to 319.6 K (39)

1,3-di-isopropoxy-2-propanol: $C_{p,m}^{o}$(liq)/$R = 48.84 + 5.332 \times 10^{-2} (T/K -298.15 K)$ from 314 to 377 K (40)

2,5,9,12-tetraoxatridecan-7-ol: $C_{\text{p,m}}^{\text{o}}(\text{liq})/R = 54.87 + 4.906{\times}10^{-2}$ (T/K -298.15 K) from 312 to 376 K (41)

1,3-bis(2,2,2-trifluoroethoxy-2-propanol: $C_{\text{p,m}}^{\text{o}}(\text{liq})/R = 52.07 + 4.665{\times}10^{-2}$ (T - 298.15/K) – $5.385{\times}10^{-5}(T$ - 298.15/ K)^2 from 235.4 to 350.0 K (42)

Table 20. Compilation of data on molar heat capacities $C_{\text{p,m}}^{\text{o}}(\text{liq})$ and heat capacity differences $\Delta_{\text{l}}^{\text{g}}C_{\text{p,m}}^{\text{o}}$ (in J·K^{-1}·mol^{-1}) at T = 298.15 K.

Compounds	$C_{\text{p,m}}^{\text{o}}(\text{liq})^{\text{a}}$	$C_{\text{p,m}}^{\text{o}}(\text{liq})^{\text{b}}$	$-\Delta_{\text{l}}^{\text{g}}C_{\text{p,m}}^{\text{o}}$
1,3-dimethoxy-2-propanol	269.3	270.7	80.6 [c]
1,3-diethoxy-2-propanol	349.2	334.5	101.4 [c]
1,3-di-isopropoxy-2-propanol	406.1	385.3	116.2 [c]
2,5,9,12-tetraoxatridecan-7-ol	456.2	486.2	129.2 [c]
1,3-bis-(2,2,2-trifluoroethoxy)-2-propanol	432.9	394.1	123.1 [c]
1-methoxy-3-tert-butoxy-2-propanol		354.5	102.8 [d]
1,3-di-(n-butoxy)-2-propanol		462.1	130.7 [d]
1,3-di-(tert-butoxy)-2-propanol		450.2	127.6 [d]
bis-(2,2,2-trifluoroethyl) ether		197.6	68.1 [d]

[a] Experimental values, [b] calculated by the group-contribution procedure [9], [c] Calculated according to [56] by using experimental heat capacities $C_{\text{p,m}}^{\text{o}}(\text{liq})$, [d] Calculated according to the procedure developed by Acree and Chickos [56] by using estimated heat capacities $C_{\text{p,m}}^{\text{o}}(\text{liq})$.

The heat capacities at the reference temperature T = 298.15 K are given in Table 20 and they were used to adjust the vaporisation enthalpies to the reference temperature T = 298.15 K (see 3.2.2) and to reduce the results of the combustion calorimetry (see 3.2.5).

Table 21. Results from the transpiration method: coefficient a and b of Equation 2, standard molar vaporization enthalpies $\Delta_l^g H_m^o$, standard molar vaporization entropies $\Delta_l^g S_m^o$, and standard molar vaporization Gibbs energies $\Delta_l^g G_m^o$ at the reference temperature T = 298.15 K

	a	$-b$	$-\Delta_{\text{l}}^{\text{g}}C_{\text{p,m}}^{\text{o}}$ [a] J·K^{-1}·mol^{-1}	$\Delta_{\text{l}}^{\text{g}}H_m^{\text{o}}$ [b] kJ·mol^{-1}	$\Delta_{\text{l}}^{\text{g}}S_m^{\text{o}}$ [c] J·K^{-1}·mol^{-1}	$\Delta_{\text{l}}^{\text{g}}G_m^{\text{o}}$ kJ·mol^{-1}
1,3-dimethoxy-2-propanol	313.3	82031.5	80.6	58.0±0.5	137.0±1.4	17.1±0.1
1,3-diethoxy-2-propanol	339.6	92041.6	101.4	61.8±0.4	142.4±0.8	19.3±0.1
1,3-di-isopropoxy-2-propanol	364.2	101321.9	116.2	66.7±0.3	152.3±0.7	21.3±0.1
2,5,9,12-tetraoxatridecan-7-ol	394.9	124276.1	129.2	85.8±0.4	170.0±1.1	35.1±0.1
1,3-bis(2,2,2-trifluoroethoxy)--2-propanol	384.1	108344.3	120.1	71.6±0.3	165.3±0.6	22.4±0.1

[a] From Table 20, [b] calculated by Equation 8 (Table C. 6), [c] calculated by Equation 9 (Table C. 6).

3.2.2. Absolute vapor pressures and thermodynamics of vaporization

The experimental vapor pressures, p_i, measured for the glycerol ethers (Table C. 6) at different temperatures were measured with help of the transpiration method. Experimental vapor pressures measured at different temperatures by the transpiration method, coefficients a and b of Equation 2, as well as values of $\Delta_{\text{l}}^{\text{g}}H_m^{\text{o}}(T)$ and $\Delta_{\text{l}}^{\text{g}}S_m^{\text{o}}(T)$ at the reference temperature T = 298.15 K are given in Table 21. The compilation of available standard molar vaporization enthalpies for the glycerol ethers is given in Table 22.

Table 22. Compilation of available vaporization enthalpies $\Delta_l^g H_m^o$ of glycerol ethers.

Compound	Method[a]	T- range	$\Delta_l^g H_m^o(T_{av})$	$\Delta_l^g H_m^o(298.15\ K)$[b]	Ref.
		K	kJ·mol⁻¹	kJ·mol⁻¹	
1,3-dimethoxy-2-propanol	T	277.7-328.7	57.8±0.4	58.0±0.5	this work
	SP			56.3±0.5	Table 27
				57.3±0.7[c]	average
1,3-diethoxy-2-propanol	T	278.4-335.0	61.1±0.2	61.8±0.4	this work
	S	278.4-344.8	60.2±0.1	61.4±0.2	this work
	SP			61.6±1.3	Table 27
				61.5±0.2[c]	average
1,3-di-isopropoxy-2-propanol	S	293.2-373.2	53.7±0.2	(57.3±0.3)	[86]
	T	281.8-334.1	65.5±0.2	66.7±0.3	this work
	SP			67.2±0.8	Table 27
				66.7±0.6[c]	average
2,5,9,12-tetraoxatridecan-7-ol	T	318.0-371.6	79.8±0.3	85.8±0.4	this work
	SP			85.9±1.1	Table 27
				85.8±0.8[c]	average
1,3-bis(2,2,2-trifluoroethoxy)- -2-propanol	S	293.2-373.2	51.8±0.4	(55.6±0.5)	[86]
	T	278.5-328.4	71.1±0.2	71.6±0.3	this work
	SP			71.4±0.1	Table 27
				71.4±0.1[c]	average
1-methoxy,3-tert-butoxy- -2-propanol	S	293.2-373.2	55.2±0.1	(58.4±0.2)	[86]
	Tb			**64.0±0.6**	Table 27
1,3-di(n-butoxy)-2-propanol	S	293.2-373.2	69.2±0.1	(73.2±0.8)	[86]
	SP			**79.2±0.9**	Table 27
1-butoxy,3-tert-butoxy- -2-propanol	S	293.2-373.2	65.0±0.7	(68.9±0.8)	[86]
	SP			**76.0±0.6**	Table 27
1,3-di(tert-butoxy)-2-propanol	*SP*			**71.8±0.9**	Table 27

[a] Techniques: T = transpiration method; S = static method; *SP* = average value from structure –property correlations (Table 27).

Vapor pressures and vaporisation enthalpies of 1,3-dimethoxy-2-propanol, 1,3-diethoxy-2-propanol, 2,5,9,12-tetraoxatridecan-7-ol have been measured for the first time. Absolute vapor pressures of a series of glycerol based ethers, including the 1,3-di-isopropoxy-2-propanol and 1,3-bis(2,2,2-trifluoroethoxy)-2-propanol were measured by Garcia *et al.* [86] (Figure C. 1, Figure C. 2) by using the static method. To our surprise, there is great disagreement between the static and our transpiration results. The only possible reason is that during the static measurements, the amount of water remaining in the samples was responsible for the systematic pressure increase at all temperatures. In contrast, in our transpiration (or gas-saturation) experiments we were able to withdraw the residual water amount by long flashing of the sample inside the saturator with the carrier gas. This was done before the start of the vapor pressure determination at an elevated temperature that was close to the upper limit of the temperature range. The absence of traces of water was demonstrated by a series of experiments at this temperature where the vapor pressure remained constant within the reasonable time. In order to ascertain our transpiration results, the vapor pressures of 1,3-diethoxy-2-propanol were additionally measured by the static method

(Table C. 7). However, the vapor pressures of 1,3-diethoxy-2-propanol as measured by both methods were in very good agreement (Figure C. 2).

Garcia *et al.* [86] did not derive vaporization enthalpies from their results. For the sake of comparison, their experimental vapor pressures were treated with Equations 2, 8 and 9 and vaporization enthalpies of the 1,3-di-isopropoxy-2-propanol and 1,3-bis(2,2,2-trifluoroethoxy)-2-propanol, as well as for 1-methoxy,3-tert-butoxy-2-propanol, 1,3-di(n-butoxy)-2-propanol, 1-butoxy,3-tert-butoxy-2-propanol were estimated and adjusted to the reference temperature $T = 298.15$ K by using the $\Delta_l^g C_{p,m}^o$–values given in Table 20. in the same way as our own transpiration results. These results are compiled in Table 22. It has turned out that vaporization enthalpies for 1,3-di-isopropoxy-2-propanol and 1,3-bis(2,2,2-trifluoroethoxy)-2-propanol derived from the static experiments are significantly lower in comparison with our new transpiration results. Also, their $\Delta_l^g H_m^o$(298.15 K)-results for 1-methoxy,3-tert-butoxy-2-propanol, 1,3-di(n-butoxy)-2-propanol, 1-butoxy,3-tert-butoxy-2-propanol seem to be in error.

3.2.3. Validation of experimental vaporization enthalpies with help of the normal boiling temperatures

Table 23. Correlation of vaporization enthalpies, $\Delta_l^g H_m^o$(298.15 K), of alkoxyethanols and glycerol ethers with their T_b normal boiling points.

R	T_b[a]	$\Delta_l^g H_{m(exp)}^o$[b]	$\Delta_l^g H_{m(calc)}^o$[c]	Δ
	K	kJ·mol⁻¹	kJ·mol⁻¹	kJ·mol⁻¹
R-O-CH₂-CH₂-OH				
Me	397.2	45.2	46.7	-1.5
Et	408.8	48.2	49.0	-0.8
iPr	417.6	50.1	50.8	-0.7
nBu	441.5	56.6	55.5	1.1
tBu	428.1	52.8	52.9	-0.1
CH₃OCH₂	466.1	61.2	60.5	0.7
R-O-CH₂-CH(OH)-CH₂-O-R				
Me/Me	445.7	58.0	56.4	1.6
Et/Et	465.1	61.8	60.3	1.5
iPr/iPr	510.2	66.7	69.2	-2.5
tBu//Me	490.3		65.3	
nBu/nBu	558.2		78.8	
nBu/tBu	547.5		76.7	
tBu/tBu	536.1		74.4	

[a] Boiling points, T_b, [48], [b] data from Table C. 8 and Table 21, [c] calculated using Equation 43.

Having in mind, that the vaporization enthalpies of 1,3-dimethoxy-2-propanol, 1,3-diethoxy-2-propanol, 2,5,9,12-tetraoxatridecan-7-ol have been measured for the first time, as well as that significant data disagreement was observed for 1,3-di-isopropoxy-2-propanol and 1,3-

bis(2,2,2-trifluoroethoxy)-2-propanol, any kind of validation for our new data is highly desired. A correlation of the enthalpies of vaporization with the normal boiling temperatures is one of the possible options to establish the consistency of the $\Delta_l^g H_m^o$(298.15 K)-results [24,54]. The literature data available on the normal boiling temperatures, T_b, for the glycerol ethers of the general formula R-O-CH$_2$-CH(OH)-CH$_2$-O-R were taken for correlation with the $\Delta_l^g H_m^o$(298.15 K)-values measured in this work with help of the transpiration method (Table 23). In order to extend database for this correlation we additionally involved a series of alkoxy-ethanols R-O-CH$_2$-CH$_2$-OH (R = Me, Et, iPr, n-Bu, tBu, and CH$_3$OCH$_2$), where reliable data on vaporization enthalpies are available (Table C. 10). The high quality and consistency of the available $\Delta_l^g H_m^o$(298.15 K)-values for alkoxy-ethanols has been separately confirmed by correlation with their normal boiling temperatures (Table C. 10). Numerical values used for the the $\Delta_l^g H_m^o$(298.15 K)- T_b correlation are given in Table 23.

Table 24. Correlation of vaporization enthalpies, $\Delta_l^g H_m^o$(298.15 K), of fluoroalkachols with their T_b normal boiling points.

CAS	Compound	$T_b{}^a$	$\Delta_l^g H_{m(exp)}^{o}{}^b$	$\Delta_l^g H_{m(calc)}^{o}{}^c$	Δ
		K	kJ·mol^{-1}	kJ·mol^{-1}	kJ·mol^{-1}
75-89-8	CF$_3$CH$_2$-OH	347.1	44.0	43.7	0.3
374-01-6	CF$_3$CH(CH$_3$)-OH	351.1	44.8	44.6	0.2
2358-54-5	CF$_3$CH$_2$-O-CH$_2$CH$_2$-OH	406.5	-	57.3	
691-26-9	CF$_3$CH$_2$-OCH$_2$-CH(OH)-CH$_2$O-CH$_2$CF$_3$	470.1	71.6	71.8	-0.2
76-37-9	CHF$_2$-CF$_2$CH$_2$-OH	385.1	53.6	52.4	1.2
422-05-9	CF$_3$-CF$_2$CH$_2$-OH	355.1	44.4	45.6	-1.2
2240-88-2	CF$_3$-CH$_2$CH$_2$-OH	372.6	-	49.6	

^{a} Boiling points, T_b, [48], ^{b} data from Table C. 8, ^{c} Calculated using Equation 44.

It has turned out, that the $\Delta_l^g H_m^o$(298.15 K)-values correlate linearly with T_b values with both sets of glycerol ethers and alkoxy-ethanols. For the joined set (Table 23), we derived the following linear correlation:

$$\Delta_l^g H_m^o(298.15 \text{ K}) / (\text{kJ·mol}^{-1}) = -32.5 + 0.1993 \times T_b \text{ with } (R^2 = 0.959) \qquad (43)$$

As can be seen from Table 23, enthalpies of vaporization determined by Equation 43 agree with the experimental values on the general level around 1 kJ·mol^{-1}. The only significant deviation of 2.5 kJ·mol^{-1} was found for 1,3-di-isopropoxy-2-propanol. However, it should be mentioned that the boiling temperatures for this compound are in disarray, *e.g.* 485-489 K [87] and 475 K [86] are significantly lower than the value taken into the correlation (Table 23).

It is well established, that fluorine-containing compounds exhibit peculiar thermochemical properties compared to their hydrocarbon analogues [88,89]. For example, the enthalpy of

vaporization of (2,2,2-trifluoroethyl)-benzene $\Delta_l^g H_m^o$(298.15 K) = 46.1 kJ·mol^{-1} [90] is significantly higher compared to the similarly shaped ethylbenzene $\Delta_l^g H_m^o$(298.15 K) = 42.3 kJ·mol^{-1} [91]. For this reason, the fluorine-containing glycerol ether 1,3-bis(2,2,2-trifluoroethoxy)-2-propanol does not fit the correlation developed by Equation 43. Hence, we additionally collected boiling points and vaporization enthalpies of a series of fluoroalkachols (Table 24) in order to establish consistency of the new $\Delta_l^g H_m^o$(298.15 K)-value for 1,3-bis(2,2,2-trifluoroethoxy)-2-propanol separately. For these fluorine-containing compounds (Table 24), we derived the following linear correlation:

$$\Delta_l^g H_m^o(298.15 \text{ K}) /(\text{kJ·mol}^{-1}) = -35.6 + 0.2285 \times T_b \text{ with } (R^2 = 0.995) \tag{44}$$

It is apparent from Table 23, that the theoretical enthalpies of vaporization estimated by Equation 44 agree with the experimental values on the general level around 1 kJ·mol^{-1}. Also, the vaporization enthalpy of 1,3-bis(2,2,2-trifluoroethoxy)-2-propanol fits perfectly in this correlation (Table 23). The good quality correlations of the $\Delta_l^g H_m^o$(298.15 K)-values with T_b values could be considered as the indicator for consistency of our new results with the data available in the literature for the similarly shaped compounds. It can be seen from Table 22 and Table 23, that differences between experimental and calculated according to Equation 43 or Equation 44 values are mostly below 1 kJ·mol^{-1}. Consequently, the uncertainties of enthalpies of vaporization which are estimated from the correlation $\Delta_l^g H_m^o$(298.15 K) – T_b are evaluated with ±1.0 kJ·mol^{-1}.

3.2.4. Structure-property relationships: validation of experimental vaporization enthalpies

Structure-property relationships in organic chemistry are always helpful to establish consistency of available experimental data.

3.2.4.1. Correlation between structurally similar compounds

It is reasonable to expect parallels between in $\Delta_l^g H_m^o$(298.15 K) in series of glycerol ethers R-O-CH$_2$-CH(OH)-CH$_2$-O-R with the vaporization enthalpies of similarly shaped alkoxyethanols R-O-CH$_2$-CH$_2$-OH. We plotted these enthalpies in Figure 13, with the numerical data compiled in Table 25. From these data, we derived the following linear correlation:

$$\Delta_l^g H_m^o(298.15 \text{ K})_{GE} /(\text{kJ·mol}^{-1}) = -22.2 + 1.765 \times \Delta_l^g H_m^o(298.15 \text{ K})_{AE} \text{ with } (R^2 = 0.997) \tag{45}$$

As can be seen from Table 25, enthalpies of vaporization determined by Equation 45 agree with the experimental values on the general level around 1 kJ·mol^{-1}. Hence, these quantitatively logical structure-property relationships between glycerol ethers and the parent alkoxyethanols can be considered as a strong evidence of consistency for vaporization enthalpies evaluated in this study.
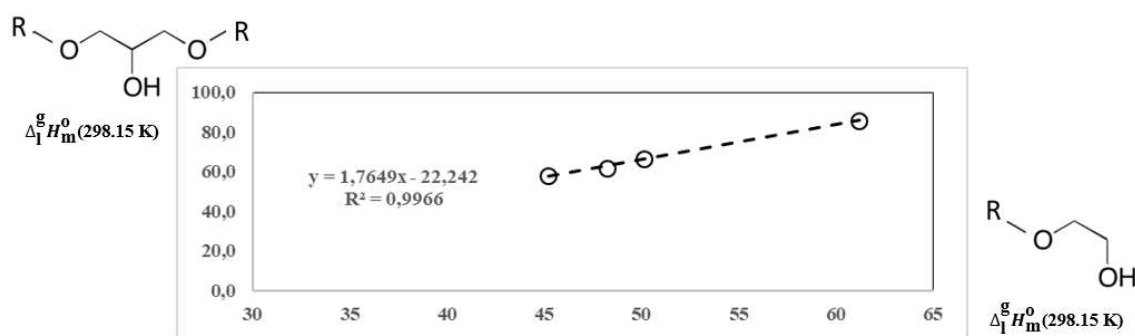
Figure 13. Correlation of vaporization enthalpies $\Delta_l^g H_m^o$(298.15 K) of glycerol ethers R-O-CH$_2$-CH(OH)-CH$_2$-O-R with the vaporization enthalpies of similarly shaped alkoxyethanols R-O-CH$_2$-CH$_2$-OH (data are in kJ·mol^{-1}).

Table 25. Correlation of vaporization enthalpies, $\Delta_l^g H_m^o$(298.15 K), of alkoxyethanols (AE) with those of glycerol ethers (GE), data are in kJ·mol^{-1}.

R	R-O-CH$_2$-CH$_2$-OH Exp.[a]	R-O-CH$_2$-CH(OH)-CH$_2$-O-R Exp.[b]	Calc.[c]	Δ
Me	45.2	58.0	57.6	0.4
Et	48.2	61.8	62.9	-1.1
iPr	50.1	66.7	66.2	0.5
Bu	56.6	-	77.7	-
tBu	52.8	-	71.0	-
CH$_3$OCH$_2$	61.2	85.8	85.8	0.0

[a] Experimental data from Table C. 8, [b] data from Table 21, [c] Calculated using Equation 45.

3.2.4.2. Assessment of vaporization enthalpies based on the structural analogy

Vaporization enthalpy is the measure of intensity of the *inter*-molecular interactions in the liquid state. However, *inter*-molecular interactions in the glycerol ethers and in the alkoxyethanols are complemented with the *intra*-molecular hydrogen bonding (HB) between hydroxyl and ether groups [92]. The strength of this *intra*-molecular HB is definitely dependent on the substituents R attached to the ether group. The apparent structural analogy between alkoxyethanols and glycerol ethers is presented in Figure 14.
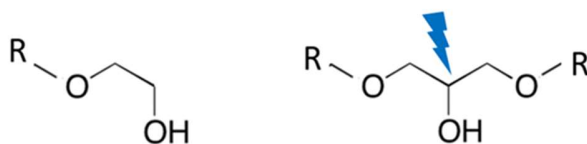
Figure 14. Apparent structural analogy between alkoxyethanols and glycerol ethers.

Indeed, the R-O-CH$_2$-CH$_2$-OH structure can be considered as the substructure of the glycerol ethers R-O-CH$_2$-CH(OH)-CH$_2$-O-R. This structural pattern could be used for a quick appraisal of

vaporization enthalpies of the glycerol ethers as well as for the test of the data consistency as follows.

Let us consider the $\Delta_{l}^{g} H_{m}^{o}(298.15\,\text{K}) = 48.2$ kJ·mol^{-1} [91] of 2-ethoxy-ethanol as the starting value for the developing a system of contributions to the enthalpy of vaporization. The choice of this particular molecule is stipulated by the observation that as a rule the thermodynamic properties of the first representative (usually methyl-substituted) of a homologous series of organic and ionic compounds are slightly different (or non-additive) compared to the other members of the series (*e.g.* ethyl, propyl, butyl, *etc.*) [23,93]
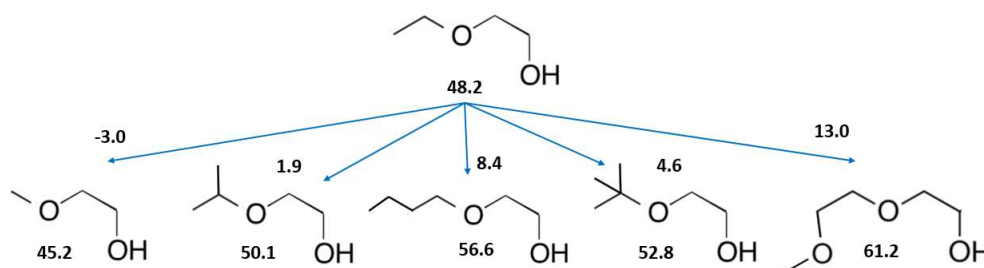
Figure 15. Developing a system of contributions Δ^{R} to the enthalpy of vaporization based on the $\Delta_{l}^{g} H_{m}^{o}(298.15\,\text{K}) = 48.2$ kJ·mol^{-1} of 2-ethoxy-ethanol [91]. Experimental vaporization enthalpies of 2-methoxyethanol, 2-isopropoxyethanol, 2-n-butoxyethanol, 2-tertbutoxyethanol, and 3,6-dioxa-1-heptanol are given in Table C. 8.

Table 26. Comparison of experimental and theoretical vaporization enthalpies, $\Delta_{l}^{g} H_{m}^{o}(298.15\,\text{K})$, of glycerol ethers (data are in kJ·mol^{-1}).

R-O-CH$_2$-CH(OH)-CH$_2$-O-R	Exp.[a]	Eq.44[b]	Eq.45[c]	Eq.46[d]	Eq.47[e]	Theor.[f]	Δ
1	2	3	4	5	6	7	8
Me/Me	58.0±0.5	56.4	57.6	55.8	55.4	56.3±0.5	1.7
Et/Et	61.8±0.4	60.3	62.9	-	-	61.6±1.3	0.2
iPr/iPr	66.7±0.3	69.2	66.2	65.6	67.9	67.2±0.8	-0.5
tBu//Me	(58.4±0.2)	65.3		63.4	63.4	**64.0±0.6**	*-5.6*
nBu/nBu	(73.2±0.8)	78.8	77.7	78.6	81.7	**79.2±0.9**	*-6.0*
nBu/tBu	(68.9±0.8)	76.7		74.8	76.4	**76.0±0.6**	*-7.1*
tBu/tBu	-	74.4	71.0	71.0	71.0	71.8±0.9	-
CH$_3$OCH$_2$/CH$_2$OCH$_3$	85.8±0.4	-	85.8	87.8	84.0	85.9±1.1	-0.1
CF$_3$CH$_2$/CH$_2$CF$_3$	71.6±0.3	71.8 [g]	-	-	71.3	71.5±0.1	0.1

[a] Experimental data from Table 22, [b,c] calculated using Equation 44, [c] calculated using Equation 45, [d] calculated analogously to Equation 477, [e] calculated analogously to Equation 8, [f] Average value calculated from results given in columns 3-6, [f] Calculated using Equation. 43.

As it shown in Figure 15 we have calculated the individual differences Δ^{R}, when systematically subtracted experimental vaporization enthalpy of 2-ethoxyethanol from experimental vaporization enthalpies of 2-methoxyethanol, 2-isopropoxyethanol, 2-n-butoxyethanol, 2-tert-butoxyethanol, and 3,6-dioxa-1-heptanol. What these differences Δ^{R} are talking about? They are generally

reflecting two contributions. The first one accounts for the changing of the alkylsubstituent (length and branching). The second contribution is responsible for the impact of type of the alkylsubstituent on the strength *intra*-molecular HB. Having in mind the disagreement between our new $\Delta_l^g H_m^o$(298.15 K)-values with the results from Garcia *et al.* [86] it is very practical to use the Δ^R-values to assess the expected value of vaporization enthalpy for the glycerol ethers. To do this we used the 1,3-di-ethoxy-2-propanol as the starting or the "centerpiece" molecule with the $\Delta_l^g H_m^o$(298.15 K) = 61.8 kJ·mol^{-1} (Table 22). Thus, in order to assess the vaporization enthalpy *e.g.* of 1,3-diisopropoxy-2-propanol we simply need to add two contributions Δ^{iPr} = 1.9 kJ·mol^{-1} (Figure 15) to the experimental vaporization enthalpy of 1,3-diethoxy-2-propanol:

$$\Delta_l^g H_m^o(298.15 \text{ K, 1,3-di-isopropoxy-2-propanol}) = \Delta_l^g H_m^o(298.15 \text{ K, 1,3-di-ethoxy-2-propanol}) +$$

$$2\times\Delta^{iPr} = (61.8 + 2\times1.9) = 65.6 \text{ kJ·mol}^{-1} \qquad (46)$$

This estimate is in a good agreement with the transpiration result $\Delta_l^g H_m^o$(298.15 K, 1,3-di-isopropoxy-2-propanol) = 66.7±0.3 kJ·mol^{-1} (Table 22). Following this way, we have estimated vaporization enthalpies of all glycerol ethers measured in this work. Results are compiled in Table 26, column 5. Comparison of experimental and theoretical values, estimated according to Equation 46 reveal an agreement at the level generally below 2 kJ·mol^{-1}. Taking into account the simplified way to estimate the desired quantity, such an agreement could be considered as sufficient to establish internal consistency of the new experimental data.

3.2.4.3. Evaluation of vaporization enthalpies based on the "centerpiece" model

Evaluation of vaporization enthalpies based on the structural analogy is very simple and ostensive procedure, provided that sufficient amount of structural analogous with the reliable thermodynamic data can be found in the literature. However, in order to generalize this approach, it is reasonable to develop evaluation of vaporization enthalpies based on the "centerpiece" model combined with a group-additivity increments.

To do this we again start with the 1,3-diethoxy-2-propanol as the "centerpiece" molecule with the $\Delta_l^g H_m^o$(298.15 K) = 61.8 kJ·mol^{-1} (Table 22). In order to modify this "centerpiece" 1,3-diisopropoxy-2-propanol into the required 1,3-di-isopropoxy-2-propanol we suggest the pathway illustrated in Figure 16. In general, we need only to reshape the *ethyl* substituent into the *iso-propyl* substituent (both at the left and the right side of the molecule) by subtracting of two CH$_2$[O, C] increments and by addition of two CH [O, 2C] increments instead. One of the CH$_3$[C] groups was already present in the starting structure, hence we attach two additional CH$_3$[C] groups (also both at the left and the right side). The numerical values of increments are given in Table 27. The final

theoretical value of 1,3-diisopropoxy-2-propanol vaporization enthalpy is expressed by the following equation:

$\Delta_l^g H_m^o$(298.15 K, 1,3-di-isopropoxy-2-propanol) = $\Delta_l^g H_m^o$(298.15 K, 1,3-di-ethoxy-2-propanol) -

2×CH$_2$[O, C] + 2×CH[O, 2C] + 2×CH$_3$[C] = (61.8 - 2×3.21 + 2×0.60 + 2×5.65) = 67.9 kJ·mol^{-1} (47)

Table 27. Group-additivity values for calculation of enthalpies of formation and enthalpies of vaporization of glycerol ethers at 298.15 K (in kJ·mol^{-1}).

Increment	$\Delta_l^g H_m^o$(298.15 K)	$\Delta_f H_m^o$(g, 298.15 K)
CH$_3$[C] = CH$_3$[O]	5.65	-41.8
CH$_2$[2C]	4.98	-20.9
CH[3C]	3.01	-10.0
C[4C]	0.01	-0.4
O[2C]	7.89	-100.1
CH$_2$[O, C]	3.21	-33.6
CH[O, 2C]	0.60	-26.1
C[O, 3C]	-0.30	-16.4
CH$_2$[OH, 2C]	4.70	-33.2
CH[OH, 3C]	2.05	-29.1
OH[C]	32.15	-159.7
CF$_3$[C]	10.45[b]	-

[a] The numerical values of increments from [81,94,95], [b] Derived as described in Figure C. 4.

These data are also in a good agreement with the transpiration result $\Delta_l^g H_m^o$(298.15 K, 1,3-di-isopropoxy-2-propanol) = 66.7±0.3 kJ·mol^{-1} (Table 21). Following this way, we have estimated vaporization enthalpies of all glycerol ethers measured in this work. Results are compiled in Table 26, column 6. The theoretical values, estimated according to Equation 47 are in agreement with the transpiration results (the deviations are generally below 2 kJ·mol^{-1}) proving the internal consistency of the new experimental data.
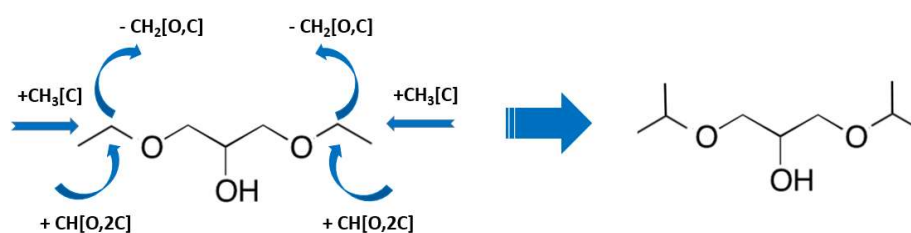
Figure 16. Using the 1,3-diethoxy-2-propanol as the "centerpiece" for estimation vaporization enthalpy of 1,3-diisopropoxy-2-propanol with help of increments given in Table 27.

The structure-property relationships discussed in Section 3.4 has helped to establish the internal consistency of *experimental* and *theoretical* $\Delta_l^g H_m^o$(298.15 K)-values. The compilation of the *theoretical* results is given in Table 26 (columns 3-6). In order to get more confidence, we have averaged the results from different theoretical approaches and the averaged value is given in Table 26, column 7. These *theoretical* values (Table 26, column 7) can be now fair compared with the

experimental results (Table 26, column 2). As it apparent from Table 26, column 8, the agreement is excellent at the level generally below 0.5 kJ·mol⁻¹. Even the somewhat larger deviation (of 1.7 kJ·mol⁻¹) observed for 1,3-dimethoxy-2-propanol is quite expected due to the peculiarities of the first representatives of homologous series, as it has been already mentioned above. In this context, the systematic deviations (at the level of 7 kJ·mol⁻¹) of $\Delta_l^g H_m^o$(298.15 K)-results for 1-methoxy,3-tert-butoxy-2-propanol, 1,3-di-(n-butoxy)-2-propanol, and 1-butoxy,3-tert-butoxy-2-propanol (Table 26, column 2) seem to be the clear evidence of problems with the static method used by Garcia *et al.* [86]. As a consequence, we suggest the *theoretical* values given in bold in Table 26 (column 7) as the reliable $\Delta_l^g H_m^o$(298.15 K)-values for the thermochemical calculations with these three glycerol ethers.

3.2.5. Standard molar enthalpies of formation from combustion calorimetry

Specific energies of combustion $\Delta_c u°$ were calorimetrically measured in series of five experiments for each glycerol ether. Auxiliary quantities required for the reduction of the combustion results are collected in Table C. 11. Compilation of combustion results for $\Delta_c u°$ and $\Delta_c H_m^o$ with glycerol ethers are given in Table C. 12. These results where referenced to the following reactions:

1,3-dimethoxy-2-propanol: $C_5H_{12}O_3$(liq) + 6.5×O_2(g) = 5×CO_2(g) +6×H_2O(liq) (48)

1,3-diethoxy-2-propanol: $C_7H_{16}O_3$(liq) + 9.5×O_2(g) = 7×CO_2(g) +8×H_2O(liq) (49)

1,3-di-isopropoxy-2-propanol: $C_9H_{20}O_3$(liq) + 12.5×O_2(g) = 9×CO_2(g) +10×H_2O(liq) (50)

2,5,9,12-tetraoxatridecan-7-ol: $C_9H_{20}O_5$(liq) + 11.5×O_2(g) = 9×CO_2(g) +10×H_2O(liq) (51)
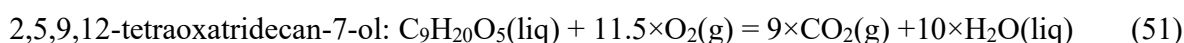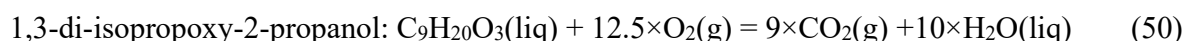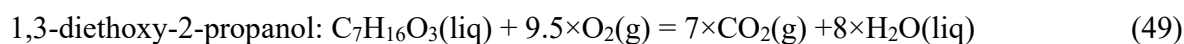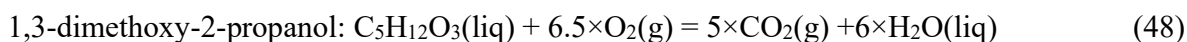
Combustion experiments with 1,3-bis(2,2,2-trifluoroethoxy)-2-propanol require rotating-bomb combustion calorimeter. Unfortunately, this device was under reconstruction during period of the current project. Combustion experiments with glycerol ethers were performed for the first time and the final results are compiled in Table 28, column 3.

Table 28. Compilation of thermochemical data for glycerol ethers at *T*=298.15 K (*p*°=0.1 MPa, in kJ·mol⁻¹).

compound	$\Delta_c H_m^o$(liq)	$\Delta_f H_m^o$(liq)	$\Delta_l^g H_m^{o\,a}$	$\Delta_f H_m^o$(g)$_{exp}$	$\Delta_f H_m^o$(g)$_{theor}$[b]
1	2	3	4	5	6
1,3-dimethoxy-2-propanol	-084.4±1.6	-598.1±1.8	57.3±1.4	-540.8±2.3	-540.5±1.5
1,3-diethoxy-2-propanol	-4370.2±1.3	-671.1±1.6	61.5±0.4	-609.6±1.6	-609.6±2.1
1,3-diisopropoxy-2-propanol	-5654.9±2.5	-745.0±2.8	66.7±1.2	-678.3±3.0	-680.7±2.1
2,5,9,12-tetraoxatridecan-7-ol	-5442.1±2.3	-957.8±2.6	85.8±1.6	-872.0±3.1	-868.1±2.1
1,3-bis(2,2,2-trifluoroethoxy)-2-propanol			71.4±0.2		-1902.7±2.1

[a] From Table 21., [b] averaged quantum-chemical results from G3MP2, G4MP2 and G4, calculations (Table 27).

3.2.6. Gas-phase standard molar enthalpies of formation: experiment and theory

The experimental gas-phase standard molar enthalpies of formation $\Delta_f H_m^o(g)_{exp}$ are derived (Table 28, column 5) from the evaluated experimental vaporization enthalpies (Table 21) and results from combustion calorimetry (Table C. 12) according to common thermochemical equations:

$$\Delta_f H_m^o(g, 298.15 \text{ K})_{exp} = \Delta_l^g H_m^o(298.15 \text{ K}) + \Delta_f H_m^o(\text{liq}, 298.15 \text{ K})_{exp} \qquad (52)$$

Since thermochemical data on glycerol ethers were measured for the first time, we used the high-level quantum-chemical calculations to support the reliability of our new results. In the past decade, the high-level composite quantum-chemical methods become a valuable tool for obtaining *theoretical* $\Delta_f H_m^o(g, 298.15)$-values with so-called "chemical accuracy" of 4-5 kJ·mol^{-1} [30,96,97]. The quantum-chemical methods differ considerably in terms computing power and time. In this work we tested G3MP2, G4MP2 and G4 methods to get the *theoretical* $\Delta_f H_m^o(g, 298.15)$-values of glycerol ethers for validation of our new *experimental* results. An agreement or disagreement between the *theoretical* and *experimental* $\Delta_f H_m^o(g, 298.15 \text{ K})$-values provides a valuable indicator of the data mutual consistency.

1,3-dimethoxy-2-propanol   1,3-diethoxy-2-propanol   1,3-di-isopropoxy-2-propanol

2,5,9,12-tetraoxatridecan-7-ol   1,3-bis(2,2,2-trifluoroethoxy)-2-propanol
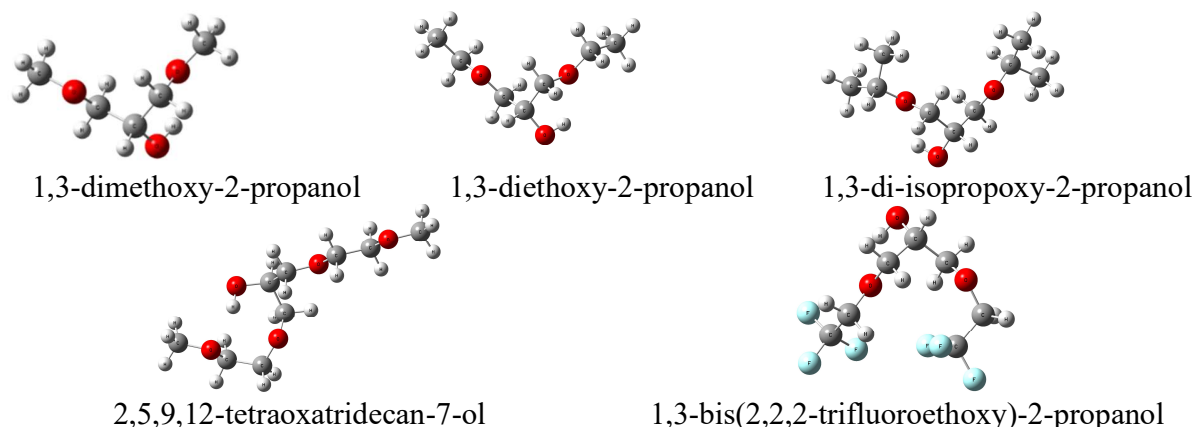
Figure 17. The most stable conformers of glycerol ethers: 1,3-dimethoxy-2-propanol, 1,3-diethoxy-2-propanol, 1,3-diisopropoxy-2-propanol, 2,5,9,12-tetraoxatridecan-7-ol, and 1,3-bis(2,2,2-trifluoroethoxy)-2-propanol.

The search for the lowest energy conformers was carried out in three steps ((MD $\rightarrow$ GGA DFT functional $\rightarrow$ Meta-GGA DFT functional) using the ADF 16 program [36]. First, all possible conformers of glycerol ethers were generated with the preservation of connectivity (molecular graph) and in each case, the structure was optimized by the method of molecular mechanics in the UFF force field. Further, the geometry of the first 100 low-lying conformers of the considered ethers was optimized within the framework of PBE/DZP on a large grid, and for the obtained 50 lowest-energy conformers (PBE/DZP), the structure was re-optimized using M06L/DZP on an

ultra-large grid. In each case, Slater Cartesian orbitals were used. It should be noted that after each of the three steps, the sequence of energy-aligned structures of glycerol ethers was different (although the differences in total electron energy were insignificant in the range of 1-3 kJ·mol⁻¹). Therefore, for the first three low-lying conformers obtained using both PBE/DZP and M06L/DZP, the enthalpy of formation was calculated using the composite methods G3MP2 [98], G4MP2 [99], and G4 [100] methods in the GAUSSIAN 09 program [101]. It was found that the differences between the stable conformers did not exceed 3 kJ·mol⁻¹.

Admittedly, the glycerol ethers are flexible molecules, but it has been found that the most stable conformer for each ether differs from other less stable conformers by 5-6 kJ·mol⁻¹. According to our general experience, for such case only the most stable conformer contributes to the theoretical enthalpy of formation, and conformers with the energy difference $\geq$ 5-10 kJ·mol⁻¹ are practically not populated in the gas phase [102]. Such a simplification can be used for large molecules with abundant flexibility with sufficient accuracy. For example, for glycerol a theoretical value $\Delta_f H_m^o$(g, 298.15 K) = -582.9 kJ·mol⁻¹ for calculated for a single most stable conformer by using the G4 method and the atomization procedure is already in very good agreement with the recommended experimental result $\Delta_f H_m^o$(g, 298.15 K)$_{exp}$ = -578.8±0.6 kJ·mol⁻¹ [102]. As a consequence, all theoretical enthalpies of formation in this work were derived from the most stable conformers of glycerol ethers, which are shown in Figure 17.

Table 29. Experimental and theoretical gas-phase enthalpies of formation $\Delta_f H_m^o$(g) at T = 298.15 K (p° = 0.1 MPa) for glycerol ethers as calculated by different methods (in kJ·mol⁻¹).

compound	G3MP2 AT[b]	G4MP2 AT[c]	G4 AT[d]	G4 WBR	$\Delta_f H_m^o$(g)$_{theor}$ [e]	Exp.[a]
1,3-dimethoxy-2-propanol	-540.9	-540.4	-540.3	-540.5[f]	-540.5±1.5	-540.8±2.3
1,3-diethoxy-2-propanol	-611.4	-608.9	-609.0		-609.6±2.1	-609.6±1.6
1,3-di-isopropoxy-2-propanol	-683.7	-679.5	-679.8		-680.7±2.1	-678.3±3.0
2,5,9,12-tetraoxatridecan-7-ol	-870.2	-866.0	-869.0		-868.1±2.1	-872.0±3.1
1,3-bis(2,2,2-trifluoroethoxy)-2-propanol	-1917.3	-1899.0	-1896.2		-1902.7±2.1	

[a] From Table 28, [b] calculated by the G3MP2 method according to the atomization procedure and corrected with Equation 53 (Table C. 13), [c] calculated by the G4MP2 method according to the atomization procedure and corrected with Equation 54 (Table C. 14), [d] calculated by the G4 method according to the atomization procedure and corrected with Equation 55 (Table C. 15), [e] the *theoretical* value; calculated as the average from G3MP2, G4MP2 and G4 results, [f] average value calculated by the G4 method according to the well-balanced reactions (Figure C. 5, Table C. 16).

The H_{298}-values have been converted to the standard molar enthalpies of formation $\Delta_f H_m^o$(g, 298.15 K)$_{theor}$ using the atomization (AT) reaction. As a rule, the enthalpies of formation derived from the atomization reaction deviate systematically from the experimental values [79]. However, simple linear correlations between the AT-calculated and the *experimental* enthalpies of formation help to "correct" the results and to obtain reliable theoretical values. The *experimental* and

quantum-chemical $\Delta_f H_m^o$(g, 298.15 K)-values, which were used to establish "corrections" are given in Table C. 13 - Table C. 15. The following linear correlations individual for each composite method were established (in kJ·mol^{-1}):

$$\Delta_f H_m^o(g)_{theor} = 1.0050 \times \Delta_f H_m^o(g, AT) + 2.5 \qquad \text{with } R^2 = 0.9998 \qquad \text{for G3MP2} \quad (53)$$
$$\Delta_f H_m^o(g)_{theor} = 1.0015 \times \Delta_f H_m^o(g, AT) - 1.2 \qquad \text{with } R^2 = 0.9998 \qquad \text{for G4MP2} \quad (54)$$
$$\Delta_f H_m^o(g)_{theor} = 0.9965 \times \Delta_f H_m^o(g, AT) + 2.0 \qquad \text{with } R^2 = 0.9998 \qquad \text{for G4} \quad (55)$$

Using these correlations, the "corrected" enthalpies of formation of glycerol ethers have been calculated (Table 29). Another conventional way to convert the H_{298}-values to the standard molar enthalpies of formation $\Delta_f H_m^o$(g, 298.15 K)$_{theor}$ is using the "well-balanced reactions" (*WBR*) [96]. Using the *WBR* method we designed three reactions for 1,3-dimethoxy-2-propanol (Figure C. 5) with the reference compounds where reliable experimental gas-phase enthalpies of formation $\Delta_f H_m^o$(g, 298.15 K) are available in the literature (Table C. 16). The average enthalpy of formation of 1,3-dimethoxy-2-propanol derived from the WBR method is indistinguishable from those calculated by the "corrected" atomization reaction (Table 29). The final gas-phase *theoretical* standard molar enthalpies of formation, $\Delta_f H_m^o$(g)$_{theor}$, are summarized in Table 29. As can be seen from this table, the "corrected" atomization G3MP2, G4MP2 and G4 gas-phase-enthalpies of formation of glycerol ethers are in very close agreement. Therefore, we calculated the weighted average value for each compound in Table 29 and designated it as the *theoretical* values, $\Delta_f H_m^o$(g, 298.15 K)$_{theor}$, for comparison with the *experimental* values, $\Delta_f H_m^o$(g, 298.15 K)$_{exp}$, compiled in Table 28. Comparison of column 5 with column 6 in Table 28 shows good agreement between the *theoretical* and *experimental* $\Delta_f H_m^o$(g, 298.15 K)-values for each compound. This good agreement can be considered as proof of the internal consistency of the thermochemical results evaluated in this work (Table 28).

3.2.7. Evaluation of the gas-phase enthalpies of formation based on the "centerpiece" model

Even if a remarkable correspondence between the *experimental* and *theoretical* $\Delta_f H_m^o$(g, 298.15 K)-values has been established, additional validation of the evaluated results with the aid of structure-property relationships is desirable. In 3.2.4.3 we used the "centerpiece" model for evaluation of vaporization enthalpies. The same model can be applied for evaluation of the gas-phase standard molar enthalpies of formation. In Figure 18 it is shown, how to derive enthalpies of formation of 1,3-diethoxy-2-propanol and 1,3-di-isopropoxy-2-propanol starting from 1,3-dimethoxy-2-propanol.
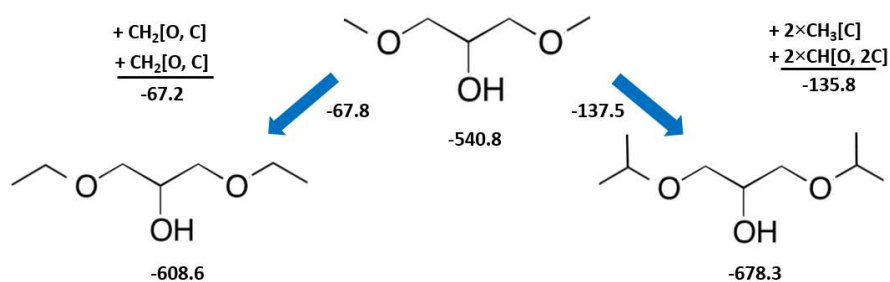
Figure 18. Using the "centerpiece" model for evaluation of the gas-phase standard molar enthalpies of formation, $\Delta_f H_m^o$(g, 298.15 K)$_{exp}$, of 1,3-dimethoxy-2-propanol, 1,3-diethoxy-2-propanol, and 1,3-diisopropoxy-2-propanol. The numerical values are taken from Table 27 and Table 28 and they are given in kJ·mol^{-1}.

Indeed, if we add two enthalpic contributions CH$_2$[O, C] (Table 27) to the experimental value $\Delta_f H_m^o$(g, 298.15 K)$_{exp}$ = -578.8±0.6 kJ·mol^{-1} of 1,3-dimethoxy-2-propanol, we obtain the enthalpy of formation of 1,3-diethoxy-2-propanol (Figure 18). This calculation is very simple to validate: the difference between the experimental enthalpies of formation of 1,3-diethoxy-2-propanol and 1,3-dimethoxy-2-propanol of -67.8 kJ·mol^{-1} is very close to the sim of two contributions CH$_2$[O, C] of -67.2 kJ·mol^{-1}, as it can be seen in Figure 18. In the similar way it is possible to calculate the enthalpy of formation of 1,3-di-isopropoxy-2-propanol starting from the "centerpiece" 1,3-di-methoxy-2-propanol (Figure 18). The good agreement observed among the *theoretical* and *experimental* $\Delta_f H_m^o$(g, 298.15 K)-values for glycerol ethers, as well as the logical structure-property relationships demonstrated on Figure 18 can be considered as an evidence of the internal consistency of thermochemical results evaluated in this work (Table 28).

Chapter 4 Commodity Chemicals and Fuels from Biomass: Thermodynamic Properties of Levoglucosan Derivatives

4.1. Introduction

Cellulose is the inexhaustible, sustainable, and fascinating renewable source for industrially important chemicals and fuels. Cellulose-derived platform chemicals not only offer viable substitutes for most petroleum-based polymers, but also enable the development of novel functional materials [103]. The thermochemical studies of platform chemicals, such as ethylene glycol [92], 5-hydroxymethylfurfural [73,104], levulinic acid [74], lactic acid [105], resulting from the conversion of cellulose have been systematically conducted in our laboratory.

In the focus of this work are dihydro-levoglucosenone (or cyrene) and levoglucosenone (Figure 19). Cyrene may be derived from cellulosic waste and it is considered as a potential "green" replacement for industrial polar aprotic solvents, such as dimethyl-formamide and N-

methyl-pyrrolidinone, that are facing increased regulation for their toxicity [106]. The selective pyrolytic conversion of cellulose or cellulose-containing materials produces levoglucosenone, a highly functionalized chiral structure. The highly functionalized structure of levoglucosenone makes it an attractive chiral synthon for the synthesis of a wide variety of natural and unnatural compounds [107].

dihydro-levoglucosenone
(cyrene) [537716-82-8]

levoglucosenone
[37112-31-5]

levoglucosan
[498-07-7]
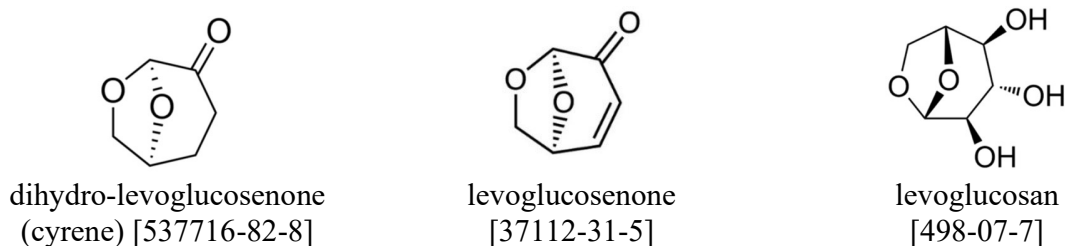
Figure 19. Compounds studied in the research.

Admittedly, reliable thermochemical data are required for the design and development of new compounds and technologies [108–110]. The thermochemical properties of cyrene and levoglucosenone are relevant for large-scale manufacture. In this work we measured vapour pressures of cyrene and levoglucosenone and the standard molar vaporization enthalpies, $\Delta_l^g H_m^o$(298.15 K) were derived. We used calorimetry to measure combustion energies of cyrene and levoglucosenone for the first time. We used different empirical methods, structure-property correlations, and the high-level quantum-chemical calculations for validation and evaluation of new experimental results.

4.2. Results and discussion

All experimental results and intermediate discussion are presented in our article [111]. Due to the subject of the manuscript, it was decided to observe here the part of the research connected with the issue of valorization of levoglucosan derivatives.

4.2.1. Energetics of levoglucosan derivatives valorization

An essential aspect of the use of renewable carbon sources is the production of platform molecules from biomass and the upgrading of these molecules into valuable products. Levoglucosan is the valuable intermediate obtained from thermal degradation of cellulose component of biomass [112]. The general reaction for this process is shown in Figure 20. The enthalpy of this reaction, $\Delta_r H_m^o$(298.15 K) = 156 kJ·mol^{-1}, was calculated according to the Hess´s Law with help of the experimental standard molar enthalpy of formation, $\Delta_f H_m^o$(g, 298.15 K) = -830.4±2.9 kJ·mol^{-1}, of levoglucosan evaluated in this work (Table D. 1) and the $\Delta_f H_m^o$(cr, 298.15 K) = -985±7 kJ·mol^{-1}, per mole of monomeric units for the microcrystalline cellulose [113]. The reaction enthalpy, $\Delta_r H_m^o$(298.15 K) = 44 kJ·mol^{-1}, for this process is significantly lower when

calculations are performed with the liquid phase levoglucosan as the final product. In this case, $\Delta_f H_m^o$(liq, 298.15 K) = -942.1±3.1 kJ·mol^{-1}, of levoglucosan was derived from its $\Delta_f H_m^o$(cr, 298.15 K) and $\Delta_{cr}^l H_m^o$(298.15 K), evaluated in [111] and Table D. 1.
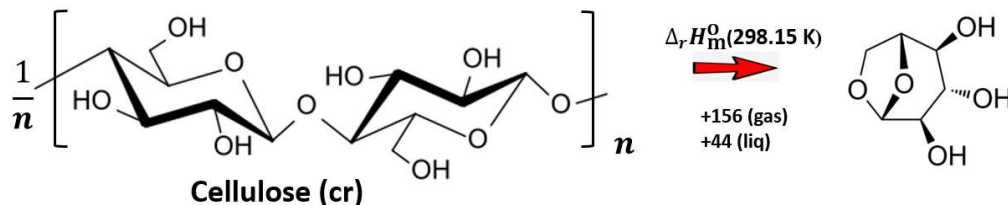
Figure 20. The thermal degradation of cellulose to obtain levoglucosan. The enthalpies of reaction are given in kJ·mol^{-1}.

Levoglucosan can be also obtained from dehydration of biomass-derived sugars [114]. The energetics of this process can be assessed with help of a model reaction with α-D-glucose shown in Figure 21. The enthalpy of this reaction, $\Delta_r H_m^o$(298.15 K) = 202 kJ·mol^{-1}, was calculated with help of the gas-phase experimental standard molar enthalpy of formation of levoglucosan (Table D. 1) and the $\Delta_f H_m^o$(cr, 298.15 K) = -1273.3±1.1 kJ·mol^{-1} [115]. Also, in this case the reaction enthalpy, $\Delta_r H_m^o$(298.15 K) = 46 kJ·mol^{-1}, for this dehydration process is significantly lower when calculations are performed with the liquid phase levoglucosan as the final product.
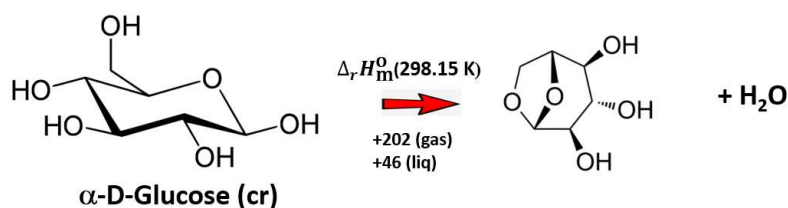
Figure 21. The dehydration of α-D-glucose to obtain levoglucosan. The enthalpies of reaction are given in kJ·mol^{-1}.

There are many ways to use levoglucosan to produce the commodity chemicals [116]. The production of levoglucosenone via levoglucosan dehydration using Brønsted solid acid catalysts in tetrahydrofuran was reported just recently [117]. The reaction is shown in Figure 22.
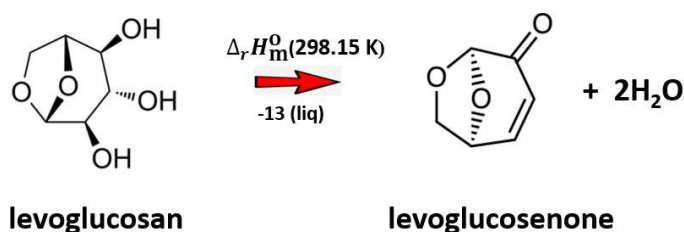
Figure 22. The dehydration of levoglucosan to obtain levoglucosenone. The enthalpy of reaction is given in kJ·mol^{-1}.

The 100% levoglucosan conversion with the levoglucosenone selectivity of up to 59% was achieved. The use of propylsulfonic acid functionalized silica catalysts increased the production of levoglucosenone by a factor of two compared to the use of homogeneous acid catalysts. Such promising reaction parameters open the way for large-scale development of this process. The reaction enthalpy for the reaction shown in Figure 22 is therefore important for optimizing the heat balances. The enthalpy of this reaction, $\Delta_r H_m^o$(liq, 298.15 K) = -12.8±3.9 kJ·mol^{-1}, was calculated with help of the liquid-phase standard molar enthalpy of formation of levoglucosan $\Delta_f H_m^o$(liq, 298.15 K) = -942.1±3.1 kJ·mol^{-1}, and the $\Delta_f H_m^o$(liq, 298.15 K) = -383.3±1.5 kJ·mol^{-1} of levoglucosenone (Table D. 1).

$\Delta_r H_m^o$(298.15 K)

+ H$_2$

-114 (liq)

levoglucosenone   **cyrene**
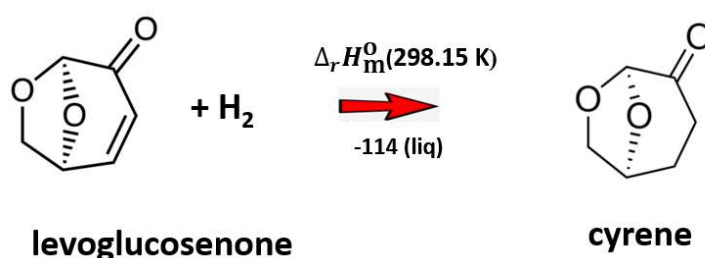
Figure 23. The hydrogenation of levoglucosenone to obtain cyrene (dihydro-levoglucosenone). The enthalpy of reaction is given in kJ·mol^{-1}.

The levoglucosenone can be hydrogenated to cyrene (dihydrolevoglucosenone) according to the reaction given in Figure 23 [116]. The reaction enthalpy, $\Delta_r H_m^o$(liq, 298.15 K) = -114.4±2.3 kJ·mol^{-1}, which was calculated from our new data (Table D. 1) for both reaction participants, is in agreement with the enthalpy of hydrogenation of cyclohexene to cyclohexane, $\Delta_r H_m^o$(liq, 298.15 K) = -117.9±1.0 kJ·mol^{-1}, calculated with data taken from the literature [115]. The relatively high exothermic effect of the hydrogenation reaction must be taken into account when developing the technology for temperature management.

Another promising process of the isomerization of levoglucosenone to hydroxymethyl furfural in an aqueous solvent system with a sulfuric acid catalyst was reported recently [118]. The reaction network is presented in Figure 24. The isomerization enthalpy, $\Delta_r H_m^o$(liq, 298.15 K) = -34.3±2.7 kJ·mol^{-1}, was calculated from our new data for levoglucosenone (Table D. 1) and $\Delta_f H_m^o$(liq, 298.15 K) = -417.6±1.4 kJ·mol^{-1} for hydroxymethyl furfural from our previous work [104]. Furthermore, optimizing the isomerization of levoglucosenone could allow for the production of hydroxymethyl furfural or levulinic acid [74] in high yield, which can in turn be converted to fuels [119] and platform chemicals [104]. The reaction enthalpy, $\Delta_r H_m^o$(liq, 298.15 K) = -74.7±2.5 kJ·mol^{-1}, was calculated from $\Delta_f H_m^o$(liq, 298.15 K) = -425.1±0.4 kJ·mol^{-1} for

formic acid [115] and $\Delta_f H_m^o$(liq, 298.15 K) = -638.8±2.1 kJ·mol^{-1} for levulinic acid from our previous work [74].
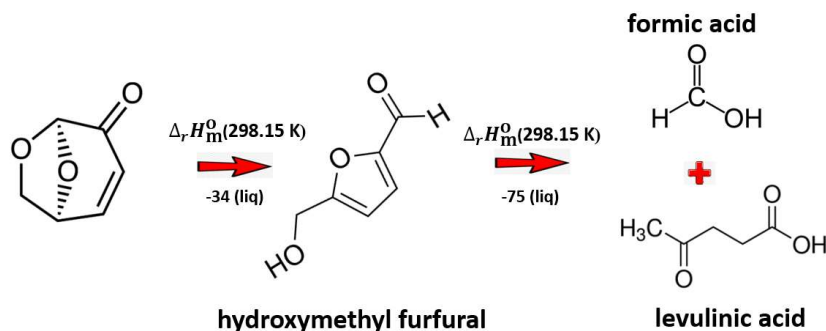
Figure 24. The isomerization of levoglucosenone to hydroxymethyl furfural and subsequent of hydroxymethyl furfural to formic and levulinic acids.

Chapter 5 Prediction of thermodynamic properties. Centerpiece approach applied to aminoalcohols: how do we avoid confusion and get reliable results?

5.1. Introduction

The group additivity (GA) approach offers an excellent way of assessing the thermodynamic properties of molecules whose properties have not been measured. One of the most popular GA approach was developed by Sydney W. Benson [1]. A group is defined by Benson as "a polyvalent atom (ligancy ≥ 2) in a molecule together with all of its ligands." The sum of the groups that constitute a molecule of interest provides a quick appraisal of a thermodynamic property. The GA works well for the gas-phase standard molar enthalpies of formation $\Delta_f H_m^o$(g, 298.15 K). The GA performance for the liquid phase enthalpies of formation, $\Delta_f H_m^o$(liq, 298.15 K), is less successful because the intermolecular interactions between the molecules are randomly distributed among the groups. This fact aggravates the accuracy of the prediction considerably. In contrast, the standard molar enthalpies of vaporization, $\Delta_l^g H_m^o$(298.15 K), obey sufficiently well to the additivity rules. An important step in this direction was made by and co-workers [120] who showed that group additivity can be used to estimate the $\Delta_l^g H_m^o$(298.15 K)-values of organic and organometallic compounds with good precision. In his later work [24], Sydney W. Benson also expanded the GA method for calculating enthalpy of vaporization. We endorsed and followed Benson's approach and re-evaluated the group contributions using the updated $\Delta_f H_m^o$(g, 298.15 K), $\Delta_f H_m^o$(liq, 298.15 K), and $\Delta_l^g H_m^o$(298.15 K) data [81]. The crucial advantage of the Benson´s method is that the energetics of a molecule of interest can be collected from scratch. However, many interactions between nearest and non-nearest neighbour groups, between substituents, and

between fragments of the molecule are not taken into account by this procedure [60]. In the original Benson´s scheme, such interactions are included as a list of individual "non-additive "contributions. However, the variety of possible structures of organic compounds is countless, so that the list of individual "non-additive" contributions can be endless.
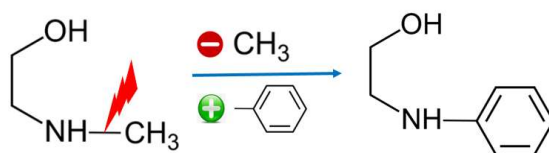
Figure 25. Calculations of vaporization enthalpy, $\Delta_l^g H_m^o$(298.15 K), of 2-(phenyl-amino)-ethanol from 2-(methyl-amino)-ethanol using the "centerpiece" approach.

In our most recent work [25,38] we develop a "centerpiece" approach that is closely related to the conventional group-contribution methods [24,81]. In the latter methods the molecule of interest is collected completely from well-defined group contributions. In contrast, the idea of this "centerpiece" approach is to select a "core" molecule that may possibly close mimic the structure of the molecule of interest, but the selected "centerpiece" molecule has the well-established thermodynamic properties. Different substituents can be attached (or subtracted) to this "centerpiece" in different positions. The visualisation of the "centerpiece" approach is given in Figure 25.

2-(methyl-amino)-ethanol [109-83-1]

1-(dimethylamino)-2-propanol [108-16-7]

2-(dimethylamino)-1-propanol [15521-18-3]

2-(phenyl-amino)-ethanol [122-98-5]

2-(benzyl-amino)-ethanol [104-63-2]
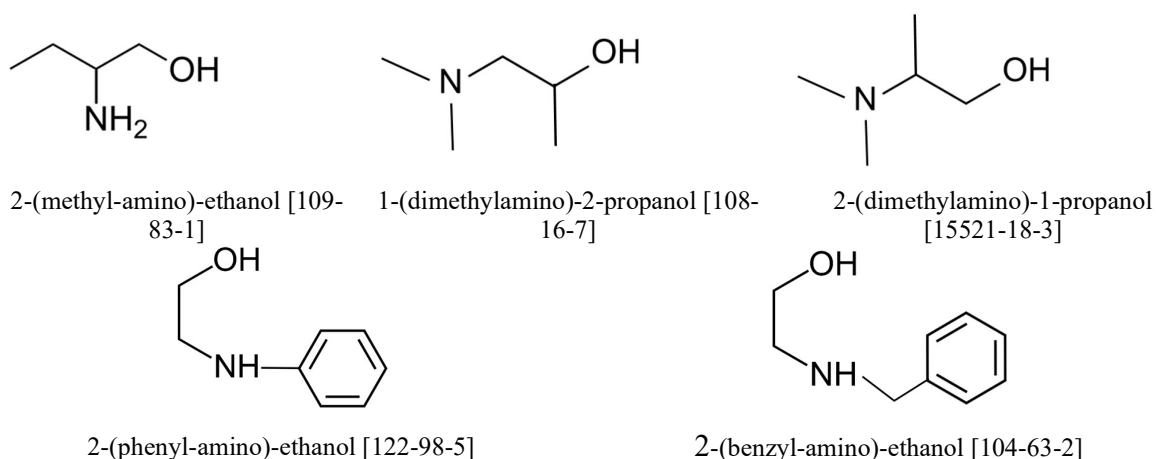
Figure 26. Branched and phenyl-substituted aminoalcohols studied in this work.

For the prediction, *e.g.* the enthalpy of vaporization of 2-(phenyl-amino)-ethanol, a similarly shaped 2-(methyl-amino)-ethanol, can be seen as a well suited "centerpiece". Indeed, the latter molecule already bears the energetic contribution due to the inherent intra-molecular hydrogen bond (intra-HB), which is the most significant feature of amino-ethanols. The experimental vaporization enthalpy of 2-(methyl-amino)-ethanol is well-established in the literature [121,122]. Using this value as the "centerpiece", we can therefore exchange the methyl-

group CH$_3$ with the phenyl-group C$_6$H$_5$ and estimate the desired $\Delta_l^g H_m^o$(298.15 K)-value for of 2-(phenyl-amino)-ethanol. It should be noted that the conventional GA method to such predictions will not work because intra-HB is not parameterized at all. To validate the "centrepiece" approach to aminoalcohols, we examined the series of aminoalcohols shown in Figure 26.

The focus of this work was on vapor pressures measurements and the standard molar vaporization enthalpies, $\Delta_l^g H_m^o$(298.15 K). We used different empirical and structure-property correlation methods for validation and evaluation of new and available experimental results. We used the evaluated $\Delta_l^g H_m^o$(298.15 K)-values for aminoalcohols listed in Figure 26 in order to show the success and limitations of the "centrepiece" approach.

5.2. Results and discussion

5.2.1. Absolute vapor pressures and thermodynamics of vaporization

The primary experimental results on vapor pressures for the DL-2-amino-1-butanol, 1-(dimethylamino)-2-propanol, 2-(phenyl-amino)-ethanol and 2-(benzyl-amino)-ethanol from the transpiration method are summarized in Table E.2.

The vapor pressures for DL-2-amino-1-butanol and 1-(dimethylamino)-2-propanol were measured for the first time. The vapor pressures at different temperatures for 2-(phenyl-amino)-ethanol are reported by Stull [53]. These data correspond to the significantly higher temperature range and a comparison is not possible. The vapor pressures temperature dependence for 2-(benzyl-amino)-ethanol was measured by Razzouk *et al.* [123] using the static method. The comparison of the available data is given in Figure E.1. Our perspiration results are significantly lower compared to those of the static technique. It has turned out that the purity of the sample used by Razzouk *et al.* [123] was only 97.7% according to gas chromatography as determined after vapor pressure measurements. In our experience with the static method, the remaining 2.3% impurities could significantly increase the vapor pressure if the impurities have a higher volatility. However, this apparent disagreement led us to look for additional data that would help resolve the observed contradictions. As a matter of fact, the SciFinder [34] compiles experimental boiling temperatures at various pressures. The accuracy of this data is questionable as it comes from the distillation of a compound after its synthesis and not from special physico-chemical studies. However, the numerous data on boiling temperatures at standard pressure, as well as at reduced pressures provide at least a reliable level of the experimental vapor pressures and a reliable trend of the dependence of the vapor pressure temperature. As can be seen in Figure E.1, the boiling points data agree fair with our transpiration results, but not with those from the static method. After

we have resolved the contradictions observed in this way for 2-(benzyl-amino)-ethanol, we have systematically (Table E. 3) collected the data available in SciFinder for amino alcohols (Figure 26). These data were used to derive vaporization enthalpies of aminoalcohols (Table 30). The "empirical" results derived in this way are designated in Table 30 as *SF*-values. The compilation of the standard molar enthalpies of vaporization of aminoalcohols at the reference temperature T = 298.15 K, calculated according to Equation 8 is given in Table 30.

Table 30. Compilation of the standard molar enthalpies of vaporization $\Delta_l^g H_m^o$ of substituted aminoalcohols.

Compound	M^a	T- range	$\Delta_l^g H_m^o(T_{av})$	$\Delta_l^g H_m^o$(298.15 K)
		K	kJ·mol^{-1}	kJ·mol^{-1}
2-(methyl-amino)-ethanol [109-83-1]				**57.7±0.2** [122]
2-(ethyl-amino)-ethanol [110-73-6]				**60.8±0.2** [124]
DL-2-amino-1-butanol	T	303.2-333.5	64.0±0.4	65.5±0.5
1-(dimethylamino)-2-propanol [108-16-7]	*SF*	333-400	42.3±0.6	47.3±0.7
	T_b	400		44.9±1.5
	T	276.2-308.2	46.3±0.2	45.7±0.3
				45.6±0.2 ^{c}
2-(dimethylamino)-1-propanol [15521-18-3]	SF	341-423	45.8±0.5	51.6±0.7
	T_b	420.5		50.3±1.5
				51.4±0.6
2-(phenyl-amino)-ethanol [122-98-5]	n/a	377.2-552.8	65.5±1.5	78.8±1.7 [53]
	SF	383-560	68.6±1.4	83.6±1.6
	T_b	553		85.0±1.5
	Add			83.3±1.0
	J_x			83.4±1.0
	T	308.1-348.5	79.8±0.3	82.3±0.4
				82.6±0.3
2-(benzyl-amino)-ethanol 104-63-2	S	292.8-362.9	71.7±0.6	(74.5±0.7) [123]
	SF	379-562	78.5±3.6	92.4±3.7
	T_b	(562)		87.0±1.5
	Add			86.2±1.0
	J_x			83.5±1.0
	T	302.2-344.4	82.2±0.3	84.5±0.4
				84.7±0.4

^{a} Techniques: T = transpiration method; S = static method; n/a = method is not available; SF - from experimental boiling temperatures reported at different pressures compiled by the SciFinder [34] (see text); J_x – from correlation of experimental vaporization enthalpies with Kovats´s indices (see text); Add = calculated according to the "centerpiece" approach.

5.2.2. Correlation of vaporization enthalpies with normal boiling temperatures

The relation of vaporization enthalpy to boiling point is a well-established phenomenon and Trouton's rule is the best evidence of this. According to our experience, the amino alcohols are thermally stable compounds, that boil between 400 K and 560 K [48,55,78], depending on their size and structure. In the paper [124] it was established a linear correlation of $\Delta_l^g H_m^o$(298.15 K)-values with T_b values were found for the set containing *primary* and *secondary* aminoalcohols (kJ·mol^{-1}):

$$\Delta_l^g H_m^o(298.15 \text{ K}) = -35.3 + 0.2193 \times T_b \text{ with } (R^2 = 0.966) \tag{56}$$

The results calculated from this correlation were in agreement with those derived from other methods within of ±1.5 kJ·mol^{-1}. Equation 56 was used to calculate vaporization enthalpies of 1-(dimethylamino)-2-propanol, 2-(dimethylamino)-1-propanol, 2-(phenyl-amino)-ethanol, and 2-(benzyl-amino)-ethanol, which are given in Table 30 and designated as the T_b -values.

5.2.3. Kovats´s retention indices for validation of experimental vaporization enthalpies

As anticipated, the following linear correlation was obtained when the $\Delta_l^g H_m^o$(298.15 K)-values are correlated with J_x-values for the structurally parent set of aminoalcohols collected in Table 31:

$$\Delta_l^g H_m^o(298.15\ K)/(kJ·mol^{-1}) = 29.6 + 0.0399 \times J_x \text{ with } (R^2 = 0.996) \qquad (57)$$

Table 31. Correlation of vaporization enthalpies, $\Delta_l^g H_m^o$(298.15 K), of aminoalcohols with their Kovats´s indices (J_x)

| CAS | Compound | J_x [a] | $\Delta_l^g H_m^o$(298 K)$_{exp}$ [b] | $\Delta_l^g H_m^o$(298 K)$_{calc}$ [c] | Δ |
			kJ·mol^{-1}	kJ·mol^{-1}	kJ·mol^{-1}
109-83-1	2-(methyl-amino)-ethanol	700	57.7±0.2 [122]	57.5	0.2
110-73-6	2-(ethyl-amino)-ethanol	786	60.8±0.2 [124]	61.0	-0.2
122-98-5	2-(phenyl-amino)-ethanol	1347	82.3±0.4 [d]	83.3	-1.1
104-63-2	2-(benzyl-amino)-ethanol	1349	84.5±0.4 [d]	83.4	1.1

[a] Kovats´s indices, J_x, on the standard non-polar column OV-1 [125], [b] data from Table 30, [c] calculated with Equation 67, [d] Experimental data measured by using the transpiration method (Table 30).

The "theoretical" results derived from this correlation are given in Table 30 and designated as J_x. The vaporization enthalpies derived from the correlations with Kovats´s indices (Table 31, column 5) are in a good agreement with those obtained by the transpiration method (Table 30). Such good agreement can be seen as additional validation of the experimental data measured in this work by using the transpiration method (Table 30). It can be seen from Table 31, that differences between experimental and calculated according to Equation 57 vaporization enthalpies are at the level of 1 kJ·mol^{-1} in the worst cases. Hence, the uncertainties of enthalpies of vaporization which are estimated from the correlation the $\Delta_l^g H_m^o$(298.15 K) - J_x are evaluated with ±1.0 kJ·mol^{-1}.

5.2.4. Evaluation of available vaporization enthalpies

As can be seen from Table 30, the vaporization enthalpies, $\Delta_l^g H_m^o$(298.15 K), derived from vapor pressures measured by the conventional methods, as well as those derived from the SciFinder [34] data are in good agreement for aminoalcohols compiled in this table. Such a good agreement has reinforced usefulness of the experimental boiling temperatures reported at different pressures compiled by the SciFinder for evaluation of the scarce thermodynamic data. Additional validation of the $\Delta_l^g H_m^o$(298.15 K)-values collected in Table 30 was conducted with the correlation

$\Delta_l^g H_m^o$(298.15 K) – T_b. The results obtained from this correlation agree within the experimental uncertainties with values derived with other methods.

Also, the $\Delta_l^g H_m^o$(298.15 K)-values derived with help chromatographic retention indices, J_x, agree well with values derived for aminoalcohols with other methods. The "theoretical" T_b–values and J_x-values derived from both correlations, as well as the "empirical" SF-values are valuable to support the level of enthalpy of vaporization derived from other methods, especially in cases where data are scarce. The experimental and "theoretical" vaporization enthalpies derived for each amino-alcohol are given in Table 30. From this table can be seen, that for every compound agreement among $\Delta_l^g H_m^o$(298.15 K)-values, which were derived in different ways, all lie within the assigned error bars. To get more confidence and reliability, the weighted average (the uncertainty was used as a weighing factor) for of aminoalcohols given in Table 30 is calculated. These values are highlighted in bold and are recommended for thermochemical calculations performed in the following section.

5.2.5. Prediction of vaporization enthalpies of aminoalcohols with the "centerpiece" approach

The general idea of the "centerpiece" approach is already shown in Figure 25. Now this idea is applied to predicting the $\Delta_l^g H_m^o$(298.15 K)-values, which have been carefully evaluated in Table 30. First of all, let us complete the prediction shown in Figure 25 with help of the experimental vaporization enthalpy of 2-(methyl-amino)-ethanol $\Delta_l^g H_m^o$(298.15 K) = 57.7±0.2 kJ·mol^{-1} given in Table 30. According to the idea, the vaporization enthalpy of 2-(phenyl-amino)-ethanol is derived by cutting the CH_3-group (with its contribution to vaporization enthalpy of 6.33 kJ·mol^{-1}, given in Table E. 4) and attaching the C_6H_5-group (with its contribution to vaporization enthalpy of 31.7 kJ·mol^{-1}, given in Table E. 4) instead. The resulting "additive" value $\Delta_l^g H_m^o$(298.15 K) = 83.1±1.0 kJ·mol^{-1} is very close to the transpiration result $\Delta_l^g H_m^o$(298.15 K) = 82.3±0.4 kJ·mol^{-1} (Table 30).

Another option for predicting the vaporization enthalpy of 2-(phenyl-amino)-ethanol is to start from the experimental vaporization enthalpy of 2-(ethyl-amino)-ethanol $\Delta_l^g H_m^o$(298.15 K) = 60.8±0.2 kJ·mol^{-1} given in Table 30. In this case, in order to derive the desired value, it is needed to cut off the CH_3 and CH_2 groups and append the C_6H_5 group instead. The resulting "additive" value $\Delta_l^g H_m^o$(298.15 K) = 83.3±1.0 kJ·mol^{-1} is also very close to the transpiration result value $\Delta_l^g H_m^o$(298.15 K) = 82.3±0.4 kJ·mol^{-1} (Table 30). It is even easier to predict the vaporization enthalpy of 2-(benzyl-amino)-ethanol starting from the same "centerpiece" 2-(ethyl-amino)-

ethanol as it shown in Figure 27. The resulting "additive" value $\Delta_l^g H_m^o(298.15$ K$) = 86.2\pm1.0$ kJ·mol^{-1} for 2-(benzyl-amino)-ethanol agrees within the combined uncertainties with the transpiration result $\Delta_l^g H_m^o(298.15$ K$) = 84.5\pm0.4$ kJ·mol^{-1} (Table 30).
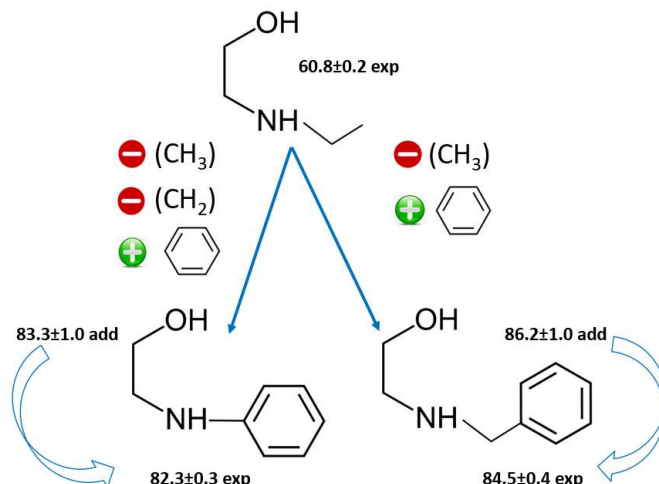
Figure 27. Calculations of vaporization enthalpies of of 2-(phenyl-amino)-ethanol and of 2-(benzyl-amino)-ethanol using the "centerpiece" approach.

The examples of the "centerpiece" approach application given in Figure 25 and Figure 27 show a generally possible way to obtain a reliable prediction even starting from different species. However, this method cannot be considered as universal, as the selection of the starting "centerpiece" requires some preliminary knowledge of effects that arise when substituents are placed in close proximity in the germinal or vicinal position on the alkane skeleton. This idea is demonstrated in Figure 28. Using the "centerpiece" approach, the vaporization enthalpy of DL-2-amino-1-butanol can be estimated starting from 2-amino-ethanol, 2-amino-1-propanol, and from 2-amino-1-pentanol. Experimental data for these aminoalcohols are given in Table E. 5.
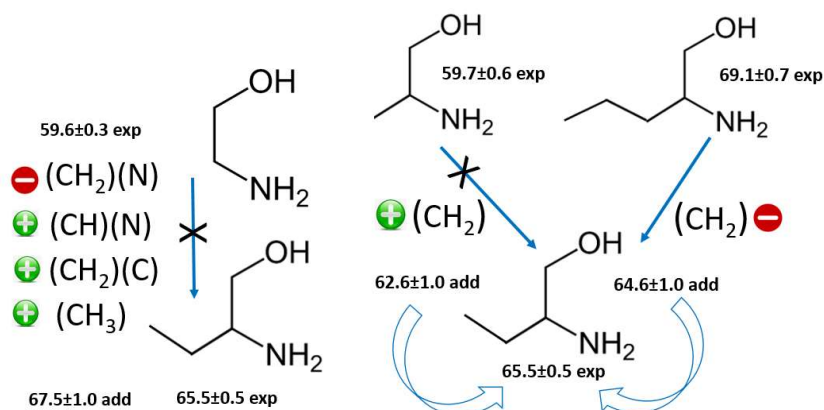
Figure 28. Calculations of vaporization enthalpy of DL-2-amino-1-butanol using the "centerpiece" approach.

The four steps required to construct DL-2-amino-1-butanol from 2-amino-ethanol are shown in Figure 28 (left). The resulting "additive" value $\Delta_l^g H_m^o(298.15\ K) = 67.5\pm1.0\ kJ\cdot mol^{-1}$ is clearly overestimated compared to the transpiration result $\Delta_l^g H_m^o(298.15\ K) = 65.5\pm0.5\ kJ\cdot mol^{-1}$ (Table 30). Maybe there are too many construction steps to get a correct result? Starting with 2-amino-1-propanol, the number of steps is considerably lower (Figure 28, middle). But even in this case the "additive" value $\Delta_l^g H_m^o(298.15\ K) = 62.6\pm1.0\ kJ\cdot mol^{-1}$ is clearly underestimated compared to the transpiration result $\Delta_l^g H_m^o(298.15\ K) = 65.5\pm0.5\ kJ\cdot mol^{-1}$ (Table 30). What is wrong with the centerpiece approach? Starting with 2-amino-1-pentanol, we also need only one step to construct DL-2-amino-1-butanol (Figure 28, right). Finally, the "additive" result $\Delta_l^g H_m^o(298.15\ K) = 64.6\pm1.0\ kJ\cdot mol^{-1}$ comparable to the experiment can be got. What can be the reason for the trial and error observed in all three cases?
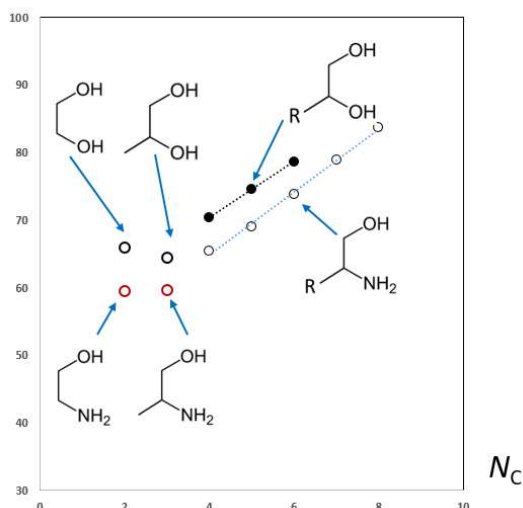
$\Delta_l^g H_m^o(298.15\ K)$

Figure 29. Chain-length dependence of vaporization enthalpies $\Delta_l^g H_m^o(298.15\ K)/kJ\cdot mol^{-1}$ in 1,2-alkanediols and in 2-amino-1-alkanols. N_C is the total number of C-atoms in the molecule.
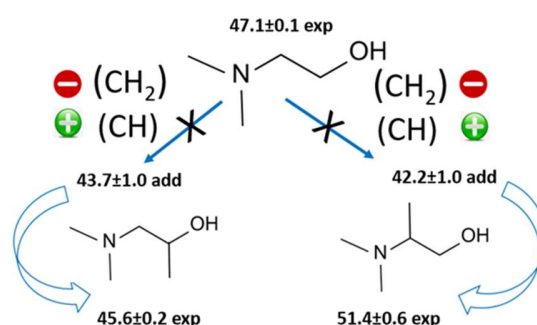
Figure 30. Calculations of vaporization enthalpies of 2-(dimethyl-amino)-1-propanol and 1-(dimethyl-amino)-2-propanol using the "centerpiece" approach.

At first glance, none of the three starting molecules 2-aminoethanol, 2-amino-1-propanol and 2-amino-1-pentanol are very different. But it is not correct. It is known that the energetics of amino alcohols and 1,2-alkanediols is determined by the intra-molecular hydrogen bonding [92,126]. Let us first consider 1,2-alkanediols, for which a plausible explanation was given in our previous work [92]. With the 1,2-alkanediols, an unusual sequence of the $\Delta_l^g H_m^o(298.15\ K)$-values was observed with increasing chain length (in $kJ\cdot mol^{-1}$): 1,2-ethanediol (66.0±0.2), 1,2-

propanediol (64.5±0.2), 1,2-butanediol (70.4±0.3), 1,2-pentanediol (74.6±0.3), and 1,2-hexanediol (78.7±0.3) [92]. Such behaviour of 1,2-alkanediols can be explained by a strong intra-HB, which obviously dominates in the liquid state. In the case of 1,2-propanediol, the addition of an external methyl group leads to a steric hindrance to the formation of an intra-HB. Because of this steric hindrance, the enthalpy of vaporization of 1,2-propanediol is reduced compared to 1,2-ethanediol. However, an attachment of the next alkyl fragments to the 1,2-ethanediol unit does not have the same effect as with the first substitution, since the added fragments are further away from the hydroxyl groups, which form the intra-HB. With increasing chain length in 1,2-butanediol and 1,2-pentanediol, the substitution effect on the intra-HB is already compensated and the $\Delta_l^g H_m^o$(298.15 K)-values become linearly dependent on the chain length (Figure 29).

As can be seen in Figure 29, the trend similar to that of 1,2-alkanediols applies to amino alcohols: the strongest intra-HB is in 2-amino-ethanol. However, already in 2-amino-1-propanol, the CH_3 group, which is located in the close proximity of the amino-group, reduces the strength of the intra-HB for steric reasons. Similar to 1,2-alkanediols, an attachment of the next alkyl fragments to 2-amino-ethanol does not have the same effect as with the first substitution. As a consequence, the vaporization enthalpies of 2-amino-ethanol and 2-amino-1-propanol are out of the linear correlation shown in Figure 29. The linearity of the chain length dependence of the enthalpy of vaporization begins with 2-amino-1-butanol. Such a peculiar energetic behaviour that has been observed in amino alcohols can now explain the trial and error observed with three "centerpieces" shown in Figure 28. Indeed, using 2-aminoethanol and 2-amino-1-propanol to predict the enthalpy of vaporization of 2-amino-1-butanol could be considered as a typical "error", as both molecules have much more individual characteristics than is applicable for group additivity. In contrast, using the 2-amino-1-pentanol as the "centerpieces" is optimal for the prediction, since according to the Figure 29, this molecule is already out of perturbation specific for the smaller homologues.

Another important factor for the selection of the "centerpiece" molecule is illustrated in Figure 30. Let us try to predict vaporization enthalpies of two branched aminoalcohols: enthalpies of 2-(dimethyl-amino)-1-propanol and 1-(dimethyl-amino)-2-propanol starting from $\Delta_l^g H_m^o$(298.15 K) = 47.1±0.1 kJ·mol^{-1} [127] of 2-(dimethyl-amino)-ethanol as the "centerpiece" molecule. In both cases only replacement the CH_2 group with the CH group and adding the contribution for the CH_3 group as it shown in Figure 30 is required. In both cases, however, the "additive" results do not agree with the experimental values evaluated in Table 30.

The obvious reason for the observed disagreement is the appearance of steric repulsions between substituents, since they occur in close proximity on the small skeleton. Due to these repulsions the tightness of the packaging of the molecules in the liquid is unique for each type of branching. Therefore, the correct selection of the "centerpiece" molecule is hardly possible.

The consequence for proper use of the "centerpiece" approach is that the small branched molecules and molecules with strong steric interactions (*e.g.* 2-amino-2-methyl-1-propanol) must be excluded from application. Nonetheless, the "centerpiece" approach with different types of organic and metal-organic compounds is tested by our group. The reliable results have been already obtained for aldehydes and esters [128], substituted benzenes [25,38], and for *tris*(beta-diketonato)iron complexes [129].

In summary, the compilation of experimental results evaluated in Table 30 made it possible to validate three different approaches (SF, T_b, and "centerpiece") in order to reliably assess the $\Delta_l^g H_m^o$(298.15 K) values for organic and metal-organic compounds.

Chapter 6 Evaluation of vaporization thermodynamics of pure aminoalcohols

6.1. Introduction

The CO_2 capture and sequestration processes have been widely reported to reduce emissions to the atmosphere, using systems based on solid sorbents, ionic liquids, advanced membrane, porous materials, amines, and aminoalcohols [130]. The amino alcohols that are practically used in CO_2 capture processes after combustion are mono-, di-, tri-ethanolamine, and N-methyl-di-ethanolamine. It is therefore desirable to synthesize new amino alcohols that incorporate the benefits of amine mixtures in the same molecule or that could provide new materials for mixing in a formulated solvent [131]. Synthetic approaches based on rational molecular design allow for a systematic modification of the structure of aminoalcohols by an appropriate placement of substituent functional groups, especially the hydroxyl function, relative to the position of the amino group [131,132]. The performance of these modified and branched aminoalcohols in aqueous solutions with regard to the solubility of CO_2 is significantly higher than that of conventional amino alcohols [131]. Admittedly, knowledge of reliable thermodynamic data is generally essential for the design and development of new synthetic routes [133]. In this paper we studied the series of aminoalcohols shown in Figure 31.

2-amino-2-methyl-1-propanol

3-(dimethyl-amino)-1-propanol

1-(dimethyl-amino)-2-propanol
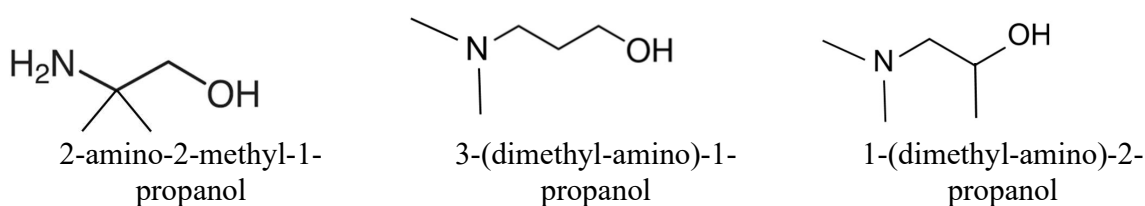
Figure 31. Aminoalcohols studied in this work using the transpiration method.

2-(ethyl-amino)-1-ethanol

2-(iso-propyl-amino)-1-ethanol

3-(diethyl-amino)-1-propanol
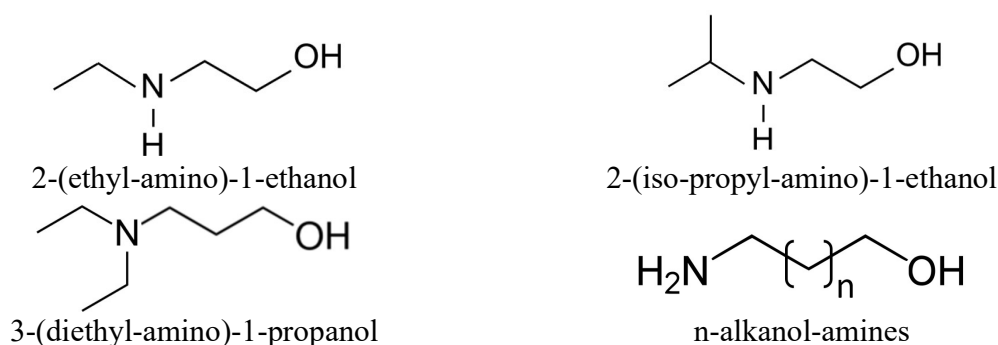
n-alkanol-amines

Figure 32. Aminoalcohols evaluated in this work: 2-(ethyl-amino)-1-ethanol, 2-(iso-propyl-amino)-1-ethanol, 3-(diethyl-amino)-1-propanol, and n-alkanol-amines with n = 1 – 4 (or 3-amino-1-propanol, 4-amino-1-butanol, 5-amino-1-pentanol, 6-amino-1-hexanol).

2-(n-propyl-amino)-ethanol

2-(n-butyl-amino)-ethanol

2-(t-butyl-amino)-ethanol

1-amino-2-methyl-2-propanol

4-amino-4-methyl-2-pentanol

2-amino-3-methyl-1-butanol

1-amino-3-methyl-2-butanol

2-amino-4-methyl-1-pentanol
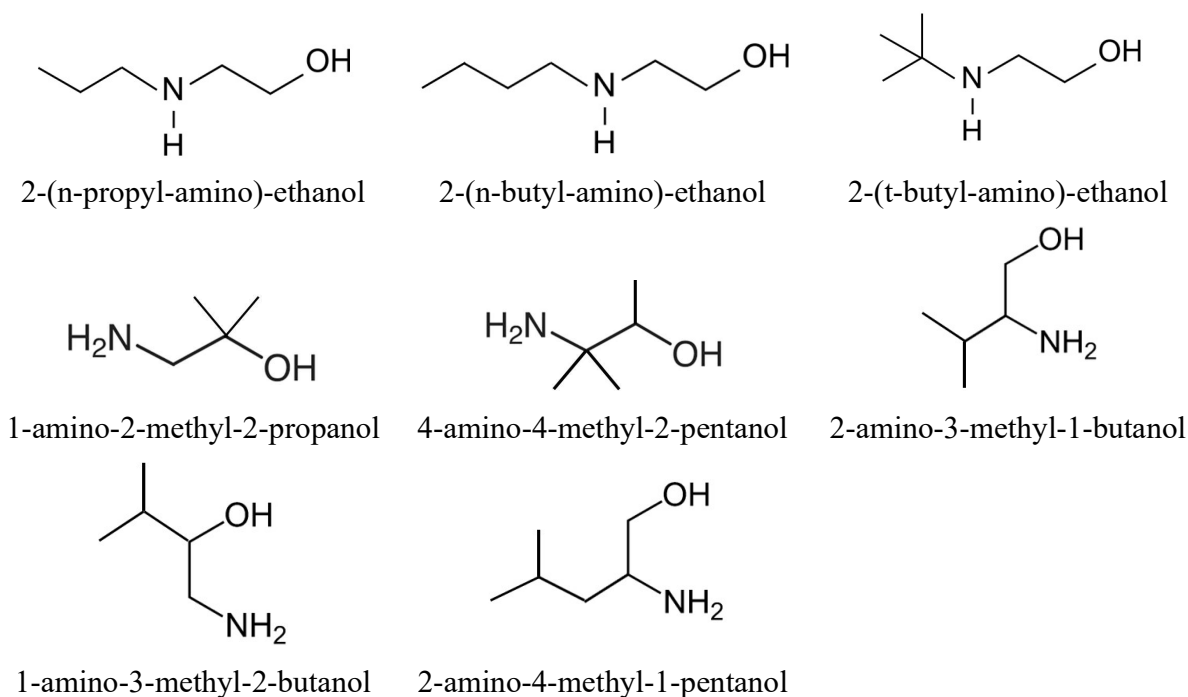
Figure 33. Aminoalcohols with the known T_b-values, which were used in this work to predict $\Delta_l^g H_m^o(298.15 \text{ K})$.

They are used as individual compounds as well as synthetic formulations consisting of mixtures of amino alcohols and some chemical additives. The advantages that can be derived from aminoalcohols mixtures are also limited to commercially available individual aminoalcohols.

The focus of this work was on vapour pressures measurements and the standard molar vaporization enthalpies, $\Delta_l^g H_m^o$(298.15 K). In addition, vapour pressures of differently structured amino alcohols available in the literature (Figure 32) were collected and evaluated. We used different empirical and structure-property correlation methods for validation and evaluation of new and available experimental results. The evaluated $\Delta_l^g H_m^o$(298.15 K)-values were correlated with the normal boiling temperatures, T_b, of aminoalcohols. A robust linear correlation was established for primary and secondary aminoalcohols. The tertiary aminoalcohols exhibit their own line.

We collected the T_b-values for the branched alkyl-substituted aminoalcohols (Figure 33) and predicted their vaporization enthalpies using the developed correlations. We collected the T_b-values for the branched alkyl-substituted amino alcohols (Figure 33) and predicted their enthalpies of vaporization based on the correlations developed.

6.2.   Results and discussion

6.2.1. Absolute vapour pressures and thermodynamics of vaporization

Experimental data on the vapor pressures for 2-amino-2-methyl-1-propanol have been presented in Chapter 7. The primary experimental results on 3-(dimethyl-amino)-1-propanol, and 1-(dimethyl-amino)-2-propanol from the transpiration method are summarized in Table E.2.

The vapour pressures over the liquid sample of 1-(dimethyl-amino)-2-propanol were measured for the first time. In contrast, the vapour pressures measurements over the liquid 2-amino-2-methyl-1-propanol have been a popular endeavor in the past [134–138].

The available vapour pressures for 3-(dimethyl-amino)-1-propanol, measured by ebulliometry [139] and with the static method [137] are significantly different (Figure F. 1). However, our new transpiration results are more in line with the ebulliometric results, even if the temperature ranges of the two studies are very different (Figure F. 1). This apparent disagreement led us to look for additional data that would help resolve the observed contradictions. As a matter of fact, SciFinder [122] compiles experimental boiling temperatures at various pressures. The accuracy of this data is questionable as it comes from the distillation of a compound after its synthesis and not from special physico-chemical studies. However, the numerous data on boiling temperatures at standard pressure, as well as at reduced pressures provide at least a reliable level of the experimental vapour pressures and a reliable trend of the dependence of the vapour pressure temperature. As can be seen in Figure F. 1, the boiling points taken from SciFinder agree well with the ebulliometric and transpiration results, but not with those from the static method. After have resolved contradictions observed for for 3-(dimethyl-amino)-1-propanol in this way, we have

systematically collected the data available in SciFinder for amino alcohols, which are shown in Figure 31 - Figure 33. These data were used to derive vaporization enthalpies of aminoalcohols (Table 32). The compilation of the standard molar enthalpies of vaporization of aminoalcohols at the reference temperature $T = 298.15$ K, calculated according to Equation 8 is given in Table 32.

6.2.2. Evaluation of available vaporization enthalpies

As can be seen from Table 32, the vaporization enthalpies, $\Delta_l^g H_m^o$(298.15 K), derived from vapour pressures measured by the conventional methods, as well as those derived from the SciFinder data are in good agreement for aminoalcohols compiled in this table. Such a good agreement has reinforced usefulness of the experimental boiling temperatures reported at different pressures compiled by the SciFinder for evaluation of the scarce thermodynamic data.

Table 32. Compilation of the standard molar enthalpies of vaporization $\Delta_l^g H_m^o$ of substituted aminoalcohols.

Compound	M[a]	T- range	$\Delta_l^g H_m^o(T_{av})$	$\Delta_l^g H_m^o$(298.15 K)	Ref.
		K	kJ·mol⁻¹	kJ·mol⁻¹	
2-amino-ethanol [141-43-5]	T			**59.6±0.3**	[122]
2-(ethyl-amino)-ethanol	SF	351-443	53.3±4.9	60.0±5.0	this work
[110-73-6]	T	282.5-321.3	60.8±0.3	61.0±0.4	[122]
	S	243.1-308.1	62.5±0.1	60.8±0.2	[140]
				60.8±0.2	average
2-(iso-propyl-amino)-ethanol	S	248.1-308.1	64.6±0.1	62.9±0.2	[140]
[109-56-8]	S	298.1-342.9	61.5±0.1	63.1±0.3	[140]
	E	363.2-438.2	52.1±0.4	60.0±0.5	[141]
				62.7±0.2	average
2-amino-2-methyl-1-propanol (liq)	SF	342-440	56.4±0.6	62.9±0.8	[134]
[124-68-5]	E	373.3-436.9	53.6±0.1	61.4±0.6	[135]
	E	364.1-425.5	55.2±0.4	62.1±0.7	[136]
	S	293.3-373.0	60.3±0.3	62.6±0.4	[137]
	E	347.5-452.0	54.9±0.3	62.0±0.6	[138]
	T	306.3-333.7	60.5±0.3	62.1±0.5	[134]
	J_x			61.9±1.0	[134]
	T	290.3-333.4	61.5±0.2	62.3±0.3	this work
				62.2±0.2	average
2-amino-2-methyl-1-propanol (cr)	T	274.4-288.2	67.3±0.6	67.0±1.1	this work
3-(dimethlyamino)-1-propanol	SF	341-438	46.7±0.7	53.4±0.8	this work
[3179-63-3]	S	283.2-373.1	56.6±1.5	58.6±1.6	[137]
	E	352.3-433.7	47.6±0.2	54.5±0.5	[139]
	T	275.6-319.3	55.1±0.2	54.9±0.3	this work
				54.8±0.2	average
3-(diethlyamino)-1-propanol	SF	335-463	54.4±4.6	63.5±4.7	this work
[622-93-5]	E	353.9-442.2	53.4±0.5	62.1±0.7	[139]
				62.2±0.8	
3-amino-1-propanol	E	348.2-368.2	58.5±2.7	62.3±2.8	[142]
[156-87-6]	E	372.3-459.0	56.2±0.1	63.5±0.6	[143]
	T	288.3-321.7	62.3±0.4	62.7±0.5	[122]
	SF	333-461	56.6±1.2	62.9±1.3	[134]
	T	287.2-328.2	61.7±0.1	62.2±0.3	[134]
	J_x			63.3±1.0	[134]
				62.3±0.3	
4-amino-1-butanol	SF	328-481	61.9±2.8	69.7±2.9	[134]

[13325-10-5]	J_x			68.5±1.0	[134]
	T	288.2-329.2	68.1±0.3	68.8±0.4	[134]
				68.8±0.4	average
5-amino-1-pentanol	SF	352-495	64.2±1.3	74.7±1.5	[134]
[2508-29-4]	J_x			72.3±1.0	[134]
	T	292.0-333.1	71.1±0.2	72.3±0.3	[134]
				72.4±0.3	
6-amino-1-hexanol	SF	393-508	62.6±1.9	76.3±2.1	[134]
[4048-33-3]	J_x			77.0±1.0	[134]
				76.9±0.9	
1-(dimethylamino)-2-propanol	T	276.4-306.7	45.8±0.2	45.3±0.3	this work
[108-16-7]					

[a] Techniques: T = transpiration method; J_x – from correlation of experimental vaporization enthalpies with Kovats´s indices; S = static method; E = ebulliometry; n/a = method is not available; SF - from experimental boiling temperatures reported at different pressures compiled by the SciFinder [122].

Additional validation of the $\Delta_l^g H_m^o$(298.15 K)-values collected in Table 32 was conducted in our recent work using chromatographic retention indices for aminoalcohols [134]. We derived reliable linear correlation between vaporization enthalpies and Kovats´s indices, J_x, of aminoalcohols. The "theoretical" results derived from this correlation are given in Table 32 and designated as J_x. These results are valuable to support the level of enthalpy of vaporization derived from other methods, especially in cases where data are scarce *(e.g.* for 4-amino-1-butanol, 5-amino-1-pentanol, and 6-amino-1-hexanol). The experimental and "theoretical" vaporization enthalpies derived for each amino-alcohol are given in Table 32. From this table can be seen, that for every compound agreement among $\Delta_l^g H_m^o$(298.15 K-values, which were derived in different ways, all lie within the assigned error bars. To get more confidence and reliability, we calculated the weighted average (the uncertainty was used as a weighing factor) for most of aminoalcohols given in Table 32.

6.2.3. Correlation of vaporization enthalpies with normal boiling temperatures

The relation of vaporization enthalpy to boiling point is a well-established phenomenon and Trouton's rule is the best evidence of this. According to our experience, the amino alcohols are thermally stable compounds, that boil between 430 K and 530 K [48,78,144], depending on their size and structure. The variety of aminoalcohols structures feasible for synthesis and CO_2 capture, as well as the scarce thermodynamic data have prompted us to correlate $\Delta_l^g H_m^o$(298.15 K)-values evaluated in this work (Table 32) with the normal boiling temperatures, T_b, which can easily be found in the literature [48,78,144]. Provided that a reliable correlation can be found, enthalpies of vaporization of numerous aminoalcohols can be assessed by means of their boiling points. The compilation of the correlated data is given in Table 33 and Table 34.

Table 33. Correlation of vaporization enthalpies $\Delta_l^g H_m^o$(298.15 K) of primary and secondary aminoalcohols with their T_b normal boiling temperatures.

CAS	Compound	T_b [a]	$\Delta_l^g H_m^o$(298.15 K)$_{exp}$ [b]	$\Delta_l^g H_m^o$(298.15 K)$_{calc}$ [c]	Δ
		K	kJ·mol^{-1}	kJ·mol^{-1}	kJ·mol^{-1}
96-20-8	2-amino-1-butanol	451	64.4±0.3 [134]	63.6	0.8
78-96-6	1-amino-2-propanol	433	59.2±0.4 [134]	59.7	-0.5
13552-21-1	1-amino-2-butanol	442	63.6±0.3 [134]	61.6	2.0
133325-10-5	4-amino-1-butanol	479	68.8±0.4	69.8	-1.0
2508-29-4	5-amino-1-pentanol	495	72.4±0.3	73.2	-0.8
4048-33-3	6-amino-1-hexanol	508	76.9±0.9	76.1	0.8
124-68-5	2-amino-2-methyl-1-propanol	440	62.2±0.2	61.2	1.0
109-83-1	2-(methyl-amino)-ethanol	431	57.7±0.2 [122]	59.3	-1.6
110-73-6	2-(ethyl-amino)-ethanol	443	60.8±0.2	61.8	-1.0
109-56-8	2-(iso-propyl-amino)-ethanol	446	62.7±0.2	62.5	0.2

[a] Normal boiling temperatures are from [48,78,144], [b] values evaluated in Table 32 or taken from literature, [c] calculated using Equation 58.

Table 34. Correlation of vaporization enthalpies $\Delta_l^g H_m^o$(298.15 K) of tertiary aminoalcohols with their T_b normal boiling temperatures.

CAS	Compound	T_b [a]	$\Delta_l^g H_m^o$(298.15 K)$_{exp}$ [b]	$\Delta_l^g H_m^o$(298.15 K)$_{calc}$ [c]	Δ
		K	kJ·mol^{-1}	kJ·mol^{-1}	kJ·mol^{-1}
108-01-0	2-(dimethyl-amino)-ethanol	407	47.1±0.1 [122]	46.8	0.3
100-37-8	2-(diethyl-amino)-ethanol	436	52.6±0.2 [122]	53.9	-1.3
108-16-7	1-(dimethylamino)-2-propanol	397	45.3±0.3	44.9	0.4
3179-63-3	3-(dimethlyamino)-1-propanol	437	54.8±0.2	54.6	0.2
622-93-5	3-(diethlyamino)-1-propanol	463	62.2±0.8	61.5	0.7

[a] Normal boiling temperatures are from [25,48,78], [b] values evaluated in Table 32 or taken from literature, [c] Calculated using Equation 58.

For the set containing *tertiary* aminoalcohols (Table 34), the linear correlation was as follows (kJ·mol^{-1}):

$$\Delta_l^g H_m^o(298.15 \text{ K}) = -61.1 + 0.2650 \times T_b \text{ with } (R^2 = 0.986) \quad (59)$$

As can be seen from Table 33 and Table 34, the results calculated from the two correlations with the boiling temperatures agree well with those derived from other methods. Such good agreement can be seen as evidence of the internal consistency of the experimental data on the $\Delta_l^g H_m^o$(298.15 K) evaluated in this work (Table 32). From Table 33 and Table 34 it can be seen that differences between experimental and calculated according to Equation 58 and Equation 59 values are mostly below 2 kJ·mol^{-1}. Consequently, the uncertainties of enthalpies of vaporization which are estimated from the correlation $\Delta_l^g H_m^o$(298.15 K) – T_b, are weighted with ±1.5 kJ·mol^{-1}.

6.2.4. Prediction of vaporization enthalpies of branched aminoalcohols with the help of normal boiling temperatures and group additivity

Having established correlations between vaporization enthalpies of aminoalcohols and their boiling points, we decided to apply these correlations to predict data for a set of branched species collected in Table 35.

Table 35. Compilation of the standard molar enthalpies of vaporization $\Delta_l^g H_m^o$ of branched alkyl-substituted aminoalcohols.

Compound	M[a]	T- range	$\Delta_l^g H_m^o (T_{av})$	$\Delta_l^g H_m^o$(298.15 K)
		K	kJ·mol^{-1}	kJ·mol^{-1}
2-(n-propyl-amino)-ethanol	SF	364-473	55.5±1.1	64.8±1.3
[16369-21-4]	T_b	463.2		66.2±1.5
	Add			65.3±1.5
				65.4±0.8
2-(n-butyl-amino)-ethanol	SF	364-478	56.2±1.6	66.4±1.9
[111-75-1]	T_b	478.2		69.5±1.5
	Add			69.8±1.5
				68.9±0.9[c]
2-(t-butyl-amino)-ethanol	SF	340-450	54.9±1.5	63.0±1.6
[4620-70-6]	T_b	449.7		63.4±1.5
	Add			62.9±1.5
				63.1±0.9
1-amino-2-methyl-2-propanol	SF	338-424	50.9±0.5	56.6±0.7
[2854-16-2]	T_b	424		57.7±1.5
				56.8±0.6
4-amino-4-methyl-2-pentanol	SF	344-448	50.7±0.6	58.9±0.8
[4404-98-2]	T_b	448		62.9±1.5
				59.8±0.7
2-amino-3-methyl-1-butanol	SF	348-459	58.1±2.1	66.1±2.2
[16369-05-4]	T_b	459		65.4±1.5
	Add			68.0±1.5
				66.6±1.0
1-amino-3-methyl-2-butanol	SF	349-467	52.2±1.8	(60.4±1.9)
[17687-58-0]	T_b	467		67.1±1.5
	Add			68.0±1.5
				67.6±1.1
2-amino-4-methyl-1-pentanol	SF	371-467	63.6±2.0	73.8±2.1
	Add			72.5±1.5
				73.0±1.2

[a] Techniques: SF - from experimental boiling temperatures reported at different pressures compiled by the SciFinder [34]; T_b – from correlation of experimental vaporization enthalpies with the normal boiling temperatures; Add – estimated using group-additivity.

Using the T_b-values available in the literature [48,78], the vaporization enthalpies were estimated with Equation 58 and given in Table 35. The advantage of this set is that not only T_b-values have been found in the literature, but also a sufficient amount of boiling temperatures at reduced pressures compiled by SciFinder. We approximated the latter values with Equation 2 and calculated the $\Delta_l^g H_m^o$(298.15 K) for comparison with those obtained from the $\Delta_l^g H_m^o$(298.15 K) – T_b correlation (Table 35). As can be seen from this table, the agreement between the T_b and SF

estimates, with the exception of 1-amino-3-methyl-2-butanol, is fair, which gives confidence to the empirical methods applied for the prediction.

Taking into account very uncertain sources for boiling temperatures, which were compiled from SciFinder and internet sources [48,78], we nevertheless decided to validate the $\Delta_l^g H_m^o$(298.15 K)-estimates in Table 35 using group additivity. In our most recent work [25,38] we develop a "centerpiece" approach that is closely related to the conventional group-contribution methods [1,81]. In the latter methods the molecule of interest is collected completely from well-defined group contributions. The idea of this "centerpiece" approach is to select a "core" molecule that may possibly close mimic the structure of the molecule of interest, but the selected "centerpiece" molecule has the well-established thermodynamic properties. Different substituents can be attached (or subtracted) to this "centerpiece" in different positions. The visualisation of the "centerpiece" approach is given in Figure 34.
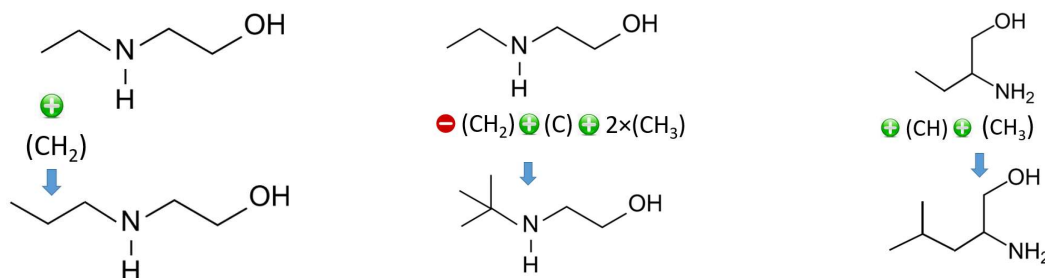
Figure 34. Calculations of vaporization enthalpies of 2-(n-propyl-amino)-ethanol, 2-(t-butyl-amino)-ethanol, and 2-amino-4-methyl-1-pentanol using the "centerpiece" approach.

Indeed, starting from the vaporization enthalpy of 2-(ethyl-amino)-ethanol $\Delta_l^g H_m^o$(298.15 K) = 60.8±0.2 kJ·mol^{-1} evaluated in Table 32, it is easy to estimate the vaporization enthalpy of 2-(n-propyl-amino)-ethanol (Figure 34, left) simply by adding the CH$_2$-contribution (Table 36). The calculation of the vaporization enthalpy of 2-(t-butyl-amino)-ethanol is relatively more sophisticated and requires three iterations given in Figure 34 (middle).

Another "centerpiece" is better suited for a proper estimation of the vaporization enthalpy of 2-amino-4-methyl-1-pentanol (Figure 34, right). The structurally parent "centerpiece" is the 2-amino-1-butanol [96-20-8] with the vaporization enthalpy $\Delta_l^g H_m^o$(298.15 K) = 64.9±0.3 kJ·mol^{-1} evaluated in our recent work [134]. Only two contributions (CH) and (CH$_3$) have to be added to this value in order to obtain the desired enthalpy of vaporization of 2-amino-4-methyl-1-pentanol (Figure 34, right). The enthalpic contributions required for the "centerpiece" approach and used for calculations of the "Add"-values are compiled in Table 36. Following this pattern, the $\Delta_l^g H_m^o$(298.15 K) –values for the branched aminoalcohols were estimated and designated in Table

35 as "Add". It makes oneself conspicuous, that the all "Add"- values are in a good agreement with the T_b and SF estimates (Table 35).

Table 36. Group-additivity values Γ_i for calculation of enthalpies of vaporization, $\Delta_l^g H_m^o$(298.15 K), of alkanes, amines, and aminoalcohols at 298.15 K (in kJ mol^{-1}) [81,95,145].

	$\Delta_l^g H_m^o$(298.15 K)
	Γ_i
Alkanes	
C-(C)(H)$_3$	6.33
C-(C)$_2$(H)$_2$	4.52
C-(C)$_3$(H)	1.24
C-(C)$_4$	-2.69
Amines	
C-(N)(C)(H)$_3$	6.33
C-(N)(C)(H)$_2$	2.9
C-(N)(C)$_2$(H)	-2.0
C-(N)(C)$_3$	-7.7
N-(C)(H)$_2$	18.0
N-(C)$_2$(H)	12.6
N-(C)$_3$	4.9
Alcohols	
C-(O)(C)(H)$_3$	6.33
C-(O)(C)(H)$_2$	4.7
C-(O)(C)$_2$(H)	1.3
C-(O)(C)$_3$	-3.8
HO-(C)	31.5

In summary, the compilation of the experimental results evaluated in Table 32 made it possible to validate three different approaches (SF, T_b, and "centerpiece") in order to reliably assess the $\Delta_l^g H_m^o$(298.15 K) values for amino alcohols, required for the heat management of the CO_2 capture processes.

Chapter 7 Paving the way to the sustainable hydrogen storage: thermochemistry of aminoalcohols as precursors for the liquid organic hydrogen carriers

7.1. Introduction

The reversible hydrogenation/dehydrogenation reactions of small aromatic molecules have attracted a great deal of interest in recent years due to their potential application in the development of liquid organic hydrogen carriers (LOHCs). The idea behind the LOHC is that the hydrogen is stored in a molecule that contains double bonds via a catalytic reaction. The hydrogen accumulated in this way can be released at any time and at any location via a catalytic dehydrogenation reaction. In this context, chemical hydrogen storage and transport systems are of great interest. These should

make it possible to store significant amounts of hydrogen and to release pure hydrogen on demand. However, finding affordable but efficient hydrogen storage systems remains a challenge for the upcoming hydrogen economy. In our recent studies [146,147], we have shown that alkyl-substituted pyrazines can be considered as a seminal LOHCs, provided that efficient, large-scale synthesis of these compounds is developed.

The methods of making pyrazine derivatives are limited. In industry, substituted pyrazines are synthesized by the catalytic condensation of ethylenediamine with vicinal diols such as propylene glycol [148]. A very simple and environmentally friendly method for the preparation of substituted pyrazines has been reported just recently [149]. A highly selective formation of 2,5-alkyl-substituted pyrazines was achieved by base-metal catalysed dehydrogenative self-coupling of 2-aminoalcohols. There are two crucial advantages of the latter method. The first one is that the replacement of noble-metal-based catalysts by catalysts based on low-toxicity, earth-abundant base metals is a significant for development of the cost-effective homogeneous catalysis. The second advantage is that there are enough effective methods of 2-aminoalcohols synthesis from cheap and readily available starting materials that opens up a promising routes towards sustainable production of aminoalcohols from renewable sources. For example, an efficient and environmentally benign method of coupling reaction of amino acids with aldehydes or ketones to synthesise various aminoalcohols at room temperature is described [150]. Taking into account both advantages of alkyl-pyrazine synthesis from aminoalcohols, such protocol can be considered as very suitable for the further development of large-scale commercial processes.

| 1-amino-2-alcohols | 2-amino-1-alcohols | n-alkanol-amines | 2-amino-2-methyl-1-propanol |
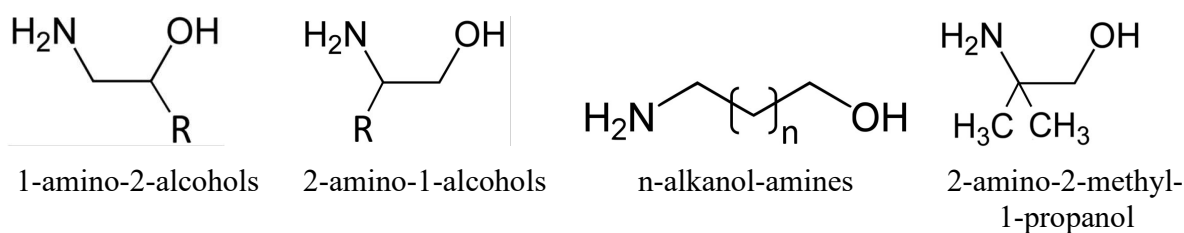
Figure 35. Aminoalcohols studied in this work: 1-amino-2-alcohols with R = alkyl C1-C6; 2-amino-1-alcohols with R = alkyl C1-C6; n-alkanol-amines with n = 1 – 4 (or 3-amino-1-propanol, 4-amino-1-butanol, 5-amino-1-pentanol, 6-amino-1-hexanol); 2-amino-2-methyl-1-propanol.

Another area of application also motivated this study. Aminoalcohols are easily complexed with various transition metals. Such complexes are broadly used in different fields: catalysis, inhibitors, electroplating, and dyes [151]. Moreover, these features are successfully used to obtain a wide range of volatile organometallic compounds that are used as precursors in chemical vapor deposition or atomic layer deposition technologies to provide inorganic materials of various types

and compositions [152,153]. From this point of view, amino alcohols can be used both as independent ligands [154] and, what has proven to be more valuable, as additional co-ligands [152,153]. Since the numerous settings can be varied (type, number and position of the substituents in the carbon skeleton and length of the carbon chain), these ligands give related complexes additional possibilities to control thermal stability and volatility. Admittedly, knowledge of reliable thermodynamic data in general is essential for the design and development of new compounds and technologies. In this paper we studied the series of aminoalcohols shown in Figure 35. The focus of this work was on vapour pressures measurements and the standard molar vaporization enthalpies, $\Delta_l^g H_m^o$(298.15 K). We used different empirical and structure-property correlations method for validation and evaluation of new experimental results.

Moreover, in order to fulfil the expectation that thermodynamic data on aminoalcohols can be useful for optimization of alkyl-pyrazines (as seminal liquid organic hydrogen carriers) synthesis, we used new data in combination with our previous thermochemical data on alkyl-pyrazines to calculate energetics of dehydrogenative self-coupling of 2-aminoalcohols.

7.2. Results and discussion

7.2.1. Absolute vapour pressures and thermodynamics of vaporization

The primary experimental results on vapour pressures for 2-amino-2-methyl-1-propanol, 1-amino-2-propanol, 4-amino-1-butanol, and 5-amino-1-pentanol from the transpiration method are summarized in Table G.2.

The vapour pressures for 1-amino-2-butanol, 4-amino-1-butanol, and 5-amino-1-pentanol were measured for the first time. Vapour pressures measurements on 2-amino-2-methyl-1-propanol have been a popular endeavor in the past [135–138,155]. As can be seen from Figure G. 1, the vapour pressures available for the 2-amino-2-methyl-1-propanol, measured by the ebulliometry and static method are remarkably consistent. The main motivation for carrying out the new measurements was to investigate possible peculiarities of aminoalcohols under the conditions of the transpiration experiments. Our new transpiration results are in agreement with the static results reported by Belabbaci *et al*. [137] in the comparable temperature range (Figure G. 1). No specifics were observed which gives confidence in using the transpiration method for this class of compound.

The complete lack of data for 1-amino-2-butanol, 4-amino-1-butanol, and 5-amino-1-pentanol prompted us to use experimental boiling temperatures at different pressures compiled by SciFinder [34]. The accuracy of this data is questionable as it comes from the distillation of a

compound after its synthesis and not from special physico-chemical studies. However, the numerous data on boiling temperatures at standard pressure, as well as at reduced pressures provide at least a reliable level of the experimental vapour pressures and a reliable trend of the dependence of the vapour pressure temperature. For example, in Figure G. 1 for 2-amino-2-methyl-1-propanol the boiling points at different pressures compiled by SciFinder are in fair agreement with the precise ebulliometric and static measurements. In this work for the sake of comparison, we have systematically collected the data available in SciFinder for aminoalcohols presented in Figure 35. The comparisons of our new results with those of SciFinder are shown in Figure G. 2 - Figure G. 5. To our surprise, the agreement observed for 2-amino-1-butanol (Figure G. 2), 3-amino-1-propanol (Figure G. 3), 4-amino-1-butanol (Figure G. 4), and 5-amino-1-pentanol (Figure G. 5) can be considered sufficient to obtain the reliable trend of the temperature dependencies of the vapour pressures. The SciFinder data involved in data acquisition are summarized in Table G. 3. Vapour pressures for 1-amino-2-propanol are available from the static method [155] and from the compilation by Stephenson and Malanowski [43]. The significant disagreement is shown in Figure G. 6. Unfortunately, the compilation by Stephenson and Malanowski [43] provides only the Antoine approximation coefficients. Information on the method and purity of the compound is missing and the reason for the disagreement observed for 1-amino-2-propanol cannot be explained.

Table 37. Compilation of the standard molar enthalpies of vaporization $\Delta_l^g H_m^o$ of aminoalcohols.

Compound, CAS	M^a	T- range	$\Delta_l^g H_m^o(T_{av})$	$\Delta_l^g H_m^o(298.15\ K)$
		K	kJ·mol^{-1}	kJ·mol^{-1}
2-amino-ethanol [141-43-5]	T			**59.6±0.3** [122]
2-amino-1-propanol	SF	353-449	53.4±1.2	59.9±1.3
[6168-72-5]	J_x			59.7±1.0
	N_c			59.7±1.0
				59.7±0.6 ^{c}
2-amino-1-butanol	SF	324-452	57.5±1.1	64.0±1.2
[96-20-8]	T	278.3-333.9	64.9±0.3	65.2±0.4 [155]
	J_x			64.3±1.0
	N_c			64.5±1.0
				64.9±0.3
2-amino-1-pentanol	J_x			68.7±1.0
[16369-14-5]	N_c			69.4±1.0
				69.1±0.7
2-amino-1-hexanol	SF	371-464	64.1±1.5	74.3±1.6
[5665-74-7]	J_x			73.2±1.0
	N_c			74.2±1.0
				73.8±0.7
2-amino-1-heptanol [74872-95-0]	N_c			79.0±1.0
2-amino-1-octanol [16369-15-6]	N_c			83.8±1.0
2-amino-2-methyl-	SF	342-440	56.4±0.6	62.9±0.8
1-propanol	E	373.3-436.9	53.6±0.1	61.4±0.6 [135]
[124-68-5]	E	364.1-425.5	55.2±0.4	62.1±0.7 [136]
	S	293.3-373.0	60.3±0.3	62.6±0.4 [137]

Compound	Technique	Temp range	Value	Value (ref)
	E	347.5-452.0	54.9±0.3	62.0±0.6 [138]
	T	306.3-333.7	60.5±0.3	62.1±0.5
	J_x			61.9±1.0
				62.2±0.2
1-amino-2-propanol [78-96-6]	n/a	306-431	51.0±1.5	(55.5±1.6) [43]
	S	326.8-372.9	56.3±0.1	59.3±0.4 [155]
	J_x			59.2±1.0
				59.2±0.4
1-amino-2-butanol [13552-21-1]	SF	348-443	55.9±0.7	62.8±0.9
	T	278.3-318.2	63.8±0.3	63.7±0.4
	J_x			63.8±1.0
				63.6±0.3
1-amino-2-pentanol [5343-35-1]	SF	348-469	59.3±5.2	67.8±5.3
	J_x			68.2±1.0
	GA			68.4±1.0
				68.3±0.7
1-amino-2-hexanol [72799-62-3]	GA			73.2±1.0
1-amino-2-heptanol [51411-48-4]	GA			78.0±1.0
1-amino-2-octanol [4255-35-0]	GA			82.8±1.0
3-amino-1-propanol [156-87-6]	E	348.2-368.2	58.5±2.7	62.3±2.8 [142]
	E	372.3-459.0	56.2±0.1	63.5±0.6 [143]
	T	287.2-328.2	61.7±0.1	62.2±0.3 [155]
	SF	333-461	56.6±1.2	62.9±1.3
	J_x			63.3±1.0
				62.3±0.3
4-amino-1-butanol [13325-10-5]	SF	328-481	61.9±2.8	69.7±2.9
	T	288.2-329.2	68.1±0.3	68.8±0.4
	J_x			68.5±1.0
				68.8±0.4
5-amino-1-pentanol [2508-29-4]	SF	352-495	64.2±1.3	74.7±1.5
	J_x			72.3±1.0
	T	292.0-331.1	71.1±0.2	72.3±0.3
				72.4±0.3
6-amino-1-hexanol [4048-33-3]	SF	393-508	62.6±1.9	76.3±2.1
	J_x			77.0±1.0
				76.9±0.9

[a] Techniques: T = transpiration method; J_x – from correlation of experimental vaporization enthalpies with Kovats´s indices; S = static method; E = ebulliometry; n/a = method is not available; SF - from experimental boiling temperatures reported at different pressures compiled by SciFinder [34]; N_c – from correlation of experimental vaporization enthalpies with the number of C-atoms in the molecule; GA – the appropriate number of contributions $[CH_2]$ = 4.8 kJ·mol^{-1} was added to the experimental vaporization enthalpy of 1-amino-2-butanol, as the representative of the homologous series of 1-amino-2-alkanol.

The compilation of the standard molar enthalpies of vaporization of aminoalcohols at the reference temperature T = 298.15 K, calculated according to Equation 8 is given in Table 37.

As can be seen from Table 37, the vaporization enthalpies, $\Delta_l^g H_m^o$(298.15 K), derived from vapour pressures measured by the conventional methods as well as those derived from the SciFinder data are in good agreement for 2-amino-1-butanol, 2-amino-2-methyl-1-propanol, 1-amino-2-butanol, 4-amino-1-butanol, and 5-amino-1-pentanol. Such a good agreement has reinforced valuability of the experimental boiling temperatures compiled by the SciFinder for the evaluation of the scarce thermodynamic data. Nevertheless, the additional validation of

vaporization enthalpies, $\Delta_l^g H_m^o$(298.15 K), which were derived for aminoalcohols in Table 37, is necessary.

7.2.2. Kovats´s retention indices for validation of experimental vaporization enthalpies

In this work we measured Kovats´s indices for aminoalcohols in the temperature range from 363K to 393 K with the capillary column DB-1 (Table G. 4). In addition, some literature data available on the retention indices for aminoalcohols on DB-1 [156] were taken for correlation with the $\Delta_l^g H_m^o$(298.15 K)-values evaluated in this work (Table 37). The results of this correlation are given in the Table 38.

Table 38. Correlation of vaporization enthalpies, $\Delta_l^g H_m^o$(298.15 K), of aminoalcohols with their Kovats´s indices (J_x).

CAS	Compound	J_x [a]	$\Delta_l^g H_m^o$(298 K)$_{exp}$ [b]	$\Delta_l^g H_m^o$(298 K)$_{calc}$ [c]	Δ
			kJ·mol⁻¹	kJ·mol⁻¹	kJ·mol⁻¹
141-43-5	2-amino-ethanol	698 [156]	59.6	59.4	0.2
6168-72-5	2-amino-1-propanol	704	59.9	59.7	0.2
96-20-8	2-amino-1-butanol	809	64.9 [e]	64.3	0.6
16369-14-5	2-amino-1-pentanol	907	-	68.7	-
5665-74-7	2-amino-1-hexanol	1009	74.3	73.2	1.1
124-68-5	2-amino-2-me-1-propanol	755 [156]	62.1 [d]	61.9	0.2
78-96-6	1-amino-2-propanol	693	59.3	59.2	0.1
13552-21-1	1-amino-2-butanol	797	63.7 [d]	63.8	-0.1
5343-35-1	1-amino-2-pentanol	897 [156]	67.8	68.2	-0.4
156-87-6	3-amino-1-propanol	785 [156]	62.2 [d]	63.3	-1.1
133325-10-5	4-amino-1-butanol	904 [156]	68.8	68.5	0.3
2508-29-4	5-amino-1-pentanol	988 [156]	72.3	72.3	0.0
4048-33-3	6-amino-1-hexanol	1094 [156]	76.3	77.0	-0.7

[a] Kovats´s indices at 393 K, J_x, on the standard non-polar column DB-1 measured in this work, [b] data from Table 37, [c] Calculated with Equation 60, [d] experimental data measured by using the transpiration method (Table 37).

It is known, that the $\Delta_l^g H_m^o$(298.15 K)-values correlate linearly with Kovats`s indices in various homologous series of alkanes, alkylbenzenes, aliphatic ethers, alcohols, or in a series of structurally similar compounds [157]. As anticipated, the following linear correlation was obtained when the $\Delta_l^g H_m^o$(298.15 K)-values are correlated with J_x-values for the structurally parent set of aminoalcohols collected in Table 38:

$$\Delta_l^g H_m^o(298.15 \text{ K}) /(\text{kJ·mol}^{-1}) = 28.5 + 0.0443 \times J_x \text{ with } (R^2 = 0.992) \tag{60}$$

The vaporization enthalpies derived from the correlations with Kovats´s indices (Table 38) are in a good agreement with those obtained by the transpiration method (Table 37). Such good

agreement can be seen as additional validation of the experimental data measured in this work by using the transpiration method (Table 37). It can be seen from Table 38, that differences between experimental and calculated according to Equation 60 vaporization enthalpies are mostly below 1 kJ·mol^{-1}. Hence, the uncertainties of enthalpies of vaporization which are estimated from the correlation the $\Delta_l^g H_m^o$(298.15 K) - J_x are evaluated with ±1.0 kJ·mol^{-1}.

7.2.3. Chain-length dependence for validation of experimental vaporization enthalpies

Admittedly, the $\Delta_l^g H_m^o$(298.15 K)-values correlate linearly with the number of C-atoms within the homologues series of organic compounds [157]. For example, n-alkanes with the chain-length $N_C = 2$ to 11 exhibit the following linear dependency (in kJ·mol^{-1}):

$$\Delta_l^g H_m^o(298.15 \text{ K}) = 1.03 + 5.06 \times N_C \quad \text{(with } R^2 = 0.9982) \quad (61)$$

Also n-alkanols with the chain-length $N_C = 2$ to 11 obey the following linear dependency (in kJ·mol^{-1}):

$$\Delta_l^g H_m^o(298.15 \text{ K}) = 33.2 + 4.74 \times N_C \quad \text{with } (R^2 = 0.9983) \quad (62)$$

Another example, n-alkylamines with the chain-length $N_C = 2$ to 11 show their own linear dependence (in kJ·mol^{-1}):

$$\Delta_l^g H_m^o(298.15 \text{ K}) = 16.5 + 4.82 \times N_C \quad \text{with } (R^2 = 0.9993) \quad (63)$$

The data included in these correlations are summarized in Table G. 5.

It is evident from Equation 61-63 that the (CH₂)-contribution to the $\Delta_l^g H_m^o$(298.15 K)-value in n-alkanes (5.06 kJ·mol^{-1}) is slightly higher compared to those in n-alkanols (4.78 kJ·mol^{-1}) or in n-alkylamines (4.82 kJ·mol^{-1}). Are aminoalcohols something special in regard to the chain-length dependence?

Table 39. Correlation of vaporization enthalpies, $\Delta_l^g H_m^o$(298.15 K), of 2-amino-1-alcohols with the chain length (NC).

CAS	Compound	N_C	$\Delta_l^g H_m^o$(298 K)$_{exp}$[a]	$\Delta_l^g H_m^o$(298 K)$_{calc}$[b]	Δ
6168-72-5	2-amino-1-propanol	3	59.9	59.7	0.2
96-20-8	2-amino-1-butanol	4	64.9	64.5	0.4
16369-14-5	2-amino-1-pentanol	5	-	69.4	-
5665-74-7	2-amino-1-hexanol	6	74.3	74.2	0.1
74872-95-0	2-amino-1-heptanol	7	-	79.0	-
16369-15-6	2-amino-1-octanol	8	-	83.8	-

[a] Experimental data from Table 37, [b] calculated with Equation 64.

The evaluated in this work $\Delta_l^g H_m^o$(298.15 K)-data on 2-amino-1-alkanols are collected in Table 39. The chain-length dependence developed for this series is given by the following equation (in kJ·mol^{-1}):

$$\Delta_l^g H_m^o(298.15 \text{ K}) = 45.3 + 4.81 \times N_C \qquad \text{with } (R^2 = 0.9998) \qquad (64)$$

It is quite obvious that the (CH_2)-contributions to the $\Delta_l^g H_m^o(298.15 \text{ K})$ derived for n-alkanols, n-alkyl-amines, and 2-amino-1-alkanols are hardly distinguishable. This observation can serve as a valuable indicator of internal consistency of our new experimental results. Moreover, the (CH_2)-contribution of 4.8 kJ·mol^{-1} can be also propagated to the series of on 1-amino-2-alkanols, where the reliable experimental $\Delta_l^g H_m^o(298.15 \text{ K})$-values are known only for 1-amino-2-propanol and 1-amino-2-butanol (Table 37). In order to assess the vaporization enthalpies for 1-amino-2-alkanols with the chain-length N_C = 5 to 8, the contribution (CH_2) = 4.8 kJ·mol^{-1} was subsequently added staring from the experimental value $\Delta_l^g H_m^o(298.15 \text{ K})$ = 63.7±0.4 kJ·mol^{-1} of 1-amino-2-butanol (Table 37). The $\Delta_l^g H_m^o(298.15 \text{ K})$-values for 1-amino-2-alkanols calculated in this additive manner are given in Table 37 and Tables G.1, G.5, G.6 and designated as "GA" (or calculated by the Group-Additivity).

Contrary to our expectations, the very good $(\Delta_l^g H_m^o(298.15 \text{ K}) - N_C)$ correlation was also obtained for the series n-alkanol-amines (3-amino-1-propanol, 4-amino-1-butanol, 5-amino-1-pentanol, and 6-amino-1-hexanol):

$$\Delta_l^g H_m^o(298.15 \text{ K}) = 48.6 + 4.76 \times N_C \qquad \text{with } (R^2 = 0.9998) \qquad (65)$$

The experimental data used for correlation are compiled in Table G. 6. The presence of the strong intra-molecular hydrogen bonding in 3-amino-1-propanol, and the absence of such a feature in 4-amino-1-butanol, 5-amino-1-pentanol, and 6-amino-1-hexanol are known [158]. To our surprise however, the vaporization enthalpy of 3-amino-1-propanol correlates perfectly with the species with the longer chain between amino and hydroxyl groups. Perhaps this observation might be explained by the significant prevalence of the inter-molecularly bound species compared to the intra-molecularly bound species in the liquid aminoalcohols.

7.2.4. Evaluation of available vaporization enthalpies

Information on $\Delta_f H_m^o(\text{liq}, 298.15 \text{ K})$ for eighteen aminoalcohols has been collected in Table 37. Unfortunately, most of these compounds are not commercially available in sufficient quantities for vapour pressure measurements using conventional techniques (ebulliometry, statics, transpiration, *etc.*). In order to obtain information about vaporization thermodynamics of a possibly broad scope of aminoalcohols structures, we applied the empirical method $(\Delta_l^g H_m^o(298.15 \text{ K}) - N_C$ correlation), structure-property relationships $(\Delta_l^g H_m^o(298.15 \text{ K}) - N_C$ correlations), as well as the GA procedure (development of the suitable CH_2-contribution). The experimental and "theoretical" vaporization enthalpies derived for each amino-alcohol are given in Table 37. From this table can

be seen, that for every compound agreement among $\Delta_l^g H_m^o$(298.15 K)-values, which were derived in different ways, all lie within the assigned error bars. To get more confidence and reliability, we calculated the weighted average (the uncertainty was used as a weighing factor) for most of aminoalcohols given in Table 37. These values are highlighted in bold and are recommended for thermochemical calculations.

7.2.5. Energetics of dehydrogenative coupling reactions of aminoalcohols leading to alkyl-pyrazines

The promising environmentally friendly dehydrogenative coupling of 2-aminoalcohols to form 2,5-disubstituted symmetrical pyrazines homogeneously catalyzed by a Mn-pincer complex was reported by Daw *et al.* [149]. The typical reactions R1 to R3 are given in Figure 36. A particular attraction of these reactions is that two molecules of aminoalcohols will release three molecules of H_2 and only water if 2,5-di-alkyl-substituted pyrazines can be obtained. The synthesis is carried out at 423 K with a conversion of 99% and an isolated yield of up to 95%.

The enthalpies of reactions, $\Delta_r H_m^o$(liq, 298.15 K), were calculated according to the Hess´s Law with help of standard molar enthalpies of formation, $\Delta_f H_m^o$(liq, 298.15 K), of reactions R_1-R_3 participants. The gas phase enthalpies of formation, $\Delta_f H_m^o$(g, 298.15 K), of numerous aminoalcohols were recently estimated using the high-level quantum-chemical composite method G4 [159]. These values for 2-amino-1-propanol, 2-amino-1-butanol, and 2-amino-1-pentanol (Table G. 7), have been combined with the $\Delta_l^g H_m^o$(298.15 K)-values for these aminoalcohols evaluated in this work (Table 37). The resulting liquid phase enthalpies of formation, $\Delta_f H_m^o$(liq, 298.15 K), are given in Table 41. The $\Delta_f H_m^o$(liq, 298.15 K)-values for alkyl-pyrazines were evaluated in our recent works [146,147] and they are given in Table 40, column 3.
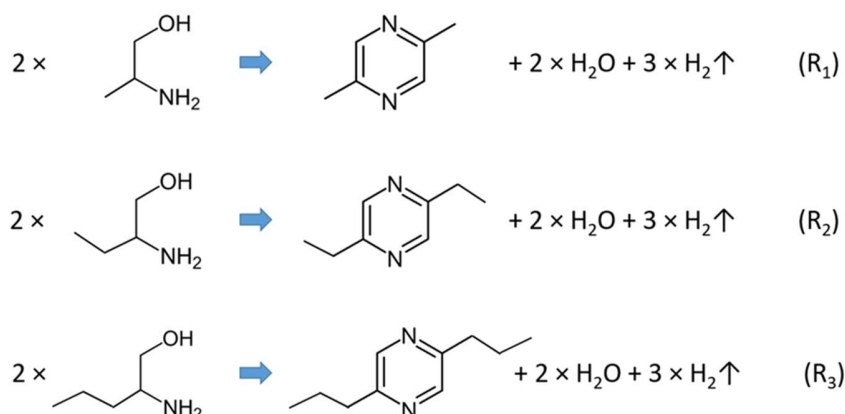
Figure 36. Dehydrogenative coupling reactions of aminoalcohols leading to alkyl-pyrazines.
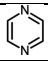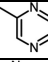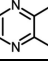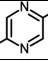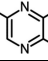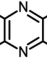
Table 40. Energetics of R1 – R3 dehydrogenative coupling reactions of aminoalcohols at T = 298.15 K (p° =0.1 MPa) (in kJ·mol-1).

Reaction	$\Delta_f H_m^o(AA)$ [a]	$\Delta_f H_m^o(AP)$ [b]	$\Delta_r H_m^{o}$ [c]
R$_1$	-300.8±3.7	67.0±2.0	97.0±4.2
R$_2$	-325.7±3.6	25.8±3.0	104.8±4.7
R$_3$	-353.4±3.8	-28.6±3.0	106.6±4.8

[a] Data for aminoalcohols from Table G.7, [b] data for alkyl-pyrazines from Table G. 8, [c] calculated according to the Hess´s Law applied to reactions R$_1$ – R$_3$ and $\Delta_f H_m^o$(liq, H$_2$O) = (-285.83 ± 0.04) kJ·mol^{-1} [32].

The resulting reactions R$_1$-R$_3$ enthalpies, $\Delta_r H_m^o$(298.15 K), calculated using the Hess´s Law are given in Table 40, column 4. Surprisingly, it has turned out that the dehydrogenative coupling reactions of aminoalcohols are strongly endothermic with the reaction enthalpies at the level of 100 kJ·mol^{-1}. This aspect must be taken into account when optimizing the synthetic conditions. The energetic effects of all three reactions are not very different, but the slight dependence on the chain length does not seem to be important within the experimental error bars.

Table 41. Reaction enthalpies of hydrogenation/dehydrogenation of pyrazine derivatives, at T = 298.15 K in kJ·mol^{-1} [146,147].

Compounds		$\Delta_r H_m^o$(liq)[a]	$\Delta_r H_m^o$/H$_2$ [b]
pyrazine		-178.7	-59.7
methyl-pyrazine		-173.2	-57.7
2,3-dimethyl-pyrazine		-161.6	-53.9
2,5-dimethyl-pyrazine		-163.9	-54.6
tri-methyl-pyrazine		-155.0	-51.7
tetra-methyl-pyrazine		-145.4	-48.5

[a] Calculated according to the Hess´s Law applied to chemical reaction, e.g. for pyrazine C$_4$H$_4$N$_2$(liq) + 3 H$_2$ (g) = C$_4$H$_{10}$N$_2$(liq), [b] reaction enthalpy per mole of hydrogen in kJ·mol^{-1}/H$_2$

In our recent works [146,147], we have shown that pyrazine and alkyl substitute pyrazines can be considered as prospective candidates for LOHC. The energetics of hydrogenation/dehydrogenation of pyrazine derivatives is significantly lower compared to other seminal LOHC candidates. For example, for 2,5-dimethyl-pyrazine, the reaction enthalpy per mole of hydrogen $\Delta_r H_m^o$ = -54.6 kJ·mol^{-1}/H$_2$ (Table 40) is considerably lower than those for the commercially available biphenyl with $\Delta_r H_m^o$ = -64.6 kJ·mol^{-1}/H$_2$ [160] or commercial thermofluids based on benzyltoluenes (Marlothem LH$^®$) and dibenzyltoluenes (Marlotherm SH$^®$) (-63.5 and -65.4 kJ·mol^{-1}/H$_2$, respectively) [161]. Moreover, the reaction enthalpy for 2,5-dimethyl-pyrazine is comparable with enthalpy of hydrogenation of N-ethyl-carbazole (-50.5 kJ·mol^{-1}/H$_2$)

[161–163]. It has also been found that a consequent methylation of the pyrazine ring (methyl, dimethyl, trimethyl, and tetramethyl) decreases even more significantly (Table 41) the liquid phase reaction enthalpy per mole of hydrogen (from -59.7 kJ·mol^{-1} observed for unsubstituted pyrazine to -48.5 kJ·mol^{-1} for tetra-methyl-pyrazine) [146,147].

Chapter 8 Thermochemical properties and dehydrogenation thermodynamics of indole derivates

8.1. Introduction

Liquid Organic Hydrogen Carrier (LOHC) are a promising way of storing hydrogen by reversible, catalytic hydrogenation of an aromatic compound. The hydrogen-rich form of an LOHC is the corresponding alicyclic component, which can be stored stably at ambient conditions. For dehydrogenation, i.e. hydrogen release, the hydrogenated LOHC is heated to temperatures of usually 250 to 310 °C [164]. In this reaction, hydrogen is set free and the aromatic form of the carrier is recovered for further storage cycles. To enable dehydrogenation at lower temperatures, there are two main options. First, the partial pressure of hydrogen can be reduced, either by lowering total pressure or by dilution with an inert gas. Second, the heat of reaction for the endothermic reaction can be lowered. Thus, LOHC materials with lower enthalpy of reaction for dehydrogenation are needed. Nitrogen-containing aromatic systems turn out to be very promising in this regard [165].

N-ethyl carbazole has drawn much attention in recent years as a nitrogen-containing LOHC. An alternative to carbazole-type LOHCs are indoles. A carbazole molecule can basically be understood as an indole molecule with four additional carbon atoms, forming a further six-membered ring fused with the indole molecule. Hence, indole and its derivatives cannot only be used as a LOHC material itself, as it is frequently proposed [166–169], but can also serve as model components for understanding the chemistry of carbazole-type LOHCs [170].

The dehydrogenation of per-hydrogenated indole (H8-indole) proceeds via two main steps: first, dehydrogenation to indoline and, second, dehydrogenation to indole (Figure 37):
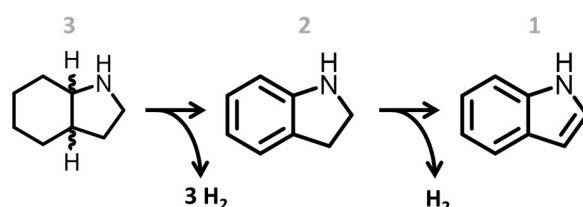
Figure 37. Reaction scheme for the dehydrogenation of H8-indole

Stopping the reaction at the stage of indoline would still provide 75 % of the total stored hydrogen, but to recover everything the reaction has to proceed to indole. The question, if the indoline is dehydrogenated further to indole or if first further H8-indole is dehydrogenated, before dehydrogenation of indoline starts, is not solely governed by catalysis, but also by the reaction thermodynamics.

In this study, measurements of the thermochemical properties of indole and its partially (indoline) and fully (H8-indole) hydrogenated derivatives are reported. From the difference in these substance properties, particularly the reaction enthalpies, conclusions on the thermodynamics of the reaction network can be drawn. To enhance the scope and improve the understanding of the model component indole as a basis for carbazole-type LOHCs, the evaluation also includes the methylated derivatives with the methyl group on the carbon-atom next to the nitrogen-atom.

8.2. Results and discussion

8.2.1. Heat capacity measurements

Heat capacities for the indole derivatives, except for 2-methylindole were measured for the first time. The only available for comparison data set was on 2-methylindole measured with help of the high-precision cryogenic adiabatic calorimetry [171]. The maximum deviation of our data from the literature is 1,5% in the temperature range from 240 up to 294 K, but such deviation of the DSC results from the adiabatic calorimetry results is typical. The heat capacities for the indole derivatives derived in this work are given in Table H. 1 and Table H. 2. The heat capacities at the reference temperature $T = 298.15$ K (Table 42) have been used for the temperature adjustments of experimental vaporization enthalpies as follows.

Table 42. Compilation of data on molar heat capacities $C_{p,m}^o$(g, cr or liq) and heat capacity differences $\Delta_{cr,l}^g C_{p,m}^o$ (in J·K^{-1}·mol^{-1}) at $T = 298.15$ K.

Compounds	$C_{p,m}^o$(g) [a]	$C_{p,m}^o$(cr)	$-\Delta_{cr}^g C_{p,m}^o$ [b]	$C_{p,m}^o$(liq)	$-\Delta_l^g C_{p,m}^o$ [b]
indole (cr)	120.9	162.2 [c]	**25.1**(41.3)	208.9 [d]	-
indoline (liq)	127.5	-	-	219.5 [c] 213.3 [172]	**67.7**(92.0)
H8-indole (liq)	151.5	-	-	242.3 [c]	**73.6**(93.0)
2-methyl-indole (cr)	146.1[171]	175.5 [171] [e] 179.9 [c]	**27.1**(29.4)	224.6 [171]	**69.0**(78.5)
2-methyl-indoline (liq)	174.0	-	-	251.3 [c]	**75.9**(77.3)
2-methyl-H8-indole (liq)	178.6	-	-	266.5 [c]	**79.9**(84.4)

[a] Calculated in this work using RRHO approach of statistical thermodynamics [173], [b] calculated according to the [27] by using experimental heat capacities $C_{p,m}^o$ (cr or liq), [c] measured with DSC, [d] calculated by the group-contribution procedure developed by Acree and Chickos [27], [e] measured with the adiabatic calorimeter [171].

8.2.2. Vapor pressures and thermodynamics of sublimation /vaporization

Experimental vapor pressures measured at different temperatures by the transpiration method, coefficients a and b of Equation 2, as well as values of $\Delta_{cr,l}^{g} H_m^o(T)$ and $\Delta_{cr,l}^{g} S_m^o(T)$ are given in Table 43. The method for calculating the combined uncertainties of the vaporization/sublimation enthalpies includes uncertainties from the experimental conditions of transpiration, uncertainties in vapor pressure and uncertainties due to the temperature adjustment to $T = 298.15$ K as described elsewhere [75,76,174].

The compilation of available standard molar vaporization/sublimation enthalpies for the indole derivatives is given in Table 44. Vapor pressures and vaporisation enthalpies of H8-indole, 2-methyl-indoline, and 2-methyl-H8-indoline have been measured for the first time. Vapor pressures and sublimation/vaporization enthalpies of the indole and indoline were frequently reported in the literature (Table 44). For the sake of comparison, the reported in the literature enthalpies of vaporisation/sublimation of indole derivatives were adjusted to the reference temperature $T = 298.15$ K by using the $\Delta_{cr,l}^{g} C_{p,m}^o$–values given in Table 42 in the same way as our own transpiration results.

Table 43. Results from the transpiration method: coefficient a and b of Equation 2, standard molar sublimation/vaporization enthalpies $\Delta_{cr,l}^{g} H_m^o$, standard molar sublimation/vaporization entropies $\Delta_{cr,l}^{g} S_m^o$, and standard molar sublimation/vaporization Gibbs energies $\Delta_{cr,l}^{g} G_m^o$ at the reference temperature $T = 298.15$ K.

	a	b	$-\Delta_{cr,l}^{g} C_{p,m}^o$ [a] $J \cdot K^{-1} \cdot mol^{-1}$	$\Delta_{cr,l}^{g} H_m^o$ [b] $kJ \cdot mol^{-1}$	$\Delta_{cr,l}^{g} S_m^o$ [c] $J \cdot K^{-1} \cdot mol^{-1}$	$\Delta_{cr,l}^{g} G_m^o$ $kJ \cdot mol^{-1}$
indole (cr)	283.3	-82861.1	25.1	75.4±1.3	162.5±2.4	26.9±0.04
indoline (liq)	290.8	-80648.7	67.7	60.5±0.6	127.4±1.6	11.5±0.20
H8-indole (liq)	293.7	-75474.3	73.6	53.5±0.7	124.4±1.6	16.5±0.06
2-methyl-indole (cr)	304.5	-93204.6	27.1	85.1±1.2	181.7±1.4	31.0±0.04
2-methyl-indoline (liq)	307.7	-85660.1	75.9	63.0±0.4	136.1±0.8	11.6±0.20
2-methyl-H8-indoline (liq)	311.3	-81609.0	79.9	57.8±0.8	135.6±1.8	17.3±0.06

[a] Calculated according to the procedure developed by Acree and Chickos by using experimental heat capacities $C_{p,m}^o$ (cr or liq) from this table, [b] calculated by Equation 8, [c] calculated by Equation 9.

For the indole, except for one extremely high [175] and one extremely low [176] value, other available sublimation enthalpies from the Knudsen-effusion and from the transpiration method are in a good agreement (Table 44). Moreover, the recently developed indirect method based on the high-precision solution calorimetry results [177,178], also provides the sublimation enthalpy of indole in close agreement with the conventional methods (Table 44). To get more confidence, we have derived a weighted average from the ten entries for the sublimation enthalpy of indole, and the result is $\Delta_{cr}^{g} H_m^o(298.15 \text{ K}) = 75.0\pm0.4$ kJ·mol^{-1}.

The vaporization enthalpy of the indoline measured in this work is within the combined uncertainty of those measured in our lab previously [179] (Table 44), as well as from the result measured by using the "vacuum sublimation" drop microcalorimetric method [180]. We have derived the weighted average from the tree entries for the vaporisation enthalpy of indoline, and the result is $\Delta_l^g H_m^o$(298.15 K) = 60.7±0.5 kJ·mol⁻¹.

Table 44. Compilation of available enthalpies of sublimation/vaporization $\Delta_{cr,l}^g H_m^o$.

Compound/CAS	Methodᵃ	T- range	$\Delta_{cr,l}^g H_m^o(T_{av})$	$\Delta_{cr,l}^g H_m^o$(298.15 K)	Ref.
		K	kJ·mol⁻¹	kJ·mol⁻¹	
indole (cr)	K	283-328	74.9±2.0	75.1±2.0	[181]
	VG	283-301	70.0±2.0	(69.9±2.0)	[176]
	K	291.8-319.1	74.2±2.8	74.4±3.0	[42]
	K	298-315	95.0±4.0	(95.1±4.0)	[175]
	K	275-303	77.8±3.4	77.6±3.4	[182]
	K	275.2-291.1	78.4±2.2	78.0±2.8	[180]
	T	290.4-325.2	73.7±0.8	74.0±1.2	[179]
	SC			75.0±2.0	[177]
	SC			75.0±1.7	[178]
	SC			75.3±1.7	[178]
				74.9±0.6	Table 45
	T	293.1-323.2	75.1±0.7	75.4±1.3	this work
				75.0±0.4	average
indoline (liq)	DC	329.1	65.6±0.6	61.9±1.9	[180]
	E	380.9-547.3	50.9±0.2	61.6±1.7	[172]
	T	280.6-338.3	60.3±0.4	61.0±0.8	[179]
	T	288.7-335.2	59.6±0.5	60.5±0.6	this work
				60.8±0.9 ᶜ	average
H8-indole (liq)	T	277.9-329.2	53.3±0.4	53.5±0.7	this work
2-methyl-indole (cr)	DC	360.1	91.7±1.0	87.6±2.4	[171,183]
				85.5±1.0	Table 45
	T	298.3-330.1	84.7±0.4	85.1±1.2	this work
				85.5±0.7	average
2-methyl-indole (liq)	IP	340.0-430.0	66.3±0.2	72.1±1.0	[171,172]
	E	427.3-595.0	58.0±0.2	72.2±2.2	[171,172]
				72.1±0.9	average
2-methyl-indoline (liq)	T	283.2-333.0	62.4±0.3	63.0±0.4	this work
2-methyl-H8-indole (liq)	T	275.1-313.2	58.2±0.6	57.8±0.8	this work

ᵃ Techniques: DC = drop calorimetry; T = transpiration method; K = Knudsen effusion method; SC = method based on solution calorimetry; VG = viscosity gauge; IP = inclined piston method; E = Ebulliometry.

The value $\Delta_{cr}^g H_m^o$ = 65.6±0.6 kJ·mol⁻¹ at 329.1 K was directly determined for 2-methyl-indole with a drop microcalorimetric technique, combined with an enthalpy for the gas phase of $\Delta_{298.15\,K}^{329.1\,K} H_m^o$(g) estimated with the group-contribution method of Stull et al. [77]. Chirico et al. [171] recalculated their value to be 87.6± 2.4 kJ·mol⁻¹ at 298.15 K by including the enthalpy for the gas phase computed with the quantum-chemical methods, rather than the very approximate

group-contribution method. The latter value is in agreement with our new transpiration result $\Delta_{cr}^{g}H_{m}^{o}$(298.15 K) = 85.1±1.2 kJ·mol⁻¹ within the combined experimental uncertainties (Table 44).

8.2.3. Thermodynamics of solid-liquid, solid-gas, and liquid-gas phase transitions

2-Methyl-indole is crystalline at room temperature. The consistency of enthalpies of sublimation, vaporization and fusion for this compound was established as follows. Indeed, for indole, the sublimation enthalpy $\Delta_{cr}^{g}H_{m}^{o}$(298.15 K) = 75.4±1.3 kJ·mol⁻¹ was measured using transpiration below the melting point (Table 44) and the vaporization enthalpy $\Delta_{l}^{g}H_{m}^{o}$(298.15 K) = 65.3±0.6 kJ·mol⁻¹ was derived from vapor pressures measured above the melting point in our previous work [179] (Table 45). The consistency of phase transitions available for the indole can be easily established and the experimental enthalpy of fusion for this compound $\Delta_{cr}^{l}H_{m}^{o}$(298.15 K) = 9.6±0.4 kJ·mol⁻¹ (Table 45) as follows:

$$\Delta_{cr}^{g}H_{m}^{o}(298.15 \text{ K, indole}) = 65.3 + 9.6 = 74.9 \pm 0.7 \text{ kJ·mol}^{-1} \qquad (66)$$

This estimate is in a good agreement with the transpiration experiment $\Delta_{cr}^{g}H_{m}^{o}$(298.15 K) = 75.4±1.3 kJ·mol⁻¹ (Table 44)

Table 45. Thermodynamics of phase transitions of indoles (in kJ·mol⁻¹).

Compounds	T_{fus}, K	$\Delta_{cr}^{l}H_{m}^{o}$ at T_{fus}	Ref	$\Delta_{cr}^{l}H_{m}^{o}$ [a]	$\Delta_{l}^{g}H_{m}^{o}$ [b]	$\Delta_{cr}^{g}H_{m}^{o}$
					298.15K	
1	2	3	4	5	6	7
indole	325.9	10.6±0.5	[184]			
	326.3	10.9±0.5	[185]			
	325.9	10.6±0.2	[179]			
	325.5	12.1±1.0	[177]			
	325.7	10.9±0.3	this work			
	325.9	**10.7±0.2**	average	9.6±0.4	65.3±0.6[179]	**74.9±0.7**
2-methylindole	329.4	15.7±1.0	[186]			
	332.0	14.84±0.03	[171]			
	331.1	14.7±0.2	this work			
	332.0	**14.8±0.1**	average	13.4±0.4	72.1±0.9	**85.5±1.0**

[a] The experimental enthalpies of fusion $\Delta_{cr}^{l}H_{m}^{o}$ measured at T_{fus} were adjusted to 298.15 K with help of the equation [27]: $\Delta_{cr}^{l}H_{m}^{o}$(298.15 K)/(J·mol⁻¹) = $\Delta_{cr}^{l}H_{m}^{o}$(T_{fus}/K) – ($\Delta_{cr}^{g}C_{p,m}^{o}$-$\Delta_{l}^{g}C_{p,m}^{o}$)×[($T_{fus}$/K) – 298.15 K], [b] from Table 44.

In this way we also validated the phase transition data available for 2-methylindole as follows. The consistent vaporization enthalpies for this compound were measured by Chirico et al. [171] by using the inclined-piston manometry and ebulliometry (Table 44). The fusion enthalpy is evaluated in Table 45:

$$\Delta_{cr}^{g}H_{m}^{o}(298.15 \text{ K, 2-methylindole}) = 72.1 + 13.4 = 85.5 \pm 1.0 \text{ kJ·mol}^{-1} \qquad (67)$$

This indirect result is in agreement with the transpiration experiment $\Delta_{cr}^{g}H_{m}^{o}$(298.15 K) = 85.1±1.2 kJ·mol⁻¹ and with those from the drop microcalorimetric technique $\Delta_{cr}^{g}H_{m}^{o}$(298.15 K) = 87.6±2.4

kJ·mol^{-1} (Table 44). The agreement of data on indole and 2-methyl-indole supports the consistency of the solid-liquid, solid-gas, and liquid-gas phase transitions derived for these compounds in this work.

8.2.4. Validation of experimental vaporization enthalpies of indole derivatives with help of the structure-property relationships

Having in mind, that the vaporisation enthalpies of H8-indole, 2-methyl-indoline, and 2-methyl-H8-indoline have been measured for the first time, any kind of validation for these new data is highly desired. Structure-property relationships are always helpful in this context.
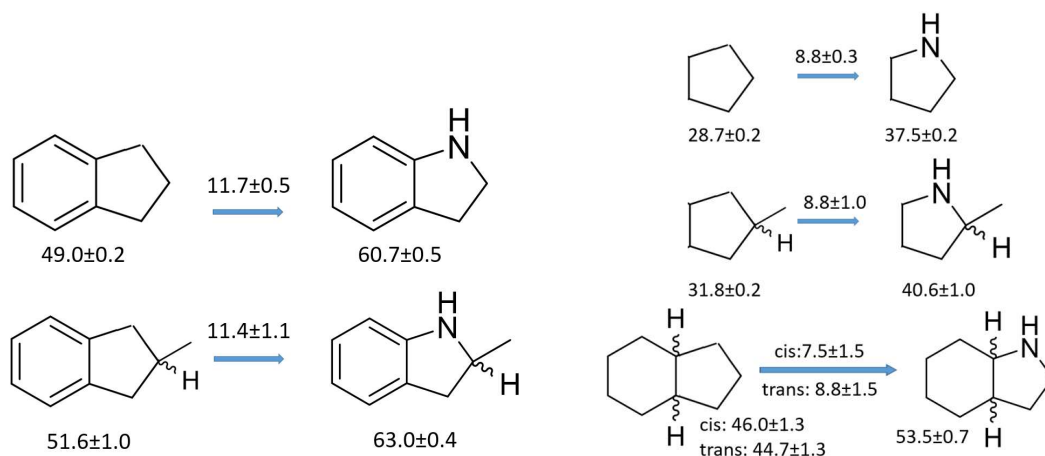
Figure 38. Validation of experimental vaporization enthalpies, $\Delta_l^g H_m^o$(298.15 K), of indole derivatives with help of the comparison with similarly shaped cyclic hydrocarbons: series indane – indoline (left) and series cyclopentane – pyrrolidines (right). All data are given in kJ·mol^{-1}.

It is reasonable to find out parallels between vaporization enthalpies in series of experimental vaporization enthalpies derived in this work for indole derivatives with the vaporization enthalpies of similarly shaped cyclic hydrocarbons given in Figure 38. As expected, for the series indane – indoline derivatives (Figure 38, left) the differences in $\Delta_l^g H_m^o$(298.15 K) of indane and indoline, as well as for 2-methyl-indane and 2-methyl-indoline are perfectly the same. Also for the series cyclopentane – pyrrolidines (Figure 38, right) the differences in $\Delta_l^g H_m^o$(298.15 K) between cyclopentane and pyrrolidine is exactly the same as the difference between methyl-cyclopentane and methyl-pyrrolidine. For the pair octahydro-1H-indene – H8-indole the difference of vaporization enthalpies shows the same level of 8 kJ·mol^{-1}. Hence, these quantitatively logical structure-property relationships between hydrocarbons and the parent molecules with inserted nitrogen atom can be considered as a strong evidence of consistency for vaporization enthalpies evaluated in this study.

8.2.5. Combustion calorimetry: standard molar enthalpies of formation

Specific energies of combustion $\Delta_c u°$ were measured in series of five experiments for each compound. Table H. 6 and Table H. 7 list results of combustion experiments for indole derivatives. Auxiliary data required for the reduction of the combustion results are presented in Table H. 4, Table H. 5 that list results of a typical combustion experiment for each compound. Combustion results for $\Delta_c u°$ and $\Delta_c H_m^o$ are reported in Table H. 6 and Table H. 7, where these refer to the reactions:

indole: $C_8H_7N(cr) + 9.75 \times O_2(g) = 8 \times CO_2(g) + 3.5 \times H_2O(liq) + 0.5\ N_2(g)$ (68)

indoline: $C_8H_9N(liq) + 10.25 \times O_2(g) = 8 \times CO_2(g) + 4.5 \times H_2O(liq) + 0.5\ N_2(g)$ (69)

H8-indole: $C_8H_{15}N(liq) + 11.75 \times O_2(g) = 8 \times CO_2(g) + 7.5 \times H_2O(liq) + 0.5\ N_2(g)$ (70)

2-methyl-indole: $C_9H_9N(cr) + 11.25 \times O_2(g) = 9 \times CO_2(g) + 4.5 \times H_2O(liq) + 0.5\ N_2(g)$ (71)

2-methyl-indoline: $C_9H_{11}N(liq) + 11.75 \times O_2(g) = 8 \times CO_2(g) + 5.5 \times H_2O(liq) + 0.5\ N_2(g)$ (72)

2-methyl-H8-indole: $C_9H_{17}N(liq) + 13.25 \times O_2(g) = 8 \times CO_2(g) + 8.5 \times H_2O(liq) + 0.5\ N_2(g)$ (73)
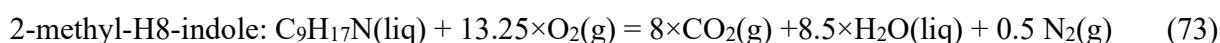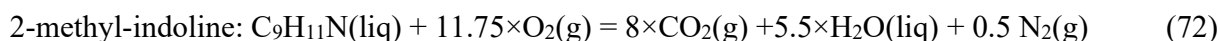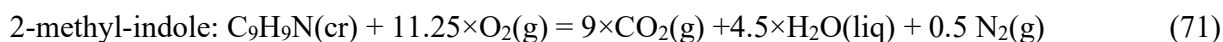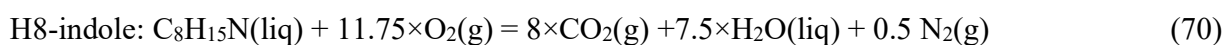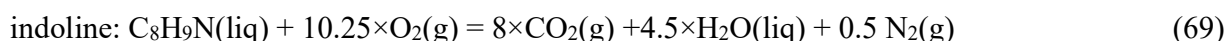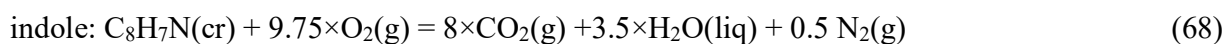
The $\Delta_f H_m^o$(cr or liq)-values of indole derivatives were obtained (Table 46) applying the Hess´s Law to Equations 68-73 with help of recommended by CODATA data [32]; uncertainties are calculated according to the guidelines developed by Olofsson [187]. The compilation of thermochemical results derived in this work is given in Table 46.

Table 46. Compilation of thermochemical data for indole derivatives at T=298.15 K ($p°$=0.1 MPa, in kJ·mol^{-1}).

compound	$\Delta_c H_m^o$(cr,l)	$\Delta_f H_m^o$(cr,l)	$\Delta_{cr,l}^g H_m^{o\ a}$	$\Delta_f H_m^o$(g)$_{exp}$	$\Delta_f H_m^o$(g)$_{theor}$[b]
1		2	3	4	5
indole (cr)	-4278±30 [188]	(130±30)			
	-4265±4 [189]	(117±5)			
	-4240.5±5.0 [175]	92.0±5.1			
	-4235.0±0.7 [190]	86.5±1.3			
	-4236.0±1.4 [179]	87.6±1.8			
	-4235.8±1.3 [this work]	87.3±1.6			
		87.2±0.9	**75.0±0.4**	**162.2±1.0**	160.9±1.5
indoline (liq)	-4492.4±2.2 [180]	58.1±2.4			
	-4497.7±2.0 [79]	63.4±2.2			
	-4494.0±1.0 [172]	59.7±1.5			
	-4493.6±1.3 [this work]	59.3±1.7			
		60.0±0.9	**60.8±0.9**	**120.8±1.3**	117.5±1.4
H8-indole (liq)	-5174.3±1.5 [this work]	-117.5±1.8	53.5±0.7	-64.0±1.9	-63.1±1.4
2-methyl-indole (cr)	-4865.6±2.4 [183]	37.7±2.7			
	-4864.8±1.1 [171]	36.9±2.6			
	-4862.6±1.5 [this work]	34.8±1.9			
		36.1±1.3	**85.5±0.7**	**121.6±1.5**	121.3±2.0
2-methyl-indoline	-5130.8±1.5 [this work]	17.2±1.9	63.0±0.4	80.2±1.9	80.3±1.6
2-methyl-H8-indole	-5814.1±1.8 [this work]	-157.1±2.1	57.8±0.8	-99.3±2.2	-99.5±1.3

[a] From Table 44, [b] averaged quantum-chemical results from G4, G3MP2, and CBS-APNO calculations (Table 47).

Berthelot and Andre [188] were the first to determine the enthalpy of combustion of indole. Stern and Klebs [189] determined the enthalpy of combustion of indole in the crystalline state at 298.15 K. Both results are significantly more negative than all later determinations. Zimmerman and Geisenfelder [175] reported thermochemical data for a large number of the nitrogen containing compounds. However, purities of their samples are ill defined and we ascribed to the combustion enthalpy measured in their work a generous uncertainty of $\pm$ 5 kJ·mol^{-1}. Good [190] from one of the most experienced Bartlesville laboratory performed combustion experiments with a sample of purity 99.90 mol percent. The value determined by Good is in accord with our recent as well as with the new combustion result measured for the indole in the current study (Table 46).

The enthalpy of combustion for indoline in the liquid state was determined earlier by Ribeiro da Silva et al. [180], as well as in our previous study [79]. Both these values were in fair agreement within the combined experimental uncertainties (Table 46). Our new combustion enthalpy value agrees well with both previous results and corresponds to the place in between.

The enthalpy of combustion for 2-methylindole in the crystalline state was determined previously by Ribeiro da Silva et al. [183] and by Chirico et al. [171]. Their values agree well with that obtained here (Table 46). In order to get more confidence, we have derived the weighted average values for indole, indoline, and 2-methyl-indole (Table 46) and recommended them for further thermochemical calculations. Combustion experiments with H8-indole, 2-methyl-indoline, and 2-methyl-H8-indole were performed for the first time and results are compiled in Table 46.

8.2.6. Gas-phase standard molar enthalpies of formation: experiment and theory

The experimental gas-phase standard molar enthalpies of formation $\Delta_f H^o_m(g)_{exp}$ are derived from experimental results on vapor pressure measurements and results from combustion calorimetry according to common thermochemical equations:

$$\Delta_f H^o_m(g, 298.15 \text{ K})_{exp} = \Delta_{cr}^g H^o_m(298.15 \text{ K}) + \Delta_f H^o_m(cr, 298.15 \text{ K})_{exp} \qquad (74)$$

$$\Delta_f H^o_m(g, 298.15 \text{ K})_{exp} = \Delta_l^g H^o_m(298.15 \text{ K}) + \Delta_f H^o_m(liq, 298.15 \text{ K})_{exp} \qquad (75)$$

Results obtained with help Equations 74 and 75 are given in Table 46, column 5. Since thermochemical data on three indole derivatives were measured for the first time, we used the high-level quantum-chemical calculations to support the reliability of our new results.

Search for structures of the stable conformations was performed using the UFF method [36]. Optimization of conformers was performed by using G3MP2. Structures of main conformers were identified with the Amsterdam Density Functional (ADF) program [36] with help of M06L/TZ2P and M06/QZ4P methods. Basis sets were built with Slater-type orbital functions.

Harmonic frequencies were calculated with help of M06L/TZ2P method. Enthalpies H_{298} of the most stable conformers for each compound (Figure 39) were calculated by using and G4 G3MP2, and SBS-APNO methods.

Structure	Name	Figures	Structure	Name	Figures
	Indole			Indoline	
	H8-Indole			2-Methyl-Indole	
	2-Methyl-Indoline			H8-2-Methyl-Indole	
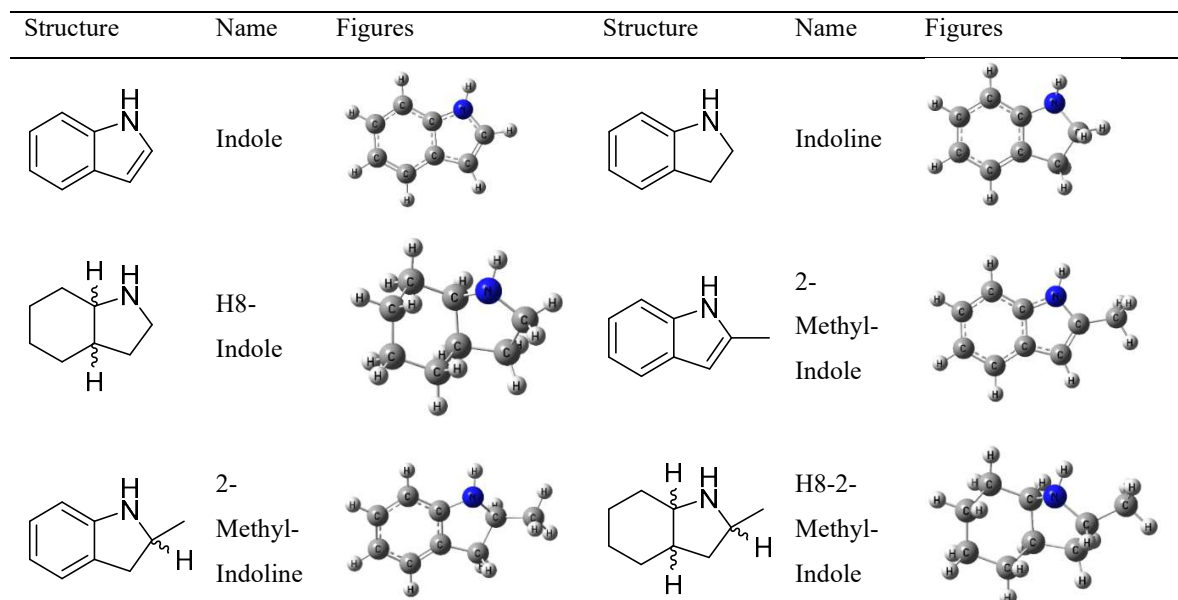
Figure 39. The most stable conformers of indole derivatives.

The H_{298}-values have been converted to the standard molar enthalpies of formation $\Delta_f H_m^o$(g, 298.15 K)$_{theor}$ using the atomization (AT), as well as using the "well-balanced reactions" (WBR) [96]. For the *WBR* method we designed 5-6 reactions for each indole derivative (Table H. 9 - Table H. 14). Using reliable experimental gas-phase enthalpies of formation $\Delta_f H_m^o$(g, 298.15 K) of the reference compounds (Table H. 15), the theoretical gas phase enthalpies were calculated. Results of quantum-chemical calculations are summarized in Table 47.

Table 47. Experimental and theoretical gas-phase enthalpies of formation $\Delta_f H_m^o$(g) at T = 298.15 K ($p°$ = 0.1 MPa) for indole derivatives as calculated by different methods (in kJ·mol^{-1}).

compound	Exp.[a]	G4 AT[b]	G4 WBR[c]	G3MP2 AT[b]	G3MP2 WBR[c]	CBS-APNO WBR[c]	$\Delta_f H_m^o$(g)$_{theor}$[d]
indole	162.2±1.0	160.4±3.5	161.0±1.3	158.8±4.1	160.9±1.1	161.2±2.0	160.9±1.5
indoline	120.8±1.3	117.6±3.5	117.3±1.4	116.0±4.1	117.7±1.1	117.6±1.3	117.5±1.4
H8-indole	-64.0±1.9	-63.5±3.5	-64.1±1.6	-60.5±4.1	-63.3±1.2	-62.7±1.1	-63.1±1.4
2-methyl-indole	121.6±1.5	120.2±3.5	121.7±1.8	118.9±4.1	121.8±1.6	120.7±2.7	121.3±2.0
2-methyl-indoline	80.2±1.9	79.4±3.5	80.1±1.4	78.0±4.1	80.5±1.3	80.7±1.7	80.3±1.6
2-methyl-H8-indole	-99.3±2.2	-100.4±3.5	-100.4±1.5	-97.3±4.1	-99.6±1.2	-99.1±1.0	-99.5±1.3

[a] From Table 46, [b] Calculated by the G4 or G3MP2, [c] Calculated by the G4, G3MP2, and CBS-APNO, [d] Calculated for each compound as the weighted average from columns 3 to 7 from this Table.

In our recent work we systematically use the G4 and the G3MP2 methods for thermochemical calculations [30,59–61,79,179]. As it quite apparent from Table 47, the G4 *theoretical* values $\Delta_f H_m^o$(g, 298.15 K)$_{theor}$ are practically indistinguishable from the *experimental*

results, regardless of atomization or WBR procedure is applied. Table 47 also demonstrates that the G3MP2 *theoretical* values $\Delta_f H_m^o$(g, 298.15 K)$_{theor}$ calculated according to the *WBR* are also in good agreement with the *experimental* values $\Delta_f H_m^o$(g, 298.15 K)$_{exp}$. The CBS-APNO results derived with help of the WBR are also in very good agreement with the *experimental* values $\Delta_f H_m^o$(g, 298.15 K)$_{exp}$.

8.2.7. Validation of experimental enthalpies of formation of indole derivatives with help of structure-property relationships

Even having remarkable agreement between the *experimental* and *theoretical* $\Delta_f H_m^o$(g, 298.15 K)-values, the additional validation of the evaluated results with help of structure-property relationships is desired. For this purpose, in Figure 40 we separated the studied compounds in to vertical lines: the line indole → indoline → H8-indole, as well as the line 2-methyl-indole → 2-methyl-indoline → 2-methyl-H8-indole. Both lines represent virtual hydrogenation reactions. At a first glance we would expect that introduction of the methyl substituent into the five-membered ring (left line) could hardly change the energetics of these virtual hydrogenation reactions in comparison to the methylated indole derivatives (right line).
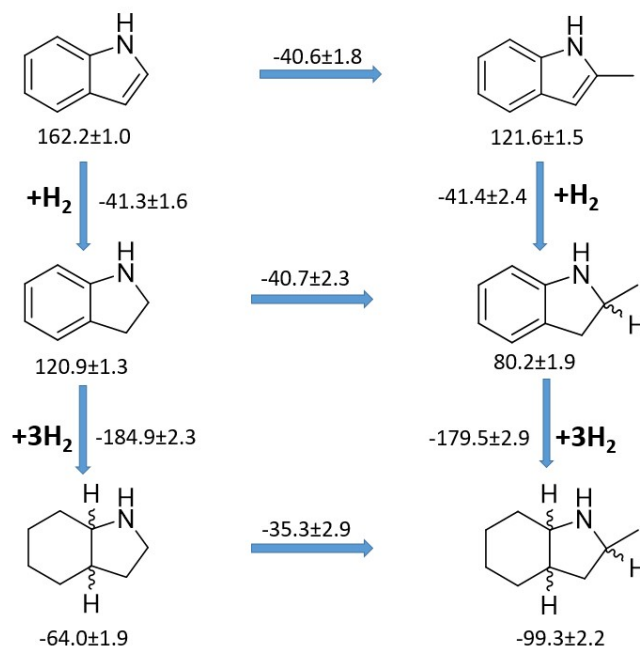
Figure 40. Virtual hydrogenation reactions of indole derivatives. The *experimental* values $\Delta_f H_m^o$(g, 298.15 K)$_{exp}$ are taken from Table 46 and they are given in kJ·mol^{-1}.

Indeed, as it can be seen on Figure 40, the hydrogenation enthalpies presented by arrows from the top (indole) to the bottom (H8-indole) in the left line are indistinguishable (within the experimental uncertainties) from analogous reactions presented in the right line. Moreover, the

enthalpic effect from introduction of the methyl-substituent to the species given in the left line (indole → indoline → H8-indole) is also remarkably constant for the indole (40.6 ± 1.8 kJ·mol^{-1}) and indoline (40.7 ± 2.3 kJ·mol^{-1}). This enthalpic effect is slightly lower (35.3 ± 2.9 kJ·mol^{-1}) for the pair H8-indole to 2-methyl-H8-indole, but this light decrease could be explained by appearing of the ring-strains in both aliphatic cyclic compounds, which are usually very specific for each cyclic specie.

The good agreement observed among the *theoretical* and *experimental* $\Delta_f H_m^o$(g, 298.15 K)-values for indole derivatives, as well as the logical structure-property relationships demonstrated on Figure 40 can be considered as an evidence of the internal consistency of thermochemical results evaluated in this work (Table 46). This can be recommended now as reliable benchmark properties for further thermochemical calculations of hydrogenation/dehydrogenation reactions involving these compounds.

8.2.8. Standard molar thermodynamic functions of indole derivatives

The possibility to assess the ideal gas and condensed phase properties of organic compounds is of importance for material sciences, engineering, and biochemistry. The basic thermodynamic equation for the Gibbs free energy:

$$\Delta_f G_m^o = \Delta_f H_m^o - T \times \Delta_f S_m^o \tag{76}$$

is responsible for the quick appraisal of feasibility of chemical processes. Hence, it is highly desirable to assess values of $\Delta_f H_m^o$ and $\Delta_f S_m^o$ from the experiments, computations, or combining theoretical and experimental methods.

8.2.8.1. Computation of heat capacities and entropies for the ideal-gas state

The ideal gas state thermodynamic properties including heat capacity, absolute entropy of individual compounds and equimolar racemic mixtures for molecules with stereo isomers were calculated with "rigid rotator harmonic oscillator" approach [173].

The complete results from computation of heat capacities and entropies for the ideal-gas state are given for each compound in Table H. 16 - Table H. 21, as well as the values referenced to the T= 298.15 K are compiled in Table 44, Table 48 and Table 49. The thermodynamic properties for indole, indoline, and H8-indole were previously calculated by Steele and Chirico [172]. The entropies for indole agree within 0.2% at 300 K, in case of indoline deviation does not exceed 2%. The results for H8-indole were estimated by using additive scheme and can be used only as rough estimation.

The values of entropy in the ideal gas state S_m^o(g, 298.15 K) can be now used for calculation of standard molar thermodynamic functions of formation of the indole derivatives as follows.

8.2.8.2. Standard molar thermodynamic functions of formation

Table 48. Thermodynamic properties of indole derivatives (in J·K^{-1}·mol^{-1} at T = 298.15 K).

Compound	$\Delta_{cr,l}^g S_m^o$ [a]	S_m^o(g)[b]	S_m^o(cr,l)[c]
	exp.	calc.	calc.
indole (cr)	162.5±2.4	332.3	169.8
indoline (liq)	127.4±1.6	342.8	215.4
H8-indole (liq)	124.4±1.6	385.5	247.3
2-methyl-indole (cr)	181.7±1.4	368.8 [171]	187.1
2-methyl-indoline (liq)	136.1±0.8	405.0	263.1
2-methyl-H8-indole (liq)	135.6±1.8	406.1	269.2

[a] From Table 44, [b] calculated using the RRHO approach [173], [c] calculated as sum of S_m^o(g) from this table and entropy of sublimation/vaporization $\Delta_{cr,l}^g S_m^o$(298.15 K).

The standard molar entropies S_m^o(cr/l, 298.15 K), of indole derivatives (Table 45) were calculated by the subtracting of the contribution $\Delta_{cr,l}^g S_m^o$ from the entropy in the ideal gas state S_m^o(g, 298.15 K) derived in previous section. Numerical values of molar entropies S_m^o(cr,l, 298.15 K) for the indole derivatives are given in Table 48, last column.

Table 49. Experimental standard molar thermodynamic properties of indoles at T = 298.15 K.

Compound	State	$\Delta_f H_m^o$ [a]	$\Delta_f S_m^o$	$\Delta_f G_m^o$	S_m^o [b]	$C_{p,m}^o$ [c]
		kJ·mol^{-1}	J·K^{-1}·mol^{-1}	kJ·mol^{-1}	J·K^{-1}·mol^{-1}	J·K^{-1}·mol^{-1}
indole	cr	87.2±0.9	-428.7	215.0	169.8	162.2
	gas	162.2±1.0	-266.2	241.6	332.3	120.9
indoline	liq	60.2±1.2	-513.7	213.3	215.4	219.5
	gas	120.8±1.3	-386.3	236.0	342.8	127.5
H8-indole	liq	-117.5±1.8	-873.3	142.9	247.3	242.3
	gas	-64.0±1.9	-735.1	155.2	385.5	151.5
2-methyl-indole	cr	36.1±1.3	-550.1	200.1	184.7 [171]	175.5 [171]
	gas	121.6±1.5	-366.0	230.7	368.8 [171]	146.1 [171]
2-methyl-indoline	liq	17.2±1.9	-602.2	196.8	263.1	251.3
	gas	80.2±1.9	-460.3	217.4	405.0	174.0
2-methyl-H8-indole	liq	-157.1±2.1	-987.7	137.4	269.2	266.5
	gas	-99.3±2.2	-850.8	154.4	406.1	178.6

[a] from Table 46, [b], from Table 48, [c] From Table 42.

The standard molar entropies of formation, $\Delta_f S_m^o$, in the gas and in the condensed (cr or liq) phase were calculated on the basis of reaction 77:

$$a\ C_{graphite} + (b/2)\ H_2(g) + (c/2)\ N_2(g) = C_aH_bN_c\ (g\ or\ cr\ or\ liq) \qquad (77)$$
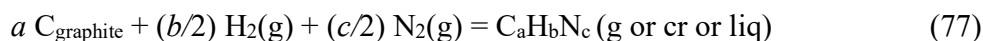
using the S_m^o-values given in Table 45 and the values of entropy of formation for $C_{graphite}$ (5.74±0.13) J·K^{-1}·mol^{-1}, for H_2(g) (130.52±0.02) J·K^{-1}·mol^{-1}, and for N_2(g) (191.61±0.01) J·K^{-1}·mol^{-1} recommended by Chase [144].

Values of the standard Gibbs energies of formation, $\Delta_f G_m^o$, were estimated from the values of $\Delta_f H_m^o$, and $\Delta_f S_m^o$ (Table 48). The standard molar thermodynamic functions in the condensed and in the gas phase collected in Table 48 can be used for optimization of technology for the industrially important hydrogenation/dehydrogenation reactions, as well as for validation of theoretical and empirical methods for prediction of thermodynamic properties.

8.2.9. Thermodynamics of hydrogen release and uptake

The reaction equilibria of hydrogenation and dehydrogenation are governed by the Gibbs energy of reaction $\Delta_r G$. Hydrogenation reaction of different aromatics mainly differ in terms of the enthalpic contribution to the Gibbs energy of reaction, while the entropic contributions are usually quite similar. Complete hydrogenation of indole is accompanied by a heat release of $\Delta_r H_m^o = -56.6$ kJ mol^{-1}(H$_2$) (for 2-methyl indole a value of -55.2 kJ mol^{-1}(H$_2$) is derived; note: all reaction enthalpies are reported relative to 1 mol hydrogen, not 1 mol indole). Thus, hydrogenation of indole is significantly less exothermal than hydrogenation of homocyclic LOHCs like dibenzyl toluene with a reaction enthalpy of -68.1 kJ mol^{-1}(H$_2$). This has tremendous consequences on hydrogen release. Due to the lower reaction enthalpy, dehydrogenation of 8H-indole is possible at much lower temperatures.

However, there are certain differences. Most important in this regard is the stepwise nature of the reaction. The dehydrogenation of H8-indole to indoline has a reaction enthalpy of 61.6 kJ mol^{-1}(H$_2$) (59.8 kJ mol^{-1}(H$_2$) for 2-methyl-H8-indole). Enthalpy of reaction for further dehydrogenation of indoline to indole is only 41.3 kJ mol^{-1}(H$_2$) (41.4 kJ mol^{-1}(H$_2$) for 2-methyl-indoline). This corresponds to a significant difference in the Gibbs energies of reaction. While dehydrogenation of H8-indole to indoline is accompanied with a Gibbs energy change of 25.6 kJ mol^{-1}(H$_2$) at standard conditions and is thus still clearly limited by reaction equilibrium, dehydrogenation of indoline to indole only requires a change in Gibbs energy of 5.5 kJ mol^{-1}(H$_2$). Therefore, dehydrogenation of indoline to indole is thermodynamically possible at temperatures slightly above ambient. Under reaction conditions for H8-indole dehydrogenation, indoline is thermodynamically quite unstable.

4. References

[1]   S.W. Benson, Thermochemical Kinetics. Methods for the Estimation of Thermochemical Data and Rate Parameters, John Wiley & Sons, Inc., New York, 1968. https://doi.org/https://doi.org/10.1002/bbpc.19690730226.

[2]   J.S. Chickos, S. Hosseini, D.G. Hesse, Determination of vaporization enthalpies of simple organic molecules by correlations of changes in gas chromatographic net retention times, Thermochim. Acta. 249 (1995) 41–62. https://doi.org/10.1016/0040-6031(95)90670-3.

[3]   E. Kováts, Gas-chromatographische Charakterisierung organischer Verbindungen. Teil 1: Retentionsindices aliphatischer Halogenide, Alkohole, Aldehyde und Ketone, Helv. Chim. Acta. 41 (1958) 1915–1932. https://doi.org/10.1002/hlca.19580410703.

[4]   D.H. Zaitsau, S.P. Verevkin, A.Y. Sazonova, Vapor pressures and vaporization enthalpies of 5-nonanone, linalool and 6-methyl-5-hepten-2-one. Data evaluation, Fluid Phase Equilib. 386 (2015) 140–148. https://doi.org/https://doi.org/10.1016/j.fluid.2014.11.026.

[5]   D. Kulikov, S.P. Verevkin, A. Heintz, Enthalpies of vaporization of a series of aliphatic alcohols: Experimental results and values predicted by the ERAS-model., Fluid Phase Equilib. 192 (2001) 187–207. https://doi.org/10.1016/S0378-3812(01)00633-1.

[6]   K. V. Zherikova, S.P. Verevkin, Ferrocene: Temperature adjustments of sublimation and vaporization enthalpies, Fluid Phase Equilib. 472 (2018) 196–203. https://doi.org/10.1016/j.fluid.2018.05.004.

[7]   D.H. Zaitsau, A.A. Pimerzin, S.P. Verevkin, Fatty acids methyl esters: Complementary measurements and comprehensive analysis of vaporization thermodynamics, J. Chem. Thermodyn. 132 (2019) 322–340. https://doi.org/10.1016/j.jct.2019.01.007.

[8]   G. Pei, J. Xiang, G. Li, S. Wu, F. Pan, X. Lv, A Literature Review of Heat Capacity Measurement Methods BT - 10th International Symposium on High-Temperature Metallurgical Processing, in: T. Jiang, J.-Y. Hwang, D. Gregurek, Z. Peng, J.P. Downey, B. Zhao, O. Yücel, E. Keskinkilic, R. Padilla (Eds.), Springer International Publishing, Cham, 2019: pp. 569–577.

[9]   J.S. Chickos, S. Hosseini, D.G. Hesse, J.F. Liebman, Heat capacity corrections to a standard state: a comparison of new and some literature methods for organic liquids and solids, Struct. Chem. 4 (1993) 271–278. https://doi.org/10.1007/BF00673701.

[10]   E.S. Domalski, E.D. Hearing, Estimation of the Thermodynamic Properties of C-H-N-O-

S-Halogen Compounds at 298.15 K, J. Phys. Chem. Ref. Data. 22 (1993) 805–1159. https://doi.org/10.1063/1.555927.

[11]   J.S. Chickos, W.E. Acree, Enthalpies of vaporization of organic and organometallic compounds, 1880-2002, J Phys. Chem. Ref. Data. 32 (2003) 519–878. https://doi.org/10.1063/1.1529214.

[12]   J.S. Chickosa, W.E. Acree, Enthalpies of sublimation of organic and organometallic compounds. 1910-2001, J. Phys. Chem. Ref. Data. 31 (2002) 537–698. https://doi.org/10.1063/1.1475333.

[13]   S.P. Verevkin, D.H. Zaitsau, V.N. Emel'yanenko, A. V Yermalayeu, C. Schick, H. Liu, E.J. Maginn, S. Bulut, I. Krossing, R. Kalb, V.N. Emel'yanenko, A. V Yermalayeu, C. Schick, H. Liu, E.J. Maginn, S. Bulut, I. Krossing, R. Kalb, Making Sense of Enthalpy of Vaporization Trends for Ionic Liquids: New Experimental and Simulation Data Show a Simple Linear Relationship and Help Reconcile Previous Data, J. Phys. Chem. B. 117 (2013) 6473–6486. https://doi.org/10.1021/jp311429r.

[14]   Y.U. Paulechka, D.H. Zaitsau, G.J. Kabo, A.A. Strechan, Vapor pressure and thermal stability of ionic liquid 1-butyl-3-methylimidazolium Bis(trifluoromethylsulfonyl)amide, Thermochim. Acta. 439 (2005) 158–160. https://doi.org/10.1016/j.tca.2005.08.035.

[15]   E.C.W. Clarke, D.N. Glew, Evaluation of thermodynamic functions from equilibrium constants, Trans. Faraday Soc. 62 (1966) 539. https://doi.org/10.1039/tf9666200539.

[16]   Y.U. Paulechka, D.H. Zaitsau, G.J. Kabo, On the difference between isobaric and isochoric heat capacities of liquid cyclohexyl esters, J. Mol. Liq. 115 (2004) 105–111. https://doi.org/10.1016/j.molliq.2004.03.002.

[17]   V.N. Emel'yanenko, S.P. Verevkin, Benchmark thermodynamic properties of 1,3-propanediol: Comprehensive experimental and theoretical study, J. Chem. Thermodyn. 85 (2015) 111–119. https://doi.org/10.1016/j.jct.2015.01.014.

[18]   S.P. Verevkin, Vapour pressures and enthalpies of vaporization of a series of the linear n-alkyl-benzenes, J. Chem. Thermodyn. 38 (2006) 1111–1123. https://doi.org/10.1016/j.jct.2005.11.009.

[19]   S.P. Verevkin, E.L. Krasnykh, T. V. Vasiltsova, A. Heintz, Determination of ambient temperature vapor pressures and vaporization enthalpies of branched ethers, J. Chem. Eng. Data. 48 (2003) 591–599. https://doi.org/10.1021/je0255980.

[20]   P.A.A. Nesterov I.A., Nesterova T.N., Thermodynamics of sorption and evaporation of alkylbenzenes. III. Critical pressures, Izv. Univ. Chem. Chem. Technol. 43 (2000) 22–30.

[21]   The Sadtler Standard Gas Chromatography Retention Index Library, Sadtler-Heyden, Bio-Rad Laboratories, Sadtler Division, Philadelphia, 1986.

[22]   J.S. Chickos, J.A. Wilson, Vaporization Enthalpies at 298.15 K of the n-Alkanes from C21 to C28 and C30, J. Chem. Eng. Data. 42 (1997) 190–197. https://doi.org/10.1021/je960089h.

[23]   V.N. Emel'yanenko, S.P. Verevkin, B. Koutek, J. Doubsky, V.N. Emel'yanenko, S.P. Verevkin, B. Koutek, J. Doubsky, Vapour pressures and enthalpies of vapourization of a series of the linear aliphatic nitriles, J. Chem. Thermodyn. 37 (2005) 73–81. https://doi.org/10.1016/j.jct.2004.08.004.

[24]   S.W.S.W. Benson, New Methods for Estimating the Heats of Formation, Heat Capacities, and Entropies of Liquids and Gases, J. Phys. Chem. A. 103 (1999) 11481–11485. https://doi.org/10.1021/jp992971a.

[25]   S.P. Verevkin, M.E. Konnova, V. V. Turovtsev, A. V. Riabchunova, A.A. Pimerzin, Weaving a Network of Reliable Thermochemistry around Lignin Building Blocks: Methoxy-Phenols and Methoxy-Benzaldehydes, Ind. Eng. Chem. Res. 59 (2020) 22626–22639. https://doi.org/10.1021/acs.iecr.0c04281.

[26]   C. Plato, A.R. Glasgow, Differential scanning calorimetry as a general method for determining the purity and heat of fusion of high-purity organic chemicals. Application to 95 compounds, Anal. Chem. 41 (1969) 330–336. https://doi.org/10.1021/ac60271a041.

[27]   J.S.C. W. Acree Jr., Phase transition enthalpy measurements of organic and organometallic compounds and ionic liquids. Sublimation, vaporization, and fusion enthalpies from 1880 to 2015. Part 2. C11–C192, J. Phys. Chem. Ref. Data. 46 (2017) 013104.

[28]   C. Gobble, J. Chickos, S.P. Verevkin, Vapor Pressures and Vaporization Enthalpies of a Series of Dialkyl Phthalates by Correlation Gas Chromatography, J. Chem. Eng. Data. 59 (2014) 1353–1365. https://doi.org/10.1021/je500110d.

[29]   G. Bikelyte, M. Hartel, J. Stierstorfer, K. TM, P. AA, V. SP, Benchmark properties of 2-, 3-and 4-nitrotoluene: Evaluation of thermochemical data with complementary experimental and computational methods, J. Chem. Thermodyn. 111 (2017) 271–278. https://doi.org/10.1016/j.jct.2017.03.029.

[30]   E. VN, Z. KV, F. Agapito, S. JAM, V. SP, V.N. Emel'yanenko, K. V. Zaitseva, F. Agapito, J.A. Martinho Simões, S.P. Verevkin, Benchmark thermodynamic properties of methylanisoles: Experimental and theoretical study, J. Chem. Thermodyn. 85 (2015) 155–

162. https://doi.org/10.1016/j.jct.2015.02.001.

[31]   S.P. Verevkin, A. Heintz, Thermochemistry of substituted benzenes: quantification of ortho-, para-, meta-, and buttress interactions in alkyl-substituted nitrobenzenes, J. Chem. Thermodyn. 32 (2000) 1169–1182. https://doi.org/https://doi.org/10.1006/jcht.2000.0589.

[32]   E.U. Franck, J. D. Cox, D. D. Wagman, V. A. Medvedev: CODATA - Key Values for Thermodynamics, aus der Reihe: CODATA, Series on Thermodynamic Properties. Hemisphere Publishing Corporation, New York, Washington, Philadelphia, London 1989. 271 Seiten, Preis: £ 28.00, Berichte Der Bunsengesellschaft Für Phys. Chemie. 94 (1990) 93–93. https://doi.org/10.1002/bbpc.19900940121.

[33]   J.D. Cox, D.D. Wagman, V.A. Medvedev, CODATA key values for thermodynamics, Hemisphere Pub. Corp., New York, 1989.

[34]   SciFinder Discovery Platform, Am. Chem. Sosciety. (2021). https://scifinder.cas.org.

[35]   M.E. Wieser, N. Holden, T.B. Coplen, J.K. Böhlke, M. Berglund, W.A. Brand, P. De Bièvre, M. Gröning, R.D. Loss, J. Meija, T. Hirata, T. Prohaska, R. Schoenberg, G. O'Connor, T. Walczyk, S. Yoneda, X.-K. Zhu, Atomic weights of the elements 2011 (IUPAC Technical Report), Pure Appl. Chem. 85 (2013) 1047–1078. https://doi.org/10.1351/PAC-REP-13-03-02.

[36]   G. te Velde, F.M. Bickelhaupt, E.J. Baerends, C. Fonseca Guerra, S.J.A. van Gisbergen, J.G. Snijders, T. Ziegler, Chemistry with ADF, J. Comput. Chem. 22 (2001) 931–967. https://doi.org/10.1002/jcc.1056.

[37]   V.N. Emel'yanenko, M.A. Varfolomeev, V.B. Novikov, V. V Turovtsev, Y.D. Orlov, Thermodynamic Properties of 1,4-Benzoquinones in Gaseous and Condensed Phases: Experimental and Theoretical Studies, J. Chem. Eng. Data. 62 (2017) 2413–2422. https://doi.org/10.1021/acs.jced.7b00354.

[38]   S.P. Verevkin, V. V. Turovtsev, I. V. Andreeva, Y.D. Orlov, A.A. Pimerzin, Webbing a network of reliable thermochemistry around lignin building blocks: tri-methoxy-benzenes, RSC Adv. 11 (2021) 10727–10737. https://doi.org/10.1039/D1RA00690H.

[39]   S.P. Verevkin, V.N. Emel'yanenko, R. Siewert, A.A. Pimerzin, Thermochemistry of the lignin broken bits, Fluid Phase Equilib. 522 (2020) 112751. https://doi.org/10.1016/j.fluid.2020.112751.

[40]   R. Siewert, V.N. Emel'yanenko, S.P. Verevkin, Thermochemistry of phthalic acids: Evaluation of thermochemical data with complementary experimental and computational methods, Fluid Phase Equilib. 517 (2020) 112582.

https://doi.org/10.1016/j.fluid.2020.112582.

[41]   I. V. Andreeva, M.A. Varfolomeev, S.P. Verevkin, Thermochemistry of di-substituted benzenes: Ortho-, meta-, and para-hydroxyacetophenones, J. Chem. Thermodyn. 140 (2020) 105893. https://doi.org/10.1016/j.jct.2019.105893.

[42]   N. Serpinskii, VV., Voitkevich SA., Lyuboshich, Results of vapor pressure determinations for 36 flavours, All-Union Sci. Reserach Inst. Synth. Nat. Aromat. Princ. 4 (1954) 125– 130.

[43]   R.M. Stephenson, S. Malanowski, Handbook of the Thermodynamics of Organic Compounds, Springer Netherlands, Dordrecht, 1987. https://doi.org/10.1007/978-94-009-3173-2.

[44]   Khorevskaya AS, No Title, Byk SSh. Zh Prikl Khim. 40 (1967) 464.

[45]   L.M.P.F. Amaral, M.A.V. Ribeiro da Silva, Calorimetric study of 2′-methylacetophenone and 4′-methylacetophenone, J. Chem. Thermodyn. 57 (2013) 301–305. https://doi.org/10.1016/j.jct.2012.08.034.

[46]   L.M.P.F. Amaral, P. Szterner, V.M.F. Morais, M.A.V. Ribeiro da Silva, Thermochemical study of the isomeric compounds: 3-acetylbenzonitrile and benzoylacetonitrile, J. Chem. Thermodyn. 91 (2015) 452–458. https://doi.org/10.1016/j.jct.2015.08.008.

[47]   A.R.R.P. Almeida, M.J.S. Monte, Vapour pressures and phase transition properties of four substituted acetophenones, J. Chem. Thermodyn. 107 (2017) 42–50. https://doi.org/10.1016/j.jct.2016.12.012.

[48]   Guidechem.com database, (n.d.). https://www.guidechem.com/.

[49]   M.V. Roux, M. Temprado, J.S. Chickos, Y. Nagano, Critically Evaluated Thermochemical Properties of Polycyclic Aromatic Hydrocarbons, J. Phys. Chem. Ref. Data. 37 (2008) 1855–1996. https://doi.org/10.1063/1.2955570.

[50]   W. V. Steele, R.D. Chirico, S.E. Knipmeyer, A. Nguyen, Vapor Pressure of Acetophenone, (±)-1,2-Butanediol, (±)-1,3-Butanediol, Diethylene Glycol Monopropyl Ether, 1,3-Dimethyladamantane, 2-Ethoxyethyl Acetate, Ethyl Octyl Sulfide, and Pentyl Acetate, J. Chem. Eng. Data. 41 (1996) 1255–1268. https://doi.org/10.1021/je9601117.

[51]   R.R. Dreisbach, S.A. Shrader, Vapor Pressure–Temperature Data on Some Organic Compounds, Ind. Eng. Chem. 41 (1949) 2879–2880. https://doi.org/10.1021/ie50480a054.

[52]   G.R. Nicholson, M. Szwarc, J.W. Taylor, The heats of formation of diacetyl and of benzyl methyl ketone in the vapour phase, J. Chem. Soc. (1954) 2767–2769. https://doi.org/10.1039/JR9540002767.

[53] D.R. Stull, Vapor Pressure of Pure Substances. Organic and Inorganic Compounds, Ind. Eng. Chem. 39 (1947) 517–540. https://doi.org/10.1021/ie50448a022.

[54] S.P. Verevkin, M.E. Konnova, V.N. Emeĺyanenko, A.A. Pimerzin, Weaving a web of reliable thermochemistry around lignin building blocks: Vanillin and its isomers, J. Chem. Thermodyn. 157 (2021) 106362. https://doi.org/10.1016/j.jct.2020.106362.

[55] PubChem, open chemistry database at the National Institutes of Health (NIH), (n.d.). https://pubchem.ncbi.nlm.nih.gov/.

[56] W. Acree, J.S. Chickos, Phase Transition Enthalpy Measurements of Organic and Organometallic Compounds. Sublimation, Vaporization and Fusion Enthalpies From 1880 to 2015. Part 1. C 1 − C 10, J. Phys. Chem. Ref. Data. 45 (2016) 033101. https://doi.org/10.1063/1.4948363.

[57] Timmermans J., Freezing points of organic compounds. VVI New determinations, Bull Soc Chim Belg. 61 (1952) 393.

[58] W. Acree, J.S. Chickos, Phase Transition Enthalpy Measurements of Organic and Organometallic Compounds. Sublimation, Vaporization and Fusion Enthalpies From 1880 to 2015. Part 1. C 1 − C 10, J. Phys. Chem. Ref. Data. 45 (2016) 033101. https://doi.org/10.1063/1.4948363.

[59] K. V. Zherikova, A.A. Svetlov, N. V. Kuratieva, S.P. Verevkin, Structure–property relationships in halogenbenzoic acids: Thermodynamics of sublimation, fusion, vaporization and solubility, Chemosphere. 161 (2016) 157–166. https://doi.org/10.1016/j.chemosphere.2016.06.111.

[60] S.P. Verevkin, V.N. Emel'yanenko, R.N. Nagrimanov, Nearest-Neighbor and Non-Nearest-Neighbor Interactions between Substituents in the Benzene Ring. Experimental and Theoretical Study of Functionally Substituted Benzamides, J. Phys. Chem. A. 120 (2016) 9867–9877. https://doi.org/10.1021/acs.jpca.6b10332.

[61] V.N. Emel'yanenko, K. V. Zaitseva, R.N. Nagrimanov, B.N. Solomonov, S.P. Verevkin, Benchmark Thermodynamic Properties of Methyl- and Methoxybenzamides: Comprehensive Experimental and Theoretical Study, J. Phys. Chem. A. 120 (2016) 8419–8429. https://doi.org/10.1021/acs.jpca.6b08027.

[62] R.D. Chirico, A. Kazakov, A. Bazyleva, V. Diky, K. Kroenlein, V.N. Emel′yanenko, S.P. Verevkin, Critical Evaluation of Thermodynamic Properties for Halobenzoic Acids Through Consistency Analyses for Results from Experiment and Computational Chemistry, J. Phys. Chem. Ref. Data. 46 (2017) 023105.

https://doi.org/10.1063/1.4983656.

[63] S.P. Verevkin, V.N. Emel'yanenko, D.H. Zaitsau, Thermochemistry of Substituted Benzamides and Substituted Benzoic Acids: Like Tree, Like Fruit?, ChemPhysChem. 19 (2018) 619–630. https://doi.org/10.1002/cphc.201701132.

[64] M.A. Varfolomeev, D.I. Abaidullina, B.N. Solomonov, S.P. Verevkin, V.N. Emel'yanenko, Pairwise Substitution Effects, Inter- and Intramolecular Hydrogen Bonds in Methoxyphenols and Dimethoxybenzenes. Thermochemistry, Calorimetry, and First-Principles Calculations, J. Phys. Chem. B. 114 (2010) 16503–16516. https://doi.org/10.1021/jp108459r.

[65] M. Graglia, N. Kanna, D. Esposito, Lignin Refinery: Towards the Preparation of Renewable Aromatic Building Blocks, ChemBioEng Rev. 2 (2015) 377–392. https://doi.org/10.1002/cben.201500019.

[66] Y. Furutani, Y. Dohara, S. Kudo, J. Hayashi, K. Norinaga, Theoretical Study on Elementary Reaction Steps in Thermal Decomposition Processes of Syringol-Type Monolignol Compounds, J. Phys. Chem. A. 122 (2018) 822–831. https://doi.org/10.1021/acs.jpca.7b09450.

[67] S. P. Verevkin, Substituent effects on the benzene ring. Prediction of the thermochemical properties of alkyl substituted hydroquinones, Phys. Chem. Chem. Phys. 1 (1999) 127–131. https://doi.org/10.1039/A806706F.

[68] R.S. Kalb, E.N. Stepurko, V.N. Emel'yanenko, S.P. Verevkin, Carbonate based ionic liquid synthesis (CBILS®): thermodynamic analysis, Phys. Chem. Chem. Phys. 18 (2016) 31904–31913. https://doi.org/10.1039/C6CP06594E.

[69] A.Y. Russo, M.E. Konnova, I. V Andreeva, S.P. Verevkin, Vaporization thermodynamics of compounds modeling lignin structural units, Fluid Phase Equilib. 491 (2019) 45–55. https://doi.org/https://doi.org/10.1016/j.fluid.2019.03.004.

[70] M.A.R. Matos, M.S. Miranda, V.M.F. Morais, Calorimetric and Theoretical Determination of Standard Enthalpies of Formation of Dimethoxy- and Trimethoxybenzene Isomers, J. Phys. Chem. A. 104 (2000) 9260–9265. https://doi.org/10.1021/jp001928g.

[71] G. Nichols, J. Orf, S.M. Reiter, J. Chickos, G.W. Gokel, The vaporization enthalpies of some crown and polyethers by correlation gas chromatography, Thermochim. Acta. 346 (2000) 15–28. https://doi.org/https://doi.org/10.1016/S0040-6031(99)00405-0.

[72] M. Voges, F. Schmidt, D. Wolff, G. Sadowski, C. Held, Thermodynamics of the alanine

aminotransferase reaction, Fluid Phase Equilib. 422 (2016) 87–98. https://doi.org/10.1016/j.fluid.2016.01.023.

[73] A. Stark, B. Ondruschka, D.H. Zaitsau, S.P. Verevkin, Biomass-Derived Platform Chemicals: Thermodynamic Studies on the Extraction of 5-Hydroxymethylfurfural from Ionic Liquids, J. Chem. Eng. Data. 57 (2012) 2985–2991. https://doi.org/10.1021/je300529j.

[74] V.N. Emel'yanenko, E. Altuntepe, C. Held, A.A. Pimerzin, S.P. Verevkin, E. VN, E. Altuntepe, C. Held, P. AA, V. SP, Renewable platform chemicals: Thermochemical study of levulinic acid esters, Thermochim. Acta. 659 (2018) 213–221. https://doi.org/10.1016/j.tca.2017.12.006.

[75] S.P. Verevkin, A.Y. Sazonova, V.N. Emel'yanenko, D.H. Zaitsau, M.A. Varfolomeev, B.N. Solomonov, K. V. Zherikova, V.N. Emel'yanenko, D.H. Zaitsau, M.A. Varfolomeev, B.N. Solomonov, K. V. Zherikova, V.N. Emel'yanenko, D.H. Zaitsau, M.A. Varfolomeev, B.N. Solomonov, K. V. Zherikova, Thermochemistry of halogen-substituted methylbenzenes, J. Chem. Eng. Data. 60 (2015) 89–103. https://doi.org/10.1021/je500784s.

[76] V.N. Emel'yanenko, S.P. Verevkin, V.N. Emel'Yanenko, S.P. Verevkin, Benchmark thermodynamic properties of 1,3-propanediol: Comprehensive experimental and theoretical study, J. Chem. Thermodyn. 85 (2015) 111–119. https://doi.org/10.1016/j.jct.2015.01.014.

[77] S.G.C. Stull, R.D., Westrum E.F., The Chemical Thermodynamics of Organic Compounds, J. Wiley, New York, 1969.

[78] The National Institute of Standards and Technology (NIST), (n.d.). https://pubchem.ncbi.nlm.nih.gov/.

[79] S.P. Verevkin, V.N. Emel'yanenko, A.A. Pimerzin, E.E. Vishnevskaya, Thermodynamic Analysis of Strain in the Five-Membered Oxygen and Nitrogen Heterocyclic Compounds, J. Phys. Chem. A. 115 (2011) 1992–2004. https://doi.org/10.1021/jp1090526.

[80] H. Hatakeyama and T. Hatakeyama, Biopolymers, Springer Berlin Heidelberg, Berlin, Heidelberg, 2010. https://doi.org/10.1007/978-3-642-13630-6.

[81] S.P. Verevkin, V.N. Emel'yanenko, V. Diky, C.D. Muzny, R.D. Chirico, M. Frenkel, New Group-Contribution Approach to Thermochemical Properties of Organic Compounds: Hydrocarbons and Oxygen-Containing Compounds, J. Phys. Chem. Ref. Data. 42 (2013) 033102. https://doi.org/10.1063/1.4815957.

[82]   V.N. Emel'yanenko, A. V. Yermalayeu, M. Voges, C. Held, G. Sadowski, S.P. Verevkin, V.N. Emel′yanenko, A. V. Yermalayeu, M. Voges, C. Held, G. Sadowski, S.P. Verevkin, Thermodynamics of a model biological reaction: A comprehensive combined experimental and theoretical study, Fluid Phase Equilib. 422 (2016) 99–110. https://doi.org/10.1016/j.fluid.2016.01.035.

[83]   A. Leal-Duaso, P. Pérez, J.A. Mayoral, E. Pires, J.I. García, Glycerol as a source of designer solvents: physicochemical properties of low melting mixtures containing glycerol ethers and ammonium salts, Phys. Chem. Chem. Phys. 19 (2017) 28302–28312. https://doi.org/10.1039/C7CP04987K.

[84]   B.S. Flowers, M.S. Mittenthal, A.H. Jenkins, D.A. Wallace, J.W. Whitley, G.P. Dennis, M. Wang, C.H. Turner, V.N. Emel'yanenko, S.P. Verevkin, J.E. Bara, 1,2,3-Trimethoxypropane: A Glycerol-Derived Physical Solvent for CO2 Absorption, ACS Sustain. Chem. Eng. 5 (2017) 911–921. https://doi.org/10.1021/acssuschemeng.6b02231.

[85]   S. Qian, X. Liu, V.N. Emel'yanenko, P. Sikorski, I. Kammakakam, B.S. Flowers, T.A. Jones, C.H. Turner, S.P. Verevkin, J.E. Bara, Synthesis and Properties of 1,2,3-Triethoxypropane: A Glycerol-Derived Green Solvent Candidate, Ind. Eng. Chem. Res. 59 (2020) 20190–20200. https://doi.org/10.1021/acs.iecr.0c03789.

[86]   J.I. García, H. García-Marín, J.A. Mayoral, P. Pérez, Green solvents from glycerol. Synthesis and physico-chemical properties of alkyl glycerol ethers, Green Chem. 12 (2010) 426–434. https://doi.org/10.1039/B923631G.

[87]   C.S. Khadzhibekov, S. N.; Tulyaganov, S. R.; Sultankulov, A.; Kadyrov, 3. Some aspects of synthesis of 1,3-dialkoxy-2-propanols, Dokl. Akad. Nauk UzSSR. (1985) 40–41.

[88]   S.P. Verevkin, Predicting Enthalpy of Vaporization of Ionic Liquids: A Simple Rule for a Complex Property, Angew. Chemie Int. Ed. 47 (2008) 5071–5074. https://doi.org/10.1002/anie.200800926.

[89]   D. Hasty, J. Drapekin, T. Subramanian, T.C. Winter, J.S. Chickos, A.A. Samarov, A. V Yermalayeu, S.P. Verevkin, Applications of Correlation Gas Chromatography and Transpiration Studies for the Evaluation of the Vaporization and Sublimation Enthalpies of Some Perfluorinated Hydrocarbons, J. Chem. Eng. Data. 57 (2012) 2350–2359. https://doi.org/10.1021/je300504f.

[90]   F. Schaffer, S.P. Verevkin, H.-J. Rieger, H.-D. Beckhaus, C. Rüchardt, Geminal Substituent Effects, 15. Enthalpies of Formation of a Series of Fluorinated Hydrocarbons and Strain-Free Group Increments to Assess Polar and Anomeric Stabilization and Strain,

Liebigs Ann. 1997 (1997) 1333–1344. https://doi.org/10.1002/jlac.199719970709.

[91]   V.V. Majer, V.V. Svoboda, H. v. Kehiaian, Enthalpies of vaporization of organic compounds: A critical review and data compilation, Blackwell Scientific Publications, Oxford, 1985.

[92]   S.P. Verevkin, Determination of vapor pressures and enthalpies of vaporization of 1,2-alkanediols, Fluid Phase Equilib. 224 (2004) 23–29. https://doi.org/https://doi.org/10.1016/j.fluid.2004.05.010.

[93]   S.P. Verevkin, D.H. Zaitsau, V.N. Emel'yanenko, A. V Yermalayeu, C. Schick, H. Liu, E.J. Maginn, S. Bulut, I. Krossing, R. Kalb, Making Sense of Enthalpy of Vaporization Trends for Ionic Liquids: New Experimental and Simulation Data Show a Simple Linear Relationship and Help Reconcile Previous Data, J. Phys. Chem. B. 117 (2013) 6473–6486. https://doi.org/10.1021/jp311429r.

[94]   S.P. Verevkin, Improved Benson Increments for the Estimation of Standard Enthalpies of Formation and Enthalpies of Vaporization of Alkyl Ethers, Acetals, Ketals, and Ortho Esters, J. Chem. Eng. Data. 47 (2002) 1071–1097. https://doi.org/10.1021/je020023o.

[95]   G.N. Roganov, P.N. Pisarev, V.N. Emel'yanenko, S.P. Verevkin, Measurement and Prediction of Thermochemical Properties. Improved Benson-Type Increments for the Estimation of Enthalpies of Vaporization and Standard Enthalpies of Formation of Aliphatic Alcohols, J. Chem. Eng. Data. 50 (2005) 1114–1124. https://doi.org/10.1021/je049561m.

[96]   S.E. Wheeler, K.N. Houk, P. v. R. Schleyer, W.D. Allen, A Hierarchy of Homodesmotic Reactions for Thermochemistry, J. Am. Chem. Soc. 131 (2009) 2547–2560. https://doi.org/10.1021/ja805843n.

[97]   K. V. Zaitseva, V.N. Emel'yanenko, F. Agapito, A.A. Pimerzin, M.A. Varfolomeev, S.P. Verevkin, Benchmark thermochemistry of methylbenzonitriles: Experimental and theoretical study, J. Chem. Thermodyn. 91 (2015) 186–193. https://doi.org/10.1016/j.jct.2015.07.025.

[98]   L.A. Curtiss, P.C. Redfern, K. Raghavachari, V. Rassolov, J.A. Pople, Gaussian-3 theory using reduced Möller-Plesset order, J. Chem. Phys. 110 (1999) 4703–9. https://doi.org/10.1063/1.478385.

[99]   B. Narayanan, P.C. Redfern, R.S. Assary, L.A. Curtiss, Accurate quantum chemical energies for 133 000 organic molecules, Chem. Sci. 10 (2019) 7449–7455. https://doi.org/10.1039/C9SC02834J.

[100] L.A. Curtiss, P.C. Redfern, K. Raghavachari, Gaussian-4 theory, J. Chem. Phys. 126 (2007) 084108. https://doi.org/10.1063/1.2436888.

[101] M.J. Frisch, G.W. Trucks, H.B. Schlegel, G.E. Scuseria, M.A. Robb, J.R. Cheeseman, G. Scalmani, V. Barone, B. Mennucci, G.A. Petersson, H. Nakatsuji, M. Caricato, X. Li, H.P. Hratchian, A.F. Izmaylov, J. Bloino, G. Zheng, J.L. Sonnenberg, M. Hada, M. Ehara, K. Toyota, R. Fukuda, J. Hasegawa, M. Ishida, T. Nakajima, Y. Honda, O. Kitao, H. Nakai, T. Vreven, J.A. Montgomery Jr., J.E. Peralta, F. Ogliaro, M.J. Bearpark, J. Heyd, E.N. Brothers, K.N. Kudin, V.N. Staroverov, R. Kobayashi, J. Normand, K. Raghavachari, A.P. Rendell, J.C. Burant, S.S. Iyengar, J. Tomasi, M. Cossi, N. Rega, N.J. Millam, M. Klene, J.E. Knox, J.B. Cross, V. Bakken, C. Adamo, J. Jaramillo, R. Gomperts, R.E. Stratmann, O. Yazyev, A.J. Austin, R. Cammi, C. Pomelli, J.W. Ochterski, R.L. Martin, K. Morokuma, V.G. Zakrzewski, G.A. Voth, P. Salvador, J.J. Dannenberg, S. Dapprich, A.D. Daniels, Ö. Farkas, J.B. Foresman, J. V Ortiz, J. Cioslowski, D.J. Fox, Gaussian 09, Revision D.01, (2016).

[102] S.P. Verevkin, D.H. Zaitsau, V.N. Emel'yanenko, A.A. Zhabina, Thermodynamic properties of glycerol: Experimental and theoretical study, Fluid Phase Equilib. 397 (2015) 87–94. https://doi.org/10.1016/j.fluid.2015.03.038.

[103] A. Guleria, G. Kumari, S. Saravanamurugan, Cellulose valorization to potential platform chemicals, in: Biomass, Biofuels, Biochem., Elsevier, 2020: pp. 433–457. https://doi.org/10.1016/B978-0-444-64307-0.00017-2.

[104] S.P. Verevkin, V.N. Emel'yanenko, E.N. Stepurko, R. V Ralys, D.H. Zaitsau, A. Stark, Biomass-Derived Platform Chemicals: Thermodynamic Studies on the Conversion of 5-Hydroxymethylfurfural into Bulk Intermediates, Ind. Eng. Chem. Res. 48 (2009) 10087–10093. https://doi.org/10.1021/ie901012g.

[105] V.N. Emel'yanenko, S.P. Verevkin, C. Schick, E.N. Stepurko, G.N. Roganov, M.K. Georgieva, The thermodynamic properties of S-lactic acid, Russ. J. Phys. Chem. A. 84 (2010) 1491–1497. https://doi.org/10.1134/S0036024410090074.

[106] J. Sherwood, M. De bruyn, A. Constantinou, L. Moity, C.R. McElroy, T.J. Farmer, T. Duncan, W. Raverty, A.J. Hunt, J.H. Clark, Dihydrolevoglucosenone (Cyrene) as a bio-based alternative for dipolar aprotic solvents, Chem. Commun. 50 (2014) 9650–9652. https://doi.org/10.1039/C4CC04133J.

[107] M.B. Comba, Y. Tsai, A.M. Sarotti, M.I. Mangione, A.G. Suárez, R.A. Spanevello, Levoglucosenone and Its New Applications: Valorization of Cellulose Residues, European

J. Org. Chem. 2018 (2018) 590–604. https://doi.org/10.1002/ejoc.201701227.

[108] J.E. Bara, T.K. Carlisle, C.J. Gabriel, D. Camper, A. Finotello, D.L. Gin, R.D. Noble, Guide to CO2 Separations in Imidazolium-Based Room-Temperature Ionic Liquids, Ind. Eng. Chem. Res. 48 (2009) 2739–2751. https://doi.org/10.1021/ie8016237.

[109] S. Srinivasan, J. Billeter, D. Bonvin, Extent-based incremental identification of reaction systems using concentration and calorimetric measurements, Chem. Eng. J. 207–208 (2012) 785–793. https://doi.org/https://doi.org/10.1016/j.cej.2012.07.063.

[110] Z. JS, Z. CY, L. GT, L. GS, Measuring enthalpy of fast exothermal reaction with infrared thermography in a microreactor, Chem. Eng. J. 295 (2016) 384–390. https://doi.org/10.1016/j.cej.2016.01.100.

[111] V.S. Andreeva IV, Pimerzin AA, Turovtsev VV, Bara JE, Richardson D, Commodity Chemicals and Fuels from Biomass: Thermodynamic Properties of Levoglucosan Derivatives, Chem. Eng. J. submited (2021).

[112] A. Shaw, X. Zhang, L. Kabalan, J. Li, Mechanistic and kinetic investigation on maximizing the formation of levoglucosan from cellulose during biomass pyrolysis, Fuel. 286 (2021) 119444. https://doi.org/10.1016/j.fuel.2020.119444.

[113] A. V Blokhin, O. V Voitkevich, G.J. Kabo, Y.U. Paulechka, M. V Shishonok, A.G. Kabo, V. V Simirsky, Thermodynamic Properties of Plant Biomass Components. Heat Capacity, Combustion Energy, and Gasification Equilibria of Cellulose, J. Chem. Eng. Data. 56 (2011) 3523–3531. https://doi.org/10.1021/je200270t.

[114] I. Itabaiana Junior, M. Avelar do Nascimento, R.O.M.A. de Souza, A. Dufour, R. Wojcieszak, Levoglucosan: a promising platform molecule?, Green Chem. 22 (2020) 5859–5880. https://doi.org/10.1039/D0GC01490G.

[115] S.P.K. J.B. Pedley, R.D. Naylor, Thermochemical data of organic compounds, Chapman an, New York, 1986.

[116] H. Xin, X. Hu, C. Cai, H. Wang, C. Zhu, S. Li, Z. Xiu, X. Zhang, Q. Liu, L. Ma, Catalytic Production of Oxygenated and Hydrocarbon Chemicals From Cellulose Hydrogenolysis in Aqueous Phase, Front. Chem. 8 (2020). https://doi.org/10.3389/fchem.2020.00333.

[117] O. Oyola-Rivera, J. He, G.W. Huber, J.A. Dumesic, N. Cardona-Martínez, Catalytic dehydration of levoglucosan to levoglucosenone using Brønsted solid acid catalysts in tetrahydrofuran, Green Chem. 21 (2019) 4988–4999. https://doi.org/10.1039/C9GC01526D.

[118] S.H. Krishna, T.W. Walker, J.A. Dumesic, G.W. Huber, Kinetics of Levoglucosenone

Isomerization, ChemSusChem. 10 (2017) 129–138.
https://doi.org/10.1002/cssc.201601308.

[119] Y. Román-Leshkov, C.J. Barrett, Z.Y. Liu, J.A. Dumesic, Production of dimethylfuran for liquid fuels from biomass-derived carbohydrates, Nature. 447 (2007) 982–985. https://doi.org/10.1038/nature05923.

[120] M. Ducros, J.F. Gruson, H. Sannier, Estimation des enthalpies de vaporisation des composes organiques liquides. Partie 1. Applications aux alcanes, cycloalcanes, alcenes, hydrocarbures benzeniques, alcools, alcanes thiols, chloro et bromoalcanes, nitriles, esters, acides et aldehydes, Thermochim. Acta. 36 (1980) 39–65. https://doi.org/https://doi.org/10.1016/0040-6031(80)80109-2.

[121] W. V. Steele, R.D. Chirico, S.E. Knipmeyer, A. Nguyen, Vapor Pressure, Heat Capacity, and Density along the Saturation Line, Measurements for Cyclohexanol, 2-Cyclohexen-1-one, 1,2-Dichloropropane, 1,4-Di- tert -butylbenzene, (±)-2-Ethylhexanoic Acid, 2-(Methylamino)ethanol, Perfluoro- n -heptane, and Sulfolan, J. Chem. Eng. Data. 42 (1997) 1021–1036. https://doi.org/10.1021/je9701036.

[122] S. Kapteina, K. Slowik, S.P. Verevkin, A. Heintz, Vapor Pressures and Vaporization Enthalpies of a Series of Ethanolamines, J. Chem. Eng. Data. 50 (2005) 398–402. https://doi.org/10.1021/je049761y.

[123] A. Razzouk, A. Hajjaji, I. Mokbel, P. Mougin, J. Jose, Experimental vapor pressures of 1,2-bis(dimethylamino)ethane, 1-methylmorpholine, 1,2-bis(2-aminoethoxy)ethane and N-benzylethanolamine between 273.18 and 364.97K, Fluid Phase Equilib. 282 (2009) 11–13. https://doi.org/10.1016/j.fluid.2009.04.006.

[124] P.A. Verevkin SP, Andreeva IV, Evaluation of vaporization thermodynamics of pure amino-alcohols, J Mol Liq. (2021) submitted.

[125] F. Liu, Y. Liang, C. Cao, N. Zhou, Theoretical prediction of the Kovat's retention index for oxygen-containing organic compounds using novel topological indices, Anal. Chim. Acta. 594 (2007) 279–289. https://doi.org/10.1016/j.aca.2007.05.023.

[126] A.-M. Kelterer, M. Ramek, Intramolecular hydrogen bonding in 2-aminoethanol, 3-aminopropanol and 4-aminobutanol, J. Mol. Struct. THEOCHEM. 232 (1991) 189–201. https://doi.org/https://doi.org/10.1016/0166-1280(91)85254-5.

[127] M.I. Nouria C-B-A, Dergal F, Negadi L, Measurement and correlation of the (vapor + liquid) equilibria of pure 4-ethylmorpholine, 1,2-dimethylisopropylamine and N,N-dimethylethanolamine, and their binary aqueous solutions, J Chem Thermodyn. 63 (2013)

44–51.

[128] R. Siewert, D.H. Zaitsau, V.N. Emel'yanenko, S.P. Verevkin, Biomass Valorization: Thermodynamics of the Guerbet Condensation Reaction, J. Chem. Eng. Data. 64 (2019) 4904–4914. https://doi.org/10.1021/acs.jced.9b00419.

[129] K. V Zherikova, S.P. Verevkin, Error or exemption to the rule? Development of a diagnostic check for thermochemistry of metal–organic compounds, RSC Adv. 10 (2020) 38158–38173. https://doi.org/10.1039/D0RA06880B.

[130] I.S. Omodolor, H.O. Otor, J.A. Andonegui, B.J. Allen, A.C. Alba-Rubio, Dual-Function Materials for CO 2 Capture and Conversion: A Review, Ind. Eng. Chem. Res. 59 (2020) 17612–17631. https://doi.org/10.1021/acs.iecr.0c02218.

[131] A.G.H.W. K. Maneeintra, R.O. Idem, P. Tontiwachwuthikul, Synthesis, Solubilities, and Cyclic Capacities of Amino Alcohols for CO2 Capture from Flue Gas Streams, Energy Procedia. 1 (2009) 1327–1334.

[132] G.S. More, R. Srivastava, Synthesis of amino alcohols, cyclic urea, urethanes, and cyclic carbonates and tandem one-pot conversion of an epoxide to urethanes using a Zn–Zr bimetallic oxide catalyst, Sustain. Energy Fuels. 5 (2021) 1498–1510. https://doi.org/10.1039/D0SE01912G.

[133] T. Niemi, I. Fernández, B. Steadman, J.K. Mannisto, T. Repo, Carbon dioxide-based facile synthesis of cyclic carbamates from amino alcohols, Chem. Commun. 54 (2018) 3166–3169. https://doi.org/10.1039/C8CC00636A.

[134] P.A. Verevkin SP, Andreeva IV, Konnova ME, Portnova SV, Zherikova KV, Paving the way to the sustainable hydrogen storage: thermochemistry of amino-alcohols as precursors for the liquid organic hydrogen carriers, J Chem Thermodyn. (2021) submitted.

[135] P. GD, C. Anastasi, V. EC, G.D. Pappa, C. Anastasi, E.C. Voutsas, Measurement and thermodynamic modeling of the phase equilibrium of aqueous 2-amino-2-methyl-1-propanol solutions, Fluid Phase Equilib. 243 (2006) 193–197. https://doi.org/10.1016/j.fluid.2006.03.014.

[136] J.R. A. Barreau, P. Mougin, C. Lefebvre, Q.M. Luu Thi, Ternary Isobaric Vapour-Liquid Equilibria of Methanol + N-Methyldiethanolamine + Water and Methanol + 2-Amino-2-methyl-1-propanol + Water Systems, J. Chem. Eng. Data. 52 (2007) 769–773.

[137] A. Belabbaci, N. Chiali-Baba Ahmed, I. Mokbel, L. Negadi, Investigation of the isothermal (vapour+liquid) equilibria of aqueous 2-amino-2-methyl-1-propanol (AMP), N-benzylethanolamine, or 3-dimethylamino-1-propanol solutions at several temperatures,

J. Chem. Thermodyn. 42 (2010) 1158–1162. https://doi.org/10.1016/j.jct.2010.04.015.

[138] G.F.V. K. Klepáčová, P.J.G. Huttenhuis, P.W.J. Derks, Vapour pressures of several commercially used alkanolamines, J. Chem. Eng. Data. 56 (2011) 2242–2248.

[139] I.M. Bernhardsen, A.A. Trollebø, C. Perinu, H.K. Knuutila, Vapour-liquid equilibrium study of tertiary amines, single and in blend with 3-(methylamino)propylamine, for post-combustion CO2 capture, J. Chem. Thermodyn. 138 (2019) 211–228. https://doi.org/10.1016/j.jct.2019.06.017.

[140] F.M. Soares BP, Štejfa V, Ferreira O, Pinho SP, Růžička K, Vapor pressures and thermophysical properties of selected ethanolamines, Fluid Phase Equilib. 473 (2018) 245–54.

[141] A.A. Trollebø, A. Hartono, M. Usman, M. Saeed, H.F. Svendsen, Vapour-liquid equilibria in pure N-Methyl-1,3-diaminopropane (MAPA), 1,3-diaminopropane (DAP), 2-(Isopropylamino)ethanol (IPAE), N-tert-Butyldiethanolamine (N-TBDEA) and their aqueous solutions, J. Chem. Thermodyn. 141 (2020) 105965. https://doi.org/https://doi.org/10.1016/j.jct.2019.105965.

[142] E.B. A. Nath, Isothermal Vapor-Liquid Equilibria of Binary and Ternary Mixtures Containing Alcohol, Alkanolamine, and Water with a New Static Device, J. Chem. Eng. Data. 28 (1983) 370–375.

[143] Daubert TE, Vapour Pressure of Ten Pure Industrial Chemicals, in Experimental Results for DIPPR 1990-91 Projects on Phase Equilibria and Pure Component Properties, DIPPR Data Ser. 2 (1994) 143–153.

[144] Chase NW, NIST-JANAF thermochemical tables, J. Phys. Chem. Ref. Data Monogr. 9 (1998) 1–1951.

[145] S.P. Verevkin, Y. Chernyak, Vapor pressure and enthalpy of vaporization of aliphatic propanediamines, J. Chem. Thermodyn. 47 (2012) 328–334. https://doi.org/https://doi.org/10.1016/j.jct.2011.11.004.

[146] S.P. Verevkin, V.N. Emel'yanenko, R. Siewert, A.A. Pimerzin, Energetics of LOHC: Structure-Property Relationships from Network of Thermochemical Experiments and in Silico Methods, Hydrogen. 2 (2021) 101–121. https://doi.org/10.3390/hydrogen2010006.

[147] S.P. Verevkin, R.N. Nagrimanov, D.H. Zaitsau, M.E. Konnova, A.A. Pimerzin, Thermochemical properties of pyrazine derivatives as seminal liquid organic hydrogen carriers for hydrogen storage, J. Chem. Thermodyn. 158 (2021) 106406. https://doi.org/10.1016/j.jct.2021.106406.

[148] Y.S. Higasio, T. Shoji, Heterocyclic compounds such as pyrroles, pyridines, pyrollidins, piperdines, indoles, imidazol and pyrazins, Appl. Catal. A Gen. 221 (2001) 197–207. https://doi.org/10.1016/S0926-860X(01)00815-8.

[149] A. Kumar, T. Janes, N.A. Espinosa-Jalapa, D. Milstein, Selective Hydrogenation of Cyclic Imides to Diols and Amines and Its Application in the Development of a Liquid Organic Hydrogen Carrier, J. Am. Chem. Soc. 140 (2018) 7453–7457. https://doi.org/10.1021/jacs.8b04581.

[150] S. Pan, M. Jiang, J. Hu, R. Xu, X. Zeng, G. Zhong, Synthesis of 1,2-amino alcohols by decarboxylative coupling of amino acid derived α-amino radicals to carbonyl compounds via visible-light photocatalyst in water, Green Chem. 22 (2020) 336–341. https://doi.org/10.1039/C9GC03470F.

[151] M.S. Masoud, S.A. Abou El-Enein, I.M. Abed, A.E. Ali, Synthesis and Characterization of Amino Alcohol Complexes, J. Coord. Chem. 55 (2002) 153–178. https://doi.org/10.1080/00958970211879.

[152] S. Mishra, S. Daniele, Metal–Organic Derivatives with Fluorinated Ligands as Precursors for Inorganic Nanomaterials, Chem. Rev. 115 (2015) 8379–8448. https://doi.org/10.1021/cr400637c.

[153] K.I. Karakovskaya, S.I. Dorovskikh, E.S. Vikulova, I.Y. Ilyin, K. V. Zherikova, T. V. Basova, N.B. Morozova, Volatile Iridium and Platinum MOCVD Precursors: Chemistry, Thermal Properties, Materials and Prospects for Their Application in Medicine, Coatings. 11 (2021) 78. https://doi.org/10.3390/coatings11010078.

[154] J.H. Han, E.A. Jung, H.Y. Kim, D.H. Kim, B.K. Park, J.-S. Park, S.U. Son, T.-M. Chung, Atomic layer deposition of indium oxide thin film from a liquid indium complex containing 1-dimethylamino-2-methyl-2-propoxy ligands, Appl. Surf. Sci. 383 (2016) 1–8. https://doi.org/10.1016/j.apsusc.2016.04.120.

[155] S.P.V. R. Siewert, D.H. Zaitsau, P. Stange, R. Ludwig, The strength of intramolecular hydrogen bonding in amino-alcohols, PCCC. (2021) submitted.

[156] C.T. Peng, Prediction of retention indices, J. Chromatogr. A. 903 (2000) 117–143. https://doi.org/10.1016/S0021-9673(00)00901-8.

[157] E.L. Krasnykh, S.P. Verevkin, B. Koutek, J. Doubsky, Vapour pressures and enthalpies of vaporization of a series of the linear n-alkyl acetates, J. Chem. Thermodyn. 38 (2006) 717–723. https://doi.org/10.1016/j.jct.2005.08.003.

[158] K.Z. Haufa, M.A. Czarnecki, Molecular Structure and Hydrogen Bonding of 2-

Aminoethanol, 1-Amino-2-Propanol, 3-Amino-1-Propanol, and Binary Mixtures with Water Studied by Fourier Transform Near-Infrared Spectroscopy and Density Functional Theory Calculations, Appl. Spectrosc. 64 (2010) 351–359. https://doi.org/10.1366/000370210790918445.

[159] N. Hatefi, W.R. Smith, Ideal-Gas Thermochemical Properties for Alkanolamine and Related Species Involved in Carbon-Capture Applications, J. Chem. Eng. Data. 66 (2021) 1592–1599. https://doi.org/10.1021/acs.jced.0c00742.

[160] D.H. Zaitsau, V.N. Emel'yanenko, A.A. Pimerzin, S.P. Verevkin, Benchmark properties of biphenyl as a liquid organic hydrogen carrier: Evaluation of thermochemical data with complementary experimental and computational methods, J. Chem. Thermodyn. 122 (2018) 1–12. https://doi.org/10.1016/j.jct.2018.02.025.

[161] K. Müller, K. Stark, V.N. Emel'yanenko, M.A. Varfolomeev, D.H. Zaitsau, E. Shoifet, C. Schick, S.P. Verevkin, W. Arlt, Liquid Organic Hydrogen Carriers: Thermophysical and Thermochemical Studies of Benzyl- and Dibenzyl-toluene Derivatives, Ind. Eng. Chem. Res. 54 (2015) 7967–7976. https://doi.org/10.1021/acs.iecr.5b01840.

[162] S.P. Verevkin, V.N. Emel'yanenko, A. Heintz, K. Stark, W. Arlt, Liquid Organic Hydrogen Carriers: An Upcoming Alternative to Conventional Technologies. Thermochemical Studies., Ind. Eng. Chem. Res. 51 (2012) 12150–12153. https://doi.org/10.1021/ie301898m.

[163] V.N. Emel'yanenko, M.A. Varfolomeev, S.P. Verevkin, K. Stark, K. Müller, M. Müller, A. Bösmann, P. Wasserscheid, W. Arlt, Hydrogen Storage: Thermochemical Studies of N-Alkylcarbazoles and Their Derivatives as a Potential Liquid Organic Hydrogen Carriers, J. Phys. Chem. C. 119 (2015) 26381–26389. https://doi.org/10.1021/acs.jpcc.5b10392.

[164] P. Preuster, C. Papp, P. Wasserscheid, Liquid Organic Hydrogen Carriers (LOHCs): Toward a Hydrogen-free Hydrogen Economy, Acc. Chem. Res. 50 (2017) 74–85. https://doi.org/10.1021/acs.accounts.6b00474.

[165] R.H. Crabtree, Nitrogen-Containing Liquid Organic Hydrogen Carriers: Progress and Prospects, ACS Sustain. Chem. Eng. 5 (2017) 4491–4498. https://doi.org/10.1021/acssuschemeng.7b00983.

[166] L. Li, M. Yang, Y. Dong, P. Mei, H. Cheng, Hydrogen storage and release from a new promising Liquid Organic Hydrogen Storage Carrier (LOHC): 2-methylindole, Int. J. Hydrogen Energy. 41 (2016) 16129–16134. https://doi.org/10.1016/j.ijhydene.2016.04.240.

[167] V. Zubar, J.C. Borghs, M. Rueping, Hydrogenation or Dehydrogenation of N-Containing Heterocycles Catalyzed by a Single Manganese Complex, Org. Lett. 22 (2020) 3974–3978. https://doi.org/10.1021/acs.orglett.0c01273.

[168] Y. Dong, M. Yang, L. LL, T. Zhu, C. XD, C. HS, Study on reversible hydrogen uptake and release of 1,2-dimethylindole as a new liquid organic hydrogen carrier, Int. J. Hydrogen Energy. 44 (2019) 4919–4929. https://doi.org/10.1016/j.ijhydene.2019.01.015.

[169] A. Søgaard, M. Scheuermeyer, A. Bösmann, P. Wasserscheid, A. Riisager, Homogeneously-catalysed hydrogen release/storage using the 2-methylindole/2-methylindoline LOHC system in molten salt-organic biphasic reaction systems, Chem. Commun. 55 (2019) 2046–2049. https://doi.org/10.1039/C8CC09883B.

[170] P. Bachmann, M. Schwarz, J. Steinhauer, F. Späth, F. Düll, U. Bauer, T. Nascimento Silva, S. Mohr, C. Hohner, M. Scheuermeyer, P. Wasserscheid, J. Libuda, H.-P. Steinrück, C. Papp, Dehydrogenation of the Liquid Organic Hydrogen Carrier System Indole/Indoline/Octahydroindole on Pt(111), J. Phys. Chem. C. 122 (2018) 4470–4479. https://doi.org/10.1021/acs.jpcc.7b12625.

[171] R.D. Chirico, E. Paulechka, A. Bazyleva, A.F. Kazakov, Thermodynamic properties of 2–methylindole: Experimental and computational results for gas-phase entropy and enthalpy of formation, J. Chem. Thermodyn. 125 (2018) 257–270. https://doi.org/10.1016/j.jct.2018.05.029.

[172] W. V. Steele, R.D. Chirico, Thermodynamics and the hydrodenitrogenation of indole: Part 1, Thermodynamic properties of indoline and 2-methylindole: Part 2, Gibbs energies of reaction in the hydrodenitrogenation of indole: Part 3, Thermodynamic equilibria and comparison with literatu, Pittsburgh, PA, and Morgantown, WV (United States), 1989. https://doi.org/10.2172/6124014.

[173] M.L. Frenkel, Thermodynamics of Organic Compounds in the Gas State, T.E.E.S.T.R. Center., 1994.

[174] S.P. Verevkin, V.N. Emel'yanenko, V.N. Emel'yanenko, Transpiration method: Vapor pressures and enthalpies of vaporization of some low-boiling esters, Fluid Phase Equilib. 266 (2008) 64–75. https://doi.org/10.1016/j.fluid.2008.02.001.

[175] G.H. Zimmermann, H., Über die Mesomerieenergie von Azolen, Zeitschrift Für Elektrochemie, Berichte Der Bunsengesellschaft Für Phys. Chemie. 65 (1961) 368–371. https://doi.org/https://doi.org/10.1002/bbpc.19610650412.

[176] A. Aihara, A study of hydrogen bondings by the measurement of vapour pressures,

Nippon kagaku zassi, 1955.

[177] B.N. Solomonov, R.N. Nagrimanov, T.A. Mukhametzyanov, Additive scheme for calculation of solvation enthalpies of heterocyclic aromatic compounds. Sublimation/vaporization enthalpy at 298.15K, Thermochim. Acta. 633 (2016) 37–47. https://doi.org/https://doi.org/10.1016/j.tca.2016.03.031.

[178] R.N. Nagrimanov, A.A. Samatov, T.M. Nasyrova, B.N. Solomonov, Non-additivity in the solvation enthalpies of NH-containing compounds and estimation of their sublimation enthalpies at 298K, J. Mol. Liq. 246 (2017) 119–123. https://doi.org/https://doi.org/10.1016/j.molliq.2017.09.029.

[179] S.P. Verevkin, V.N. Emel'yanenko, A.A. Pimerzin, E.E. Vishnevskaya, Thermodynamic Analysis of Strain in Heteroatom Derivatives of Indene, J. Phys. Chem. A. 115 (2011) 12271–12279. https://doi.org/10.1021/jp203650d.

[180] M.A. V. Ribeiro da Silva, J.I.T.A. Cabral, J.R.B. Gomes, Experimental and Computational Study on the Molecular Energetics of Indoline and Indole, J. Phys. Chem. A. 112 (2008) 12263–12269. https://doi.org/10.1021/jp8065212.

[181] N. Serpinskii, VV, Voitkevich, SA, Lyuboshich, Determination of the saturated vapor pressures of several fragrant substances. II (Russian edition), Zh. Fiz. Khim. 28 (1954) 810–813.

[182] M.R. Arshadi, Determination of heats of sublimation of organic compounds by a mass spectrometric–knudsen effusion method, J. Chem. Soc. Faraday Trans. 1 Phys. Chem. Condens. Phases. 70 (1974) 1569. https://doi.org/10.1039/f19747001569.

[183] M.A. V Ribeiro da Silva, J.I.T.A. Cabral, J.R.B. Gomes, Combined experimental and computational study of the energetics of methylindoles, J. Chem. Thermodyn. 41 (2009) 1193–1198. https://doi.org/https://doi.org/10.1016/j.jct.2009.05.018.

[184] W.-S.D. Szafranski, A., olid–liquid phase diagrams of some binary mixtures of key organic coal compounds (biphenyl, naphthalene, alkylnaphthalenes, diphenyl ether, indole), Int. DATA Ser. Sel. Data Mix. Ser. A. 1 (1984) 40–50.

[185] C. Yokoyama, T. Ebina, S. Takahashi, Solid-liquid equilibria of six binary mixtures containing indole, J. Chem. Eng. Data. 38 (1993) 583–586. https://doi.org/10.1021/je00012a028.

[186] et al. Peyrot, L., Etude thermochimique de dérivés d'une hydrazine indoliques d'intérêt pharmaceutique, Calorimétrie Anal. Therm. (1997).

[187] G. Olofsson, Assignment of uncertainties, in Combustion Calorimetry: Experimental

Chemical Thermodynamics, Pergamon, New York, 1979.

[188] A.G. Berthelot M., Nouvelles recherches sur les chaleurs de formation et de combustion de divers composes azotes et autres, Ann. Chirm. Phys. 17 (1899) 433.

[189] A. Stern, G. Klebs, Calorimetrische Bestimmungen bei einfachen und mehrkernigen Pyrrolderivaten, Justus Liebig's Ann. Der Chemie. 504 (1933) 287–297. https://doi.org/10.1002/jlac.19335040118.

[190] W.D. Good, Enthalpies of combustion of nine organic nitrogen compounds related to petroleum, J. Chem. Eng. Data. 17 (1972) 28–31. https://doi.org/10.1021/je60052a038.

[191] Majer, V.; Svoboda, V., Enthalpies of Vaporization of Organic Compounds: A Critical Review and Data Compilation, Blackwell Scientific Publications, Oxford, 1985.

[192] M. Colomina, C. Latorre, R. Perez-Ossorio, Heats of combustion of five alkyl phenyl ketones, Pure Appl. Chem. 2 (1961) 133–136. https://doi.org/10.1351/pac196102010133.

[193] Wadso I., Heats of hydrolysis of phenyl acetate and phenyl thiolacetate, Acta Chem Scand. 14 (1960) 561–565.

[194] R.G. Simões, F. Agapito, H.P. Diogo, M.E.M. da Piedade, Enthalpy of Formation of Anisole: Implications for the Controversy on the O–H Bond Dissociation Enthalpy in Phenol, J. Phys. Chem. A. 118 (2014) 11026–11032. https://doi.org/10.1021/jp507267f.

[195] L.A. Curtiss, P.C. Redfern, K. Raghavachari, V. Rassolov, J.A. Pople, Gaussian-3 theory using reduced Mo/ller-Plesset order, J. Chem. Phys. 110 (1999) 4703–4709. https://doi.org/10.1063/1.478385.

[196] V. V Turovtsev, Y.D. Orlov, I.A. Kaplunov, Y.A. Fedina, V. V Zubkov, Errors of the most popular functionals in the calculation of the electron energy and enthalpy of formation of compounds, J. Phys. Conf. Ser. 1352 (2019) 012058. https://doi.org/10.1088/1742-6596/1352/1/012058.

[197] J. Dykyj, J.; Seprakova, M.; Maulech, Physikalische Eigenschaften des Athylenglykols und Seiner Derivate (II) Dampftensionen von Alkoxyathanolen und Aneren Drivaten des Athylenglykols, Chem. Zvesti. 11 (1957) 461–466.

[198] C.H. Rochester, J.R. Symonds, Thermodynamic studies of fluoroalcohols. Part 1.— Vapour pressures and enthalpies of vaporization, J. Chem. Soc. Faraday Trans. 1 Phys. Chem. Condens. Phases. 69 (1973) 1267. https://doi.org/10.1039/f19736901267.

[199] J. Murata, S. Yamashita, M. Akiyama, S. Katayama, T. Hiaki, A. Sekiya, Vapor Pressures of Hydrofluoroethers, J. Chem. Eng. Data. 47 (2002) 911–915. https://doi.org/10.1021/je010322y.

[200] H.R. Henze, B.G. Rogers, Symmetrical Dialkoxyacetones, J. Am. Chem. Soc. 61 (1939) 433–435. https://doi.org/10.1021/ja01871a060.

[201] Verevkin SP, Thermochemical investigation on a-methyl-styrene and parent phenyl substituted alkenes, Thermochim. Acta. 326 (1999) 17–25.

[202] J.B. Pedley, R.D. Naylor, S.P. Kirby, J.B. Pedley, Thermochemical data of organic compounds., 2nd ed., Chapman & Hall, London, 1986.

[203] W. V Steele, R.D. Chirico, S.E. Knipmeyer, A. Nguyen, I.R. Tasker, DIPPER project 871 determination of ideal-gas enthalpies of formation for key compounds, The 1991 project results, United States, 1993. https://doi.org/10.2172/10107077.

[204] S.P. Verevkin, V.N. Emel'yanenko, S.A. Kozlova, Organic Carbonates: Experiment and ab Initio Calculations for Prediction of Thermochemical Properties, J. Phys. Chem. A. 112 (2008) 10667–10673. https://doi.org/10.1021/jp8024705.

[205] N.N. Gutner, N.M.; Lebedeva, N.D.; Dobychin, S.L.; Kiseleva, Thermochemical study of aliphatic ethers, J. Appl. Chem. USSR. 53 (1980) 1523–1525.

[206] M. Månsson, Non-bonded oxygen-oxygen interactions in straight-chain compounds, J. Chem. Thermodyn. 1 (1969) 141–151. https://doi.org/10.1016/0021-9614(69)90053-6.

[207] Karrer, P.; Nageli, C.; Hurwitz, O.; Walti, A., Polysaccharide VIII. Zur Kenntnis der Starke und der Amylosen, Ber. 4 (1921) 678–699.

[208] Skuratov, S.M.; Kozina, M.L.; Shteher, S.M.; Varushyenko, R.M., The heats of combustion of several purified compounds, Thermochem. Bull. (Moscow State Univ.). (1957) 36–37.

[209] I.M. Rocha, T.L.P. Galvão, E. Sapei, M.D.M.C. Ribeiro da Silva, M.A. V Ribeiro da Silva, Levoglucosan: A Calorimetric, Thermodynamic, Spectroscopic, and Computational Investigation, J. Chem. Eng. Data. 58 (2013) 1813–1821. https://doi.org/10.1021/je400207t.

[210] G.J. Kabo, Y.U. Paulechka, O. V Voitkevich, A. V Blokhin, E.N. Stepurko, S. V Kohut, Y. V Voznyi, Experimental and theoretical study of thermodynamic properties of levoglucosan, J. Chem. Thermodyn. 85 (2015) 101–110. https://doi.org/https://doi.org/10.1016/j.jct.2015.01.005.

[211] Y. Maham, L. G. Hepler, A. E. Mather, A. W. Hakin, R. A. Marriott, Molar heat capacities of alkanolamines from 299.1 to 397.8 K Group additivity and molecular connectivity analyses, J. Chem. Soc. Faraday Trans. 93 (1997) 1747–1750. https://doi.org/10.1039/A607568A.

[212] M. Mundhwa, A. Henni, Molar Heat Capacity of Various Aqueous Alkanolamine Solutions from 303.15 K to 353.15 K, J. Chem. Eng. Data. 52 (2007) 491–498. https://doi.org/10.1021/je0604232.

[213] D. Kulikov, S.P. Verevkin, A. Heintz, Enthalpies of vaporization of a series of linear aliphatic alcohols. Experimental measurements and application of the ERAS-model for their prediction, Fluid Phase Equilib. 192 (2001) 187–207.

[214] Sigma Aldrich, (n.d.). https://www.sigmaaldrich.com/.

[215] J.V. Braun, Cyclic Imines. V. Dihydro-p-indole and p-Indole, Berichte Der Dtsch. Chem. Gesellschaft. 45 (1912) 1274–88.

[216] V. SP, Verevkin SP, Thermochemistry of phenols: quantification of the ortho-, para-, and meta-interactions in tert-alkyl substituted phenols, J. Chem. Thermodyn. 31 (1999) 559–585. https://doi.org/10.1006/jcht.1998.0459.

[217] V.N. Emel'yanenk, S.P. Verevkin, Enthalpies of Formation and Substituent Effects of ortho-, meta-, and para-Aminotoluenes from Thermochemical Measurements and from Ab Initio Calculations, J. Phys. Chem. A. 109 (2005) 3960–3966. https://doi.org/10.1021/jp045450i.

[218] O. V. Dorofeeva, M.A. Filimonova, I.I. Marochkin, Aliphatic Amines: A Critical Analysis of the Experimental Enthalpies of Formation by Comparison with Theoretical Calculations, J. Chem. Eng. Data. 64 (2019) 5630–5647. https://doi.org/10.1021/acs.jced.9b00680.

[219] S.P. Verevkin, V.N. Emeĺyanenko, Thermodynamic properties of cyclohexanamines: Experimental and theoretical study, Thermochim. Acta. 608 (2015) 40–48. https://doi.org/https://doi.org/10.1016/j.tca.2015.03.016.

[220] O. V. Dorofeeva, M.A. Filimonova, Cyclic aliphatic amines: A critical analysis of the experimental enthalpies of formation by comparison with theoretical calculations, J. Chem. Thermodyn. 145 (2020) 106092. https://doi.org/10.1016/j.jct.2020.106092.

APPENDIX

A. Supporting information to Chapter 1.

Table A. 1. Compilation of data on molar heat capacities $C_{p,m}^o$(cr, liq) and differences $\Delta_{cr,l}^g C_{p,m}^o$ of substituted acetophenones in $J \cdot K^{-1} \cdot mol^{-1}$ at $T = 298.15$ K.

compound	$C_{p,m}^o$(cr)	$\Delta_{cr}^g C_{p,m}^o$	$C_{p,m}^o$(liq)	$\Delta_l^g C_{p,m}^o$
methylacetophenone	194.7	-30.0	237.0	-72.2
ethylacetophenone	221.6	-34.0	268.9	-80.5
cyanoacetophenone	199.7	-30.7	252.0	-76.1
acethoxyacetophenone	236.9	-36.3	300.9	-88.8

Table A. 2. Results of transpiration method: absolute vapor pressures p_i, standard ($p^0 = 0.1$ MPa) molar vaporization/sublimation enthalpies $\Delta_{l,cr}^g H_m^o$ and standard molar vaporization/sublimation entropies $\Delta_{l,cr}^g S_m^o$.

$T/$ K^a	$m/$ mg^b	$V(N_2)^c/$ dm^3	$T_a/$ K^d	Flow/ $dm^3 \cdot h^{-1}$	$p/$ Pa^e	$u(p_i)/$ Pa^f	$\Delta_{l,cr}^g H_m^o(T)/$ $kJ \cdot mol^{-1}$	$\Delta_{l,cr}^g S_m^o(T)/$ $J \cdot K^{-1} \cdot mol^{-1}$

2-methyl-acetophenone: $\Delta_l^g H_m^o(298.15 \text{ K}) = (59.3 \pm 0.4) \text{ kJ} \cdot \text{mol}^{-1}$

$$\ln(p_i/p_{ref}) = \frac{299.7}{R} - \frac{80827.5}{RT} - \frac{72.2}{R}\ln\frac{T}{298.15}; \ p_{ref} = 1 \text{ Pa}$$

$T/$ K^a	$m/$ mg^b	$V(N_2)^c/$ dm^3	$T_a/$ K^d	Flow/ $dm^3 \cdot h^{-1}$	$p/$ Pa^e	$u(p_i)/$ Pa^f	$\Delta_{l,cr}^g H_m^o(T)/$ $kJ \cdot mol^{-1}$	$\Delta_{l,cr}^g S_m^o(T)/$ $J \cdot K^{-1} \cdot mol^{-1}$
293.3	0.31	0.275	294.4	1.10	20.84	0.55	59.65	132.9
298.3	0.48	0.275	294.6	1.10	31.84	0.82	59.29	131.8
303.1	0.71	0.275	294.5	1.10	47.29	1.21	58.94	130.8
308.1	2.14	0.602	294.6	1.20	64.87	1.65	58.58	129.1
312.8	2.08	0.401	294.8	1.20	94.91	2.40	58.25	128.4
295.2	0.38	0.286	293.4	1.07	24.22	0.63	59.52	132.4
290.2	0.38	0.447	294.3	1.07	15.74	0.42	59.87	133.5
285.6	0.41	0.699	294.5	1.05	10.81	0.30	60.21	134.9
300.0	2.03	1.017	294.6	2.77	36.52	0.94	59.16	131.4
306.2	1.96	0.621	294.6	1.06	57.71	1.47	58.72	129.8
312.7	2.01	0.390	294.8	1.06	93.95	2.37	58.25	128.3
319.6	2.14	0.266	295.2	1.06	146.79	3.69	57.75	126.5
326.2	3.43	0.266	295.9	1.06	235.90	5.92	57.27	125.3
332.7	5.24	0.266	295.3	1.06	359.44	9.01	56.81	123.9

3-methyl-acetophenone: $\Delta_l^g H_m^o(298.15 \text{ K}) = (59.8 \pm 0.4) \text{ kJ} \cdot \text{mol}^{-1}$

$$\ln(p_i/p_{ref}) = \frac{296.4}{R} - \frac{81354.1}{RT} - \frac{72.2}{R}\ln\frac{T}{298.15}; \ p_{ref} = 1 \text{ Pa}$$

$T/$ K^a	$m/$ mg^b	$V(N_2)^c/$ dm^3	$T_a/$ K^d	Flow/ $dm^3 \cdot h^{-1}$	$p/$ Pa^e	$u(p_i)/$ Pa^f	$\Delta_{l,cr}^g H_m^o(T)/$ $kJ \cdot mol^{-1}$	$\Delta_{l,cr}^g S_m^o(T)/$ $J \cdot K^{-1} \cdot mol^{-1}$
285.5	0.32	1.032	295.0	5.75	2.69	0.17	60.74	131.7
290.4	0.34	0.718	295.0	8.68	2.69	0.24	60.39	130.3
295.2	0.50	0.683	297.1	13.45	2.73	0.36	60.04	129.3
298.1	0.33	0.353	294.0	17.21	1.06	0.46	59.83	128.7
300.6	0.78	0.683	298.4	21.11	2.73	0.55	59.65	128.1
303.2	0.91	0.683	299.3	24.65	2.73	0.64	59.46	127.1
303.2	0.37	0.280	294.9	24.38	1.12	0.64	59.46	127.0
308.1	0.50	0.252	299.0	36.56	1.01	0.94	59.11	126.1
312.7	1.92	0.689	296.9	51.25	1.12	1.31	58.78	125.0
319.5	2.07	0.466	298.8	82.21	1.12	2.08	58.29	123.4
326.5	2.10	0.298	296.4	129.37	1.12	3.26	57.78	121.7
333.2	3.18	0.280	296.2	208.70	1.12	5.23	57.30	120.6
334.0	3.33	0.280	296.4	218.52	1.12	5.48	57.24	120.5

$$4\text{-methyl-acetophenone: } \Delta_l^g H_m^o(298.15 \text{ K}) = (61.6\pm0.3) \text{ kJ·mol}^{-1}$$

$$\ln (p_i/p_{\text{ref}}) = \frac{299.8}{R} - \frac{83131.5}{RT} - \frac{72.2}{R}\ln\frac{T}{298.15}; \ \ p_{\text{ref}} = 1 \text{ Pa}$$

302.6	1.41	1.413	294.5	1.07	18.30	0.48	61.28	131.0
303.6	0.46	0.441	294.5	1.06	19.19	0.50	61.22	130.5
304.6	1.57	1.388	296.0	2.97	20.79	0.54	61.14	130.2
306.6	1.83	1.383	296.2	1.06	24.35	0.63	61.00	129.8
308.5	1.52	0.968	297.2	2.90	29.00	0.75	60.86	129.5
309.5	1.56	0.942	295.8	2.97	30.45	0.79	60.79	129.1
312.5	1.53	0.730	295.4	1.83	38.44	0.99	60.57	128.4
316.5	1.61	0.562	294.6	1.05	52.22	1.33	60.28	127.7
318.4	2.23	0.674	293.9	1.06	60.24	1.53	60.14	127.2
320.4	1.52	0.404	295.2	1.05	68.70	1.74	60.00	126.7
323.4	3.27	0.727	295.6	1.06	82.33	2.08	59.78	125.8
324.4	1.45	0.298	294.4	0.99	88.76	2.24	59.71	125.6
329.3	1.75	0.249	294.4	0.99	128.01	3.23	59.36	124.9
334.3	2.54	0.264	295.7	1.05	176.54	4.44	59.00	123.8
339.3	4.28	0.330	296.7	0.99	237.67	5.97	58.63	122.6
344.3	5.78	0.330	297.9	0.99	322.09	8.08	58.28	121.6
349.3	7.62	0.330	297.8	0.99	423.64	10.62	57.91	120.4
354.2	10.05	0.330	297.9	0.99	558.24	13.98	57.56	119.4

$$2\text{-cyano-acetophenone: } \Delta_l^g H_m^o(298.15 \text{ K}) = (72.9\pm0.4) \text{ kJ·mol}^{-1}$$

$$\ln (p_i/p_{\text{ref}}) = \frac{309.8}{R} - \frac{95544.7}{RT} - \frac{76.1}{R}\ln\frac{T}{298.15}; \ \ p_{\text{ref}} = 1 \text{ Pa}$$

322.9	0.18	1.186	295.8	2.74	2.63	0.07	70.97	132.1
325.3	0.18	1.004	297.6	2.87	3.13	0.08	70.79	131.3
325.3	0.18	1.004	297.3	2.87	3.08	0.08	70.79	131.2
328.2	0.19	0.852	298.3	2.84	3.90	0.10	70.57	130.6
329.2	0.19	0.770	296.4	2.43	4.23	0.11	70.50	130.4
330.0	0.19	0.730	295.6	2.74	4.41	0.12	70.43	130.1
332.1	0.18	0.601	297.0	1.03	5.20	0.16	70.27	129.6
333.2	0.19	0.555	296.4	1.08	5.77	0.17	70.19	129.5
336.1	0.17	0.412	297.4	1.03	7.06	0.20	69.97	128.7
339.9	0.20	0.358	297.3	1.08	9.64	0.27	69.68	128.1
341.1	0.16	0.258	297.7	1.03	10.45	0.29	69.59	127.8
346.0	0.67	0.770	297.6	1.08	14.92	0.40	69.21	126.8
352.9	0.63	0.466	298.5	1.08	22.99	0.60	68.69	125.0
360.1	0.69	0.323	298.3	1.08	36.57	0.94	68.14	123.4
366.9	0.90	0.269	297.9	1.08	57.34	1.46	67.62	122.2
372.4	1.25	0.269	297.2	1.08	78.82	2.00	67.21	121.1

$$3\text{-cyano-acetophenone: } \Delta_{cr}^g H_m^o(298.15 \text{ K}) = (72.9\pm0.) \text{ kJ·mol}^{-1}$$

$$\ln (p_i/p_{\text{ref}}) = \frac{332.1}{R} - \frac{106212.7}{RT} - \frac{30.7}{R}\ln\frac{T}{298.15}; \ \ p_{\text{ref}} = 1 \text{ Pa}$$

318.4	0.13	3.559	299.8	2.85	0.64	0.02	96.44	203.5
323.8	0.13	1.898	298.8	2.85	1.20	0.03	96.27	203.1
328.3	0.28	2.395	299.7	3.59	2.03	0.06	96.13	203.0
330.4	0.13	0.898	300.6	3.59	2.56	0.07	96.07	202.8
332.5	0.14	0.759	296.1	2.85	3.03	0.08	96.01	202.2
333.2	0.18	0.958	300.0	3.59	3.26	0.09	95.98	202.2
336.3	0.14	0.513	300.7	1.14	4.63	0.12	95.89	202.2
338.2	0.30	0.898	299.5	3.59	5.64	0.17	95.83	202.1
341.4	0.13	0.304	300.3	1.14	7.50	0.21	95.73	201.5

348.2	0.24	0.285	300.4	1.14	14.54	0.39	95.52	200.9
350.7	0.30	0.280	299.7	1.12	18.70	0.49	95.45	200.8
354.8	0.45	0.285	300.5	1.14	27.41	0.71	95.32	200.4
360.3	0.73	0.280	300.0	1.12	44.76	1.14	95.15	200.0
362.3	0.40	0.133	300.8	1.14	51.48	1.31	95.09	199.5

4-cyano-acetophenone: $\Delta_{cr}^{g}H_{m}^{o}(298.15\text{ K}) = (87.7\pm0.7)$ kJ·mol⁻¹

$$\ln(p_i/p_{\text{ref}}) = \frac{313.7}{R} - \frac{96872.9}{RT} - \frac{30.7}{R}\ln\frac{T}{298.15}; \ p_{\text{ref}} = 1 \text{ Pa}$$

303.2	0.14	5.398	296.6	3.00	0.46	0.02	87.57	186.6
306.3	0.14	3.599	296.8	3.00	0.64	0.02	87.47	186.2
308.2	0.16	3.249	295.2	3.00	0.82	0.03	87.41	186.3
312.2	0.14	1.849	297.0	3.00	1.25	0.04	87.29	185.8
313.2	0.10	1.230	296.0	3.08	1.37	0.04	87.26	185.6
316.2	0.14	1.200	297.2	3.00	1.95	0.05	87.17	185.5
318.1	0.12	0.854	297.2	3.01	2.30	0.06	87.11	185.1
318.2	0.12	0.923	295.8	3.08	2.29	0.06	87.11	185.0
320.2	0.14	0.800	296.6	3.00	2.95	0.08	87.04	185.2
323.1	0.17	0.753	297.4	3.01	3.91	0.10	86.96	184.8
327.1	0.16	0.476	297.8	1.10	5.76	0.17	86.83	184.3
328.0	0.14	0.367	294.0	1.10	6.25	0.18	86.80	184.2
329.2	0.13	0.311	299.6	1.10	6.94	0.20	86.77	184.0
331.1	0.63	1.281	296.2	3.08	8.37	0.23	86.71	183.9

4-cyano-acetophenone: $\Delta_{l}^{g}H_{m}^{o}(298.15\text{ K}) = (72.1\pm0.4)$ kJ·mol⁻¹

$$\ln(p_i/p_{\text{ref}}) = \frac{31081}{R} - \frac{94819.2}{RT} - \frac{76.1}{R}\ln\frac{T}{298.15}; \ p_{\text{ref}} = 1 \text{ Pa}$$

333.2	0.16	0.330	299.6	1.10	8.41	0.24	69.47	130.5
334.1	0.56	1.053	295.2	1.02	9.01	0.25	69.40	130.3
337.2	0.64	0.951	296.8	1.02	11.41	0.31	69.16	129.7
338.2	0.23	0.321	299.6	1.10	12.19	0.33	69.09	129.4
340.1	0.60	0.713	296.6	1.02	14.28	0.38	68.94	129.1
343.2	0.33	0.330	300.4	1.10	17.29	0.46	68.71	128.2
344.1	0.61	0.560	296.8	1.02	18.52	0.49	68.64	128.0
346.2	0.65	0.510	297.0	1.02	21.57	0.56	68.48	127.6
349.1	0.62	0.408	297.0	1.02	26.00	0.67	68.26	126.9
354.2	0.62	0.289	297.2	1.02	36.63	0.94	67.87	125.9
359.2	0.75	0.255	296.6	1.02	49.89	1.27	67.49	124.7
364.3	1.03	0.255	297.3	1.02	69.03	1.75	67.10	123.7
369.2	1.41	0.255	297.4	1.02	94.27	2.38	66.73	122.8

Table A. 3. Compilation of boiling points at reduced pressures from the distillation data available in the literature [34].

2-Et-acetophenone		3-Et-acetophenone		4-Et-acetophenone	
T/K	p/Pa	T/K	p/Pa	T/K	p/Pa
357.2	800	386.2	1867	367.2	533
372.2	1733	387.2	2000	371.2	667
377.2	2266	389.2	1867	385.2	1466
377.2	2133	391.2	2000	387.2	1333
381.2	2400	416.2	5308	398.2	2666
381.2	2666	517.2	101325	403.2	3066
388.2	3333			423.2	6533

| 389.2 | 4000 | | 518.2 | 101325 |
| 391.2 | 3866 | | | |
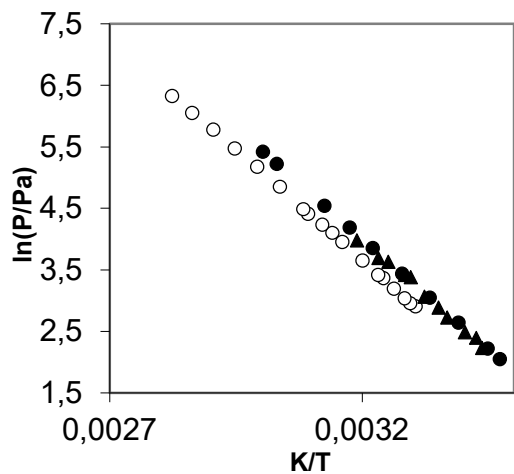
Figure A. 1. Temperature dependence of available vapor pressures for 4-methylacetophenone: ○ - this work, transpiration; ▲ – Knudsen method [42]; ● – method is not available [43].
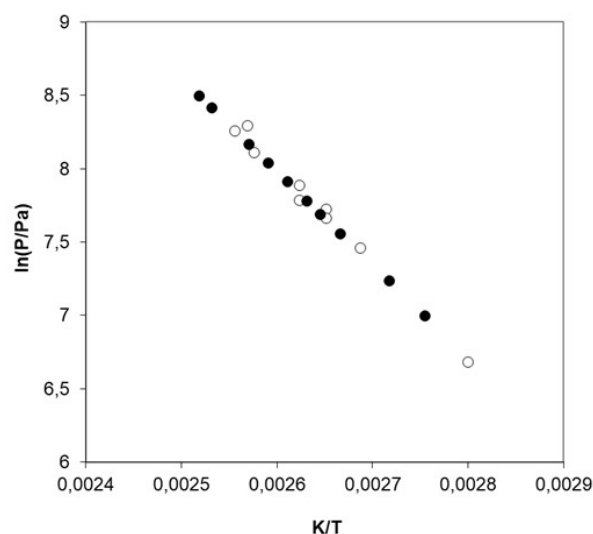
Figure A. 2. Temperature dependence of available vapor pressures for 2-ethylacetophenone: ○ - boiling temperatures at reduced pressures [34]; ● - [43].
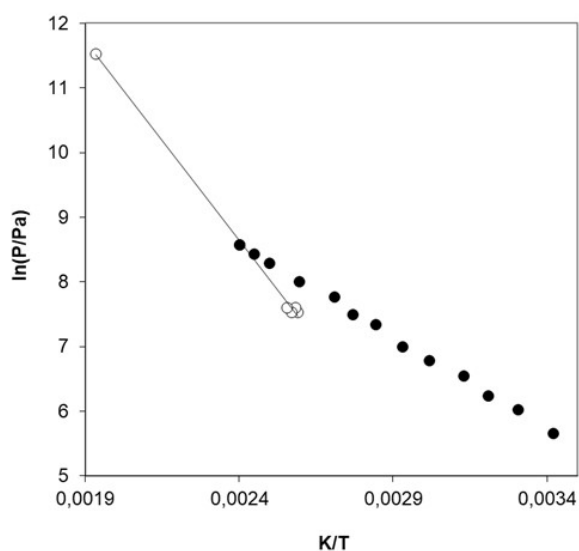
Figure A. 3. Temperature dependence of available vapor pressures for 3-ethylacetophenone: ○- boiling temperatures at reduced pressures [34]; ● – [44].
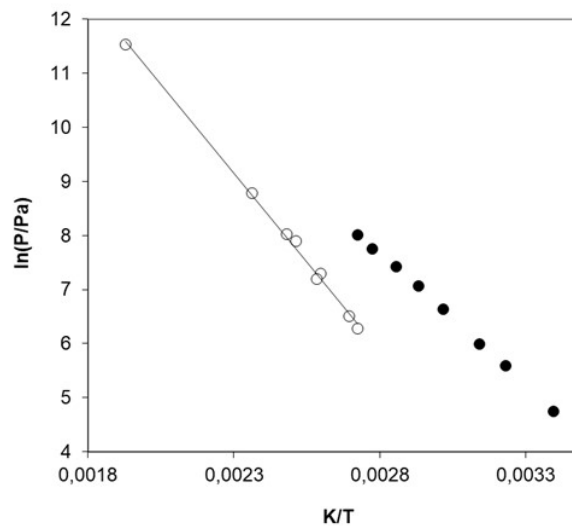
Figure A. 4. Temperature dependence of available vapor pressures for 4-ethylacetophenone: ○- boiling temperatures at reduced pressures [34]; ● - [44].
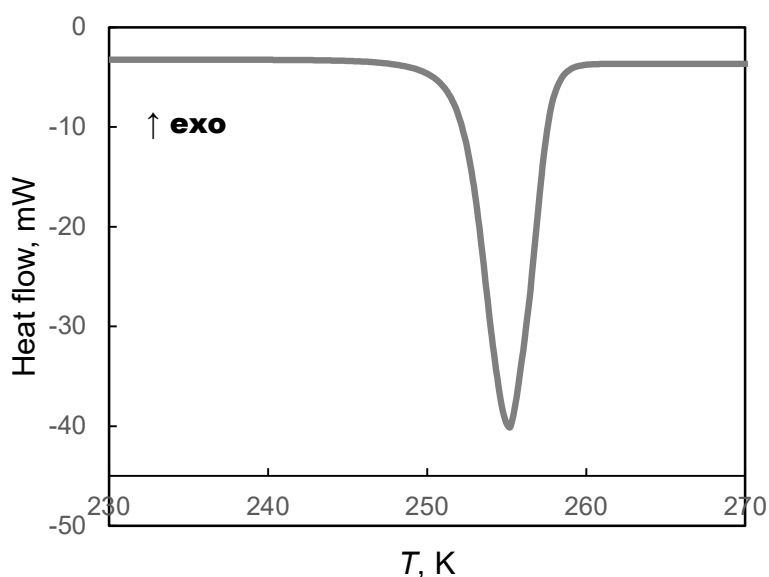
Figure A. 5. Typical thermogram of 4-methylacetophenone.

Table A. 4. Experimental thermochemical data at $T = 298.15$ K (p° = 0.1 MPa) for reference compounds (in kJ·mol^{-1}).

	$\Delta_f H_m^o$(liq)	$\Delta_l^g H_m^o$	$\Delta_f H_m^o$(g)
benzene	49.0±0.9 [49]	33.9±0.1 [49]	82.9±0.9 [49]
methylbenzene	12.0±1.1 [49]	38.1±0.1 [49]	50.1±1.1 [49]
ethylbenzene	-12.3±0.9 [115]	42.2±0.1 [191]	29.9±0.9
cyanobenzene	164.6±0.7[143]	51.1±0.1[143]	215.7±0.7
acetophenone	-142.5±1.0 [192]	55.4±0.3 [50]	-87.1±1.0
phenyl acetate	-334.8±0.9 [193]	59.0±0.3 [53]	-275.8±1.0

B. Supporting information to Chapter 2

Table B. 1. Compilation of data on molar heat capacities $C_{p,m}^o$(cr or liq) and heat capacity differences $\Delta_{cr,l}^g C_{p,m}^o$ (in J·K^{-1}·mol^{-1}) at $T = 298.15$ K for the methoxy-substituted benzenes.

Compounds	$C_{p,m}^o$(cr)[a]	$-\Delta_{cr}^g C_{p,m}^o$ [b]	$C_{p,m}^o$(liq) [a]	$-\Delta_l^g C_{p,m}^o$ [b]
1,2,3-trimethoxybenzene	243.3 [c]	37.2	335.7	97.9
1,2,4-trimethoxybenzene	243.3	37.2	335.7	97.9
1,3,5-trimethoxybenzene	243.3	37.2	335.7	97.9
3,4,5-trimethoxytoluene	270.9	41.4	364.1	105.2

Table B. 2. Compilation of data on molar heat capacities $C_{p,m}^o$(cr or liq) (in J·K^{-1}·mol^{-1}) at $T = 298.15$ K for 1,2,3-trimethoxybenzene.

T, K	$C_{p,m}^o$(cr)[a]	T, K	$C_{p,m}^o$(liq)
238	201.86	286	233.98
241	203.33	296	238.98
246	206.31	291	235.94
251	209.40	335	343.11

256	212.56	337	343.65
261	216.16	340	344.66
266	219.67	343	345.62
271	222.89	346	346.61
276	226.60	349	347.49
281	230.43		

[a] The experimental data were fitted with $C_{p,m}^o$(cr)/R = 0.0311 + 4.734×10^{-4}(T/K) from 238 to 296 K (with R = 8.314462 J·K^{-1}·mol^{-1}), $C_{p,m}^o$(cr, 298.15 K) = 240.9 J·K^{-1}·mol^{-1}

Table B. 3. Results from the transpiration method: absolute vapour pressures p$_i$, standard molar sublimation/vaporization enthalpies $\Delta_{cr,l}^g H_m^o$ and standard molar sublimation/vaporization entropies $\Delta_{cr,l}^g S_m^o$.

$T/$ K[a]	$m/$ mg[b]	$V(N_2)^c/$ dm^3	$T_a/$ K[d]	Flow/ dm^3·h^{-1}	$p_i/$ Pa[e]	$u(p_i)/$ Pa[f]	$\Delta_{cr/l}^g H_m^o(T)/$ kJ·mol^{-1}	$\Delta_{cr/l}^g S_m^o(T)/$ J·K^{-1}·mol^{-1}
1,2,3-trimethoxybenzene, $\Delta_{cr}^g H_m^o$(298.15 K) = (92.4 ± 0.7) kJ·mol^{-1}								

$$\ln(p_i/p_{ref}) = \frac{348.4}{R} - \frac{103491.0}{RT} - \frac{37.2}{R}\ln\frac{T}{298.15}$$

$T/$ K[a]	$m/$ mg[b]	$V(N_2)^c/$ dm^3	$T_a/$ K[d]	Flow/ dm^3·h^{-1}	$p_i/$ Pa[e]	$u(p_i)/$ Pa[f]	$\Delta H/$ kJ·mol^{-1}	$\Delta S/$ J·K^{-1}·mol^{-1}
288.2	2.25	102.929	295.6	2.57	0.32	0.01	92.8	216.7
291.2	1.67	51.023	295.6	2.59	0.48	0.02	92.7	216.4
294.3	1.51	31.166	295.6	2.59	0.71	0.02	92.5	215.9
297.2	1.19	16.662	295.6	2.59	1.05	0.03	92.4	215.7
300.3	0.69	6.734	295.6	2.59	1.49	0.04	92.3	215.1
303.2	0.97	6.561	295.6	2.59	2.17	0.06	92.2	214.9
306.3	1.22	5.784	295.6	2.59	3.08	0.08	92.1	214.3
308.3	1.50	5.525	295.6	2.59	3.95	0.10	92.0	214.2
310.3	1.45	4.144	295.6	2.59	5.11	0.15	91.9	214.2
312.3	1.35	3.151	295.6	2.59	6.24	0.18	91.9	213.7
314.3	1.19	2.245	295.6	2.59	7.78	0.22	91.8	213.5

1,2,3-trimethoxybenzene, $\Delta_l^g H_m^o$(298.15 K) = (73.0 ± 0.5) kJ·mol^{-1}

$$\ln(p_i/p_{ref}) = \frac{348.3}{R} - \frac{102212.3}{RT} - \frac{97.9}{R}\ln\frac{T}{298.15}$$

T	m	V	T_a	Flow	p_i	$u(p_i)$	ΔH	ΔS
318.1	1.09	1.360	295.5	2.59	11.75	0.32	71.1	148.2
321.2	1.50	1.425	295.5	2.59	15.33	0.41	70.8	147.3
324.3	1.45	1.079	295.5	2.59	19.61	0.52	70.5	146.3
327.2	1.70	0.993	295.5	2.59	25.06	0.65	70.2	145.6
331.2	2.25	0.950	295.5	2.59	34.56	0.89	69.8	144.5
334.3	2.58	0.863	295.5	2.59	43.68	1.12	69.5	143.6
337.3	2.51	0.691	295.5	2.59	53.13	1.35	69.2	142.5
340.2	3.09	0.691	295.5	2.59	65.35	1.66	68.9	141.6
343.1	2.88	0.518	295.5	2.59	81.25	2.06	68.6	140.9
346.3	2.25	0.324	295.5	2.59	101.3	2.56	68.3	140.0

1,2,4-trimethoxybenzene, $\Delta_l^g H_m^o$(298.15 K) = (75.7 ± 0.5) kJ·mol^{-1}

$$\ln(p_i/p_{ref}) = \frac{350.8}{R} - \frac{104844.6}{RT} - \frac{97.9}{R}\ln\frac{T}{298.15}$$

T	m	V	T_a	Flow	p_i	$u(p_i)$	ΔH	ΔS
309.7	0.73	3.788	293.8	3.99	2.81	0.08	74.5	153.5
314.1	0.77	2.649	294.4	3.97	4.22	0.11	74.1	152.1
319.2	0.69	1.527	294.9	3.98	6.56	0.19	73.6	150.5
324.2	0.64	0.945	294.9	2.98	9.89	0.27	73.1	148.9
329.1	0.73	0.704	294.7	2.01	15.16	0.40	72.6	147.6
329.2	1.04	1.000	301.2	3.00	15.48	0.41	72.6	147.7

329.2	0.79	0.751	300.8	3.01	15.66	0.42	72.6	147.8
332.1	0.74	0.560	297.0	1.98	19.33	0.51	72.3	146.7
332.1	0.77	0.616	301.8	1.48	18.53	0.49	72.3	146.3
334.2	0.76	0.503	295.0	2.01	21.91	0.57	72.1	145.8
335.2	0.82	0.497	301.4	1.99	24.52	0.64	72.0	145.8
338.2	0.77	0.381	300.9	1.00	29.91	0.77	71.7	144.7
339.2	0.70	0.314	294.7	0.99	32.47	0.84	71.6	144.5
341.2	0.75	0.296	300.3	0.99	37.54	0.96	71.4	143.8
342.1	1.37	0.496	298.2	0.99	40.83	1.05	71.4	143.7
344.1	0.80	0.248	294.7	0.99	46.72	1.19	71.2	143.0
344.1	0.81	0.254	300.6	0.98	47.66	1.22	71.2	143.2
345.2	1.03	0.298	298.1	0.99	51.15	1.30	71.1	142.8
347.1	0.99	0.248	295.0	0.99	58.21	1.48	70.9	142.2
348.2	1.08	0.247	297.0	0.99	64.30	1.63	70.8	142.1
350.1	1.19	0.231	294.8	0.99	75.17	1.90	70.6	141.8

1,3,5-trimethoxybenzene, $\Delta_{cr}^{g}H_m^o$(298.15 K) = (90.3 ± 0.5) kJ·mol^{-1}

$$\ln(p_i/p_{ref}) = \frac{333.9}{R} - \frac{101366.0}{RT} - \frac{37.2}{R}\ln\frac{T}{298.15}$$

288.0	0.67	72.497	296.3	4.78	0.13	0.01	90.7	202.4
296.3	0.56	21.351	296.3	4.78	0.39	0.01	90.3	201.3
298.7	0.63	18.288	296.3	5.08	0.51	0.02	90.3	200.9
303.2	0.83	13.801	296.3	5.08	0.88	0.03	90.1	200.4
304.2	1.03	15.750	296.3	6.30	0.96	0.03	90.1	200.0
307.2	0.90	9.450	296.3	6.30	1.40	0.04	89.9	199.9
308.2	0.49	4.741	296.3	5.08	1.52	0.04	89.9	199.5
311.4	1.23	7.770	296.3	6.30	2.31	0.06	89.8	199.6
314.4	1.10	5.145	296.3	6.30	3.12	0.08	89.7	199.0
316.5	0.90	3.330	296.3	3.77	3.96	0.10	89.6	198.8
317.4	1.19	4.148	296.3	6.30	4.21	0.11	89.6	198.4
319.5	1.11	2.953	296.3	3.77	5.50	0.16	89.5	198.6
320.2	1.24	3.150	296.3	6.30	5.79	0.17	89.5	198.3
323.2	1.24	2.310	296.3	6.30	7.89	0.22	89.3	197.9
325.5	1.75	2.513	296.3	3.77	10.18	0.28	89.3	197.8
326.2	1.10	1.470	296.3	6.30	10.93	0.30	89.2	197.8

1,3,5-trimethoxybenzene, $\Delta_{l}^{g}H_m^o$(298.15 K) = (68.7 ± 0.4) kJ·mol^{-1}

$$\ln(p_i/p_{ref}) = \frac{329.3}{R} - \frac{97850.6}{RT} - \frac{97.9}{R}\ln\frac{T}{298.15}$$

330.5	0.57	0.512	296.2	1.06	16.36	0.43	65.5	125.7
331.2	0.62	0.539	296.2	1.06	16.92	0.45	65.4	125.4
333.5	0.69	0.504	296.2	1.06	20.11	0.53	65.2	124.8
336.3	0.81	0.477	296.2	1.06	24.78	0.64	64.9	124.1
337.3	1.13	0.636	296.2	1.06	25.96	0.67	64.8	123.6
339.4	0.83	0.406	296.2	1.06	30.02	0.78	64.6	123.0
341.4	0.98	0.415	296.2	1.06	34.42	0.89	64.4	122.5
342.3	1.12	0.451	296.2	1.06	36.26	0.93	64.3	122.1
345.3	0.79	0.265	296.2	1.06	43.89	1.12	64.1	121.2
346.3	1.09	0.336	296.2	1.06	47.52	1.21	64.0	121.1
348.3	0.84	0.230	296.2	1.06	53.37	1.36	63.8	120.4
350.3	1.23	0.292	296.2	1.06	61.68	1.57	63.6	120.0
351.4	1.01	0.230	296.2	1.06	64.54	1.64	63.5	119.5
354.4	0.93	0.173	296.2	1.06	78.50	1.99	63.2	118.8
355.4	1.44	0.247	296.2	1.06	85.01	2.15	63.1	118.7

357.5	1.13	0.177	296.2	1.06	93.91	2.37	62.9	117.9
359.4	1.52	0.212	296.2	1.06	104.8	2.65	62.7	117.4
360.6	1.38	0.177	296.2	1.06	113.9	2.87	62.6	117.1
363.6	1.59	0.177	296.2	1.06	131.7	3.32	62.3	116.1
364.3	1.70	0.177	296.2	1.06	140.9	3.55	62.2	116.2
366.6	1.82	0.168	296.2	1.06	158.1	3.98	62.0	115.4
368.5	1.90	0.159	296.2	1.06	174.5	4.39	61.8	114.9
369.3	1.87	0.150	296.2	1.06	182.1	4.58	61.7	114.6
371.4	2.17	0.150	296.2	1.06	211.1	5.30	61.5	114.4
372.4	2.11	0.141	296.2	1.06	218.5	5.49	61.4	114.0
374.3	2.15	0.129	296.2	1.06	243.6	6.11	61.2	113.5
375.3	2.34	0.133	296.2	1.06	257.6	6.47	61.1	113.3

3,4,5-trimethoxytoluene, $\Delta_l^g H_m^o(298.15 \text{ K}) = (77.7 \pm 0.5) \text{ kJ·mol}^{-1}$

$$\ln(p_i / p_{ref}) = \frac{366.9}{R} - \frac{109273.7}{RT} - \frac{105.8}{R} \ln \frac{T}{298.15}$$

327.2	2.90	3.413	294.8	4.45	15.99	0.42	74.7	155.5
329.2	2.69	2.691	296.4	4.25	18.92	0.50	74.4	154.9
331.1	2.68	2.277	295.0	4.27	22.15	0.58	74.2	154.3
334.1	2.81	1.851	294.6	4.44	28.60	0.74	73.9	153.4
336.5	2.70	1.545	294.2	4.64	32.78	0.84	73.7	152.2
339.1	2.74	1.257	295.2	4.71	41.12	1.05	73.4	151.7
342.0	1.96	0.711	293.4	2.13	51.58	1.31	73.1	150.8
343.9	2.72	0.865	295.0	2.08	59.30	1.51	72.9	150.2
346.4	2.61	0.671	295.4	2.01	73.23	1.86	72.6	149.7
348.9	3.30	0.719	297.6	2.16	87.32	2.21	72.4	148.9
352.1	2.72	0.474	294.6	1.24	107.7	2.72	72.0	147.7
355.0	2.88	0.420	298.4	1.68	130.4	3.29	71.7	146.8
358.1	2.60	0.308	295.4	1.23	158.9	4.00	71.4	145.8
360.9	2.62	0.254	296.4	1.02	194.9	4.90	71.1	145.1
364.2	3.12	0.241	295.2	1.00	243.6	6.12	70.7	144.2
366.2	3.51	0.239	295.6	0.99	276.3	6.93	70.5	143.7

Table B. 4. Thermochemical Data at $T = 298.15$ K ($p° = 0.1$ MPa) for reference compounds (in kJ·mol^{-1}).

	$\Delta_f H_m^o(\text{liq})$	$\Delta_l^g H_m^o$	$\Delta_f H_m^o(\text{g})$
benzene	49.0±0.9 [49]	33.9±0.1 [49]	82.9±0.9 [49]
toluene	12.0±1.1 [49]	38.1±0.1 [49]	50.1±1.1 [49]
methoxybenzene	-117.1±1.4 [194]	46.4±0.3[194]	-70.7±1.4[194]

Table B. 5. All results for combustion experiments at $T = 298.15$ K ($p° = 0.1$ MPa) of the methoxy substituted benzenes.

	1,2,3-trimethoxy benzene (cr)	1,2,4-trimethoxy benzene (liq)	3,4,5-trimethoxy toluene (liq)
	28633.2	28640.8	30018.3
	28617.4	28649.1	30020.6
	28631.6	28631.5	30002.9
	28620.0	28640.3	30014.5
	28610.2	28621.4	30025.5
			30034.9
$\Delta_c u°$(cr or liq)/(J·g^{-1})	-28622.5±4.4	-28636.6±4.7	-30019.5±4.4
$\Delta_c H_m^o$(cr or liq)/(kJ·mol^{-1})	-4817.7±1.8	-4820.1±1.9	-5475.0±2.0
$\Delta_f H_m^o$(cr or liq)/(kJ·mol^{-1})	-438.9±2.1	-436.5±2.2	-460.9±2.4

Table B. 6. Experimental and theoretical gas-phase enthalpies of formation $\Delta_f H_m^o$(g) at $T = 298.15$ K ($p° = 0.1$ MPa) for substituted benzenes as calculated by G4 method (in kJ·mol^{-1}).

compound	Exp.[a]	G4		G4	
		AT	calc-exp	AT(corr)[b]	calc-exp
1,2,3-trimethoxybenzene	-346.0±2.0	-355.1	9.1	-351.8	5.8
1,2,4-trimethoxybenzene	-360.6±2.3	-364.0	3.4	-360.7	0.1
1,3,5-trimethoxybenzene	-381.6±3.2	-385.2	3.6	-382.0	0.4
3,4,5-trimethoxytoluene	-383.2±2.5	-386.6	3.4	-383.4	0.2

[a] From Table 15, [b] calculated by the G4 according to the standard atomization procedure [100], [c] results from atomization reactions were corrected with help of following equation: $\Delta_f H_m^o$(g)$_{theor}$/ kJ·mol^{-1} = 1.0023 × $\Delta_f H_m^o$(g, AT) +4.1 with R^2 = 0.9992.

Table B. 7. Experimental and theoretical gas-phase enthalpies of formation $\Delta_f H_m^o$(g) at $T = 298.15$ K ($p° = 0.1$ MPa) for substituted benzenes as calculated by G3MP2 method (in kJ·mol^{-1}).

compound	Exp.[a]	G3MP2		G3MP2	
		AT	calc-exp	AT(corr)[b]	calc-exp
1,2,3-trimethoxybenzene	-346.0±2.0	-356.6	10.6	-350.2	4.2
1,2,4-tr-methoxybenzene	-360.6±2.3	-366.2	5.6	-359.8	-0.8
1,3,5-trimethoxybenzene	-381.6±3.2	-387.3	5.7	-381.1	-0.5
3,4,5-trimethoxytoluene	-383.2±2.5	-388.5	5.3	-382.3	-0.9

[a] From Table 15, [b] calculated by the G3MP2 according to the standard atomization procedure [195], [c] results from atomization reactions were corrected with help of following equation: $\Delta_f H_m^o$(g)$_{theor}$/ kJ·mol^{-1} = 1.0064 × $\Delta_f H_m^o$(g, AT) +8.7 with R^2 = 0.9993.

Table B. 8. Experimental and theoretical gas-phase enthalpies of formation $\Delta_f H_m^o$(g) at $T = 298.15$ K ($p° = 0.1$ MPa) for substituted benzenes as calculated by G4MP2 method (in kJ·mol^{-1}).

compound	Exp.[a]	M06/QZ4P		M06/QZ4P	
		AT	calc-exp	AT(corr)[b]	calc-exp
1,2,3-trimethoxybenzene	-346.0±2.0	-359.8	13.8	-348.3	2.3
1,2,4-trimethoxybenzene	-360.6±2.3	-370.3	9.7	-358.5	-2.1
1,3,5-trimethoxybenzene	-381.6±3.2	-393.9	12.3	-381.5	-0.1

[a] From Table 15, [b] calculated by the M06/QZ4P according to the standard atomization procedure [196], [c] results from atomization reactions were corrected with help of following equation: $\Delta_f H_m^o$(g)$_{theor}$/ kJ·mol^{-1} = 0.9739 × $\Delta_f H_m^o$(g, AT) +2.1 with R^2 = 0.9992
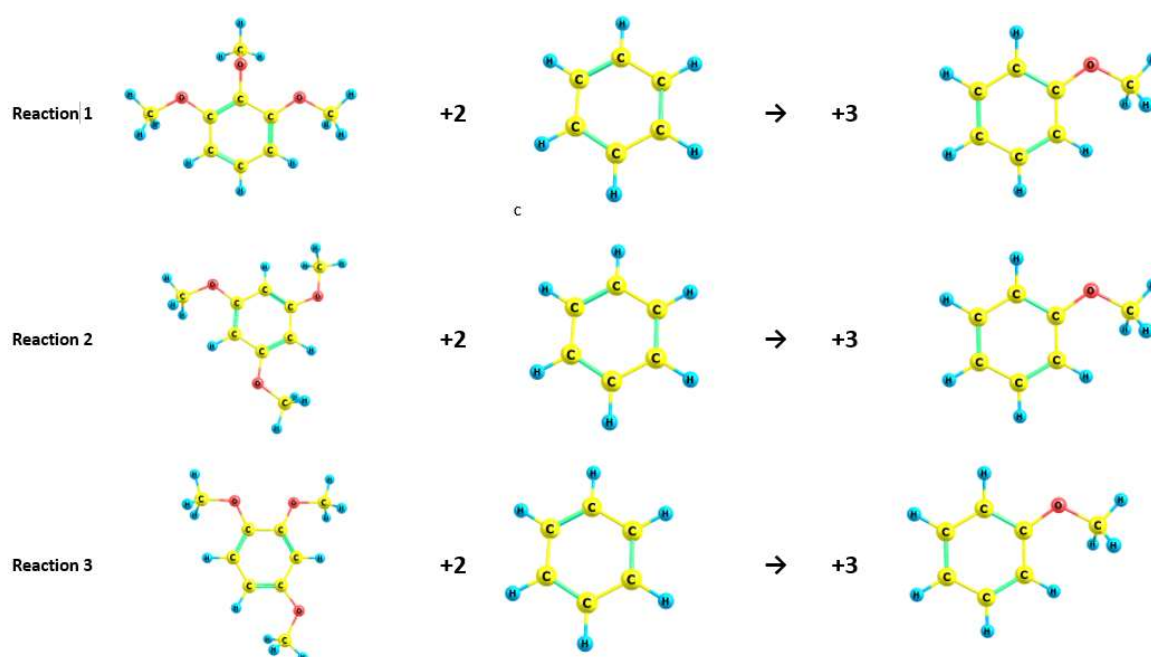
Figure B. 1. Well-balanced reactions for trimethoxybenzenes.
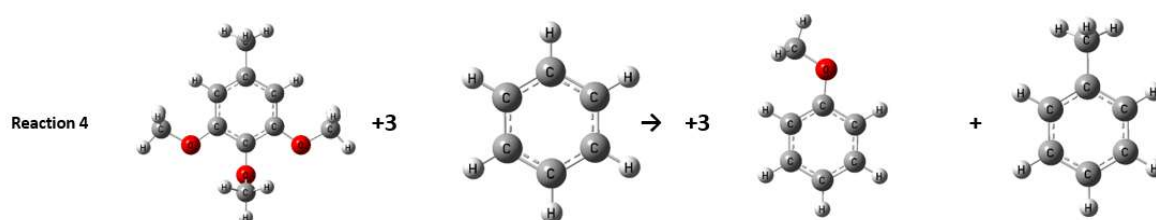
Figure B. 2. Well-balanced reaction for 3,4,5-trimethoxytoluene.

Table B. 9. Standard molar enthalpy of formation 1,2,3-trimethoxybenzene, $\Delta_f H_m^o(g)$, kJ·mol^{-1}, reaction R1.

Method	$\Delta_f H_m^o(g)$ (AT)	$\Delta_f H_m^o(g)$ Reaction R1	$\Delta_r H_m^o(g)$ Reaction enthalpy R1
G4	-355.1	-352.2	-25.7
G3MP2	-356.6	-351.5	-26.4
M06/QZ4P	-359.8	-349.3	-28.6

Table B. 10. Standard molar enthalpy of formation 1,2,4-trimethoxybenzene, $\Delta_f H_m^o(g)$, kJ·mol^{-1}, reaction R2.

Method	$\Delta_f H_m^o(g)$ (AT)	$\Delta_f H_m^o(g)$ Reaction R2	$\Delta_r H_m^o(g)$ Reaction enthalpy R2
G4	-364.0	-361.0	-16.9
G3MP2	-366.2	-361.1	-16.8
M06/QZ4P	-371.3	-360.8	-17.1

Table B. 11. Standard molar enthalpy of formation 1,3,5-trimethoxybenzene, $\Delta_f H_m^o(g)$, kJ·mol^{-1}, reaction R3.

Method	$\Delta_f H_m^o(g)$ (AT)	$\Delta_f H_m^o(g)$ Reaction R3	$\Delta_r H_m^o(g)$ Reaction enthalpy R3
G4	-385.2	-382.3	4.4
G3MP2	-387.3	-382.2	4.3
M06/QZ4P	-393.9	-383.4	5.5

Table B. 12. Standard molar enthalpy of formation 3,4,5-trimethoxytoluene, $\Delta_f H_m^o(g)$, kJ·mol^{-1}, reaction R4.

Method	$\Delta_f H_m^o(g)$ (AT)	$\Delta_f H_m^o(g)$ Reaction R4	$\Delta_r H_m^o(g)$ Reaction enthalpy R4
G4	-386.6	-381.8	-27.7
G3MP2	-388.5	-381.2	-27.4
G4MP2	-381.6	-382.1	-28.3

Table B. 13. Parameters for the development of "theoretical framework" substituents on the "centerpieces" for calculation of $\Delta_f H_m^o(g)$ of substituted benzene derivatives at 298.15 K (in kJ·mol^{-1}).

Centerpiece molecules	$\Delta_f H_m^o(g)$	$\Delta H(H \rightarrow R)$
benzene	82.9±0.9	
toluene	50.1±1.1	**-32.8**
methoxybenzene	-70.7±1.4	**-153.6**
"theoretical framework"	$\Delta_f H_m^o(g)$	Summation:
dimethoxy-benzene	***-224.3***	82.9 + (-153.6)×2
trimethoxybenzene	***-377.9***	82.9 + (-153.6)×3
trimethoxy-toluene	***-410.7***	82.9 + (-153.6)×+(-32.8)
methoxy toluene	***-103.5***	82.9 + (-153.6) + (-32.8)

Table B. 14. Parameters for pairwise nearest and non-nearest neighbour interactions of substituents on the "centerpieces" for calculation of $\Delta_f H_m^o(g)$ of substituted benzenes at 298.15 K (in kJ·mol^{-1}).

Compounds	$\Delta_f H_m^o(g)$		Pairwise interactions
			CH_3O - CH_3O
1,2-dimethoxybenzene	-210.0±2.4	(-210.0+***224.3***)	14.3
1,3-dimethoxybenzene	-224.8±2.6	(-224.8+***224.3***)	-0.5
1,4-dimethoxybenzene	-216.9±2.4	(-216.8+***224.3***)	7.4
			CH_3O - CH_3
2-methoxytoluene	-106.6±1.6	(-106.6+***103.5***)	-3.1
3-methoxytoluene	-102.6±5.0	(-102.6+***103.5***)	0.9
4-methoxytoluene	-99.0±2.0	(-99.0+***103.5***)	4.5

Table B. 15. Analysis of the total amount of pairwise nearest and non-nearest neighbour interactions of substituents on the "centerpieces" in terms of $\Delta_f H_m^o(g)$ for trimethoxy substituted benzenes at 298.15 K (in kJ·mol^{-1}).

Compound	$\Delta_f H_m^o(g)$	Actual amount of interactions	Theoretical amount of interactions	Δ^c
1	2	3	4	5
1,2,3-trimethoxybenzene	-350.6±2.4	(-350.6+377.9) = 27.3	28.1	-0.8
1,2,4-trimethoxybenzene	-360.3±1.6	(-360.3+377.9) = 17.6	21.2	-3.6
1,3,5-trimethoxybenzene	-382.1±1.2	(-382.1+377.9) = -4.2	-1.5	-2.7
3,4,5-trimethoxytoluene	-382.1±1.2	(-382.1+377.9) = 28.6	34.4	-5.8

Table B. 16. Parameters for the development of "theoretical framework" substituents on the "centerpieces" for calculation of $\Delta_l^g H_m^o$ of substituted benzenes at 298.15 K (in kJ·mol^{-1}).

Centerpiece molecules	$\Delta_l^g H_m^o$	$\Delta H(H{\rightarrow}R)$
benzene	33.9±0.1	
toluene	38.1±0.1	**4.2**
methoxybenzene	46.4±0.3	**12.5**
"theoretical framework"	$\Delta_l^g H_m^o$	Summation:
dimethoxy-benzene	**58.9**	33.9 + (12.5)×2
trimethoxybenzene	**71.4**	33.9 + (12.5)×3
trimethoxy-toluene	**75.6**	33.9 + (12.5)×3 + (4.2)
methoxy toluene	**50.6**	33.9 + (12.5) + (4.2)

Table B. 17. Parameters of pairwise nearest and non-nearest neighbour interactions of substituents on the "centerpieces" for calculation of $\Delta_l^g H_m^o$ of substituted benzenes at 298.15 K (in kJ·mol^{-1}).

	$\Delta_l^g H_m^o$		Pairwise interactions
			CH₃O - CH₃O
1,2-dimethoxybenzene	64.5±0.3	(64.5 - **58.9**)	5.6
1,3-dimethoxybenzene	59.7±0.2	(59.7 - **58.9**)	0.8
1,4-dimethoxybenzene	61.6±0.2	(61.6 - **58.9**)	2.7
			CH₃O - CH₃
2-methoxytoluene	50.2±0.4	(50.2 - **50.6**)	-0.4
3-methoxytoluene	52.8±0.5	(52.8 - **50.6**)	2.2
4-methoxytoluene	53.3±0.4	(53.3 - **50.6**)	2.7

Table B. 18. Analysis of the total amount of pairwise nearest and non-nearest neighbour interactions of substituents on the "centerpieces" in terms of $\Delta_l^g H_m^o$ for trimethoxy substituted benzenes at 298.15 K (in kJ·mol^{-1}).

Compound	$\Delta_l^g H_m^o$	Actual amount of interactions	Theoretical amount of interactions	Δ
1	2	3	4	5
1,2,3-trimethoxybenzene	73.0±0.5	(73.0 - **71.4**) = 1.6	12.0	-10.4
1,2,4-trimethoxybenzene	75.7±0.5	(75.7 - **71.4**) = 4.5	9.1	-4.6
1,3,5-trimethoxybenzene	68.7±0.4	(68.7 - **71.4**) = -2.7	2.4	-5.1
3,4,5-trimethoxytoluene	77.7±0.5	(77.7 - **75.6**) = 2.1	19.1	-17.0

C. Supporting information to Chapter 3

Table C. 1. Heat capacity of 1,3-dimethoxy-2-propanol.

T, K	$C_{\mathrm{p}}^{\mathrm{o}}{}_{\mathrm{m}}$, J·K^{-1}·mol^{-1}	T, K	$C_{\mathrm{p}}^{\mathrm{o}}{}_{\mathrm{m}}$, J·K^{-1}·mol^{-1}	T, K	$C_{\mathrm{p}}^{\mathrm{o}}{}_{\mathrm{m}}$, J·K^{-1}·mol^{-1}	T, K	$C_{\mathrm{p}}^{\mathrm{o}}{}_{\mathrm{m}}$, J·K^{-1}·mol^{-1}
232.1	246.6	254.1	253.9	277.1	261.4	300.1	270.1
233.1	247.0	255.1	254.3	278.1	261.9	301.1	270.4
234.1	247.4	256.1	254.6	279.1	262.3	302.1	270.9
235.1	247.7	257.1	254.8	280.1	262.7	303.1	271.2
236.1	248.1	258.1	255.2	281.1	263.0	304.1	271.6
237.1	248.4	259.1	255.6	282.1	263.4	305.1	271.9
238.1	248.7	260.1	255.9	283.1	263.8	306.1	272.3
239.1	248.9	261.1	256.2	284.1	264.2	307.1	272.7
240.1	249.3	262.1	256.5	285.1	264.5	308.1	273.1
241.1	249.6	263.1	256.8	286.1	264.9	309.1	273.5
242.1	250.0	264.1	257.1	287.1	265.3	310.1	273.8
243.1	250.2	265.1	257.6	288.1	265.6	311.1	274.1
244.1	250.5	266.1	257.8	289.1	265.9	312.1	274.4
245.1	250.9	267.1	258.2	290.1	266.3	313.1	274.8
246.1	251.1	268.1	258.5	291.1	266.8	314.1	275.2
247.1	251.5	269.1	258.9	292.1	267.2	315.1	275.5
248.1	251.9	270.1	259.3	293.1	267.5	316.1	275.9
249.1	252.2	271.1	260.1	294.1	267.9	317.1	276.2
250.1	252.6	272.1	259.7	295.1	268.2	318.1	276.7
251.1	252.9	273.1	260.3	296.1	267.8	319.1	277.0
252.1	253.3	274.1	260.4	297.1	269.0	320.1	277.3
253.1	253.6	275.1	260.7	298.1	269.4		
		276.1	261.0	299.1	269.7		

Table C. 2. Heat capacity of 1,3-diethoxy-2-propanol.

T, K	$C_{p}{}^{o}{}_{m}$, J·K^{-1}·mol^{-1}	T, K	$C_{p}{}^{o}{}_{m}$, J·K^{-1}·mol^{-1}	T, K	$C_{p}{}^{o}{}_{m}$, J·K^{-1}·mol^{-1}	T, K	$C_{p}{}^{o}{}_{m}$, J·K^{-1}·mol^{-1}
232.6	323.7	254.6	331.9	276.6	340.6	298.6	349.2
233.6	324.0	255.6	332.3	277.6	341.1	299.6	349.7
234.6	324.3	256.6	332.7	278.6	341.6	300.6	349.8
235.6	324.7	257.6	332.9	279.6	341.9	301.6	350.2
236.6	325.1	258.6	333.3	280.6	342.4	302.6	350.7
237.6	325.5	259.6	333.8	281.6	343.0	303.6	351.1
238.6	325.9	260.6	334.1	282.6	343.5	304.6	351.4
239.6	326.2	261.6	334.5	283.6	343.8	305.6	351.8
240.6	326.6	262.6	335.0	284.6	344.3	306.6	352.2
241.6	327.0	263.6	335.3	285.6	345.1	307.6	352.6
242.6	327.3	264.6	335.8	286.6	345.2	308.6	353.0
243.6	327.7	265.6	336.1	287.6	345.4	309.6	353.4
244.6	328.1	266.6	336.5	288.6	345.9	310.6	353.8
245.6	328.4	267.6	337.1	289.6	346.3	311.6	354.3
246.6	328.8	268.6	337.4	290.6	346.6	312.6	354.8
247.6	329.2	269.6	337.9	291.6	347.0	313.6	355.2
248.6	329.6	270.6	338.3	292.6	347.5	314.6	355.6
249.6	330.1	271.6	339.2	293.6	347.8	315.6	356.1
250.6	330.4	272.6	339.1	294.6	348.2	316.6	356.7
251.6	330.8	273.6	339.4	295.6	348.2	317.6	357.2
252.6	331.1	274.6	339.7	296.6	347.1	318.6	357.6
253.6	331.5	275.6	340.4	297.6	348.9	319.6	358.3

Table C. 3. Heat capacity of 1,3-bis-2, 2, 2-trifluoroethoxy-2-propanol.

T. K	$C_p{}^\circ{}_m$. J·K^{-1}·mol^{-1}	T. K	$C_p{}^\circ{}_m$. J·K^{-1}·mol^{-1}	T. K	$C_p{}^\circ{}_m$. J·K^{-1}·mol^{-1}	T. K	$C_p{}^\circ{}_m$. J·K^{-1}·mol^{-1}
235.4	407.03	265.1	419.54	295.2	432.12	325.1	442.98
235.9	407.15	266.1	419.96	296.2	432.52	326.2	443.62
236.9	407.58	267.1	420.37	297.2	432.89	327.2	444.02
237.9	407.98	268.1	420.83	298.2	433.31	328.2	444.32
238.9	408.43	269.1	421.31	299.2	433.74	329.2	444.79
239.9	408.86	270.1	421.77	300.1	434.05	330.2	445.11
240.9	409.48	271.1	422.16	301.2	434.77	331.2	445.55
241.9	409.70	272.1	422.63	302.2	434.60	332.2	445.83
242.9	410.09	273.1	423.08	303.2	434.41	333.2	446.15
243.9	410.50	274.1	423.49	304.2	434.66	334.2	446.56
244.9	410.92	275.1	423.94	305.2	434.96	335.2	446.97
246.1	411.42	276.1	424.36	306.2	435.37	336.2	447.18
247.1	411.81	277.1	424.76	307.2	435.76	337.2	447.52
248.1	412.38	278.1	425.29	308.2	436.14	338.2	447.98
249.1	412.88	279.1	425.68	309.3	435.44	339.2	448.26
250.1	413.38	280.1	426.10	310.2	437.46	340.2	448.52
251.1	413.73	281.1	426.47	311.2	437.78	341.2	448.98
252.1	414.10	282.2	426.75	312.2	438.16	342.2	449.35
253.1	414.49	283.2	426.71	313.2	438.52	343.2	449.65
254.1	414.92	284.2	427.66	314.2	438.92	344.2	449.95
255.1	415.29	285.2	428.28	315.2	439.28	345.2	450.11
256.1	415.68	286.2	428.67	316.2	439.63	346.2	450.60
257.1	416.09	287.2	428.89	317.2	440.02	347.2	450.81
258.1	416.50	288.2	429.30	318.2	440.53	348.2	451.09
259.1	416.87	289.2	429.71	319.2	440.80	349.2	451.42
260.1	417.47	290.2	430.11	320.2	441.09	350.0	451.90
261.1	417.80	291.2	430.49	321.2	441.42		
262.1	418.20	292.2	430.91	322.2	441.84		
263.1	418.60	293.2	431.34	323.2	442.19		
264.1	419.13	294.2	431.75	324.2	442.48		

Table C. 4. Heat capacity of 1,3-diisopropoxy-2-propanol.

T, K	$C_{p}^{o}{}_{m}$, J·K^{-1}·mol^{-1}	T, K	$C_{p}^{o}{}_{m}$, J·K^{-1}·mol^{-1}	T, K	$C_{p}^{o}{}_{m}$, J·K^{-1}·mol^{-1}	T, K	$C_{p}^{o}{}_{m}$, J·K^{-1}·mol^{-1}
314.0	412.4	330.0	420.4	346.0	427.4	362.0	434.6
315.0	412.8	331.0	420.8	347.0	428.0	363.0	435.1
316.0	413.4	332.0	421.2	348.0	428.4	364.0	435.4
317.0	413.9	333.0	421.7	349.0	428.9	365.0	435.8
318.0	414.5	334.0	422.1	350.0	429.3	366.0	436.2
319.0	415.1	335.0	422.5	351.0	429.6	367.0	436.5
320.0	415.6	336.0	422.7	352.0	430.1	368.0	436.9
321.0	416.1	337.0	423.2	353.0	430.7	369.0	437.4
322.0	416.6	338.0	423.8	354.0	431.2	370.0	437.7
323.0	417.2	339.0	424.4	355.0	431.7	371.0	438.1
324.0	417.7	340.0	424.8	356.0	432.1	372.0	438.5
325.0	418.2	341.0	425.3	357.0	432.5	373.0	438.8
326.0	418.6	342.0	425.7	358.0	432.9	374.0	439.1
327.0	418.9	343.0	426.1	359.0	433.4	375.0	439.5
328.0	419.3	344.0	426.4	360.0	433.8	376.0	439.9
329.0	419.8	345.0	426.8	361.0	434.2	377.0	440.2

Table C. 5. Heat capacity of 2, 5, 9, 12-tetraocatridecan-7-ol.

T, K	$C_{p}^{o}{}_{m}$, J·K^{-1}·mol^{-1}	T, K	$C_{p}^{o}{}_{m}$, J·K^{-1}·mol^{-1}	T, K	$C_{p}^{o}{}_{m}$, J·K^{-1}·mol^{-1}	T, K	$C_{p}^{o}{}_{m}$, J·K^{-1}·mol^{-1}
312.0	462.5	333.0	470.1	354.0	478.5	375.0	488.0
313.0	462.9	334.0	470.5	355.0	479.0	376.0	488.7
314.0	463.2	335.0	471.1	356.0	479.4		
315.0	463.5	336.0	471.7	357.0	479.9		
316.0	463.9	337.0	472.0	358.0	480.3		
317.0	464.2	338.0	472.4	359.0	480.7		
318.0	464.5	339.0	472.9	360.0	481.3		
319.0	464.9	340.0	473.2	361.0	481.7		
320.0	465.3	341.0	473.5	362.0	482.1		
321.0	465.5	342.0	473.9	363.0	482.6		
322.0	465.9	343.0	474.4	364.0	483.0		
323.0	466.2	344.0	474.8	365.0	483.6		
324.0	466.6	345.0	475.1	366.0	484.0		
325.0	467.0	346.0	475.5	367.0	484.5		
326.0	467.4	347.0	475.8	368.0	484.8		
327.0	468.2	348.0	476.3	369.0	485.3		
328.0	468.4	349.0	476.6	370.0	486.0		
329.0	468.6	350.0	477.1	371.0	486.4		
330.0	469.0	351.0	477.6	372.0	486.8		
331.0	469.4	352.0	477.9	373.0	487.3		
332.0	469.8	353.0	478.2	374.0	487.6		

Table C. 6. Results from the transpiration method: absolute vapour pressures p_i, standard molar vaporization enthalpies $\Delta_l^g H_m^o$ and standard molar vaporization entropies $\Delta_l^g S_m^o$.

$T/$ K[a]	$m/$ mg[b]	$V(N_2)^c/$ dm^3	$T_a/$ K[d]	Flow/ dm$^3\cdot$h^{-1}	$p_i/$ Pa[e]	$u(p_i)/$ Pa[f]	$\Delta_l^g H_m^o(T)/$ kJ$\cdot$mol^{-1}	$\Delta_l^g S_m^o(T)/$ J$\cdot$K$^{-1}\cdot$mol^{-1}
1,3-dimethoxy-2-propanol: $\Delta_l^g H_m^o$(298.15 K) = (58.0 ± 0.5) kJ·mol^{-1}								
$\ln(p_i/p_{ref}) = \frac{313.3}{R} - \frac{82031.4}{RT} - \frac{80.6}{R}\ln\frac{T}{298.15}$; p_{ref}= 1 Pa								
277.7	0.90	1.086	297.5	1.63	17.48	0.46	59.7	142.9
282.6	0.88	0.679	298.1	1.63	27.18	0.70	59.3	141.4
288.0	0.86	0.407	298.1	1.63	44.15	1.13	58.8	140.0
293.4	5.09	1.524	296.7	3.05	68.98	1.75	58.4	138.5
295.6	4.60	1.179	297.4	3.54	80.72	2.04	58.2	137.7
301.2	2.82	0.482	296.7	0.96	120.61	3.04	57.8	135.9
302.8	4.94	0.742	297.2	0.99	137.27	3.46	57.6	135.6
307.8	4.45	0.450	296.8	0.96	203.36	5.11	57.2	134.4
308.6	5.88	0.562	297.9	0.96	215.39	5.41	57.2	134.2
310.2	5.48	0.478	295.9	0.99	234.71	5.89	57.0	133.5
314.4	5.12	0.321	297.0	0.96	327.15	8.20	56.7	132.7
315.3	5.37	0.321	297.3	0.96	343.40	8.61	56.6	132.4
321.2	6.65	0.257	297.3	0.96	530.04	13.28	56.1	131.2
328.7	11.09	0.257	297.5	0.96	881.06	22.05	55.5	129.6
1,3-diethoxy-2-propanol: $\Delta_l^g H_m^o$(298.15 K) = (61.8 ± 0.4) kJ·mol^{-1}								
$\ln(p_i/p_{ref}) = \frac{339.6}{R} - \frac{92041.6}{RT} - \frac{101.4}{R}\ln\frac{T}{298.15}$; p_{ref}= 1 Pa								
278.4	1.55	3.807	295.5	2.86	6.92	0.20	63.8	149.5
283.2	1.62	2.474	295.6	2.86	11.04	0.30	63.3	147.9
288.3	1.43	1.380	295.8	2.86	17.36	0.46	62.8	145.9
291.0	1.67	1.296	299.8	2.88	21.88	0.57	62.5	144.9
293.5	0.84	0.501	298.0	1.00	28.02	0.73	62.3	144.2
298.5	1.90	0.749	291.7	1.05	41.55	1.06	61.8	142.2
299.4	1.63	0.621	295.7	1.55	43.75	1.12	61.7	141.7
300.7	1.62	0.551	298.0	1.00	49.40	1.26	61.6	141.4
305.0	1.32	0.313	292.7	1.07	69.59	1.76	61.1	139.9
307.7	2.59	0.501	298.0	1.00	86.62	2.19	60.8	139.1
314.3	3.46	0.393	297.1	1.07	146.54	3.69	60.2	137.2
314.4	2.96	0.340	293.8	1.07	143.45	3.61	60.2	136.9
314.6	2.17	0.251	298.1	1.00	144.59	3.64	60.1	136.8
320.6	3.95	0.286	294.7	1.07	228.12	5.73	59.5	135.1
321.3	4.01	0.276	298.2	1.00	242.74	6.09	59.5	135.0
327.4	6.21	0.286	296.2	1.07	359.35	9.01	58.8	132.9
328.4	6.20	0.267	298.4	1.00	386.96	9.70	58.7	132.7
335.0	9.71	0.267	298.6	1.00	605.56	15.16	58.1	130.9
1,3-di-isopropoxy-2-propanol: $\Delta_l^g H_m^o$(298.15 K) = (66.7 ± 0.3) kJ·mol^{-1}								
$\ln(p_i/p_{ref}) = \frac{362.2}{R} - \frac{101321.9}{RT} - \frac{116.2}{R}\ln\frac{T}{298.15}$; p_{ref}= 1 Pa								
281.8	0.94	3.336	296.4	3.03	3.97	0.10	68.58	159.1
286.9	1.15	2.528	295.4	3.03	6.40	0.18	67.99	156.7
291.0	1.22	1.820	293.9	3.03	9.33	0.26	67.51	154.9
297.8	1.19	0.897	295.7	2.99	18.52	0.49	66.72	152.6
298.7	1.16	0.819	295.4	1.82	19.85	0.52	66.61	152.1
299.6	1.33	0.848	295.3	2.99	21.92	0.57	66.50	151.9
304.5	1.21	0.518	295.3	1.55	32.57	0.84	65.94	149.8
304.5	1.21	0.513	294.9	1.06	32.86	0.85	65.93	149.8
304.6	0.81	0.342	298.6	1.08	33.37	0.86	65.93	149.9
306.5	1.29	0.455	294.5	0.97	39.53	1.01	65.71	149.2
310.4	1.14	0.301	295.7	1.06	53.04	1.35	65.26	147.5

313.4	1.12	0.227	295.2	0.97	68.34	1.73	64.91	146.6
314.3	1.87	0.360	299.8	1.08	73.24	1.86	64.80	146.2
320.3	1.98	0.244	295.5	0.97	113.22	2.86	64.11	143.8
321.0	3.20	0.360	299.8	1.08	125.35	3.16	64.02	143.8
327.0	3.58	0.270	298.1	1.08	185.74	4.67	63.32	141.4
327.1	3.38	0.244	295.7	0.97	193.11	4.85	63.31	141.6
333.8	5.93	0.270	298.2	1.08	307.78	7.72	62.53	139.3
334.1	5.59	0.244	296.1	0.97	319.47	8.01	62.50	139.3

2,5,9,12-tetraoxatridecan-7-ol: $\Delta_l^g H_m^o$(298.15 K) = (85.8 ± 0.4) kJ·mol^{-1}

$$\ln(p_i /p_{ref}) = \frac{394.9}{R} - \frac{124276.1}{RT} - \frac{129.2}{R}\ln\frac{T}{298.15}; p_{ref} = 1 \text{ Pa}$$

318.0	0.37	7.109	296.5	3.09	0.61	0.02	83.2	161.7
326.0	0.46	4.224	296.8	3.09	1.29	0.04	82.2	158.5
332.9	0.45	2.267	297.1	3.09	2.37	0.06	81.3	155.6
334.7	0.44	1.855	296.4	3.09	2.78	0.07	81.0	154.9
339.9	0.47	1.236	297.6	3.09	4.49	0.12	80.4	153.2
346.9	0.50	0.773	297.2	3.09	7.70	0.22	79.5	150.3
355.6	0.74	0.583	296.1	1.09	15.06	0.40	78.3	147.1
362.6	0.88	0.419	296.2	1.09	24.89	0.65	77.4	144.5
367.6	1.00	0.328	296.2	1.09	36.05	0.93	76.8	142.9
371.6	1.26	0.310	296.3	1.09	47.91	1.22	76.3	141.7

1,3-bis-(2,2,2-trifluoroethoxy)-2-propanol: $\Delta_l^g H_m^o$(298.15 K) = (71.6 ± 0.3) kJ·mol^{-1}

$$\ln(p_i /p_{ref}) = \frac{384.1}{R} - \frac{108344.3}{RT} - \frac{123.1}{R}\ln\frac{T}{298.15}; p_{ref} = 1 \text{ Pa}$$

278.5	0.62	3.964	295.9	2.97	1.52	0.04	74.06	173.7
284.0	0.77	2.626	295.9	2.97	2.82	0.08	73.38	171.3
291.4	0.77	1.189	296.2	2.97	6.27	0.18	72.48	168.3
293.8	0.37	0.450	295.0	1.08	7.83	0.22	72.17	167.0
294.6	2.86	3.256	294.3	2.96	8.41	0.24	72.08	166.6
298.6	0.78	0.587	296.2	1.76	12.83	0.35	71.59	165.3
300.2	0.67	0.432	294.4	1.08	14.84	0.40	71.39	164.5
303.1	2.86	1.431	295.7	2.96	19.20	0.51	71.04	163.2
307.5	1.38	0.450	294.7	1.08	29.28	0.76	70.49	161.6
314.6	2.56	0.450	295.7	1.08	54.63	1.39	69.61	158.8
321.6	2.69	0.270	295.5	1.08	95.49	2.41	68.75	156.0
328.4	4.42	0.261	295.3	1.08	161.85	4.07	67.91	153.3

Table C. 7. Absolute vapor pressures p, standard (p^o = 0.1 MPa) molar vaporization enthalpies, $\Delta_l^g H_m^o$, and standard (p^o = 0.1 MPa) molar vaporization entropies, $\Delta_l^g S_m^o$ obtained by the static method.

T^{a}/ K	p/ Pa	$u(p)^{b}$ / Pa	$\Delta_l^g H_m^o(T)^{c}$ / kJ·mol^{-1}		$\Delta_l^g S_m^o(T)$ / J·K^{-1}·mol^{-1}

1,3-diethoxy-propane-2-ol $\Delta_l^g H_m^o$(298.15 K) = (61.4±0.2) kJ·mol^{-1}

$$\ln (p/p_{ref}) = \frac{338.4}{R} - \frac{91642.5}{RT} - \frac{101.4}{R}\ln\frac{T}{298.15} ; p_{ref} = 1 \text{ Pa}$$

T/K	p/Pa	$u(p)$/Pa	ΔH		ΔS
278.4	6.96	7.0	-0.05	63.41	148.2
278.4	6.94	6.9	-0.07	63.41	148.2
280.8	8.77	8.8	-0.07	63.17	147.3
280.8	8.79	8.8	-0.05	63.17	147.3
283.2	11.08	11.1	-0.02	62.93	146.5
285.7	14.00	14.0	0.00	62.68	145.6
285.7	13.94	13.9	-0.06	62.68	145.6
288.1	17.45	17.5	-0.02	62.43	144.8
290.5	21.71	21.7	-0.01	62.19	143.9
290.5	21.80	21.8	0.06	62.18	144.0
293.0	26.93	26.9	-0.02	61.94	143.1

295.4	33.26	33.3	0.09	61.69	142.3
295.4	33.20	33.2	0.03	61.69	142.3
297.8	40.92	40.9	0.18	61.44	141.4
300.3	50.14	50.1	0.32	61.20	140.6
300.3	49.91	49.9	0.01	61.19	140.6
302.7	60.91	60.9	0.33	60.95	139.8
305.1	73.84	73.8	0.51	60.71	139.0
305.1	73.66	73.7	0.27	60.71	139.0
307.6	89.38	89.4	0.48	60.45	138.2
310.0	107.73	107.7	0.85	60.21	137.4
310.0	107.41	107.4	0.45	60.21	137.4
313.2	136.06	136.1	0.76	59.89	136.4
313.2	135.72	135.7	0.42	59.89	136.3
315.6	162.30	162.3	0.95	59.64	135.6
315.6	161.73	161.7	0.38	59.64	135.6
318.0	193.06	193.1	1.04	59.40	134.8
318.0	192.42	192.4	0.13	59.39	134.8
320.5	228.53	228.5	0.62	59.15	134.0
320.5	228.14	228.1	0.07	59.15	134.0
322.9	270.61	270.6	0.99	58.90	133.2
322.9	270.28	270.3	0.48	58.90	133.2
325.3	316.82	316.8	-0.06	58.66	132.5
325.4	317.09	317.1	-0.42	58.65	132.4
327.8	373.72	373.7	0.96	58.41	131.7
327.8	372.38	372.4	-0.62	58.40	131.7
330.2	436.10	436.1	-0.19	58.16	130.9
330.2	437.13	437.1	0.28	58.16	130.9
332.6	508.95	509.0	0.45	57.91	130.2
332.6	508.04	508.0	-1.10	57.91	130.2
335.1	591.98	592.0	-0.46	57.67	129.5
335.1	590.52	590.5	-2.66	57.66	129.4
337.5	686.62	686.6	-0.40	57.42	128.7
337.5	685.39	685.4	-2.88	57.42	128.7
339.9	792.69	792.7	-2.31	57.17	128.0
339.9	791.68	791.7	-3.79	57.17	128.0
342.3	913.53	913.5	-2.87	56.93	127.3
342.4	912.54	912.5	-6.01	56.93	127.2
344.8	1051.21	1051.2	-4.82	56.68	126.5
344.8	1048.43	1048.4	-8.82	56.68	126.5
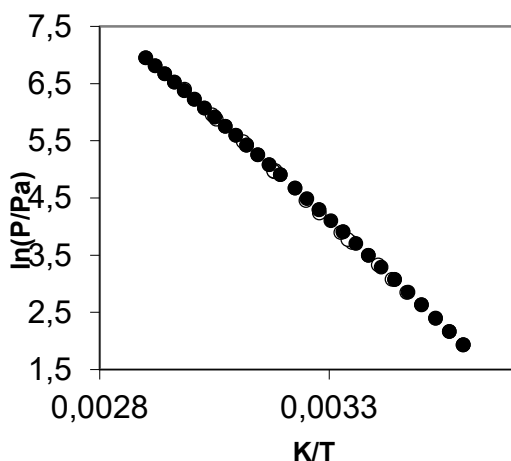
Figure C. 1. Temperature dependence of vapor pressures for 1,3-di-ethoxy-2-propanol: ○ – transpiration, this work; ● – static method, this work.
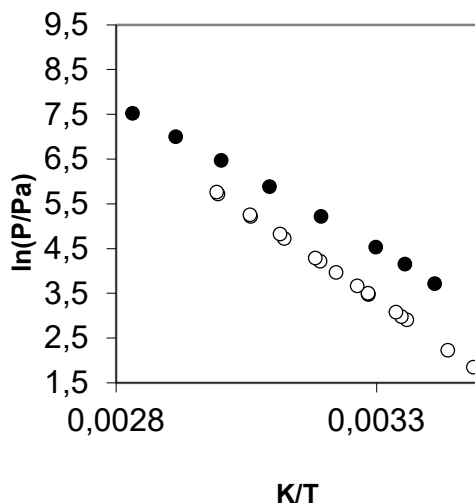
Figure C. 2. Temperature dependence of vapor pressures for 1,3-di-isopropoxy-2-propanol: ○ – this work; ● – static method [86].
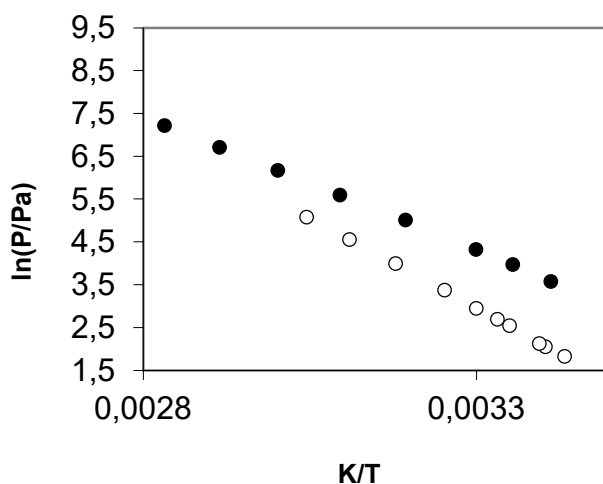
Figure C. 3. Temperature dependence of vapor pressures for 1,3-bis(2,2,2-trifluoroethoxy)-2-propanol: ○ – this work; ● – static method [86].

Table C. 8. Compilation of experimental vaporization enthalpies, $\Delta_l^g H_m^o$(298.15 K), from the literature used in the research.

CAS	Compound	Name	$\Delta_l^g H_{m(exp)}^o$	Ref.
109-86-4	CH_3-O-CH_2CH_2-OH	2-methoxyethanol	45.2±0.2	[91]
110-80-5	CH_3-CH_2-O-CH_2CH_2-OH	2-ethoxyethanol	48.2±0.2	[91]
109-59-1	$(CH_3)_2$CH-O-CH_2CH_2-OH	2-isopropoxyethanol	50.1±0.1	[91]
111-76-2	CH_3-$(CH_2)_3$-O-CH_2CH_2-OH	2-n-butoxyethanol	56.1±0.2	[91]
7580-85-0	$(CH_3)_2$CH-O-CH_2CH_2-OH	2-tertbutoxyethanol	52.8±0.6	[91]
111-77-3	CH_3-O-CH_2CH_2-O-CH_2-CH_2-OH	3,6-dioxa-1-heptanol	52.8±0.6[a]	[197]
75-89-8	CF_3CH_2-OH	2,2,2-trifluoroethanol	44.0±0.5	[198]
374-01-6	$CF_3CH(CH_3)$-OH	1,1,1-trifluoro-2-propanol	44.8±0.5	[198]
76-37-9	CHF_2-CF_2CH_2-OH	2,2,3,3-tetrafluoro-1-propanol	53.6±0.5	[198]
422-05-9	CF_3-CF_2CH_2-OH	2,2,3,3,3-pentafluoro-1-propanol	44.4±0.5	[198]
333-36-8	CF_3-CH_2-O- CH_2-CF_3	2,2,2-trifluoroethyl ether	35.2±0.2	[199]

Table C. 9. Compilation of available vaporization enthalpies $\Delta_l^g H_m^o$ of auxiliary compounds.

Compound	Method[a]	T- range	$\Delta_l^g H_m^o(T_{av})$	$\Delta_l^g H_m^o$(298.15 K)[b]	Ref.
		K	kJ·mol^{-1}	kJ·mol^{-1}	
3,6-dioxa-1-heptanol	Ebulliometry	385.5-466.2	51.3±0.3	61.2±0.6	[197]
bis(2,2,2-trifluoroethyl) ether	Static	283.2-336.9	34.5±0.1	35.2±0.2	[199]

Table C. 10. Correlation of vaporization enthalpies, $\Delta_l^g H_m^o$(298.15 K), of alkoxyethanols with their T_b normal boiling points.

R-O-CH$_2$-CH$_2$-OH	T_b[a]	$\Delta_l^g H_{m(exp)}^o$[b]	$\Delta_l^g H_{m(calc)}^o$[c]	Δ
Me	397.2	45.2	45.4	-0.2
Et	408.8	48.2	48.1	0.1
iPr	417.6	50.1	50.2	-0.1
Bu	441.5	56.6	55.8	0.8
tBu	428.1	52.8	52.7	0.1
CH$_3$OCH$_2$	466.1	61.2	61.6	-0.4

[a] Boiling pints, T_b, [48], [b] data from Table C. 7, [c] calculated using equation: $\Delta_l^g H_m^o$(298.15 K) /(kJ·mol^{-1}) = -48.2+0.2356×T_b with (R^2 = 0.995).
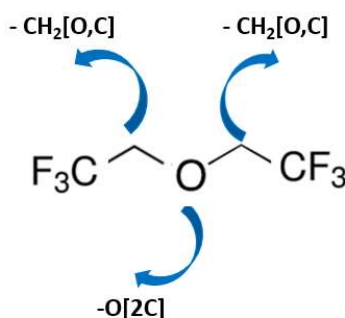
$$CF_3[C] =[\Delta_l^g H_m^0(298.15\ K)_{exp} - 2\times CH_2[O,C] - O[2C]]/2 = 10.45$$

Figure C. 4. Estimation of group-additivity contribution for the CF$_3$[C] group based on experimental vaporization enthalpy of 2,2,2-trifluoroethyl ether (Table C. 8) and increments listed in Table 27 (data are in kJ·mol^{-1})

Table C. 11. Formula, density ρ (T = 293 K), and massic heat capacity C_p (T = 298.15 K), of the materials used in the present study.

Compounds	Formula	Water content	ρ	c_p
		ppm	g·cm^{-3}	J·K^{-1} g^{-1}
1,3-dimethoxy-2-propanol	C$_5$H$_{12}$O$_3$	156	1.001 [86]	2.24
1,3-diethoxy-2-propanol	C$_7$H$_{16}$O$_3$	110	0.95 [200]	2.36
1,3-diisopropoxy-2-propanol	C$_9$H$_{20}$O$_3$	111	0.91 [87]	2.30
2,5,9,12-tetraoxatridecan-7-ol	C$_9$H$_{20}$O$_5$	286	1.039[a]	2.19
polyethylene [b]	CH$_{1.93}$		0.92	2.53
cotton [b]	CH$_{1.774}$O$_{0.887}$		1.50	1.67

[a] [34], [b] data from [201]: specific energy of combustion $\Delta_c u°$(cotton) = -16945.2 J·g^{-1}; $u(\Delta_c u°)$ = 4.2 J·g^{-1}. The specific energy of combustion $\Delta_c u°$(polyethylene) = -46357.3 J·g^{-1}; $u(\Delta_c u°)$ = 3.6 J·g^{-1}

Table C. 12. Results for combustion experiments at $T = 298.15$ K ($p° = 0.1$ MPa) for the glycerol ethers.

	1,3-dimethoxy-2-propanol	1,3-diethoxy-2-propanol	1,3-diisoproxy-2-propanol	2,5,9,12-tetraoxatridecan-7-ol
	25640.3	29444.9	32033.0	26098.9
	25635.4	29452.5	32022.2	26102.7
	25664.5	29439.5	32030.9	26092.6
	25627.2	29454.8	32028.8	26098.4
	25636.7	29440.4	32058.2	26120.8
$-\Delta_c u°$(liq) /(J·g^{-1})	25640.8±6.3	29446.4±3.1	32034.6±6.2	26102.7±4.8
$\Delta_c H_m^o$(liq) /(kJ·mol^{-1})	-3084.4±1.6	-4370.2±1.6	-5654.9±2.5	-5442.1±2.3
$\Delta_f H_m^o$(liq) /(kJ·mol^{-1})	-598.1±1.8	-671.1±1.6	-745.0±2.8	-957.8±2.6

Table C. 13. Experimental gas-phase enthalpies of formation, $\Delta_f H_m^o(g)_{exp}$, used for correlation with the G4MP2-theoretical results, $\Delta_f H_m^o(g)_{AT}$, calculated according to the atomization procedure, at 298.15 K (in kJ·mol^{-1}).

CAS	Compounds	$\Delta_f H_m^o(g)_{AT}$ [a]	$\Delta_f H_m^o(g)_{exp}$	$\Delta_f H_m^o(g)_{ATcorr}$ [b]	Δ
109-87-5	dimethoxymethane	-349.3	-348.2±0.8 [94]	-351.0	2.8
534-15-6	1,1-dimethoxyethane	-388.5	-389.7±0.8 [202]	-390.3	0.6
110-71-4	1,2-dimethoxyethane	-342.8	-342.8±0.7 [203]	-344.5	1.7
126-84-1	2,2-diethoxypropane	-496.4	-495.3±0.2 [94]	-498.3	3.0
149-73-5	trimethoxymethane	-529.8	-530.8±2.3 [94]	-531.8	1.0
122-51-0	triethoxymethane	-623.7	-630.6±1.5 [94]	-625.8	-4.8
1445-45-0	1,1,1-trimethoxyethane	-568.1	-570.8±1.6 [94]	-570.2	-0.6
24823-81-2	1,1,1-trimethoxypropane	-589.9	-589.9±1.9 [94]	-592.0	2.1
142-96-1	butylmethylether	-257.3	-258.3±1.2 [94]	-258.9	0.6
111-43-3	dipropylether	-292.7	-293.1±0.9 [94]	-291.9	-1.2
142-96-1	dibutylether	-330.3	-332.9±1.0 [94]	-332.0	-0.9
1850-14-2	tetramethoxymethane	-726.1	-727.3±1.5 [94]	-728.4	1.1
623-69-8	1,3-dimethoxy-2-propanol	-538.4		**-540.4**	
4043-59-8	1,3-diethoxy-2-propanol	-606.8		**-608.9**	
13021-54-0	1,3-diisopropoxy-2-propanol	-677.3		**-679.5**	
130670-52-9	2,5,9,12-tetraoxatridecan-7-ol	-863.5		**-866.0**	
691-26-9	1,3-bis(2,2,2-trifluoroethoxy)-2-propanol	-1895.2		**-1899.2**	

[a] Calculated by the G4MP2 method according to the standard atomization procedure [99], [b] results from atomization reactions were corrected with: $\Delta_f H_m^o(g)_{theor}/kJ·mol^{-1} = 1.0015 \times \Delta_f H_m^o(g, AT) - 1.2$ with $R^2 = 0.9998$.

Table C. 14. Experimental gas-phase enthalpies of formation, $\Delta_f H_m^o(g)_{exp}$, used for correlation with the G4-theoretical results, $\Delta_f H_m^o(g)_{AT}$, calculated according to the atomization procedure, at 298.15 K (in kJ·mol⁻¹).

CAS	Compounds	$\Delta_f H_m^o(g)_{AT}$ [a]	$\Delta_f H_m^o(g)_{exp}$	$\Delta_f H_m^o(g)_{ATcorr}$ [b]	Δ
109-87-5	dimethoxymethane	-353.9	-348.2±0.8 [94]	-350.7	-2.5
534-15-6	1,1-dimethoxyethane	-393.5	-389.7±0.8 [202]	-390.1	-0.4
110-71-4	1,2-dimethoxyethane	-347.2	-342.8±0.7 [203]	-344.0	-1.2
126-84-1	2,2-diethoxypropane	-502.5	-495.3±0.2 [94]	-498.7	-3.4
149-73-5	trimethoxymethane	-537.3	-530.8±2.3 [94]	-533.4	-2.6
122-51-0	triethoxymethane	-631.9	-630.6±1.5 [94]	-627.7	2.9
1445-45-0	1,1,1-trimethoxyethane	-576.4	-570.8±1.6 [94]	-572.4	-1.6
24823-81-2	1,1,1-trimethoxypropane	-598.6	-589.9±1.9 [94]	-594.5	-4.6
142-96-1	butylmethylether	-259.5	-258.3±1.2 [94]	-256.6	1.7
111-43-3	dipropylether	-292.7	-293.1±0.9 [94]	-289.7	3.4
142-96-1	dibutylether	-332.5	-332.9±1.0 [94]	-329.3	3.6
100-66-3	methoxybenzene	-71.3	-70.7±1.4 [194]	-69.1	1.6
103-73-1	ethoxybenzene	-105.8	-101.6±1.2 [202]	-103.4	-1.8
578-58-5	2-methylmethoxybenzene	-107.7	-106.6±1.6 [30]	-105.3	1.3
104-93-8	4-methylmethoxybenzene	-103.1	-99.3±2.0 [30]	-100.7	-1.4
994-05-8	tertamylether	-304.3	-301.5±1.7 [94]	-301.2	0.3
8021-39-4	2-methoxyphenol	-251.1	-247.3±1.8[54]	-248.2	-0.9
91-16-7	1,2-dimethoxybenzene	-211.2	-206.0±3.1[54]	-208.5	-2.5
123-91-1	1,4-dioxane	-317.8	-315.3±0.8 [202]	-314.7	0.6
110-88-3	1,3,5-trioxane	-471.0	-465.9±0.4[202]	-467.4	-1.5
108-20-3	diisopropylether	-321.5	-319.5±1.4 [94]	-318.4	1.1
616-38-6	dimethylcarbonate	-573.6	-570.7±0.6 [204]	-569.6	1.1
105-58-8	diethylcarbonate	-640.6	-637.9±0.9 [204]	-636.4	1.5
96-49-1	ethylenecarbonate	-512.5	-510.7±0.9 [204]	-508.7	2.0
108-32-7	propylenecarbonate	-556	-553.9±0.8 [204]	-552.1	1.8
4437-85-8	butylenecarbonate	-578.3	-576.7±1.2 [204]	-574.3	2.4
623-69-8	1,3-dimethoxy-2-propanol	-544.2		**-540.3**	
4043-59-8	1,3-diethoxy-2-propanol	-613.1		**-609.0**	
13021-54-0	1,3-diisopropoxy-2-propanol	-684.2		**-679.8**	
130670-52-9	2,5,9,12-tetraoxatridecan-7-ol	-874.1		**-869.0**	
691-26-9	1,3-bis(2,2,2-trifluoroethoxy)-2-propanol	-1904.9		**-1896.2**	
109-86-4	2-methoxyethanol	-373.2		-369.9	
110-80-5	2-ethoxyethanol	-407.3		-403.9	
109-59-1	2-isopropoxyethanol	-441.5		-438.0	
111-77-3	diethyleneglycolmonomethyl ether	-540.1		-536.2	

[a] Calculated by the G4 method according to the standard atomization procedure [100], [b] results from atomization reactions were corrected with help of following equation: $\Delta_f H_m^o(g)_{theor}$/ kJ·mol⁻¹ = 0.9965 × $\Delta_f H_m^o$(g, AT) + 2.0 with $R^2 = 0.9998$.
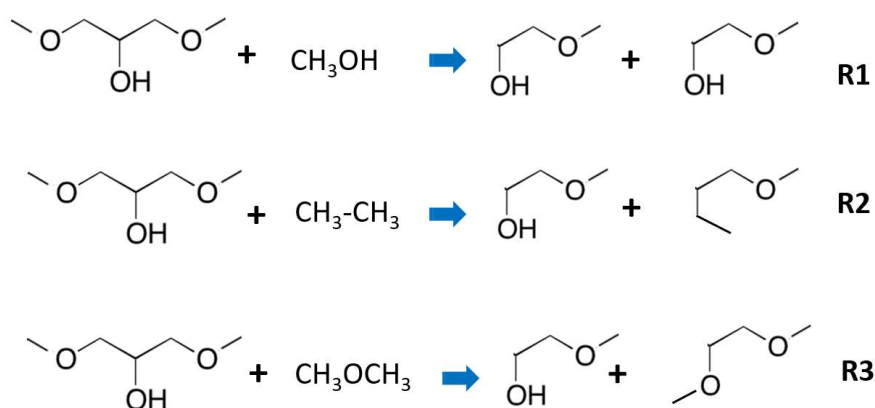
Figure C. 5. Well-balanced reactions (1-3) for calculations of standard enthalpy of formation of 1,3-dimethoxy-2-propanol.

Table C. 15. Thermochemical data at $T = 298.15$ K ($p° = 0.1$ MPa) for reference compounds (in kJ·mol^{-1}).

	$\Delta_f H_m^o(g)$
methanol	-201.5±0.3 [202]
ethane	-83.8±0.4 [202]
dimethylether	-184.1±0.5 [202]
methylpropylether	-238.2±0.7 [202]
2-methoxyethanol	-369.9±1.0 [203]
1,2-dimethoxyethane	-409.7±0.5[a]

[a] Average value calculated from [205] and [206].

Table C. 16. Standard enthalpy of formation of 1,3-dimethoxy-2-propanol, $\Delta_f H_m^o(g, 298.15$ K) kJ·mol^{-1}.

method	$\Delta_f H_m^o(g)$ (AT)	$\Delta_f H_m^o(g)$ (AT)corr	$\Delta_f H_m^o(g)$ Reaction R1	$\Delta_f H_m^o(g)$ Reaction R2	$\Delta_f H_m^o(g)$ Reaction R3	$\Delta_f H_m^o(g)$ (WBL)
G4	-544.2	**-540.3**	-544.1	-540.3	-537.5	-540.6±1.9
G4MP2	-538.4	**-540.4**	-544.0	-539.3	-536.9	-540.1±2.1
G3MP2	-540.7	**-540.9**	-543.8	-540.9	-537.5	-540.7±1.8

method	$\Delta_r H_m^o(g)$ Reaction enthalpy R1	$\Delta_r H_m^o(g)$ Reaction enthalpy R2	$\Delta_r H_m^o(g)$ Reaction enthalpy R3
G4	-0.9	16.0	8.9
G4MP2	-1.0	15.0	8.3
G3MP2	-1.2	16.6	8.9

D. Supporting information to Chapter 4

Table D. 1. Thermochemical data for dihydro-levoglucosenone (cyrene) and levoglucosenone at $T=298.15$ K ($p°=0.1$ MPa, in kJ·mol^{-1}).

compound	$\Delta_c H_m^o$(l,cr)	$\Delta_f H_m^o$(l,cr)	$\Delta_{l,cr}^g H_m^{o\ a}$	$\Delta_f H_m^o$(g)$_{exp}$	$\Delta_f H_m^o$(g)$_{theor}^{\ b}$
1	2	3	4	5	6
cyrene (liq)	-3006.7±1.5 [c]	-497.7±1.7	61.6±0.4	-436.1±1.7	-437.1±2.1
levoglucosenone (liq)	-2835.3±1.2 [c]	-383.3±1.5	64.5±1.0	-318.8±1.8	-318.8±2.1
levoglucosan (cr)	-2839.8±5.0 [207]	-950.4±5.1			
	-2831.7±1.0 [208]	-958.5±1.3			
	-2831.1±2.0 [209]	-959.1±2.1			
	-2833.4±2.9 [210]	-956.8±3.0			
		-958.1±1.0 [c]	127.7±2.8	-830.4±2.9	-831.8±2.7

[a] From [111], [b] theoretical value calculated as the average from G3MP2, and G4MP2 and G4 results [111], [c] measured in [111].

E. Supporting information to Chapter 7

Table E. 1. Compilation of data on molar heat capacities $C_{p,m}^o$ and differences $\Delta_l^g C_{p,m}^o$ of aminoalcohols, in J·K^{-1}·mol^{-1}, at 298.15 K.

compound	$C_{p,m}^o$(liq)	$-\Delta_l^g C_{p,m}^{o\ a}$
DL-2-amino-1-butanol 13054-87-0	235.4	71.8
1-(dimethylamino)-2-propanol [108-16-7]	238.8	72.7
2-(dimethylamino)-1-propanol [15521-18-3]	238.8	72.7
2-(phenyl-amino)-ethanol [122-98-5]	286.3	85.0
2-(benzyl-amino)-ethanol [104-63-2]	318.2	93.3
2-(dimethyl-amino)-ethanol	205.1 [1]	
108-01-0	211.0 [2]	
2-(diethyl-amino)-ethanol	278.3 [1]	
100-37-8	280.6 [3]	

Table E. 2. Results of transpiration method for aminoalcohols: absolute vapor pressures p, standard ($p^o = 0.1$ MPa) molar vaporization enthalpies and standard ($p^o = 0.1$ MPa) molar vaporization entropies.

$T/$ K[a]	$m/$ mg[b]	$V(N_2)^c/$ dm^3	$T_a/$ K[d]	Flow/ dm^3·h^{-1}	$p/$ Pa[e]	$u(p)/$ Pa[f]	$\Delta_{l,cr}^g H_m^o(T)$ kJ·mol^{-1}	$\Delta_{l,cr}^g S_m^o(T)$ J·K^{-1}·mol^{-1}
DL-2-amino-1-butanol [13054-87-0]: $\Delta_l^g H_m^o$(298.15 K) = (65.5±0.5) kJ·mol^{-1}								
$\ln(p/p_{ref}) = \frac{317.8}{R} - \frac{86891.6}{RT} - \frac{71.8}{R}\ln\frac{T}{298.15}$; p_{ref} = 1 Pa								
303.2	1.45	1.073	295.8	1.31	37.34	0.96	65.1	149.2
308.3	1.79	0.898	295.8	1.31	55.13	1.40	64.8	147.7
313.4	2.20	0.712	295.8	1.31	85.45	2.16	64.4	146.8
318.2	2.71	0.613	295.8	1.31	121.7	3.1	64.0	145.5
323.4	2.33	0.350	295.8	1.31	183.5	4.6	63.7	144.5
328.4	3.25	0.339	295.8	1.31	263.4	6.6	63.3	143.4
333.5	3.66	0.274	295.8	1.31	367.6	9.2	62.9	142.2
328.4	3.25	0.339	295.8	1.31	263.4	6.6	63.3	143.4
333.5	3.66	0.274	295.8	1.31	367.6	9.2	62.9	142.2
1-(dimethyl-amino)-2-propanol [108-16-7]: $\Delta_l^g H_m^o$(298.15 K) = (45.7±0.3) kJ·mol^{-1}								
$\ln(p/p_{ref}) = \frac{287.4}{R} - \frac{67352.5}{RT} - \frac{72.7}{R}\ln\frac{T}{298.15}$; p_{ref} = 1 Pa								
276.2	5.73	0.396	295.7	0.91	367.1	9.2	47.3	124.6
276.3	6.28	0.432	295.7	1.00	369.1	9.3	47.3	124.5
276.3	6.23	0.422	295.7	0.97	374.1	9.4	47.3	124.6
277.7	6.28	0.389	295.7	0.93	407.0	10.2	47.2	124.1

277.7	5.43	0.335	295.7	0.91	408.0	10.2	47.2	124.1
279.2	5.33	0.292	295.7	0.97	456.2	11.4	47.1	123.8
279.3	5.53	0.305	295.7	0.91	454.1	11.4	47.1	123.6
280.7	5.58	0.273	295.7	0.91	508.1	12.7	46.9	123.4
281.9	6.93	0.305	295.7	0.91	562.7	14.1	46.9	123.2
282.3	6.18	0.268	295.7	0.97	570.3	14.3	46.8	123.0
282.3	6.03	0.267	295.7	0.91	559.6	14.0	46.8	122.8
284.1	6.68	0.251	295.7	0.91	652.9	16.3	46.7	122.6
284.7	7.30	0.267	295.7	0.92	671.7	16.8	46.7	122.3
285.2	5.23	0.187	295.7	0.93	686.6	17.2	46.6	122.1
285.2	6.58	0.236	295.7	0.91	683.2	17.1	46.6	122.0
286.3	10.43	0.340	295.7	1.00	749.1	18.8	46.5	121.9
287.2	6.18	0.190	295.7	0.91	790.9	19.8	46.5	121.6
287.7	6.63	0.198	295.7	0.92	814.6	20.4	46.4	121.5
288.2	6.03	0.175	295.7	0.91	836.9	20.9	46.4	121.3
289.1	9.18	0.249	295.7	1.00	894.9	22.4	46.3	121.1
289.1	9.43	0.257	295.7	1.00	889.8	22.3	46.3	121.1
290.1	6.38	0.160	295.7	0.91	965.0	24.1	46.3	120.9
291.2	5.93	0.140	295.7	0.93	1022.9	25.6	46.2	120.5
291.2	6.33	0.152	295.7	0.91	1008.1	25.2	46.2	120.4
294.2	5.93	0.114	295.7	0.91	1250.2	31.3	46.0	119.8
297.2	6.89	0.107	295.7	0.92	1538.7	38.5	45.7	119.3
300.2	12.69	0.163	295.7	0.93	1842.2	46.1	45.5	118.5
303.2	14.44	0.152	295.7	0.91	2233.4	55.9	45.3	117.9
306.2	12.06	0.107	295.7	0.92	2645.6	66.2	45.1	117.1
308.2	13.61	0.107	295.7	0.92	2972.9	74.3	44.9	116.6

2-(phenyl-amino)-ethanol [122-98-5]: $\Delta_l^g H_m^o$(298.15 K) = (82.3±0.4) kJ·mol^{-1}

$$\ln (p/p_{ref}) = \frac{342.6}{R} - \frac{107623.8}{RT} - \frac{85.0}{R} \ln \frac{T}{298.15} \; ; p_{\text{ref}} = 1 \text{ Pa}$$

308.1	1.34	73.79	293.8	4.31	0.32	0.01	81.4	159.2
311.1	1.88	78.96	293.8	4.31	0.42	0.02	81.2	158.2
314.1	1.36	41.85	293.8	4.31	0.58	0.02	80.9	157.5
317.2	1.38	30.36	293.8	4.31	0.81	0.03	80.7	156.9
320.1	1.43	25.05	293.8	4.31	1.02	0.03	80.4	155.7
321.1	1.50	23.11	293.8	4.31	1.16	0.03	80.3	155.7
324.1	2.05	24.62	293.8	4.31	1.48	0.04	80.1	154.7
327.2	1.91	17.37	293.8	4.31	1.96	0.05	79.8	153.8
330.2	1.91	12.92	293.8	4.31	2.63	0.07	79.6	153.3
333.1	1.50	7.968	293.8	4.31	3.35	0.09	79.3	152.5
336.2	1.51	6.173	293.8	4.31	4.37	0.11	79.1	151.7
338.2	0.82	2.871	293.8	4.31	5.07	0.15	78.9	151.0
338.2	1.84	6.481	293.8	4.52	5.06	0.15	78.9	151.0
341.2	1.77	4.747	293.8	4.52	6.66	0.19	78.6	150.5
344.4	2.29	4.810	293.8	4.31	8.49	0.24	78.4	149.6
348.5	1.41	2.082	293.8	4.31	12.02	0.33	78.0	148.8

2-(benzyl-amino)-ethanol: $\Delta_l^g H_m^o$(298.15 K) = (84.5±0.4) kJ·mol^{-1}

$$\ln (p/p_{ref}) = \frac{360.7}{R} - \frac{112301.0}{RT} - \frac{93.3}{R} \ln \frac{T}{298.15} \; ; p_{\text{ref}} = 1 \text{ Pa}$$

302.2	0.98	68.47	294.0	4.47	0.23	0.01	84.1	170.5
305.1	1.15	59.23	294.0	4.36	0.31	0.01	83.8	169.5
308.1	1.64	58.81	294.0	4.50	0.45	0.02	83.6	168.9
311.1	1.04	28.56	294.0	4.36	0.59	0.02	83.3	167.6
314.0	1.09	22.31	294.0	4.36	0.79	0.02	83.0	166.7
317.1	1.93	29.33	294.0	4.50	1.06	0.03	82.7	165.7
319.0	1.06	12.90	294.0	4.50	1.33	0.04	82.5	165.4
321.0	0.77	7.682	294.0	4.47	1.63	0.05	82.4	164.9

323.1	0.76	6.323	294.0	4.36	1.95	0.05	82.2	164.2
326.1	1.15	7.195	294.0	4.36	2.58	0.07	81.9	163.3
329.1	1.37	6.541	294.0	4.36	3.39	0.09	81.6	162.4
331.1	0.94	3.655	294.0	4.47	4.16	0.11	81.4	162.0
332.1	1.30	4.724	294.0	4.36	4.46	0.12	81.3	161.6
335.1	1.05	2.907	294.0	4.36	5.83	0.17	81.0	160.8
338.2	0.97	2.035	294.0	4.36	7.71	0.22	80.8	160.1
341.2	0.91	1.526	294.0	4.36	9.65	0.27	80.5	159.0
344.4	1.08	1.381	294.0	4.36	12.62	0.34	80.2	158.2
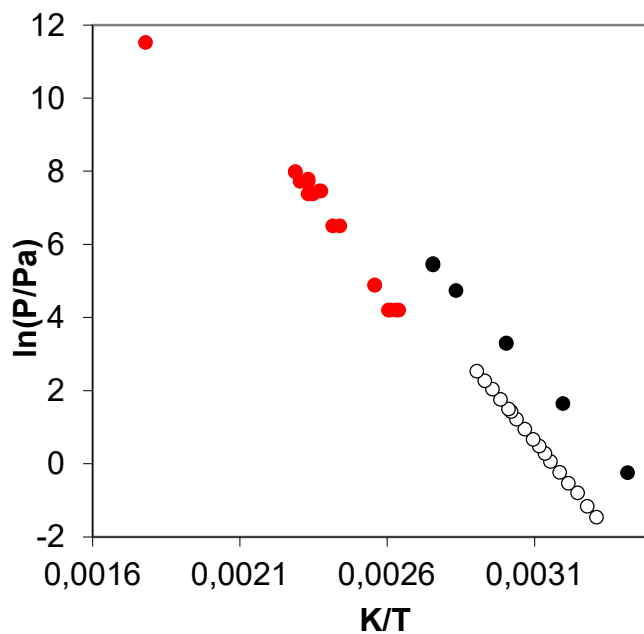
Figure E. 1. Temperature dependence of vapor pressures for the 2-(benzyl-amino)-ethanol: ○ – transpiration [this work]; ● –static method [123]; 🔴 - from experimental boiling temperatures reported at different pressures compiled by SciFinder [34].

Table E. 3. Absolute vapor pressures p, standard ($p^o = 0.1$ MPa) molar vaporization enthalpies, $\Delta_l^g H_m^o$, and standard ($p^o = 0.1$ MPa) molar vaporization entropies, $\Delta_l^g S_m^o$, derived from boiling temperatures at different pressures compiled by SciFinder [34].

T/K	p/Pa	$\Delta_l^g H_m^o(T)$/kJ·mol^{-1}	$\Delta_l^g S_m^o(T)$/J·K^{-1}·mol^{-1}
1-(dimethylamino)-2-propanol [108-16-7]: $\Delta_l^g H_m^o(298.15$ K$) = (47.3\pm0.7)$ kJ·mol^{-1}			

$$\ln (p/p_0) = \frac{289.9}{R} - \frac{68948.8}{RT} - \frac{72.7}{R}\ln \frac{T}{298.15} \; ; p_0 = 1 \text{ Pa}$$

T/K	p/Pa	$\Delta_l^g H_m^o(T)$/kJ·mol^{-1}	$\Delta_l^g S_m^o(T)$/J·K^{-1}·mol^{-1}
333	9333	44.7	114.5
336	9333	44.5	112.7
343	11999	44.0	110.6
343	11999	44.0	110.6
397	101325	40.1	101.0
398	101325	40.0	100.8
398	101058	40.0	100.8
398	102658	40.0	100.9
398	102658	40.0	100.9
399	101325	39.9	100.1
399	101325	39.9	100.1
399	101058	39.9	100.1
399	101325	39.9	100.1
400	101325	39.9	99.7
400	101325	39.9	99.7

2-(dimethylamino)-1-propanol [15521-18-3]: $\Delta_l^g H_m^o$(298.15 K) = (51.6±0.7) kJ·mol⁻¹

$$\ln (p/p_0) = \frac{295.3}{R} - \frac{73284.7}{RT} - \frac{72.7}{R}\ln\frac{T}{298.15} \; ; p_0 = 1 \text{ Pa}$$

341	5066	48.5	117.3
342	5066	48.4	116.7
342	5066	48.4	116.7
418	101325	42.9	102.7
418	101991	42.9	102.7
418	101325	42.9	102.7
418	101325	42.9	102.7
419	101325	42.8	102.5
421	101325	42.7	101.4
421	101991	42.7	101.5
421	101325	42.7	101.4
423	101325	42.5	100.5

2-(phenyl-amino)-ethanol [122-98-5]: $\Delta_l^g H_m^o$(298.15 K) = (83.6±1.6) kJ·mol⁻¹

$$\ln (p/p_0) = \frac{344.6}{R} - \frac{108915.5}{RT} - \frac{85.0}{R}\ln\frac{T}{298.15} \; ; p_0 = 1 \text{ Pa}$$

383	133	76.3	144.2
384	133	76.3	143.5
407	400	74.3	136.6
408	400	74.2	135.9
429	1600	72.4	134.4
430	1600	72.4	133.8
431	1000	72.3	129.3
432	2400	72.2	136.0
433	2400	72.1	135.4
433	1000	72.1	128.2
440	2533	71.5	131.9
443	2533	71.2	130.2
449	2533	70.7	126.9
449	2533	70.7	126.9
461	4000	69.7	124.4
548	102125	62.3	113.9
550	102125	62.2	113.1
553	101325	61.9	112.2
553	100658	61.9	112.0
555	101325	61.7	111.3
558	101325	61.5	110.2
558	100658	61.5	110.2
559	101325	61.4	109.9
560	101325	61.3	109.5

2-(benzyl-amino)-ethanol [104-63-2]: $\Delta_l^g H_m^o$(298.15 K) = (92.4±3.7) kJ·mol⁻¹

$$\ln (p/p_0) = \frac{375.5}{R} - \frac{120205.9}{RT} - \frac{93.3}{R}\ln\frac{T}{298.15} \; ; p_0 = 1 \text{ Pa}$$

379	67	84.8	162.9
380	67	84.7	162.1
383	67	84.5	159.6
384	67	84.4	158.8
391	133	83.7	159.0
391	133	83.7	159.0
410	667	81.9	158.1
414	667	81.6	155.3
421	1733	80.9	158.4
422	1733	80.8	157.7

426	1600	80.4	154.4
429	2266	80.2	155.3
429	2400	80.2	155.8
429	1600	80.2	152.4
431	2266	80.0	154.0
434	2266	79.7	152.1
437	2933	79.4	152.3
437	2933	79.4	152.3
562	101325	67.8	120.7

Table E. 4. Group-additivity values Γ_i for calculation of enthalpies of vaporization, $\Delta_l^g H_m^o(298.15$ K) of alkanes, amines and aminoalcohols at 298.15 K (in kJ mol^{-1}) [81,95,145].

	$\Delta_l^g H_m^o(298.15$ K)
Groups [a]	Γ_i
Alkanes	
C-(C)(H)$_3$	6.33
C-(C)$_2$(H)$_2$	4.52
C-(C)$_3$(H)	1.24
C-(C)$_4$	-2.69
Amines	
C-(N)(C)(H)$_3$	6.33
C-(N)(C)(H)$_2$	2.9
C-(N)(C)$_2$(H)	-2.0
C-(N)(C)$_3$	-7.7
N-(C)(H)$_2$	18.0
N-(C)$_2$(H)	12.6
N-(C)$_3$	4.9
Alcohols	
C-(O)(C)(H)$_3$	6.33
C-(O)(C)(H)$_2$	4.7
C-(O)(C)$_2$(H)	1.3
C-(O)(C)$_3$	-3.8
HO-(C)	31.5
Alkylbenzenes[b]	
Cb-(Cb)$_2$(H)	5.65
Cb-(Cb)$_2$(C)	3.44
C-(Cb)(C)(H)$_2$	3.79
C-(Cb)(C)$_2$(H)	-0.03
Cb-(Cb)$_2$(H)	-3.83

[a] The designation of groups is given according to the Benson´s original book [1], [b] The contribution for the phenyl substituent was calculated as follows: $C_6H_5 = 5\times$ [Cb-(Cb)$_2$(H)] + [Cb-(Cb)$_2$(C)] = 31.7 kJ mol^{-1}.

Table E. 5. Compilation of the standard molar enthalpies of vaporization $\Delta_l^g H_m^o(298.15$ K) of aminoalcohols [134]

Amino-alcohol/CAS	$\Delta_l^g H_m^o(298.15$ K)
2-amino-ethanol [141-43-5]	59.6±0.3
2-amino-1-propanol [6168-72-5]	59.7±0.6
2-amino-1-butanol [96-20-8]	64.9±0.3
2-amino-1-pentanol [16369-14-5]	69.1±0.7
2-amino-1-hexanol [5665-74-7]	73.8±0.7
2-amino-1-heptanol [74872-95-0]	79.0±1.0
2-amino-1-octanol [16369-15-6]	83.8±1.0

F. Supporting information to Chapter 6
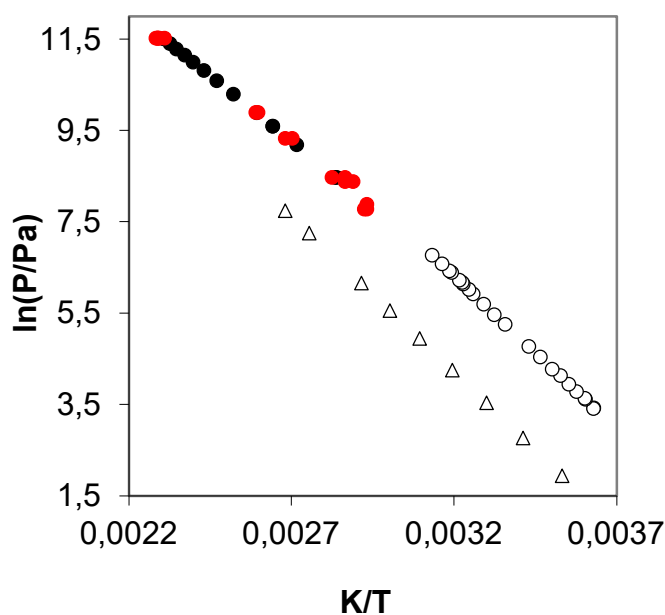
Figure F. 1. Temperature dependence of vapour pressures for the 3-(dimethylamino)-1-propanol: ○ – transpiration [this work]; △ –static method [137]; ● - ebulliometry [139]; ● - from experimental boiling temperatures reported at different pressures compiled by SciFinder [34].

Table F. 1. Compilation of data on the standard molar heat capacities $C_{p,m}^o$ and differences $\Delta_l^g C_{p,m}^o$ of aminoalcohols, in J·K^{-1}·mol^{-1}, at 298.15 K.

compound	$C_{p,m}^o$(liq)	$-\Delta_l^g C_{p,m}^o$ [a]
2-(ethyl-amino)-ethanol [110-73-6]	228.2 [1]	69.9
2-(iso-propyl-amino)-ethanol [109-56-8]	258.9 [2]	77.9
2-amino-2-methyl-1-propanol [124-68-5]	236.1 [1]	72.1
3-(dimethlyamino)-1-propanol [3179-63-3]	245.3	74.4
3-(diethlyamino)-1-propanol [622-93-5]	309.1	90.9
3-amino-1-propanol [156-87-6]	201.0 [3]	62.8
4-amino-1-butanol [13325-10-5]	241.9	73.5
5-amino-1-pentanol [2508-29-4]	273.8	81.8
6-amino-1-hexanol [4048-33-3]	305.7	90.1
1-(dimethylamino)-2-propanol [108-16-7]	238.8	72.7
2-(n-propyl-amino)-ethanol [16369-21-4]	260.7	78.4
2-(n-butyl-amino)-ethanol [111-75-1]	292.6	86.7
2-(t-butyl-amino)-ethanol [4620-70-6]	280.7	83.6
1-amino-2-methyl-2-propanol [2854-16-2]	230.0	70.4
4-amino-4-methyl-2-pentanol [4404-98-2]	287.3	85.8
2-amino-3-methyl-1-butanol [16369-05-4]	260.8	78.4
1-amino-4-methyl-2-pentanol [17687-58-0]	260.8	78.4
2-amino-4-methyl-1-pentanol [502-32-9]	292.7	86.7

Table F. 2. Results of transpiration method for aminoalcohols: absolute vapour pressures p, standard ($p^o = 0.1$ MPa) molar vaporization enthalpies and standard ($p^o = 0.1$ MPa) molar vaporization entropies.

$T/$ K^a	$m/$ mg^b	$V(N_2)^c /$ dm^3	$T_a/$ K^d	Flow/ $dm^3 \cdot h^{-1}$	$p/$ Pa^e	$u(p)/$ Pa^f	$\Delta_{l,cr}^g H_m^o(T)$ $kJ \cdot mol^{-1}$	$\Delta_{l,cr}^g S_m^o(T)$ $J \cdot K^{-1} \cdot mol^{-1}$
2-amino-2-methyl-1-propanol [124-68-5] (liq): $\Delta_l^g H_m^o(298.15\ K) = (62.3\pm0.3)$ kJ·mol^{-1}								
$\ln(p/p_{ref}) = \frac{315.1}{R} - \frac{83801.7}{RT} - \frac{72.1}{R}\ln\frac{T}{298.15}$; $p_{ref} = 1$ Pa								
290.3	1.06	0.996	295.3	0.891	29.5	0.8	62.9	149.1
291.3	1.09	0.915	295.3	0.891	33.1	0.8	62.8	149.0
292.3	0.87	0.664	295.3	0.891	36.1	0.9	62.7	148.7
294.3	1.64	1.069	295.3	0.891	42.4	1.1	62.6	148.1
294.3	0.95	0.605	295.3	0.891	43.5	1.1	62.6	148.3
297.3	1.08	0.546	295.3	0.891	54.6	1.4	62.4	147.4
299.3	1.19	0.490	295.3	0.880	66.9	1.7	62.2	147.2
302.3	1.33	0.446	295.3	0.880	82.5	2.1	62.0	146.1
305.3	1.85	0.470	295.3	0.880	108.3	2.7	61.8	145.7
308.4	1.80	0.366	295.3	0.880	135.8	3.4	61.6	144.8
313.5	2.24	0.300	295.3	0.880	205.1	5.1	61.2	143.8
318.3	3.19	0.300	295.3	0.880	291.8	7.3	60.9	142.7
323.3	3.63	0.249	295.3	0.880	400.6	10.0	60.5	141.3
328.6	3.20	0.146	295.3	0.880	598.9	15.0	60.1	140.4
333.4	4.03	0.139	295.3	0.880	792.9	19.8	59.8	139.1
2-amino-2-methyl-1-propanol [124-68-5] (cr)^g: $\Delta_{cr}^g H_m^o(298.15\ K) = (67.0\pm1.1)$ kJ·mol^{-1}								
$\ln(p/p_{ref}) = \frac{278.4}{R} - \frac{72536.4}{RT} - \frac{18.6}{R}\ln\frac{T}{298.15}$; $p_{ref} = 1$ Pa								
274.4	0.82	3.592	295.3	0.830	6.46	0.19	67.4	165.6
276.2	0.87	3.102	295.3	0.880	7.89	0.22	67.4	165.5
279.2	0.92	2.353	295.3	0.891	10.92	0.30	67.3	165.4
281.3	0.99	2.059	295.3	0.830	13.35	0.36	67.3	165.1
282.2	0.96	1.811	295.3	0.891	14.70	0.39	67.3	165.1
283.0	5.22	9.337	295.3	0.891	15.54	0.41	67.3	164.8
283.8	1.01	1.632	295.3	0.840	17.22	0.46	67.3	165.0
285.3	1.03	1.419	295.3	0.891	20.13	0.53	67.2	164.9
288.2	1.15	1.191	295.3	0.880	26.78	0.69	67.2	164.7
3-(dimethyl-amino)-1-propanol [3179-63-3]: $\Delta_l^g H_m^o(298.15\ K) = (54.9\pm0.3)$ kJ·mol^{-1}								
$\ln(p/p_{ref}) = \frac{302.5}{R} - \frac{77090.2}{RT} - \frac{74.4}{R}\ln\frac{T}{298.15}$; $p_{ref} = 1$ Pa								
275.6	2.65	2.020	294.0	1.01	32.4	0.8	56.6	138.6
275.7	2.09	1.599	294.0	1.01	32.2	0.8	56.6	138.4
277.6	2.32	1.515	294.0	1.01	37.5	1.0	56.4	137.8
277.7	2.32	1.481	294.0	1.01	38.3	1.0	56.4	137.8
279.7	2.14	1.178	294.0	1.01	44.2	1.1	56.3	137.0
281.6	2.20	1.027	294.0	1.01	52.1	1.3	56.1	136.5
283.6	2.50	0.960	294.0	1.01	62.8	1.6	56.0	136.2
285.7	2.07	0.690	294.0	1.01	72.2	1.8	55.8	135.3
288.7	2.38	0.606	294.0	1.01	94.3	2.4	55.6	134.8
291.7	2.43	0.488	294.0	1.01	119.0	3.0	55.4	133.9
298.0	2.25	0.278	294.0	1.01	192.7	4.8	54.9	132.4
301.0	3.03	0.303	294.0	1.01	238.0	6.0	54.7	131.5
304.0	2.76	0.219	294.0	1.01	299.7	7.5	54.5	130.9
307.0	3.51	0.221	294.0	1.02	375.7	9.4	54.3	130.3
308.2	4.11	0.236	294.0	1.01	413.0	10.3	54.2	130.1
309.9	5.01	0.255	294.0	1.02	464.7	11.6	54.0	129.7
310.2	3.26	0.168	294.0	1.01	457.8	11.5	54.0	129.4
311.0	29.45	1.418	294.0	2.43	491.1	12.3	54.0	129.3

313.3	2.88	0.118	294.0	1.01	576.4	14.4	53.8	128.8
314.0	27.79	1.094	294.0	2.43	599.7	15.0	53.7	128.6
316.3	2.99	0.101	294.0	1.01	697.6	17.5	53.6	128.1
319.3	2.99	0.084	294.0	1.01	835.8	20.9	53.3	127.3

1-(dimethylamino)-2-propanol [108-16-7]: $\Delta_l^g H_m^o$(298.15 K) = (45.3±0.3) kJ·mol^{-1}

$$\ln (p/p_{ref}) = \frac{285.9}{R} - \frac{66938.3}{RT} - \frac{72.7}{R} \ln \frac{T}{298.15} \; ; p_{\text{ref}} = 1 \text{ Pa}$$

276.4	5.68	0.382	295.6	0.79	378	9.5	46.8	123.1
278.4	5.68	0.329	295.6	0.79	434	11	46.7	122.6
280.4	5.73	0.289	295.6	0.79	494	12	46.6	121.9
282.3	6.00	0.263	295.6	0.79	565	14	46.4	121.4
284.4	5.79	0.217	295.6	0.79	657	16	46.3	120.9
285.3	5.89	0.211	295.6	0.79	687	17	46.2	120.6
286.3	5.79	0.190	295.6	0.79	744	19	46.1	120.4
287.3	5.62	0.171	295.6	0.79	804	20	46.1	120.2
288.3	5.79	0.164	295.6	0.79	858	21	46.0	120.0
289.3	5.84	0.155	295.6	0.81	913	23	45.9	119.7
290.5	8.17	0.203	295.6	0.76	973	24	45.8	119.3
291.7	5.95	0.135	295.6	0.81	1064	27	45.7	119.0
293.4	8.06	0.165	295.6	0.76	1175	29	45.6	118.5
294.7	6.22	0.115	295.6	0.81	1300	32	45.5	118.4
296.4	8.38	0.140	295.6	0.76	1435	36	45.4	117.9
298.7	6.22	0.088	295.6	0.81	1686	42	45.2	117.5
299.3	8.27	0.114	295.6	0.76	1721	43	45.2	117.2
300.7	6.44	0.081	295.6	0.81	1883	47	45.1	116.9
302.3	8.87	0.102	295.6	0.76	2063	52	45.0	116.5
303.7	6.38	0.067	295.6	0.81	2228	56	44.9	116.1
305.3	8.54	0.083	295.6	0.76	2433	61	44.7	115.7
306.7	7.79	0.067	295.6	0.81	2701	67	44.6	115.6

Table F. 3. Absolute vapor pressures p, standard (p^o = 0.1 MPa) molar vaporization enthalpies, $\Delta_l^g H_m^o$, and standard (p^o = 0.1 MPa) molar vaporization entropies, $\Delta_l^g S_m^o$, derived from boiling temperatures at different pressures compiled by SciFinder.

T/K	p/Pa	$\Delta_l^g H_m^o(T)$/kJ·mol^{-1}	$\Delta_l^g S_m^o(T)$/J·K^{-1}·mol^{-1}

2-(ethyl-amino)-ethanol [110-73-6]: $\Delta_l^g H_m^o$(298.15 K) = (60.0±5.0) kJ·mol^{-1}

$$\ln (p/p_{ref}) = \frac{307.5}{R} - \frac{80915.2}{RT} - \frac{69.9}{R} \ln \frac{T}{298.15} \; ; p_{ref} = 1 \text{ Pa}$$

351	1333	56.4	124.6
351	3600	56.4	132.9
353	1333	56.2	123.3
353	3600	56.2	131.6
375	13332	54.7	129.0
375	13332	54.7	129.0
376	13332	54.6	128.5
376	13332	54.6	128.5
442	101325	50.0	113.2
443	101325	50.0	113.0
443	101325	49.9	112.8

3-(dimethyl-amino)-1-propanol [3179-63-3]: $\Delta_l^g H_m^o$(298.15 K) = (53.4±0.8) kJ·mol^{-1}

$$\ln (p/p_{ref}) = \frac{297.3}{R} - \frac{75539.7}{RT} - \frac{74.4}{R} \ln \frac{T}{298.15} \; ; p_{ref} = 1 \text{ Pa}$$

341	2400	50.2	116.0
341	2666	50.2	116.9
342	2400	50.1	115.4
346	4400	49.8	117.9
349	4800	49.6	116.7

349	4400	49.6	116.0
354	4800	49.2	113.7
370	11332	48.0	111.6
373	11332	47.8	109.9
385	19998	46.9	108.3
386	19998	46.8	107.8
433	101325	43.3	100.1
436	101325	43.1	98.9
437	101325	43.1	98.7
437	101325	43.0	98.5
437	101325	43.0	98.5
437	101325	43.0	98.5
438	101325	42.9	98.1

3-(diethyl-amino)-1-propanol [622-93-5]: $\Delta_l^g H_m^o$(298.15 K) = (63.5±4.7) kJ·mol^{-1}

$$\ln (p/p_{ref}) = \frac{332.5}{R} - \frac{90642.1}{RT} - \frac{90.9}{R} \ln \frac{T}{298.15} \; ; p_{ref} = 1 \text{ Pa}$$

335	133	60.2	124.5
337	133	60.0	122.9
351	1600	58.7	132.8
353	2000	58.5	133.2
355	2666	58.4	134.2
357	2666	58.2	132.8
357	2666	58.2	132.8
358	3733	58.1	134.8
358	2666	58.1	132.0
358	2666	58.1	132.0
358	2666	58.1	132.0
359	2666	58.0	131.3
361	3733	57.8	132.7
363	3200	57.6	130.1
363	2666	57.6	128.6
365	3333	57.4	129.1
377	2133	56.4	117.4
379	2133	56.2	116.2
395	9333	54.7	118.8
462	101325	48.6	105.3
463	101325	48.6	105.1
463	101325	48.5	104.9

2-(n-propyl-amino)-ethanol [16369-21-4]: $\Delta_l^g H_m^o$(298.15 K) = (64.8±1.3) kJ·mol^{-1}

$$\ln (p/p_{ref}) = \frac{318.6}{R} - \frac{88146.8}{RT} - \frac{78.4}{R} \ln \frac{T}{298.15} \; ; p_{ref} = 1 \text{ Pa}$$

364	1467	59.6	128.6
365	1467	59.5	127.9
368	1733	59.3	127.3
370	1733	59.1	126.0
378	4000	58.5	127.9
380	4000	58.3	126.7
472	101325	51.1	108.4
472	101325	51.1	108.4
472	101325	51.1	108.4
473	101325	51.1	108.2
473	101325	51.1	108.0

2-(n-butyl-amino)-ethanol [111-75-1]: $\Delta_l^g H_m^o$(298.15 K) = (66.4±1.9) kJ·mol^{-1}

$$\ln (p/p_{ref}) = \frac{330.7}{R} - \frac{92233.2}{RT} - \frac{86.7}{R} \ln \frac{T}{298.15} \; ; p_{ref} = 1 \text{ Pa}$$

364	1467	60.7	131.5
365	1467	60.6	130.8

368	1733	60.3	130.1
370	1733	60.1	128.8
472	101325	51.3	108.8
472	101325	51.3	108.8
472	101325	51.3	108.7
473	101325	51.3	108.5
478	101325	50.8	106.3

2-(tert-butyl-amino)-ethanol [4620-70-6]: $\Delta_l^g H_m^o$(298.15 K) = (63.0±1.6) kJ·mol^{-1}

$$\ln(p/p_{ref}) = \frac{325.7}{R} - \frac{87870.6}{RT} - \frac{83.6}{R}\ln\frac{T}{298.15} ; p_{ref} = 1 \text{ Pa}$$

340	667	59.4	133.1
340	667	59.4	133.1
345	1867	59.0	137.9
354	2133	58.3	132.5
357	2666	58.0	132.3
363	3333	57.5	130.1
365	3333	57.3	128.8
449	101325	50.3	112.1
449	101325	50.3	112.1
450	101325	50.3	111.9
450	101325	50.2	111.7
450	101325	50.2	111.7

1-amino-2-methyl-2-propanol [2854-16-2]: $\Delta_l^g H_m^o$(298.15 K) = (56.6±0.7) kJ·mol^{-1}

$$\ln(p/p_{ref}) = \frac{303.8}{R} - \frac{77571.6}{RT} - \frac{70.4}{R}\ln\frac{T}{298.15} ; p_{ref} = 1 \text{ Pa}$$

338	2400	53.8	128.0
341	3333	53.6	129.0
342	3333	53.5	128.0
422	100658	47.9	113.4
423	101591	47.8	113.1
423	101325	47.8	113.0
423	101325	47.8	113.0
423	100658	47.8	113.0
424	101591	47.7	112.8
424	101325	47.7	112.8
424	101325	47.7	112.8

4-amino-4-methyl-2-pentanol [4404-98-2]: $\Delta_l^g H_m^o$(298.15 K) = (58.9±0.8) kJ·mol^{-1}

$$\ln(p/p_0) = \frac{319.3}{R} - \frac{84429.8}{RT} - \frac{85.8}{R}\ln\frac{T}{298.15} ; p_0 = 1 \text{ Pa}$$

344	1600	54.9	125.1
345	2000	54.8	126.3
345	1600	54.8	124.4
348	2000	54.6	124.5
348	2000	54.6	124.2
348	2133	54.6	124.7
349	2000	54.5	123.8
354	3200	54.0	124.0
356	3200	53.9	122.6
447	101325	46.1	103.1
448	101325	46.0	102.9
448	101325	46.0	102.7

2-amino-3-methyl-1-butanol [16369-05-4]: $\Delta_l^g H_m^o$(298.15 K) = (66.1±2.2) kJ·mol^{-1}

$$\ln(p/p_{ref}) = \frac{324.8}{R} - \frac{89505.8}{RT} - \frac{78.4}{R}\ln\frac{T}{298.15} ; p_{ref} = 1 \text{ Pa}$$

348	1067	62.2	140.9
350	1067	62.1	139.5
361	1467	61.2	134.3

363	1333	61.0	132.2
454	101325	53.9	118.8
454	95992	53.9	118.3
459	101325	53.5	116.6
459	95992	53.5	116.2

1-amino-3-methyl-2-butanol [17687-58-0]: $\Delta_l^g H_m^o$(298.15 K) = (60.4±1.9) kJ·mol^{-1}

$$\ln (p/p_{ref}) = \frac{310.7}{R} - \frac{83737.1}{RT} - \frac{78.4}{R}\ln\frac{T}{298.15} \; ; p_{ref} = 1 \text{ Pa}$$

349	1200	56.4	124.7
350	1200	56.3	124.0
351	1333	56.2	124.2
354	1333	56.0	122.1
463	101325	47.4	102.5
467	101325	47.1	101.0

2-amino-4-methyl-1-pentanol [502-32-9]: $\Delta_l^g H_m^o$(298.15 K) = (73.8±2.1) kJ·mol^{-1}

$$\ln (p/p_{ref}) = \frac{348.0}{R} - \frac{99623.0}{RT} - \frac{86.7}{R}\ln\frac{T}{298.15} \; ; p_{ref} = 1 \text{ Pa}$$

371	1467	67.4	146.6
467	101325	59.1	126.7

G. Supporting information to Chapter 7

Table G. 1. Compilation of data on molar heat capacities $C_{p,m}^o$ and differences $\Delta_l^g C_{p,m}^o$ of aminoalcohols, in J·K^{-1}·mol^{-1}, at 298.15 K.

compound	$C_{p,m}^o$(liq)	$-\Delta_l^g C_{p,m}^o$ [a]
2-amino-ethanol [141-43-5]	166.6 [211]	53.9
2-amino-1-propanol [6168-72-5]	203.5	63.5
2-amino-1-butanol [96-20-8]	235.4	71.8
2-amino-1-pentanol [16369-14-5]	267.3	80.1
2-amino-1-hexanol [5665-74-7]	299.2	88.4
2-amino-2-methyl-1-propanol [124-68-5]	236.1 [211]	72.1
1-amino-2-propanol [78-96-6]	205.0 [212]	63.5
1-amino-2-butanol [13552-21-1]	235.4	71.8
1-amino-2-pentanol [5343-35-1]	267.3	80.1
3-amino-1-propanol [156-87-6]	201.0 [212]	62.8
4-amino-1-butanol [13325-10-5]	241.9	73.5
5-amino-1-pentanol [2508-29-4]	273.8	81.8
6-amino-1-hexanol [4048-33-3]	305.7	90.1
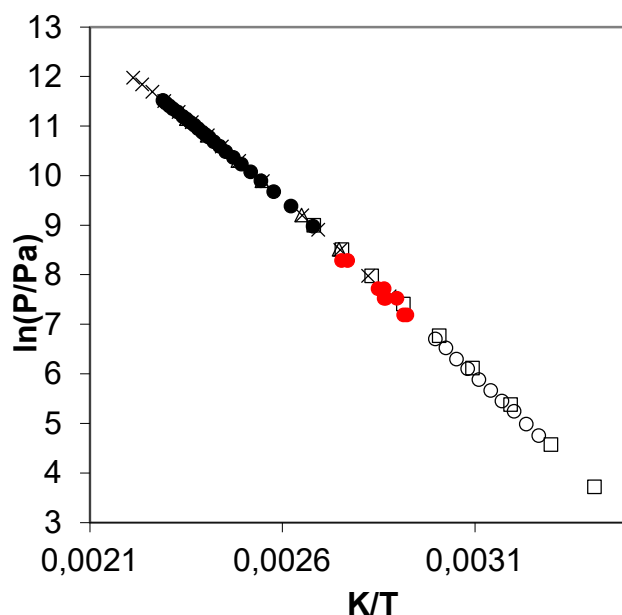
Figure G. 1. Temperature dependence of vapour pressures over the 2-amino-2-methyl-1-propanol: ○ - this work, transpiration; ● – ebulliometry [135]; × – ebulliometry [138]; Δ – ebulliometry [136]; □ – static [137]; ● – from experimental boiling temperatures reported at different pressures compiled by SciFinder [34].

Table G. 2. Results of transpiration method for aminoalcohols: absolute vapour pressures p, standard (p^o = 0.1 MPa) molar vaporization enthalpies and standard (p^o = 0.1 MPa) molar vaporization entropies.

$T/$ K^a	$m/$ mg^b	$V(N_2)^c /$ dm^3	$T_a/$ K^d	Flow/ $dm^3 \cdot h^{-1}$	$p/$ Pa^e	$u(p)/$ Pa^f	$\Delta_l^g H_m^o(T)$ $kJ \cdot mol^{-1}$	$\Delta_l^g S_m^o(T)$ $J \cdot K^{-1} \cdot mol^{-1}$
2-amino-2-methyl-1-propanol [124-68-5]: $\Delta_l^g H_m^o(298.15\ K) = (62.1 \pm 0.5)\ kJ \cdot mol^{-1}$								
$\ln(p/p_{ref}) = \frac{314.4}{R} - \frac{83574.0}{RT} - \frac{72.1}{R}\ln\frac{T}{298.15}$; p_{ref} = 1 Pa								
306.3	2.71	0.641	296.2	0.92	116.83	2.95	61.5	144.7
309.4	3.10	0.580	296.2	0.92	147.45	3.71	61.3	143.9
312.4	3.22	0.466	296.2	0.92	190.61	4.79	61.1	143.4
315.5	3.13	0.366	296.2	0.92	235.35	5.91	60.8	142.5
318.5	3.87	0.366	296.2	0.92	291.12	7.30	60.6	141.8
321.6	3.60	0.275	296.2	0.92	360.99	9.05	60.4	141.0
324.6	3.75	0.229	296.2	0.92	450.61	11.29	60.2	140.5
327.7	3.81	0.191	296.2	0.92	548.71	13.74	60.0	139.7
330.7	4.20	0.168	296.2	0.92	685.81	17.17	59.7	139.2
333.7	3.90	0.130	296.2	0.92	823.41	20.61	59.5	138.5
1-amino-2-butanol [13552-21-1]: $\Delta_l^g H_m^o(298.15\ K) = (63.7 \pm 0.4)\ kJ \cdot mol^{-1}$								
$\ln(p/p_{ref}) = \frac{317.3}{R} - \frac{85119.4}{RT} - \frac{71.8}{R}\ln\frac{T}{298.15}$; p_{ref} = 1 Pa								
278.3	0.95	3.665	295.6	2.75	7.29	0.21	65.1	154.9
283.2	0.85	2.016	295.7	2.75	11.72	0.32	64.8	153.6
283.7	1.01	2.346	295.8	2.56	12.00	0.33	64.8	153.2
288.2	1.02	1.535	296.1	2.56	18.56	0.49	64.4	152.2
290.2	1.19	1.493	295.8	2.56	22.20	0.58	64.3	151.6
293.2	1.06	0.958	295.8	2.87	30.55	0.79	64.1	151.3
295.2	1.30	1.024	295.1	2.56	35.11	0.90	63.9	150.5
298.2	1.11	0.640	295.8	2.56	47.89	1.22	63.7	150.1
298.3	1.06	0.626	296.2	1.98	46.71	1.19	63.7	149.8

301.2	1.70	0.795	296.3	2.81	59.02	1.50	63.5	149.0
303.4	1.79	0.702	295.8	2.81	70.33	1.78	63.3	148.4
303.6	1.46	0.572	295.8	2.54	70.63	1.79	63.3	148.2
303.7	1.66	0.636	296.2	2.54	72.03	1.83	63.3	148.4
305.2	1.13	0.375	296.6	1.02	83.78	2.12	63.2	148.2
308.2	0.85	0.229	296.0	0.92	102.04	2.58	63.0	147.2
308.2	0.98	0.252	296.1	1.01	107.38	2.71	63.0	147.6
308.2	2.68	0.702	296.0	2.81	105.45	2.66	63.0	147.4
313.2	1.26	0.229	296.2	0.92	152.28	3.83	62.6	146.1
313.2	1.47	0.252	296.1	1.01	161.67	4.07	62.6	146.5
318.2	2.13	0.252	295.9	1.01	232.87	5.85	62.3	145.3

4-amino-1-butanol [13325-10-5]: $\Delta_l^g H_m^o(298.15 \text{ K}) = (68.8\pm0.4) \text{ kJ·mol}^{-1}$

$$\ln(p/p_{ref}) = \frac{318.7}{R} - \frac{90738.5}{RT} - \frac{73.5}{R}\ln\frac{T}{298.15} \text{ ; } p_{ref} = 1 \text{ Pa}$$

288.2	0.40	5.017	294.8	2.69	2.21	0.06	69.6	152.3
291.3	0.41	3.808	294.8	2.69	2.95	0.08	69.3	151.3
294.1	0.41	2.945	294.8	2.64	3.80	0.10	69.1	150.5
297.3	0.42	2.198	294.8	2.64	5.28	0.16	68.9	149.9
298.2	0.41	2.047	294.8	2.67	5.51	0.16	68.8	149.3
300.2	0.39	1.582	294.8	2.64	6.86	0.20	68.7	149.1
303.2	0.54	1.691	294.8	2.67	8.86	0.25	68.5	148.2
304.2	0.44	1.275	294.8	2.64	9.49	0.26	68.4	147.8
305.2	0.42	1.081	294.8	2.70	10.57	0.29	68.3	147.7
306.1	0.44	1.063	294.8	2.71	11.37	0.31	68.2	147.5
308.2	0.43	0.887	294.8	2.66	13.44	0.36	68.1	146.8
308.2	0.43	0.878	294.8	2.70	13.58	0.36	68.1	146.9
309.3	0.41	0.769	294.8	2.71	14.65	0.39	68.0	146.5
311.2	0.42	0.653	294.8	2.70	17.49	0.46	67.9	146.2
312.3	0.42	0.608	294.8	2.70	18.92	0.50	67.8	145.8
313.3	0.56	0.709	294.8	2.66	21.68	0.57	67.7	146.0
315.2	0.40	0.449	294.8	2.70	24.32	0.63	67.6	145.2
318.4	0.58	0.486	294.8	2.65	32.63	0.84	67.3	144.8
321.3	0.53	0.359	294.8	2.70	40.71	1.04	67.1	144.0
324.3	0.59	0.314	294.8	2.70	51.50	1.31	66.9	143.4
327.2	0.63	0.270	294.8	2.70	64.65	1.64	66.7	142.8
329.2	0.74	0.270	294.8	2.70	75.34	1.91	66.5	142.4

5-amino-1-pentanol [2508-29-4]: $\Delta_l^g H_m^o(298.15 \text{ K}) = (72.3\pm0.3) \text{ kJ·mol}^{-1}$

$$\ln(p/p_{ref}) = \frac{328.4}{R} - \frac{96656.6}{RT} - \frac{81.8}{R}\ln\frac{T}{298.15} \text{ ; } p_{ref} = 1 \text{ Pa}$$

292.0	1.86	48.97	295.9	5.16	0.91	0.03	72.8	152.8
294.2	1.29	27.27	295.9	4.96	1.13	0.03	72.6	152.1
295.2	2.08	40.08	295.9	4.96	1.24	0.04	72.5	151.7
296.7	1.17	19.33	295.9	5.16	1.45	0.04	72.4	151.4
297.3	2.23	34.71	295.9	4.96	1.53	0.04	72.3	151.2
299.7	1.39	17.01	295.9	5.16	1.95	0.05	72.1	150.6
301.2	2.71	29.84	295.9	4.96	2.17	0.06	72.0	149.9
305.2	2.53	18.47	295.9	2.31	3.26	0.09	71.7	149.1
308.7	1.49	8.162	295.9	5.16	4.35	0.11	71.4	147.9
311.7	1.29	5.388	295.9	2.31	5.70	0.17	71.2	147.1
314.7	1.66	5.311	295.9	2.31	7.47	0.21	70.9	146.4
317.7	1.44	3.541	295.9	2.31	9.68	0.27	70.7	145.6
321.8	1.31	2.234	295.9	5.16	14.01	0.38	70.3	144.8
322.8	0.76	1.231	295.9	2.31	14.76	0.39	70.3	144.3
325.0	1.30	1.718	295.9	5.16	18.04	0.48	70.1	144.0
327.9	1.29	1.347	295.9	2.31	22.79	0.59	69.8	143.3
329.9	1.50	1.375	295.9	5.16	26.01	0.68	69.7	142.6

329.9	1.50	1.375	295.9	5.16	26.01	0.68	69.7	142.6
333.0	1.66	1.203	295.9	5.16	32.95	0.85	69.4	141.8
333.1	1.59	1.116	295.9	2.31	33.91	0.87	69.4	142.0

Table G. 3. Vapor pressures p, standard (p^o = 0.1 MPa) molar vaporization enthalpies, $\Delta_l^g H_m^o$, and standard (p^o = 0.1 MPa) molar vaporization entropies, $\Delta_l^g S_m^o$ obtained by the approximation of data collected from SciFinder [34].

T/ K	p/Pa	$\Delta_l^g H_m^o(T)$ /kJ·mol^{-1}	$\Delta_l^g S_m^o(T)$ /J·K^{-1}·mol^{-1}
2-amino-1-propanol [6168-72-5]: $\Delta_l^g H_m^o$(298.15 K) = (59.9±1.3) kJ·mol^{-1}			
$\ln(p/p_{ref}) = \frac{297.8}{R} - \frac{78810.3}{RT} - \frac{63.5}{R}\ln\frac{T}{298.15}$; p_{ref} = 1 Pa			
353	2000	56.4	127.1
371	5999	55.2	125.4
446	101325	50.5	113.3
448	101325	50.4	112.7
449	101325	50.3	112.1
1-amino-2-butanol [13552-21-1]: $\Delta_l^g H_m^o$(298.15 K) = (62.8±0.9) kJ·mol^{-1}			
$\ln(p/p_{ref}) = \frac{272.4}{R} - \frac{66052.3}{RT} - \frac{59.7}{R}\ln\frac{T}{298.15}$; p_{ref} = 1 Pa			
348	1600	59.2	135.7
350	1600	59.1	134.3
355	2666	58.7	135.1
356	2666	58.6	134.5
441	101325	52.5	119.2
441	95992	52.5	118.7
442	101325	52.4	118.7
443	101325	52.4	118.3
443	95992	52.4	117.8
1-amino-2-pentanol [5343-35-1]: $\Delta_l^g H_m^o$(298.15 K) = (67.8±5.3) kJ·mol^{-1}			
$\ln(p/p_{ref}) = \frac{327.8}{R} - \frac{91681.0}{RT} - \frac{80.1}{R}\ln\frac{T}{298.15}$; p_{ref} = 1 Pa			
348	467	63.8	138.6
353	533	63.4	136.0
356	1333	63.2	141.4
469	101325	54.1	115.6
2-amino-1-butanol [96-20-8]: $\Delta_l^g H_m^o$(298.15 K) = (64.0±1.2) kJ·mol^{-1}			
$\ln(p/p_{ref}) = \frac{314.6}{R} - \frac{85370.5}{RT} - \frac{71.8}{R}\ln\frac{T}{298.15}$; p_{ref} = 1 Pa			
324	267	62.1	142.3
325	267	62.0	141.5
344	1067	60.7	138.5
351	1333	60.2	135.4
353	1333	60.0	134.0
353	1067	60.0	132.2
355	1333	59.9	132.7
360	2400	59.5	134.2
360	2400	59.5	134.2
449	101325	53.1	118.4
451	101325	53.0	117.5
451	101325	53.0	117.5
452	101325	52.9	117.1
2-amino-1-hexanol [5665-74-7]: $\Delta_l^g H_m^o$(298.15 K) = (74.3±1.6) kJ·mol^{-1}			
$\ln(p/p_{ref}) = \frac{352.0}{R} - \frac{100686.4}{RT} - \frac{88.4}{R}\ln\frac{T}{298.15}$; p_{ref} = 1 Pa			
371	1600	67.9	148.5
463	98658	59.7	128.9

464	101325	59.7	128.9

3-amino-1-propanol [156-87-6]: $\Delta_l^g H_m^o$(298.15 K) = (62.9±1.3) kJ·mol^{-1}

$$\ln (p/p_{ref}) = \frac{300.5}{R} - \frac{81632.4}{RT} - \frac{62.8}{R} \ln \frac{T}{298.15} \; ; p_{ref} = 1 \text{ Pa}$$

333	267	60.7	133.0
333	400	60.7	136.3
354	1600	59.4	133.3
356	1600	59.3	132.0
358	1333	59.1	129.2
358	1733	59.1	131.4
358	1333	59.1	129.2
358	1600	59.1	130.7
358	1600	59.1	130.7
360	1733	59.0	130.1
363	1333	58.8	126.1
368	3333	58.5	130.7
371	4266	58.3	130.9
372	2666	58.3	126.4
376	4266	58.0	128.0
385	5333	57.4	124.8
386	5333	57.4	124.2
458	101325	52.9	115.5
459	101325	52.8	115.1
460	101325	52.7	114.7
461	101325	52.7	114.5
461	101325	52.7	114.3

4-amino-1-butanol [13325-10-5]: $\Delta_l^g H_m^o$(298.15 K) = (69.7±2.9) kJ·mol^{-1}

$$\ln (p/p_{ref}) = \frac{322.1}{R} - \frac{91654.7}{RT} - \frac{73.5}{R} \ln \frac{T}{298.15} \; ; p_{ref} = 1 \text{ Pa}$$

328	40	67.5	140.8
331	40	67.3	138.2
343	667	66.4	151.9
345	667	66.3	150.4
368	1333	64.6	139.6
368	1333	64.6	139.6
368	667	64.6	133.8
373	1333	64.2	136.2
377	1333	63.9	133.6
377	2000	63.9	137.0
378	1333	63.9	133.0
380	1867	63.7	134.5
380	1333	63.7	131.7
382	1867	63.6	133.2
383	2400	63.5	135.0
383	2400	63.5	134.8
475	101325	56.7	119.5
477	101325	56.6	118.7
479	101325	56.4	117.9
480	100658	56.4	117.4
481	100658	56.3	117.0

5-amino-1-pentanol [2508-29-4]: $\Delta_l^g H_m^o$(298.15 K) = (74.7±1.5) kJ·mol^{-1}

$$\ln (p/p_{ref}) = \frac{338.2}{R} - \frac{99133.0}{RT} - \frac{81.8}{R} \ln \frac{T}{298.15} \; ; p_{ref} = 1 \text{ Pa}$$

352	133	70.3	144.7
354	133	70.2	143.1
378	1067	68.2	142.6
380	1333	68.0	143.1

381	1067	68.0	140.5
383	1333	67.8	141.0
385	1333	67.6	139.7
387	1733	67.5	140.5
388	1733	67.4	139.9
392	2400	67.1	140.0
392	2266	67.1	139.5
393	2266	67.0	138.9
395	2133	66.8	137.1
395	2400	66.8	138.1
398	2266	66.6	135.7
399	2866	66.5	137.0
401	2866	66.3	135.8
494	101325	58.7	118.9
494	99992	58.7	118.8
495	101325	58.7	118.7
495	101325	58.6	118.5

6-amino-1-hexanol, 4048-33-3 (SF): $\Delta_l^g H_m^o(298.15 \text{ K}) = (76.3 \pm 2.1) \text{ kJ·mol}^{-1}$

$$\ln(p/p_{ref}) = \frac{346.6}{R} - \frac{103198.6}{RT} - \frac{90.1}{R} \ln \frac{T}{298.15}; p_{ref} = 1 \text{ Pa}$$

396	1600	67.5	136.0
399	1867	67.2	135.3
400	1867	67.1	134.7
403	2000	66.9	133.4
410	2666	66.2	131.4
412	2666	66.1	130.2
508	101325	57.4	113.1

2-amino-2-methyl-1-propanol [124-68-5]: $\Delta_l^g H_m^o(298.15 \text{ K}) = (62.9 \pm 0.8) \text{ kJ·mol}^{-1}$

$$\ln(p/p_{ref}) = \frac{316.6}{R} - \frac{84446.5}{RT} - \frac{72.1}{R} \ln \frac{T}{298.15}; p_{ref} = 1 \text{ Pa}$$

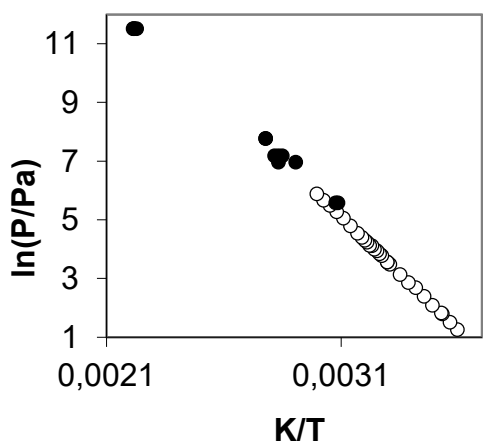|			
342	1333	59.8	138.8
343	1333	59.7	138.1
345	1867	59.6	139.5
349	1867	59.3	137.0
349	2266	59.3	138.3
349	1867	59.3	136.7
351	2266	59.1	136.9
361	4000	58.4	135.0
363	4000	58.3	133.7
431	101325	53.4	123.9
436	101325	53.0	121.6
437	101325	53.0	121.4
438	101325	52.9	121.0
438	101325	52.9	120.7
439	101325	52.8	120.5
439	101325	52.8	120.5
440	101325	52.7	119.9

Figure G. 2. Temperature dependence of vapor pressures over the 2-amino-1-butanol: ○ – transpiration [155]; ● – from experimental boiling temperatures reported at different pressures compiled by SciFinder [34].

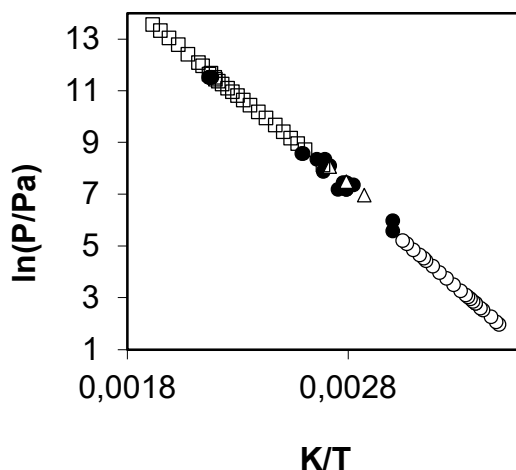**Figure G. 3.** Temperature dependence of vapor pressures over the 3-amino-1-propanol: ○ – transpiration [155]; ● – boiling points at different pressures compiled by SciFinder [34]; Δ – ebulliometry [142]; □ – ebulliometry [143].
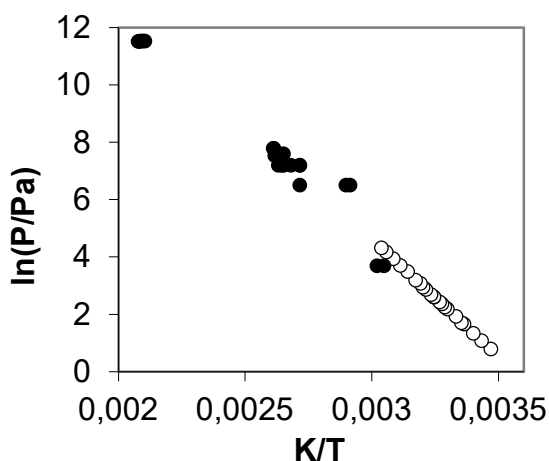

Figure G. 4. Temperature dependence of vapor pressures over the 4-amino-1-butanol: ○ – this work, transpiration; ● – boiling points at different pressures compiled by SciFinder [34].
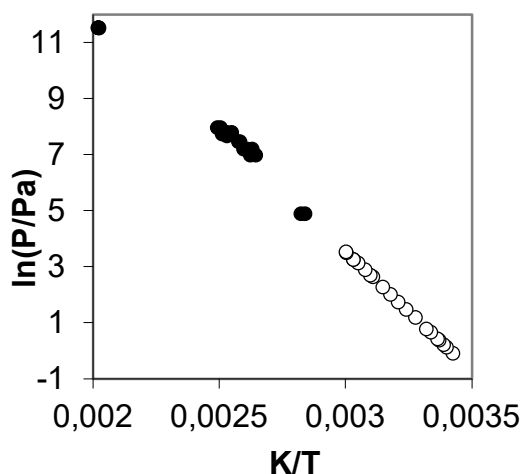

Figure G. 5. Temperature dependence of vapor pressures over the 5-amino-1-pentanol: ○ – this work, transpiration; ● – boiling points at different pressures compiled by SciFinder [34].

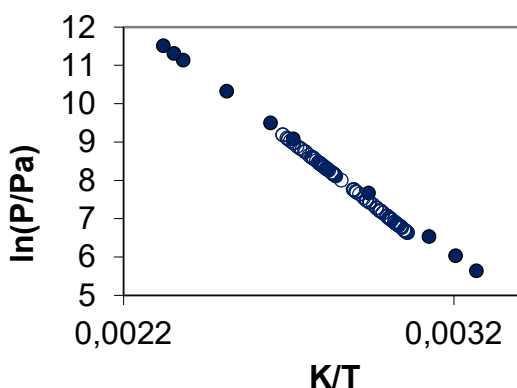**Figure G. 6.** Temperature dependence of vapor pressures over the 1-amino-2-propanol: ○ - static [155]; ● – method is not available [43].

Table G. 4. Kovat´s indices, J_x, of aminoalcohols measured on columns DB-1.

CAS	Compound	J_x	J_x	J_x	J_x
T, K		363	373	383	393
6168-72-5	2-amino-1-propanol	702	702	703	704
96-20-8	2-amino-1-butanol	806	807	808	809
16369-14-5	2-amino-1-pentanol	904	905	906	907
5665-74-7	2-amino-1-hexanol	1005	1006	1007	1009
78-96-6	1-amino-2-propanol	691	691	692	693
13552-21-4	1-amino-2-butanol	794	795	796	797

Table G. 5. Compilation of vaporization enthalpies, $\Delta_l^g H_m^o$(298.15 K), of n-alkanes, n-alcohols, n-alkylamines used for correlations with the chain length (in kJ·mol^{-1}).

compound	$\Delta_l^g H_m^o$(298.15 K) [a]	compound	$\Delta_l^g H_m^o$(298.15 K) [a]	compound	$\Delta_l^g H_m^o$(298.15 K) [a]
		methanol	37.83	methylamine	23.85
ethane		ethanol	42.5	ethylamine	26.7
n-propane	16.25	1-propanol	47.5	n-propylamine	31.3
n-butane	22.4	1-butanol	52.4	n-butylamine	35.7
n-pentane	26.75	1-pentanol	56.9	n-pentylamine	40.1
n-hexane	31.7	1-hexanol	61.1 [213]	n-hexylamine	45.1
n-heptane	36.7	1-heptanol	66.8 [213]	n-heptylamine	50.0
n-octane	41.5	1-octanol	70.1 [213]	n-octylamine	54.6
n-nonane	46.4	1-nonanol	76.9 [213]	n-nonylamine	60.0
n-decane	51.4	1-decanol	80.9 [213]	n-decylamine	64.9
n-undecane	56.4	1-undecanol	84.7 [213]	n-undecylamine	70.0

[a] From compilation by Majer and Svoboda [191].

Table G. 6. Compilation of vaporization enthalpies, $\Delta_l^g H_m^o$(298.15 K), of aminoalcohols used for correlations with the chain length (in kJ·mol^{-1}).

CAS	compound	N_C	$\Delta_l^g H_m^o$(298.15 K) [a]
78-96-6	1-amino-2-propanol	3	59.3
13552-21-1	1-amino-2-butanol	4	63.7
5343-35-1	1-amino-2-pentanol	5	68.2
72799-62-3	1-amino-2-hexanol	6	73.2
51411-48-4	1-amino-2-heptanol	7	78.0
4255-35-0	1-amino-2-octanol	8	82.8
156-87-6	3-amino-1-propanol	3	62.2
133325-10-5	4-amino-1-butanol	4	68.8
2508-29-4	5-amino-1-pentanol	5	72.3
4048-33-3	6-amino-1-hehxanol	6	76.9

[a] From Table 37.

Table G. 7. Thermochemical data at T = 298.15 K (p° =0.1 MPa) for aminoalcohols (in kJ·mol-1).

Compounds	$\Delta_f H_m^o$(g)$_{G4}$ [a]	$\Delta_l^g H_m^o$	$\Delta_f H_m^o$(liq) [b]
2-amino-1-propanol	-241.1±3.5	59.7±1.2	-300.8±3.7
2-amino-1-butanol	-261.3±3.5	64.9±0.6	-325.7±3.6
2-amino-1-pentanol	-353.4±3.5	69.1±1.4	-353.4±3.8

[a] Data from reference [159], [b] data from Table 37.

Table G. 8. Thermochemical data at $T = 298.15$ K ($p° = 0.1$ MPa) for pyrazine derivatives available in the literature [146,147] (in kJ·mol-1).

Compounds	$\Delta_f H_m^o$(liq)
methyl-pyrazine	118.7±3.5
ethyl-pyrazine	98.1±2.1
n-propyl-pyrazine	66.5±3.6
2,5-di-methyl-pyrazine	67.0±2.0
2,5-di-ethyl-pyrazine	25.8±3.0
2,5-di-n-propyl-pyrazine	-28.6±3.0

H. Supporting information to Chapter 8

Table H. 1. Compilation of data on molar heat capacities $C_{p,m}^o$(cr or liq) (in J·K^{-1}·mol^{-1}) at $T = 298.15$ K for indole, indoline, and 8H-indole.

indole		indoline		8H-indole	
T, K	$C_{p,m}^o$(cr or liq)	T, K	$C_{p,m}^o$(liq)	T, K	$C_{p,m}^o$(liq)
solid		**liquid**		**liquid**	
240	121.99	236	202.16	259	238.14
244	124.57	238	202.70	261	238.08
249	118.24	243	203.88	266	238.04
254	118.26	248	205.19	271	238.24
259	133.68	253	206.48	276	238.49
264	137.55	258	207.94	281	238.93
269	140.55	263	209.29	286	240.47
274	143.70	268	210.68	291	241.03
279	147.32	273	212.07	296	241.74
284	150.58	278	213.63	301	243.09
289	154.22	283	215.11	307	244.16
294	158.13	288	216.58	311	244.79
298	162.15	293	218.04	316	246.36
314	178.41	298	219.50	321	248.25
318	181.83	303	221.02	326	249.16
liquid		308	222.67	331	250.20
341	207.03	313	224.22	336	251.80
343	207.87	318	225.72	341	253.57
345	208.51	323	227.13	346	255.39
347	209.29	328	229.02	350	256.66
349	210.18	333	230.57		
		338	232.10		
		343	233.61		
		348	235.14		

Table H. 2. Compilation of data on molar heat capacities $C^o_{p,m}$(cr or liq) and heat capacity differences $\Delta^g_l C^o_{p,m}$ (in J·K⁻¹·mol⁻¹) at T = 298.15 K for 2-methyl-indole, 2-methyl-indoline and 2-methyl-8H-indole.

2-Me-indole		2-Me-indoline		2-Me-8H-indole	
T, K	$C^o_{p,m}$(cr or liq)	T, K	$C^o_{p,m}$(liq)	T, K	$C^o_{p,m}$(liq)
solid		**liquid**		**liquid**	
240	143.34	235	231.49	237	249.63
244	145.64	240	233.03	242	250.36
249	148.48	245	234.58	247	251.31
254	151.33	250	236.18	252	252.42
259	154.25	255	237.63	257	253.63
264	157.51	260	239.27	262	254.89
269	160.14	265	240.78	267	256.19
274	162.79	270	242.33	272	257.65
279	165.96	275	243.75	277	258.99
284	168.69	280	245.43	282	260.69
289	171.91	285	247.03	287	262.43
294	174.77	290	248.58	292	264.29
299	178.47	295	250.12	297	266.16
304	184.03	300	251.61	302	268.01
309	189.86	305	253.49	307	270.09
313	196.09	310	255.02	312	272.37
		315	256.53	317	274.62
		320	258.09	322	277.02
		325	259.56	327	279.20
		330	261.55	332	281.86
		335	263.29	337	284.34
		340	264.96	342	286.91
		345	266.48	347	289.49
		349	267.71	350	291.02

Table H. 3. Results from the transpiration method: absolute vapour pressures p_i, standard molar sublimation/vaporization enthalpies $\Delta^g_{cr,l}H^o_m$ and standard molar sublimation/vaporization entropies $\Delta^g_{cr,l}S^o_m$.

$T/$ K[a]	$m/$ mg[b]	$V(N_2)^c /$ dm³	$T_a/$ K[d]	Flow/ dm³·h⁻¹	$p_i/$ Pa[e]	$u(p_i)/$ Pa[f]	$\Delta^g_{cr/l}H^o_m(T)/$ kJ·mol⁻¹	$\Delta^g_{cr/l}S^o_m(T)/$ J·K⁻¹·mol⁻¹

indole, $\Delta^g_{cr}H^o_m(298.15\ \text{K}) = (75.4 \pm 1.3)$ kJ·mol⁻¹

$$\ln(p_i / p_{ref}) = \frac{283.3}{R} - \frac{82861.1}{RT} - \frac{25.1}{R}\ln\frac{T}{298.15}$$

$T/$ K[a]	$m/$ mg[b]	$V(N_2)^c /$ dm³	$T_a/$ K[d]	Flow/ dm³·h⁻¹	$p_i/$ Pa[e]	$u(p_i)/$ Pa[f]	$\Delta^g_{cr/l}H^o_m(T)/$ kJ·mol⁻¹	$\Delta^g_{cr/l}S^o_m(T)/$ J·K⁻¹·mol⁻¹
293.1	0.22	4.081	294.5	2.95	1.14	0.03	75.5	163.0
298.3	0.23	2.442	294.6	2.93	1.93	0.05	75.4	162.5
301.2	0.22	1.866	296.9	0.99	2.53	0.07	75.3	162.0
303.2	0.22	1.465	295.4	2.93	3.18	0.08	75.3	162.1
306.2	0.37	1.856	292.8	2.93	4.15	0.11	75.2	161.7
308.2	0.24	0.977	295.1	2.93	5.18	0.15	75.1	161.7
313.1	0.29	0.733	296.6	2.93	8.26	0.23	75.0	161.4
318.2	0.30	0.496	295.7	0.99	12.79	0.34	74.9	160.8
321.2	1.41	1.784	296.3	0.99	16.67	0.44	74.8	160.6
323.2	0.23	0.248	295.9	0.99	19.91	0.52	74.7	160.5

<p align="center">indoline. $\Delta_l^g H_m^o(298.15\ \text{K}) = (60.5 \pm 0.6)\ \text{kJ·mol}^{-1}$</p>

$$\ln(p_i / p_{ref}) = \frac{290.8}{R} - \frac{80648.7}{RT} - \frac{67.7}{R}\ln\frac{T}{298.15}$$

288.7	1.51	6.000	296.5	3.60	5.27	0.16	61.1	129.8
293.8	1.27	3.333	296.5	2.50	7.94	0.22	60.8	128.3
296.6	1.22	2.500	296.5	2.50	10.12	0.28	60.6	127.8
300.5	1.10	1.667	296.5	2.50	13.69	0.37	60.3	126.8
305.2	1.48	1.542	296.5	2.50	19.91	0.52	60.0	125.7
308.5	1.43	1.173	296.5	2.01	25.33	0.66	59.8	124.9
315.2	2.47	1.208	296.5	2.50	42.34	1.08	59.3	123.6
320.5	1.96	0.670	296.5	2.01	60.62	1.54	59.0	122.4
325.6	2.76	0.670	296.5	2.01	85.18	2.15	58.6	121.3
328.2	2.30	0.462	296.5	1.32	103.02	2.60	58.4	120.9
333.1	3.54	0.510	296.5	1.53	143.61	3.62	58.1	120.0
335.2	3.05	0.383	296.5	1.15	164.25	4.13	58.0	119.6

<p align="center">8H-indole, $\Delta_l^g H_m^o(298.15\ \text{K}) = (53.5 \pm 0.7)\ \text{kJ·mol}^{-1}$</p>

$$\ln(p_i / p_{ref}) = \frac{293.7}{R} - \frac{75474.3}{RT} - \frac{73.6}{R}\ln\frac{T}{298.15}$$

277.9	1.60	1.210	293.5	3.03	26.74	0.69	55.0	129.6
281.9	1.62	0.857	293.7	3.03	38.02	0.98	54.7	128.6
283.3	3.00	1.462	293.5	3.03	41.06	1.05	54.6	128.0
288.6	3.55	1.109	293.6	3.03	63.54	1.61	54.2	126.7
292.7	3.42	0.775	294.0	1.72	87.16	2.20	53.9	125.7
295.3	3.65	0.650	293.6	1.03	110.65	2.79	53.7	125.4
299.4	6.67	0.918	294.0	1.72	142.71	3.59	53.4	124.0
302.3	3.89	0.445	293.2	1.03	171.48	4.31	53.2	123.1
305.6	5.40	0.482	294.2	1.07	220.17	5.53	53.0	122.5
310.6	4.98	0.321	294.5	1.07	304.07	7.63	52.6	121.2
311.9	4.23	0.250	294.2	1.07	331.19	8.30	52.5	120.9
318.0	7.74	0.303	294.3	1.07	498.16	12.48	52.1	119.6
319.6	8.92	0.321	294.6	1.07	542.84	13.60	52.0	119.2
324.7	12.31	0.321	294.3	1.07	745.85	18.67	51.6	118.1
329.2	16.36	0.321	294.7	1.07	990.49	24.79	51.2	117.3

<p align="center">2-methyl-indole, $\Delta_{cr}^g H_m^o(298.15\ \text{K}) = (85.1 \pm 1.2)\ \text{kJ·mol}^{-1}$</p>

$$\ln(p_i / p_{ref}) = \frac{304.5}{R} - \frac{93204.6}{RT} - \frac{27.1}{R}\ln\frac{T}{298.15}$$

298.3	0.14	6.687	294.7	2.95	0.38	0.01	85.1	181.6
301.3	0.14	4.769	296.2	2.95	0.54	0.02	85.0	181.4
303.1	0.07	2.105	293.4	2.94	0.66	0.02	85.0	181.2
305.2	0.13	2.852	296.1	2.95	0.85	0.03	84.9	181.2
308.1	0.13	2.154	294.3	2.94	1.14	0.03	84.9	180.8
310.2	0.13	1.721	297.0	2.95	1.44	0.04	84.8	180.7
313.0	0.15	1.469	295.4	2.94	1.92	0.05	84.7	180.3
318.1	0.15	0.881	294.9	2.94	3.21	0.09	84.6	179.9
323.1	0.12	0.435	295.5	1.00	5.23	0.16	84.4	179.4
325.1	0.14	0.418	296.5	1.00	6.33	0.18	84.4	179.3
328.0	0.16	0.351	295.7	1.00	8.45	0.24	84.3	179.0
329.0	0.20	0.393	296.0	1.00	9.36	0.26	84.3	179.1
330.1	0.14	0.259	296.3	1.00	10.43	0.29	84.3	179.0

<p align="center">2-methyl-indoline, $\Delta_l^g H_m^o(298.15\ \text{K}) = (63.0 \pm 0.4)\ \text{kJ·mol}^{-1}$</p>

$$\ln(p_i / p_{ref}) = \frac{307.7}{R} - \frac{85660.1}{RT} - \frac{75.9}{R}\ln\frac{T}{298.15}$$

283.2	0.41	2.557	295.4	2.95	2.99	0.08	64.2	140.0
285.2	0.48	2.508	295.6	2.95	3.60	0.09	64.0	139.4
288.1	0.47	1.819	295.5	2.95	4.76	0.12	63.8	138.6
292.1	0.50	1.353	295.6	3.01	6.89	0.20	63.5	137.7
293.1	0.59	1.475	294.4	2.95	7.39	0.21	63.4	137.3
296.1	0.56	1.052	297.0	3.01	9.98	0.27	63.2	136.8
298.1	0.58	0.934	295.4	2.95	11.48	0.31	63.0	136.1
303.1	0.43	0.451	296.0	1.00	17.72	0.47	62.7	134.9
308.1	0.46	0.318	295.8	1.00	26.57	0.69	62.3	133.7
313.1	0.53	0.251	295.9	1.00	38.95	1.00	61.9	132.4
318.0	1.36	0.451	296.2	1.00	55.84	1.42	61.5	131.2
323.2	1.31	0.301	296.6	1.00	80.31	2.03	61.1	129.9
328.1	1.54	0.251	296.7	1.00	113.76	2.87	60.8	128.8
333.0	2.13	0.251	296.8	1.00	157.47	3.96	60.4	127.7

2-methyl-8H-indoline, $\Delta_l^g H_m^o(298.15\ \text{K}) = (57.8 \pm 0.8)\ \text{kJ·mol}^{-1}$

$$\ln(p_i/p_{ref}) = \frac{311.3}{R} - \frac{81609.0}{RT} - \frac{79.9}{R}\ln\frac{T}{298.15}$$

275.1	0.30	0.432	295.8	1.00	12.78	0.34	59.6	142.2
278.1	1.85	1.987	294.7	2.98	16.85	0.45	59.4	141.3
280.2	0.37	0.333	295.9	1.00	20.28	0.53	59.2	140.7
283.2	0.44	0.299	296.1	1.00	26.41	0.69	59.0	139.8
287.1	1.50	0.749	296.1	1.00	35.82	0.92	58.7	138.4
287.1	2.16	1.041	295.8	0.99	37.13	0.95	58.7	138.7
288.2	1.94	0.864	296.5	3.05	40.17	1.03	58.6	138.2
289.2	1.65	0.661	296.4	0.99	44.68	1.14	58.5	138.1
290.1	1.72	0.628	294.2	0.99	48.67	1.24	58.4	138.0
292.1	1.36	0.429	295.3	0.99	56.21	1.43	58.3	137.3
292.2	1.64	0.516	296.4	1.00	56.65	1.44	58.3	137.2
293.1	1.63	0.479	294.2	0.99	60.29	1.53	58.2	136.9
295.1	1.59	0.396	295.4	0.99	71.18	1.80	58.0	136.4
297.2	1.20	0.251	294.8	1.00	84.65	2.14	57.9	135.9
297.2	1.60	0.349	296.8	1.00	81.62	2.07	57.9	135.6
300.1	1.69	0.281	296.1	0.99	106.94	2.70	57.6	135.2
302.1	1.77	0.251	294.8	1.00	124.70	3.14	57.5	134.6
303.1	2.26	0.299	296.6	1.00	134.23	3.38	57.4	134.3
308.1	2.71	0.250	296.8	1.00	192.75	4.84	57.0	133.0
313.2	4.04	0.251	295.2	1.00	283.28	7.11	56.6	131.9

Table H. 4. Formula, density ρ ($T = 293$ K), and massic heat capacity C_p ($T = 298.15$ K), of the materials used in the present study. [a]

Compounds	Formula	ρ	c_p
		g·cm^{-3}	J·K^{-1} g^{-1}
indole (cr)	C_8H_7N	1.19 [190]	1.39
indoline (liq)	C_8H_9N	1.06 [214]	1.84
8H-indole (liq)	$C_8H_{15}N$	1.07 [215]	1.94
2-methyl-indole (cr)	C_9H_9N	1.07 [171]	1.37
2-methyl-indoline (liq)	$C_9H_{11}N$	0.99[c]	1.89
2-methyl-8H-indole (liq)	$C_9H_{17}N$	0.89[c]	1.91
polyethylene	$CH_{1.93}$	0.92	2.53
cotton	$CH_{1.774}O_{0.887}$	1.50	1.67

[a] Data for density and specific heat capacity of auxiliary materials are from our previous work [216]: specific energy of combustion $\Delta_c u°$(cotton) = -16945.2 J·g^{-1}; $u(\Delta_c u°)$ = 4.2 J·g^{-1}. The specific energy of combustion $\Delta_c u°$(polyethylene) = -46357.3 J·g^{-1}; $u(\Delta_c u°)$ = 3.6 J·g^{-1}.

Table H. 5. Results for typical combustion experiments at $T = 298.15$ K ($p° = 0.1$ MPa).

	indole	indoline	8H-indole	2-Me-indole	2-Me-indoline	2-Me-8H-indole
m (substance) /g	0.306886	0.343793	0.304871	0.439951	0.272299	0.206533
m'(cotton) /g	0.002179	0.002165	0.002289	0.002717	0.002313	0.002411
m"(polyethylene)/g	0.237376	0.218594	0.253545	-	0.341354	0.371671
T^i	298.14613	298.14697	298.12980	298.14910	298.15741	298.13478
T^f	299.76760	299.76241	299.82245	299.32132	298.15741	299.92875
ΔT_c /K	1.49562	1.56304	1.64719	1.10527	1.78026	1.74863
$(\varepsilon_{calor})\cdot(-\Delta T_c)$ /J	-22136.75	-23134.65	-24380.14	-16359.13	-26349.68	-25881.49
$(\varepsilon_{cont})\cdot(-\Delta T_c)$ /J	-23.60	-25.90	-27.62	-16.64	-30.06	-29.44
ΔU_{decomp} HNO$_3$ /J	28.67	29.27	26.28	26.88	25.68	22.10
ΔU_{corr} /J	9.77	9.03	7.24	8.48	9.50	7.84
$-m'\cdot\Delta_c u'$ /J	36.92	36.69	38.79	46.04	39.19	40.85
$-m"\Delta_c u'$ /J	11004.13	10133.43	11753.66	-	15824.25	17229.66
$\Delta_c u°$ /(J·g^{-1})	-36128.4	-37674.2	-41269.2	-37036.8	-38491.2	-41690.9

Table H. 6. All results for combustion experiments at $T = 298.15$ K ($p° = 0.1$ MPa) for the crystalline compounds indole and 2-methyl-indole.

	indole	2-Me-indole
	36128.4	37036.8
	36144.4	37036.4
	36126.6	37023.1
	36129.9	37046.0
	36128.0	37039.3
$\Delta_c u°$(cr) /(J·g^{-1}) [a]	-36131.5±3.3	-37036.8±3.7
$\Delta_c H_m°$(cr) /(kJ·mol^{-1}) [b]	-4235.8±1.3	-4862.6±1.5
$\Delta_f H_m°$(cr) /(kJ·mol^{-1}) [b]	87.3±1.6	34.8±1.91

Table H. 7. All results for combustion experiments at $T = 298.15$ K ($p° = 0.1$ MPa) for the liquid indole derivatives.

	indoline	H8-indole	2-Me-indoline	2-Me-H8-indole
	37674.2	41269.2	38491.2	41690.9
	37670.9	41266.9	38481.0	41700.3
	37663.9	41260.8	38473.8	41680.4
	37674.2	41253.1	38475.7	41693.8
	37683.1	41252.3	38481.7	41683.3
$\Delta_c u°$(liq) /(J·g^{-1})	-37673.3±3.1	-41260.5±3.5	-38480.7±3.0	-41689.7±3.6
$\Delta_c H_m°$(liq) /(kJ·mol^{-1})	-4493.6±1.3	-5174.3±1.5	-5130.8±1.5	-5814.1±1.8
$\Delta_f H_m°$(liq) /(kJ·mol^{-1})	59.3±1.7	-117.5±1.8	17.2±1.9	-157.1±2.1

Table H. 8. Correlation of vaporization enthalpies $\Delta_l^g H_m^o$(298.15 K) of cyclic alkanes and aromatics with their Kovats´s indices J_x.

	J_x [a]	$\Delta_l^g H_m^o$(298.15 K)$_{exp}$	$\Delta_l^g H_m^o$(298.15 K)$_{calc}$ [b]	Δ
		kJ·mol^{-1}	kJ·mol^{-1}	kJ·mol^{-1}
cyclopentane	568	28.7±0.1 [191]	28.7	0.0
methyl-cyclopentane	634	31.8±0.1 [191]	31.6	0.2
indane	1015	49.0±0.2 [79]	48.5	0.5
2-methyl-indane	1085		**51.6±1.0**	
indene	1036	50.3±0.2 [179]	49.4	0.9
2-methyl-indene	1067		**50.8±1.0**	
cis-octahydro-1H-indene	980	46.0±1.3 [115]	46.9	-0.9
trans-octahydro-1H-indene	950	44.7±1.3 [115]	45.6	-0.9
pyrrolidine		37.5±0.2 [115]		
2-methyl-pyrrolidine		40.6±1.0 [115]		

[a] Data on standard non-polar columns [78], [b] Calculated using the following equation: $\Delta_l^g H_m^o$(298.15 K) /(kJ·mol^{-1}) = 3.5+0.0443×J_x with (R^2 = 0.993).

Table H. 9. Reactions and reaction enthalpies calculated by using quantum-chemical methods for indole.

1.1

1.2

1.3

1.4.

1.5

168
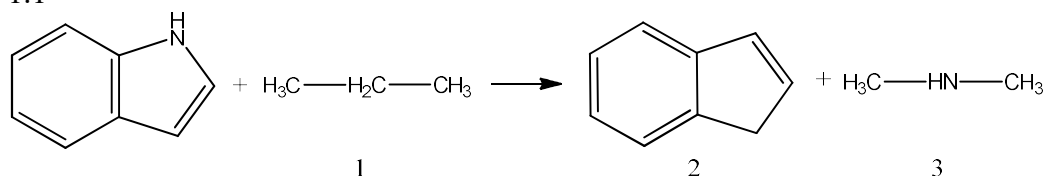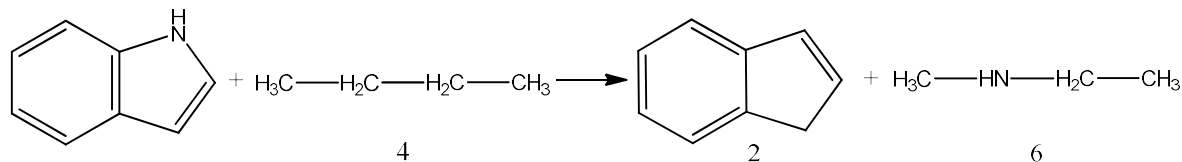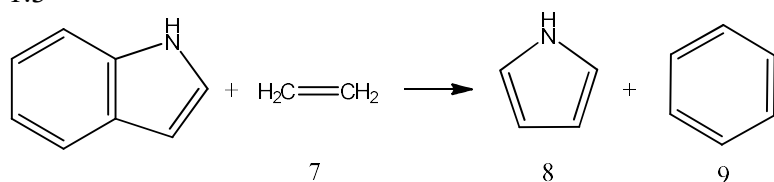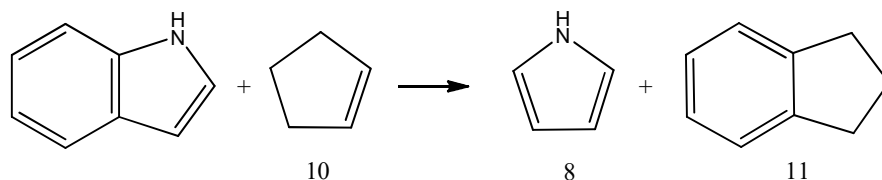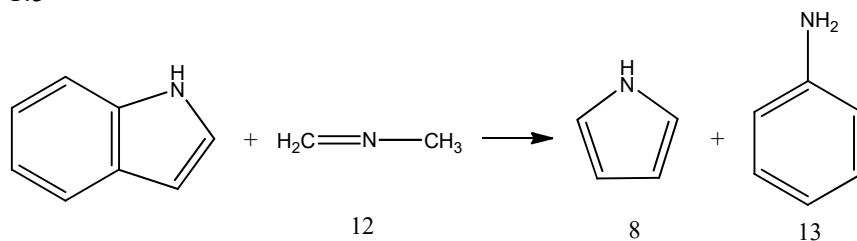
The enthalpy of formation of Indole $\Delta_f H_m^o$(g, 298.15 K), kJ/mol

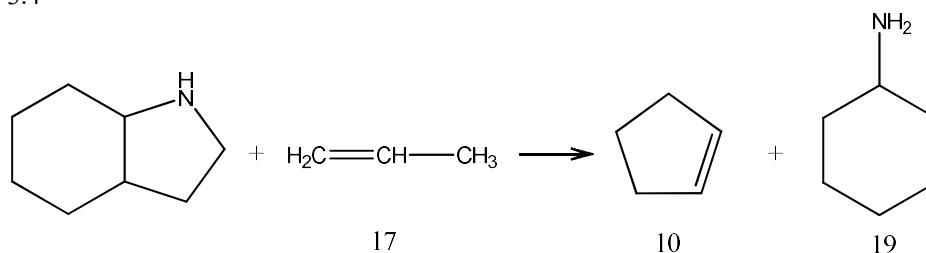| method	(AT)	Reaction 1.1	Reaction 1.2	Reaction 1.3	Reaction 1.4	Reaction 1.5*
G4	160,4	160,4	160,6	158,7	166,1	159,0
G3MP2	158,8	160,4	160,9	158,4	165,0	160,0
CBS-APNO		157,0	157,3	161,2	168,2	162,1

* In reaction (1.5) instead of the experimental value $\Delta_f H_{298}^0$ N-methyl-methaneimine value was used by G4 (AT) method.

The enthalpies of hypothetical reactions involving Indole $\Delta_r H_m^o$ (g, 298.15 K), kJ/mol

$\Delta_r H_m^o$ (g, 298.15 K)	Reaction 1.1	Reaction 1.2	Reaction 1.3	Reaction 1.4	Reaction 1.5
G4	86,4	78,9	-20,3	-31,0	-43,1
G3MP2	86,4	78,6	-20,0	-29,9	-44,2
CBS-APNO	89,8	82,2	-22,8	-33,1	-46,3

Table H. 10. Reactions and reaction enthalpies calculated by using quantum-chemical methods for indoline.

2.1
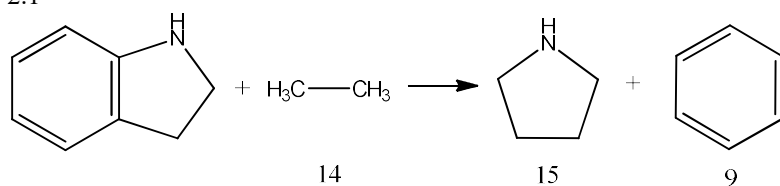
2.2
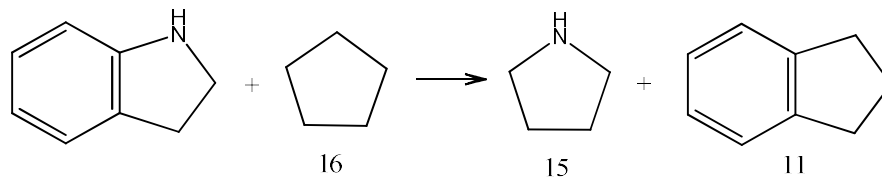
2.3
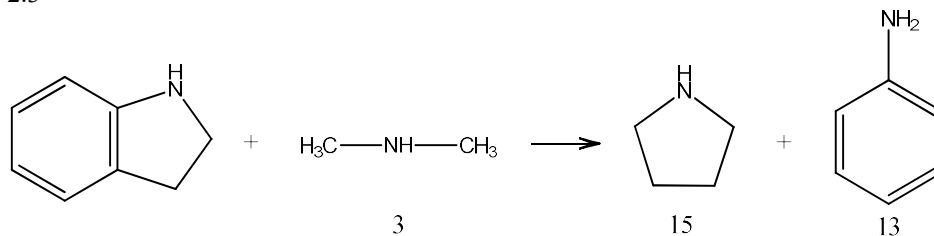
2.4
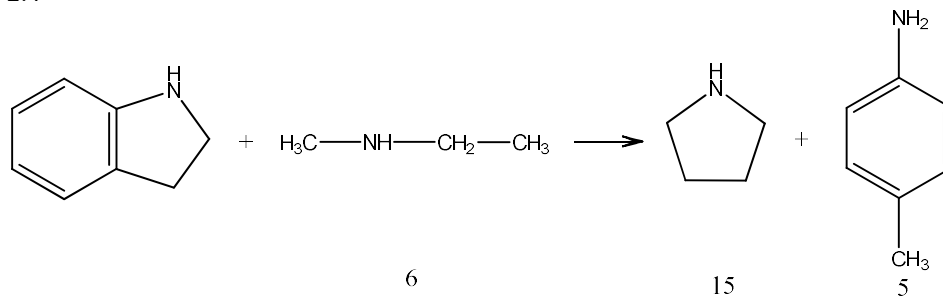
2.5
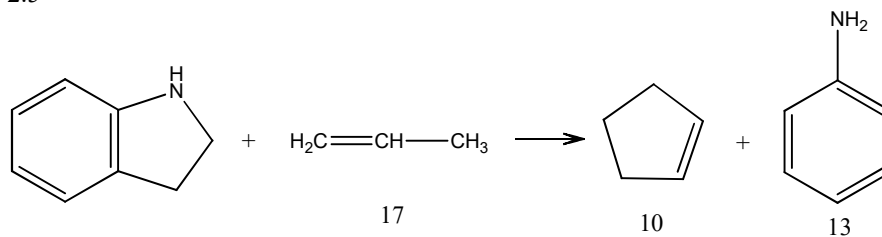
The enthalpy of formation of Indoline $\Delta_f H_m^o$(g, 298.15 K), kJ/mol

method	(AT)	Reaction 2.1	Reaction 2.2	Reaction 2.3	Reaction 2.4	Reaction 2.5
G4	117,6	115,1	121,6	117,8	118,4	113,5
G3MP2	116,0	115,4	120,4	119,1	118,5	114,9
CBS-APNO		114,2	120,7	118,9	119,4	114,6

The enthalpies of hypothetical reactions involving Indoline $\Delta_r H_m^o$ (g, 298.15 K), kJ/mol

$\Delta_r H_m^o$ (g, 298.15 K)	Reaction 2.1	Reaction 2.2	Reaction 2.3	Reaction 2.4	Reaction 2.5
G4	47,9	11,7	-15,5	-18,0	-12,5
G3MP2	47,6	12,9	-16,8	-18,1	-13,9
CBS-APNO	48,8	12,6	-16,6	-19,0	-13,6

Table H. 11. Reactions and reaction enthalpies calculated by using quantum-chemical methods for 8H-indole.

3.1
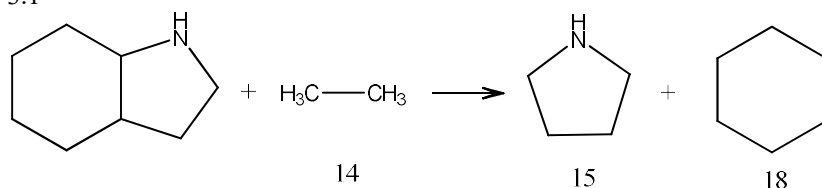
3.2
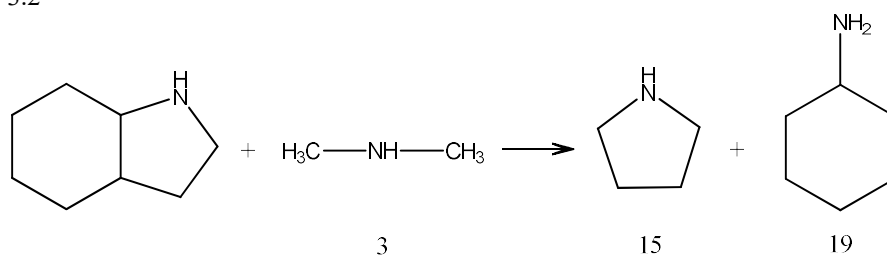
3.3
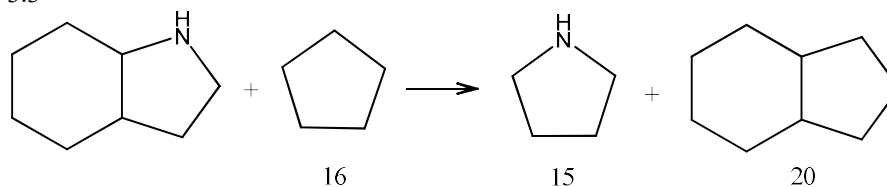
3.4

The enthalpy of formation of H8-Indole $\Delta_f H_m^o$(g, 298.15 K), kJ/mol

method	(AT)	Reaction 3.1	Reaction 3.2	Reaction 3.3 [a]	Reaction 3.3 [b]	Reaction 3.4
G4	-63,5	-67,5	-63,6	-59,9	-61,4	-68,0
G3MP2	-60,5	-66,7	-61,6	-60,4	-62,1	-65,8
CBS-APNO		-65,4	-61,0	-60,2	-61,5	-65,3

[a] – from a reaction involving cis-octahydro-1-indene, [b] – from a reaction involving trans-octahydro-1-indene.

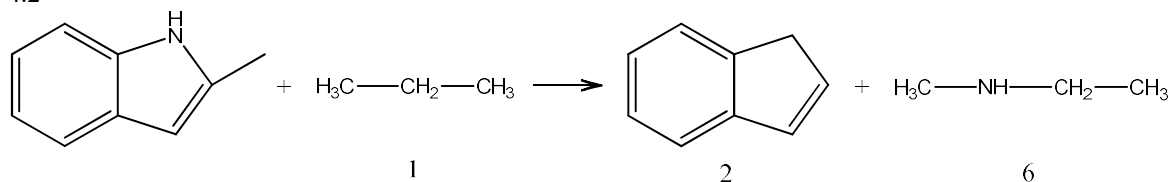| $\Delta_r H_m^o$ (g, 298.15 K)	Reaction 3.1	Reaction 3.2	Reaction 3.3 a	Reaction 3.3 b	Reaction 3.4
G4	24,5	-25,0	5,8	2,9	-21,9
G3MP2	23,7	-27,0	6,3	3,6	-24,1
CBS-APNO	22,4	-27,6	6,1	3,0	-24,6

[a] – from a reaction involving cis-octahydro-1-indene, [b] – from a reaction involving trans-octahydro-1-indene.

Table H. 12. Reactions and reaction enthalpies calculated by using quantum-chemical methods for 2-methyl-indole.

4.1
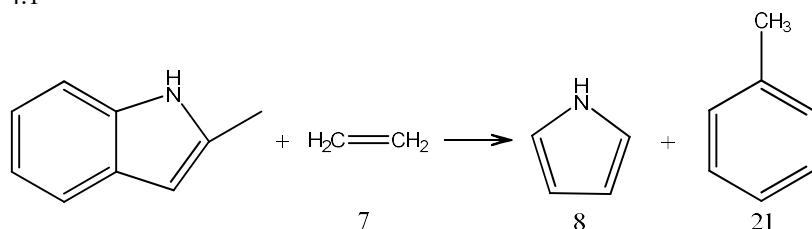
4.2

4.3
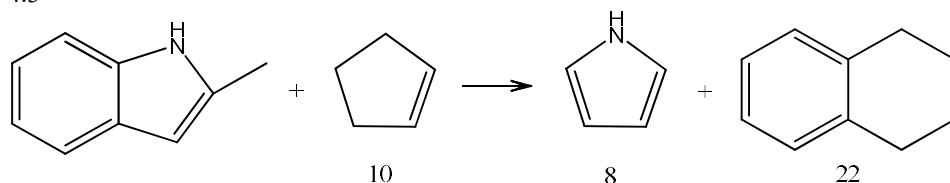
4.4
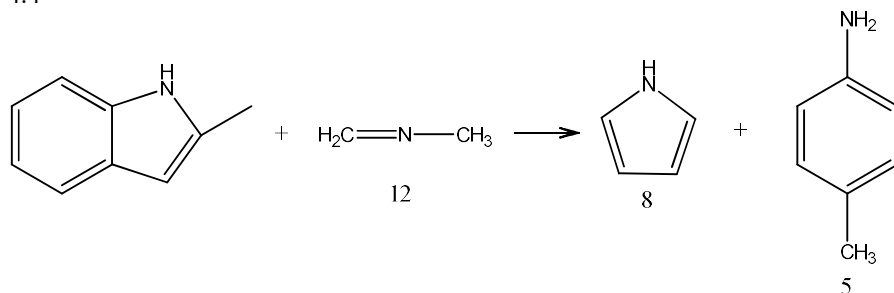
4.5
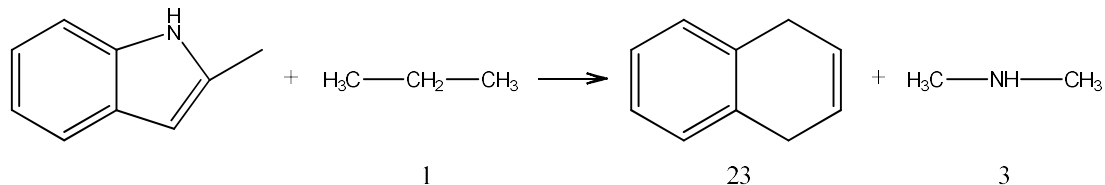
4.6
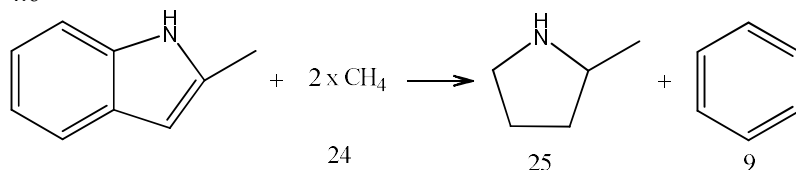
The enthalpy of formation of 2-Methyl-Indole $\Delta_f H_m^o$(g, 298.15 K), kJ/mol

method	(AT)	Reaction 4.1	Reaction 4.2	Reaction 4.3	Reaction 4.4	Reaction 4.5	Reaction 4.6
G4	120,2	119,6	120,6	127,8	119,7	120,6	117,2
G3MP2	118,9	119,0	121,4	127,1	120,4	121,1	118,4
CBS-APNO		121,0	116,6	128,7	122,2	115,2	115,2

The enthalpies of hypothetical reactions involving 2-Methyl-Indole $\Delta_r H_m^o$ (g, 298.15 K), kJ/mol

$\Delta_r H_m^o$ (g, 298.15 K)	Reaction 4.1	Reaction 4.2	Reaction 4.3	Reaction 4.4	Reaction 4.5	Reaction 4.6
G4	-13,4	98,0	-27,4	-34,0	103,9	73,3
G3MP2	-12,8	97,2	-26,7	-34,7	103,4	72,1
CBS-APNO	-14,8	102,0	-28,3	-36,5	109,3	75,3

Table H. 13. Reactions and reaction enthalpies calculated by using quantum-chemical methods for 2-methyl-indoline.
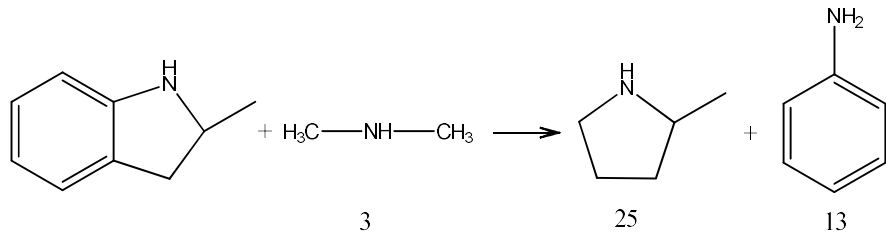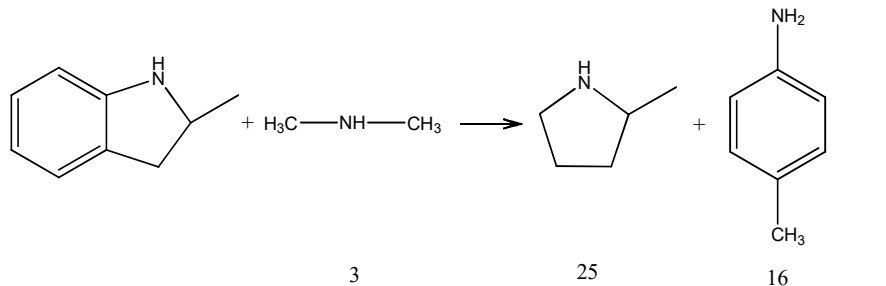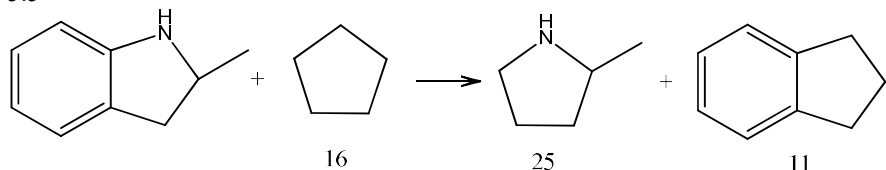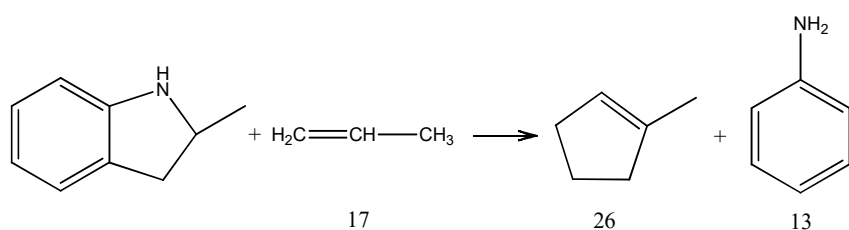
5.1

14 25 9

5.2

14 15 21

5.3

3 25 13

5.4

3 25 16

5.5

16 25 11

5.6

17   26   13
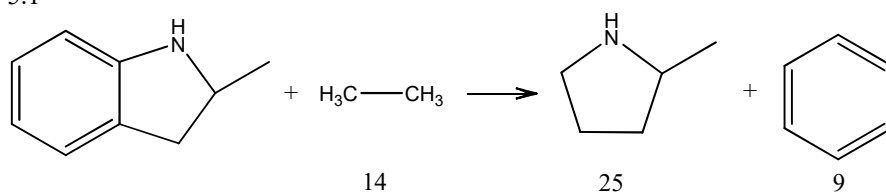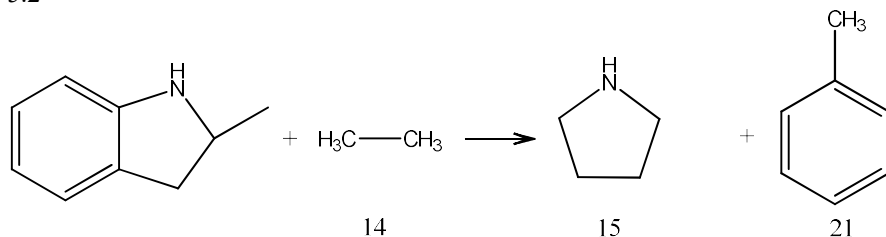
The enthalpy of formation of2-Methyl-Indoline $\Delta_f H_m^o$(g, 298.15 K), kJ/mol

method	(AT)	Reaction 5.1	Reaction 5.2	Reaction 5.3	Reaction 5.4	Reaction 5.5	Reaction 5.6
G4	79,4	77,3	78,0	80,1	80,7	84,2	76,8
G3MP2	78,0	77,9	77,9	81,6	81,6	83,3	77,6
CBS-APNO		76,1	77,1	80,9	84,2	83,1	78,4

*The enthalpies of hypothetical reactions involving2-Methyl-Indoline $\Delta_r H_m^o$ (g, 298.15 K), kJ/mol*

$\Delta_r H_m^o$ (g, 298.15 K)	Reaction 5.1	Reaction 5.2	Reaction 5.3	Reaction 5.4	Reaction 5.5	Reaction 5.6
G4	48,2	52,8	-15,3	-46,0	12,0	-13,5
G3MP2	47,6	52,9	-16,8	-46,9	12,9	-14,3
CBS-APNO	49,4	53,7	-16,1	-49,5	13,1	-15,1

Table H. 14. Reactions and reaction enthalpies calculated by using quantum-chemical methods for 2-methyl-8H-indole.
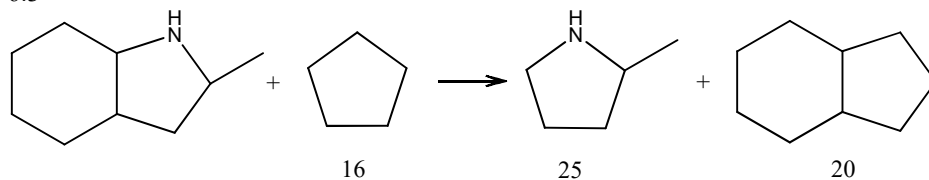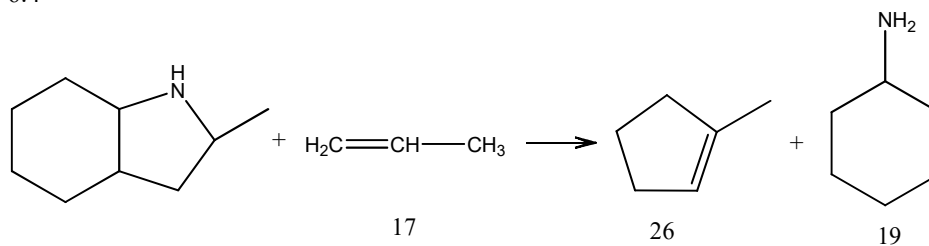
6.1

14   25   18

6.2

3   25   19

6.3

16   25   20

6.4

17   26   19
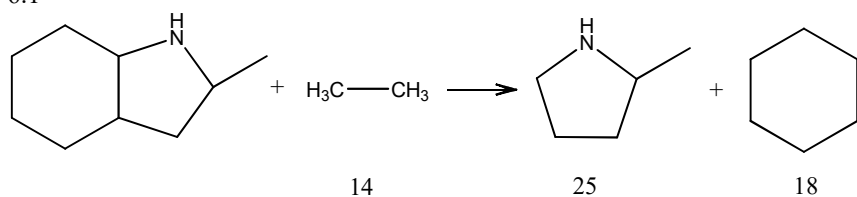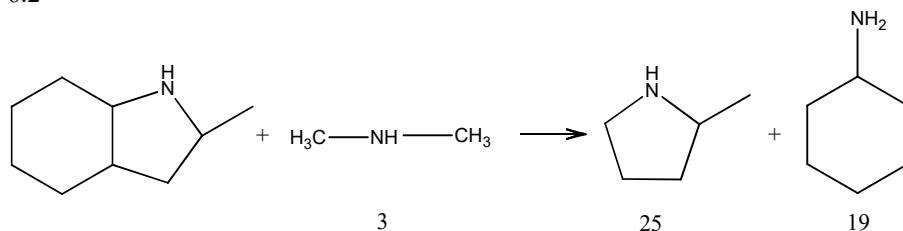
The enthalpy of formation of 8H-2-Methyl-Indole $\Delta_f H_m^o$(g, 298.15 K), kJ/mol

method	(AT)	Reaction 6.1	Reaction 6.2	Reaction 6.3 [a]	Reaction 6.3 [b]	Reaction 6.4
G4	-100,4	-104,0	-100,1	-98,0	-96,5	-103,4
G3MP2	-97,3	-103,0	-97,9	-98,3	-96,7	-101,9
CBS-APNO		-102,2	-97,7	-98,2	-97,0	-100,3
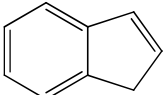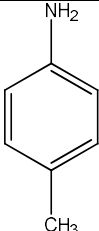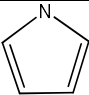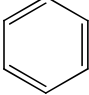
[a] – from a reaction involving trans-octahydro-1-indene, [b] – from a reaction involving cis-octahydro-1-indene.

The enthalpies of hypothetical reactions involving 8H-2-Methyl-Indole $\Delta_r H_m^o$ (g, 298.15 K), kJ/mol

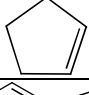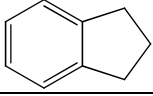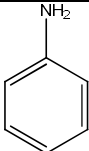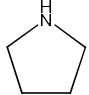| $\Delta_r H_m^o$ (g, 298.15 K)	Reaction 6.1	Reaction 6.2	Reaction 6.3 [a]	Reaction 6.3 [b]	Reaction 6.4
G4	23,5	-26,0	2,0	4,9	-24,2
G3MP2	22,5	-28,2	2,3	5,1	-25,7
CBS-APNO	21,7	-28,4	2,2	5,4	-27,3

[a] – from a reaction involving trans-octahydro-1-indene, [b] – from a reaction involving cis-octahydro-1-indene.

Table H. 15. Reference values for $\Delta_f H_m^o$ (g, 298.15 K) used for calculation reaction enthalpies in Table H. 9- Table H. 14 with help of quantum-chemical methods.

	structure	CAS	compound	formula	$\Delta_f H_m^o$(g, 298.15 K)	Ref
1	CH₃-CH₂-CH₃	74-98-6	propane	C_3H_6	-104.7 ± 0.5	[115]
2		95-13-6	indene	C_9H_8	160.7 ± 1.3	[179]
3	CH₃-NH-CH₃	124-40-4	dimethylamine	C_2H_7N	-18.6 ± 0.8	[115]
4	CH₃-CH₂-CH₂-CH₃	106-97-8	butane	C_4H_{10}	-125.6 ± 0.7	[115]
5		106-49-0	4-amino-toluene	C_7H_9N	57.0 ± 1.3	[217]
6	CH₃-NH-CH₂-CH₃	624-78-2	N-methyl-ethanamine	C_3H_9N	-46.8 ± 2.0	[218]
7	H₂C=CH₂	74-85-1	ethene	C_2H_4	52.5 ± 0.4	[115]
8		109-97-7	1-H-pyrole	C_4H_5N	108.3 ± 0.4	[115]
9		71-43-2	benzene	C_6H_6	82.6 ± 0.7	[115]
10		142-29-0	cyclo-pentene	C_5H_8	33.9 ± 1.4	[115]
11		496-11-7	indane	C_9H_{10}	60.7 ± 1.8	[79]
12	H₂C=N—CH₃	1761-67-7	N-methyl-methanimine	C_2H_5N		G4(AT)
13		62-53-3	aniline	C_6H_7N	87.1 ± 1.0	[115]
14	H₃C—CH₃	74-84-0	ethane	C_2H_6	-83.8 ± 0.4	[115]
15		123-75-1	pyrrolidine	C_4H_9N	-3.4 ± 0.8	[115]
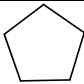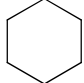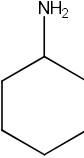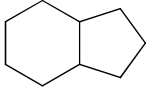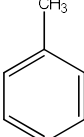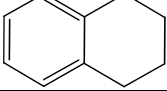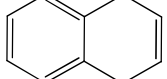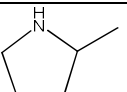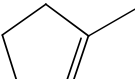
#		CAS	Name	Formula	ΔH	Ref.
16		287-92-3	cyclopentane	C_5H_{10}	-76.4 ± 0.8	[115]
17	$H_2C\!=\!CH\!-\!CH_3$	115-07-1	propene	C_3H_6	20.0 ± 0.8	[115]
18		110-82-7	cyclohexane	C_6H_{12}	-123.4 ± 0.8	[115]
19	NH_2	108-91-8	cyclohexyl-amine	$C_6H_{13}N$	-103.9 ± 1.3	[219]
20		4551-51-3	cis-octahydro-1H-indene	C_9H_{16}	-127.1 ± 2.0	[115]
20		3296-50-2	trans-octahydro-1H-indene	C_9H_{16}	-131.5 ± 2.2	[115]
21	CH_3	108-88-3	toluene	C_7H_8	50.4 ± 0.6	[115]
22		119-64-2	tetraline	$C_{10}H_{12}$	26.0 ± 2.0	[115]
23		612-17-9	1,4-dihydro-naphtalene	$C_{10}H_{10}$	138.4 ± 1.6	[201]
24	CH_4	74-82-8	methane	CH_4	-74.4 ± 0.4	[115]
25		765-38-3	2-methyl-pyrrolidine	$C_5H_{11}N$	-40.9 ± 1.6	[220]
26		693-89-0	1-methyl-cyclopentene	C_6H_{10}	-3.8 ± 0.7	[115]

Table H. 16. Thermodynamic properties of indole in the ideal gas state.

T. K	S_m^o. J K^{-1} mol^{-1}	C_{pm}^o. J K^{-1} mol^{-1}	$\frac{H-H_0}{T}$. J K^{-1} mol^{-1}	$-\frac{G-H_0}{T}$. J K^{-1} mol^{-1}
50	226.9	34.4	33.4	193.5
100	253.3	44.0	36.0	217.3
150	273.8	59.0	41.0	232.8
200	293.3	78.0	47.8	245.5
273.15	322.2	109.8	60.1	262.1
298.15	332.3	120.9	64.7	267.6
300	333.1	121.7	65.1	268.0
320	341.2	130.4	68.9	272.3
340	349.4	139.0	72.8	276.6
360	357.6	147.3	76.7	280.9
380	365.7	155.4	80.6	285.1
400	373.9	163.2	84.6	289.4
420	382.1	170.8	88.5	293.6
440	390.2	178.0	92.4	297.8
460	398.2	184.9	96.3	302.0
480	406.2	191.5	100.1	306.2
500	414.2	197.8	103.9	310.3
520	422.1	203.8	107.6	314.5
540	429.9	209.5	111.3	318.6

T, K	437.6	215.0	114.9	322.7
560	437.6	215.0	114.9	322.7
580	445.2	220.2	118.4	326.8
600	452.8	225.2	121.9	330.9

Table H. 17. Thermodynamic properties of indoline in the ideal gas state.

T, K	S_m^o, J K^{-1} mol^{-1}	C_{pm}^o, J K^{-1} mol^{-1}	$\frac{H-H_0}{T}$, J K^{-1} mol^{-1}	$-\frac{G-H_0}{T}$, J K^{-1} mol^{-1}
50	228.5	36.7	34.0	194.6
100	257.7	49.2	38.4	219.3
150	280.4	64.6	44.5	236.0
200	301.5	83.4	51.8	249.7
273.15	332.2	115.8	64.5	267.7
298.15	342.8	127.5	69.3	273.5
300	343.6	128.4	69.6	274.0
320	352.2	137.8	73.6	278.6
340	360.8	147.1	77.7	283.2
360	369.5	156.2	81.8	287.7
380	378.2	165.1	85.9	292.3
400	386.9	173.7	90.1	296.8
420	395.6	182.1	94.3	301.3
440	404.2	190.2	98.5	305.8
460	412.8	198.0	102.6	310.2
480	421.4	205.5	106.7	314.7
500	430.0	212.7	110.8	319.1
520	438.4	219.5	114.9	323.5
540	446.8	226.1	118.9	328.0
560	455.2	232.5	122.8	332.4
580	463.4	238.5	126.7	336.7
600	471.6	244.3	130.5	341.1

Table H. 18. Thermodynamic properties of racemic equimolar mixture of (R-,S-), (R-,R-), (S-,R-), (S-,S-) enantiomers of H8-indole in the ideal gas state**.**

T, K	S_m^o, J K^{-1} mol^{-1}	C_{pm}^o, J K^{-1} mol^{-1}	$\frac{H-H_0}{T}$, J K^{-1} mol^{-1}	$-\frac{G-H_0}{T}$, J K^{-1} mol^{-1}
50	246.7	43.9	36.8	209.9
100	282.5	61.3	43.5	239.0
150	310.8	79.3	51.2	259.6
200	336.3	99.6	59.8	276.5
273.15	372.9	137.1	74.4	298.5
298.15	385.5	151.5	80.0	305.6
300	386.4	152.5	80.4	306.0
320	396.7	164.4	85.1	311.6
340	407.0	176.3	89.9	317.1
360	417.4	188.2	94.9	322.5
380	427.9	200.0	99.9	328.0
400	438.5	211.6	105.0	333.4
420	449.0	222.9	110.2	338.9
440	459.7	234.0	115.4	344.3
460	470.3	244.7	120.6	349.7
480	480.9	255.1	125.8	355.1
500	491.6	265.2	131.0	360.5
520	502.2	274.9	136.2	366.0
540	512.7	284.3	141.3	371.4

560	523.2	293.3	146.4	376.8
580	533.6	302.0	151.4	382.2
600	544.1	310.0	156.4	387.7

Table H. 19. Thermodynamic properties of 2-methyl-indole in the ideal gas state from reference [171].

T, K	S_m^o, J K^{-1} mol^{-1}	C_{pm}^o, J K^{-1} mol^{-1}	$\frac{H-H_{298.15}}{T}$, J K^{-1} mol^{-1}
298.15	368.8	146.1	0.000
300	369.8	147.0	0.9063
320	379.5	156.5	10.33
340	389.3	165.9	19.21
360	399.1	175.1	27.62
380	408.8	184.1	35.62
400	418.4	192.8	43.26
420	428.1	201.3	50.59
440	437.6	209.4	57.62
460	447.1	217.2	64.39
480	456.5	224.7	70.91
500	465.8	231.9	77.21
520	475.0	238.8	83.29
540	484.2	245.4	89.18
560	493.2	251.8	94.87
580	502.2	257.8	100.4
600	511.0	263.7	105.7
620	519.7	269.3	110.9
640	528.4	274.6	116.0
660	536.9	279.8	120.8
680	545.3	284.7	125.6
700	553.6	289.5	130.2

Table H. 20. Thermodynamic properties of equimolar racemic mixture of R- and S- enantiomers of 2-methyl-indoline in the ideal gas state.

T, K	S_m^o, J K^{-1} mol^{-1}	C_{pm}^o, J K^{-1} mol^{-1}	$\frac{H-H_0}{T}$, J K^{-1} mol^{-1}	$-\frac{G-H_0}{T}$, J K^{-1} mol^{-1}
50	247.7	47.3	37.0	210.7
100	286.1	67.0	45.9	240.2
150	317.7	91.1	56.6	261.1
200	347.5	117.8	68.4	279.0
273.15	390.4	159.7	87.2	303.2
298.15	405.0	174.0	93.9	311.1
300	406.0	175.0	94.4	311.7
320	417.7	186.2	99.7	318.0
340	429.3	197.1	105.1	324.2
360	440.9	207.6	110.5	330.3
380	452.4	217.8	115.9	336.5
400	463.8	227.6	121.3	342.5
420	475.1	236.9	126.5	348.6
440	486.4	245.8	131.8	354.6
460	497.5	254.3	136.9	360.6
480	508.5	262.5	142.0	366.5
500	519.3	270.2	146.9	372.4
520	530.1	277.6	151.8	378.3

T, K	S_m^o, J K^{-1} mol^{-1}	C_{pm}^o, J K^{-1} mol^{-1}	$\frac{H-H_0}{T}$, J K^{-1} mol^{-1}	$-\frac{G-H_0}{T}$, J K^{-1} mol^{-1}
540	540.7	284.6	156.6	384.1
560	551.2	291.3	161.3	389.9
580	561.5	297.8	165.9	395.6
600	571.7	303.9	170.4	401.3

Table H. 21. Thermodynamic properties of racemic equimolar mixture of (R-,S-), (R-,R-), (S-,R-), (S-,S-) enantiomers including (R-, S- enantiomers of C2 position) of H8-2-methyl indole in the ideal gas state.

T, K	S_m^o, J K^{-1} mol^{-1}	C_{pm}^o, J K^{-1} mol^{-1}	$\frac{H-H_0}{T}$, J K^{-1} mol^{-1}	$-\frac{G-H_0}{T}$, J K^{-1} mol^{-1}
50	260.5	46.7	38.6	221.9
100	299.5	69.3	47.1	252.4
150	332.2	93.9	57.5	274.7
200	362.7	119.5	68.7	294.0
273.15	406.1	162.6	86.7	319.4
298.15	421.0	178.6	93.3	327.7
300	422.2	179.8	93.8	328.3
320	434.2	193.0	99.3	334.9
340	446.3	206.1	104.9	341.4
360	458.4	219.2	110.6	347.8
380	470.6	232.1	116.4	354.2
400	482.9	244.8	122.2	360.6
420	495.1	257.3	128.1	367.0
440	507.4	269.3	134.0	373.4
460	519.6	281.0	139.9	379.7
480	531.8	292.4	145.7	386.1
500	544.0	303.3	151.6	392.4
520	556.1	313.9	157.4	398.7
540	568.1	324.1	163.1	405.0
560	580.1	333.9	168.8	411.3
580	591.9	343.3	174.4	417.6
600	603.7	352.4	179.9	423.8